Tellus B
Chemical and Physical Meteorology

Tropical and Boreal Forest – Atmosphere Interactions: A Review

PAULO ARTAXO
HANS-CHRISTEN HANSSON
MEINRAT O. ANDREAE
JAANA BÄCK
ELIANE GOMES ALVES
HENRIQUE M. J. BARBOSA
FRIDA BENDER
EFSTRATIOS BOURTSOUKIDIS
SAMARA CARBONE
JINSHU CHI
STEFANO DECESARI
VIVIANE R. DESPRÉS
FLORIAN DITAS
EKATERINA EZHOVA
SANDRO FUZZI
NILES J. HASSELQUIST
JOST HEINTZENBERG
BRUNA A. HOLANDA
ALEX GUENTHER
HANNELE HAKOLA
LIINE HEIKKINEN
VELI-MATTI KERMINEN
JENNI KONTKANEN
RADOVAN KREJCI
MARKKU KULMALA
JOST V. LAVRIC
GERRIT DE LEEUW
KATRIANNE LEHTIPALO
LUIZ AUGUSTO T. MACHADO
GORDON MCFIGGANS
MARCO AURELIO M. FRANCO
BRUNO BACKES MELLER
FERNANDO G. MORAIS
CLAUDIA MOHR
WILLIAM MORGAN
MATS B. NILSSON
MATTHIAS PEICHL
TUUKKA PETÄJÄ
MARIA PRAß
CHRISTOPHER PÖHLKER
MIRA L. PÖHLKER
ULRICH PÖSCHL
CELSO VON RANDOW
ILONA RIIPINEN
JANNE RINNE
LUCIANA V. RIZZO
DANIEL ROSENFELD
MARIA A. F. SILVA DIAS
LARISA SOGACHEVA
PHILIP STIER
ERIK SWIETLICKI
MATTHIAS SÖRGEL
PETER TUNVED
AKI VIRKKULA
JIAN WANG
BETTINA WEBER
ANA MARIA YÁÑEZ-SERRANO
PAUL ZIEGER
EUGENE MIKHAILOV
JAMES N. SMITH
JÜRGEN KESSELMEIER

*Author affiliations can be found in the back matter of this article

COLLECTION: CONSTRAINED AEROSOL FORCINGS FOR IMPROVED CLIMATE PROJECTIONS (FORCES)

REVIEW ARTICLE

STOCKHOLM UNIVERSITY PRESS

CORRESPONDING AUTHOR:
Paulo Artaxo
Institute of Physics, University of São Paulo, Rua do Matão 1371, CEP 05508-090, São Paulo, S.P., Brazil
artaxo@if.usp.br

KEYWORDS:
Boreal forests; Tropical forests; Amazonia; biogenic emissions: fires; biomass burning; aerosol particles; climate effects

TO CITE THIS ARTICLE:
Artaxo, P, et al. 2022. Tropical and Boreal Forest – Atmosphere Interactions: A Review. *Tellus B: Chemical and Physical Meteorology*, 74(2022), 24–163. DOI: *https://doi.org/10.16993/tellusb.34*

ABSTRACT

This review presents how the boreal and the tropical forests affect the atmosphere, its chemical composition, its function, and further how that affects the climate and, in return, the ecosystems through feedback processes. Observations from key tower sites standing out due to their long-term comprehensive observations: The Amazon Tall

Tower Observatory in Central Amazonia, the Zotino Tall Tower Observatory in Siberia, and the Station to Measure Ecosystem-Atmosphere Relations at Hyytiäla in Finland. The review is complemented by short-term observations from networks and large experiments.

The review discusses atmospheric chemistry observations, aerosol formation and processing, physiochemical aerosol, and cloud condensation nuclei properties and finds surprising similarities and important differences in the two ecosystems. The aerosol concentrations and chemistry are similar, particularly concerning the main chemical components, both dominated by an organic fraction, while the boreal ecosystem has generally higher concentrations of inorganics, due to higher influence of long-range transported air pollution. The emissions of biogenic volatile organic compounds are dominated by isoprene and monoterpene in the tropical and boreal regions, respectively, being the main precursors of the organic aerosol fraction.

Observations and modeling studies show that climate change and deforestation affect the ecosystems such that the carbon and hydrological cycles in Amazonia are changing to carbon neutrality and affect precipitation downwind. In Africa, the tropical forests are so far maintaining their carbon sink.

It is urgent to better understand the interaction between these major ecosystems, the atmosphere, and climate, which calls for more observation sites, providing long-term data on water, carbon, and other biogeochemical cycles. This is essential in finding a sustainable balance between forest preservation and reforestation versus a potential increase in food production and biofuels, which are critical in maintaining ecosystem services and global climate stability. Reducing global warming and deforestation is vital for tropical forests.

1. INTRODUCTION

Tropical, temperate, and boreal forests are critical components of the climate system, and the ecosystem services they provide are essential for our society (Bonan et al., 1992, Bonan 2008, Davidson et al., 2012, Mitchard et al., 2018, IPCC SRCCL, 2019). Forest ecosystems once covered a large area of our continents and dominated in terrestrial ecosystems' water vapor processing, carbon cycling, i.e., being a major source and sink of gases and aerosol particles to and from the atmosphere (Malhi et al., 2008, Ometto et al., 2005). Thus, to a large part, they control the atmospheric composition and affect its functions, e.g., through their effect on radiation balance, clouds, and other climatic processes affecting. Until a few hundred years ago, photosynthesis was the leading mechanism controlling CO_2 atmospheric concentrations. Later use of fossil fuel emitting anthropogenic CO_2 has strongly increased the atmospheric CO_2 concentrations.

Today, land use, e.g., agriculture, occupies more land area than forests and is a significant net contributor to greenhouse gas emissions and climate change (Le Quéré et al., 2018, Pugh et al., 2019a). Land-use change also plays a prominent role in Nationally Determined Contributions (NDCs) of the Paris Agreement, with a potential to change the global carbon balance, cycling of other key chemical components, and having important regional impacts (Suni et al., 2015), as discussed in the IPCC special report on climate change, desertification, land degradation, sustainable land management, food security, and greenhouse gas fluxes in terrestrial ecosystems (IPCC SRCCL, 2019). Land ecosystems' interaction with the atmosphere does not only respond to direct land use but is also sensitive to changes in environmental conditions such as temperature, precipitation, length of seasons, and others. Ecosystems serve as a large CO_2 sink, especially in tropical regions with a fast metabolism that can absorb CO_2 from the atmosphere quickly (Canadell and Schulze 2014; Le Quéré et al., 2018, Friedlingstein et al., 2019). Changes in vegetation cover can result in regional cooling or warming through altered energy and momentum transfer between ecosystems and the atmosphere, depending on the eco-climatic conditions (Betts et al., 2001, Spracklen et al., 2008). The complex and nonlinear forest-atmosphere interactions can dampen or amplify anthropogenic climate change regionally and globally (Bonan, 2008).

Forest ecosystems are still among the most important terrestrial ecological systems in terms of ecosystem functions and services (IPBES, 2019, Blundo et al., 2021). Humans rely on healthy forests to supply energy, building materials, food, and services such as storing carbon, hosting biodiversity, and regulating climate. These biotic systems are vital for ensuring the well-being of human society and preserving global biodiversity. They also regulate the climate system, serve as large

carbon reservoirs in biomass or soil carbon pools and provide evaporative cooling processes, essential for the hydrological cycles over continental areas (Prăvălie, 2018, Trumbore et al., 2015, Grantham et al., 2020).

Forests cover $40{\cdot}10^6$ km^2 of the Earth, about 31% of global ice-free land (Song et al., 2018). Still, considerable uncertainties relate to estimates of their (and natural grasslands and savannahs) extent due to discrepancies in definitions (FAO, 2018). Globally, 60–85% of temperate and southern boreal forests are under some form of use or management (Erb et al., 2018). Comparably, about 20% of the tropical forest is estimated to be more or less managed, but this value is highly uncertain (FAO, 1999). As a comparison, the total agricultural area has been estimated to be $48{\cdot}10^6$ km^2 (FAO, 2018).

Reforestation and afforestation have been proposed as critical instruments to reduce atmospheric CO_2 concentrations (IPCC SR1.5, IPCC SRCCL 2019), which have been widely accepted as cost-effective climate change mitigation mechanisms when compared to mitigation options in the energy and transport sector (Smith et al., 2014; Griscom et al., 2017; IPCC, 2018). Additionally, forests influence water balance through the impact on evapotranspiration but also water flows and quality by reducing runoff, soil particles, and nutrients transported in run-off processes. Understanding the forest-climate interactions is important in a time where our society needs to set ambitious goals for biodiversity and ecosystem sustainability (Diaz et al., 2020, IPBES, 2019), and at the simultaneous possibility of a climate threshold where a collapse of tropical forests could happen (Hubau et al., 2020, Sullivan et al., 2020). Sullivan et al., 2020 analyzed how a long-term change in carbon stocks depended on global surface air temperature effects and found the long-term thermal sensitivity of the tropical forest carbon storage is a key uncertainty in predicting global climate change due to their complex response to climate change. The South American tropical forests were found to be more sensitive than African or Asian forests. Maximum temperature and precipitation are the most important variables to predict carbon stocks in tropical forests. They showed that the primary productivity of tropical forests starts to decrease at canopy temperatures above 32.2°C, i.e., the carbon uptake starts decreasing at this temperature. Hubau et al., 2020, when analyzing carbon stocks in Amazon and African tropical forests from 1985 to 2014, found the net carbon sink in Amazonia is decreasing, while the African tropical forests carbon sink is not changing.

The atmosphere plays a central role in all the biogeochemical cycles, including hydrology, not only as a transport vehicle but through atmospheric gas and liquid phase chemistry. The atmosphere is, of course, an integral part of the climate system. The climate is directly influenced by changes in the atmospheric composition and its influence on radiation fluxes, clouds, and precipitation. Presently the lacking knowledge about atmospheric aerosols concerning their sources, concentrations, and different atmospheric processes is the main cause of the uncertainties in climate projections (IPCC, 2013).

The tropical and boreal forests are easily separated by their different ecosystems, hydrology, and meteorology (Bonan, 2008). Thus, it appears their influence on the atmosphere is quite different, but observations of the atmosphere, its composition, its properties, and its effect on climate show similarities (Malhi et al., 2002). This review intends to establish the present knowledge on the forest–atmosphere interaction for these two important ecosystems. Due to a lack of long-term atmospheric observations, the temperate forest is not included in the review. We focus on how the tropical and boreal forest processes affect the atmosphere, its aerosols and gases, their composition, and properties over the forest. Furthermore, how the atmospheric processes in return affect the ecosystem functioning. Through the similarities and differences found in observations and modeling of the two ecosystems, the atmospheric content, and their interaction, we aim to understand better the future development of these critical ecosystems in a changing climate.

However, to put the thorough presentation of atmospheric chemistry into a broader scientific context facilitating a better understanding of reasons for observed differences and similarities, we found it necessary to introduce the two forest systems and the meteorology. The two ecosystems are strongly dependent on the climate in their respective geographical area, having specific meteorology. The clouds are an integral part of the life cycle of the aerosols, from new particle formation through growth to deposition, and a critical part of the hydrological cycle. The first section is followed by observations of the atmospheric composition, especially for aerosol particles, their chemistry, optical and hygroscopic properties, i.e., parameters impacting the regional climate forcing. Then we describe present knowledge on ecosystem emissions and uptake of greenhouse gases, water vapor, volatile organic gases, and particles. The impacts of these emissions on the observed atmospheric concentrations and physicochemical processes for the tropical and boreal forests are discussed in the perspective of observed impacts. The occurrence and impact of forest fires are mainly discussed due to their major effect on ecosystems, atmospheric composition, chemistry, and function, including the climate (Hantson et al., 2016). Other specific phenomena of major climate impact discussed are observations of new particle formation, aerosol-cloud interactions, and the hydrological cycle's impacts. We then discuss ecosystem feedback processes and the possible future of forests in a changing climate. This is discussed because of the commitment of several countries in their National Determined Contribution

(NDC) of the Paris Agreement to reduce deforestation and promote large-scale reforestation and afforestation. We finish looking at perspectives for future studies and discuss syntheses of our knowledge on the complex forest and climate relationship with its anthropogenic impacts (Roosevelt, 2013).

Unfortunately, very few sites in tropical forests have long-term comprehensive measurements of critical atmospheric properties. The ATTO tower is the only long-term site in tropical forests with the necessary characteristics to detail the seasonality of fundamental atmospheric and ecosystem properties with more than five years of continuous measurements. A few short-term studies in tropical Africa were available and integrated into this review. On the boreal component, ZOTTO and SMEAR II are two key sites on the boreal forest that provides long-term measurements. We also report a few short-term studies done in other boreal forest sites (Heintzenberg and Birmili, 2010).

2. FOREST ECOSYSTEMS AND CLIMATE

2.1. GENERAL/GLOBAL

Forest ecosystems are currently being subjected to a wide range of natural and anthropic disturbances that pose a real threat not only to forest health and the various benefits forests provide for human society but also to the overall functioning of the global climate system (Brando et al., 2019, Artaxo, 2012, Davidson and Artaxo, 2004, Grantham et al., 2020). Globally, the forests can be classified into three main forest biomes, i.e., tropical, temperate, and boreal forests. The world's forests are mainly located in Asia (31% of the global forest area), South America (21%), North and Central America (17%), Africa (17%), Europe (9%), and Oceania (5%) (Pan et al., 2013). The Earth's forests account for 80% of the planet's total plant biomass, and the amount of carbon they store in biomass and soil is more significant than the one currently present in the atmosphere (Pan et al., 2013). The total amount of carbon stored in these terrestrial systems is estimated to be about 861 Pg C, of which 44% is stored in the soil, up to 1 m-depth, 42% in live biomass, 8% in deadwood, and 5% in the litter (Pan et al., 2011). Presently the global forests are estimated to absorb about 29% of annual anthropogenic emissions of CO_2 (Le Quéré, 2018).

Figure 2.1 shows the geographical distribution of tropical, temperate, and boreal forests and some of the main issues related to their climate impacts (Prăvălie et al., 2018). Soil carbon is a crucial carbon pool, especially in temperate and boreal forests. Besides the ground carbon pool, the hydrological cycle and albedo are the main agents between climate and forests. ***Figure 2.1*** also illustrates differences in carbon allocation, evaporative cooling, and solar radiation absorption.

Globally, forests are currently subjected to the pressure of a wide range of disturbances, either natural or man-made (Grantham et al., 2020, Blundo et al., 2021). Forest perturbations can be concisely defined as all the disruptive factors that directly or indirectly threaten the ecosystems' health, functions, and services or the very existence of forests locally, regionally, or globally, affecting biodiversity or carbon storage functions (Trumbore et al., 2015).

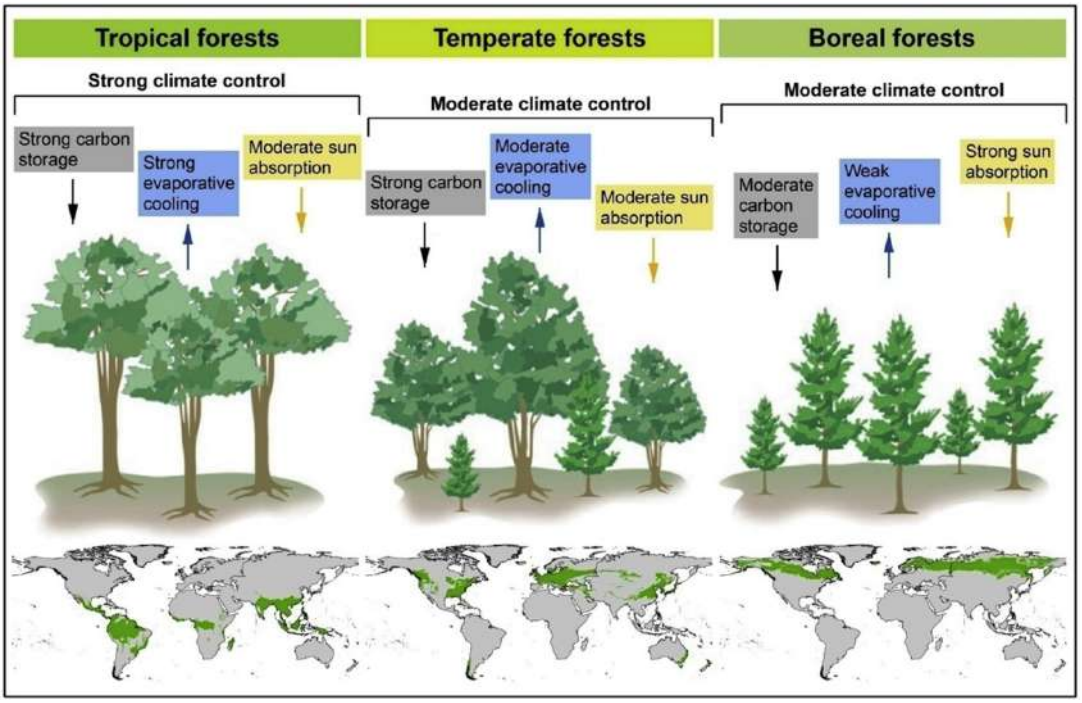

Figure 2.1 Tropical, temperate, and boreal forest geographical distribution and some of the main issues related to their climate impacts include above-ground carbon storage, evaporative cooling, and absorption of solar radiation (Prăvălie et al., 2018).

Natural successional trends in forest zones depend on disturbance regimes. Forest fires, windfalls, and the impact of pathogens and herbivores are the main factors causing drastic changes in the forest community. Fire frequency is the main successional factor in boreal forest zones of North America (Brassard and Chen 2006). The seed production in a harsh climate is episodic, and significant seed crops can be separated by as much as 12 years, causing a large variation in stand structure in natural boreal forests.

The novel stresses in the form of climate change, air pollution, invasive pests, and land-use change lead to deforestation and significant losses of stored carbon. Detecting how the increase of these stresses affects the development of the forests is a major scientific challenge requiring new observation systems to critically assess global forests' health. One of the key attributes of a healthy forest system is its ability to recover from disturbance. According to the 2015 FAO Global Forest Resources Assessment (FAO, 2015), the global forest area decreased by ~$1.3 \cdot 10^6$ km^2 (3%) in the past two and a half decades, from $41.3 \cdot 10^6$ km^2 in 1990 to $40 \cdot 10^6$ km^2 in 2015.

2.2. TROPICAL FORESTS

Tropical forests constitute about 50% of the global forest area and are present in areas with mean annual temperatures of at least 24°C and precipitation that generally exceeds 2000 mm per year. Tropical forests have very high biodiversity (IPBES, 2019). The tropical forests store large amounts of carbon, around 471 Pg C, i.e., 55% of the total global forest stocks of carbon, in the soil up to a depth of 1 m, in live biomass, deadwood, and litter (Pan et al., 2011, Blundo et al., 2021).

The degradation and fragmentation of the tropical forests in South America, Africa, and Southeast Asia, results in habitat and biodiversity loss and increased carbon emissions, and most likely disturbed hydrology and fluxes of aerosols and gases (Matricardi et al., 2020, Silva Junior et al., 2020, Mitchard, 2018, Nagy et al., 2016). Extensive remaining forests are found in the Amazon and Congo Basins and Insular Southeast Asia, with the most continuous and large area in the Amazon (Hansen et al., 2020, Lambin et al., 2003). Gross primary production (GPP) has been identified as the largest terrestrial carbon flux and the primary driver of the growing biosphere uptake of carbon. Structurally intact tropical forests sequestered about half of the global terrestrial carbon uptake over the 1990s and early 2000s, removing about 15 percent of anthropogenic carbon dioxide emissions (Hubau et al., 2020). Melnikova and Sasai, 2020 combined a diagnostic-type biosphere model with large-ensemble climate simulation data set, showing that the anthropogenic GPP effect is driven by CO_2 fertilization, projected to weaken or saturate by 2050–2150, depending on how the CO_2 concentrations will develop. The model results suggest that shortwave radiation couples with El Niño–Southern Oscillation conditions and volcanic eruptions and together drive the natural GPP effect (Melnikova and Sasai, 2020). As shortwave radiation flux at the surface is related to cloud cover, cloud-radiation feedback is important for GPP and the carbon cycling of forests (Melnikova and Sasai, 2020).

The natural Amazonian Forest was absorbing carbon at a rate of about 66 g C $m^{-2}a^{-1}$ from the '80s until 2005. However, recent measurements show the natural forest to be close to carbon-neutral, seemingly due to an increase in tree mortality, possibly due to an increase in climate extremes such as severe droughts like 2005 and 2010 (Hubau et al., 2020, Brando et al., 2014). In the Brazilian part of Amazonia, deforestation has over the last three decades cleared more than $4 \cdot 10^5$ km^2, which is about 20% of the Brazilian Amazonian Forest area. The annual rate of Amazonian deforestation was from 2004 to 2012 strongly reduced from $29 \cdot 10^3$ km^2 to $4 \cdot 10^3$ km^2 per year, showing that it is possible and feasible to reduce tropical deforestation (***Figure 2.2***). Unfortunately, from 2012 to 2021, Brazilian Amazonian deforestation increased significantly from $7.5 \cdot 10^3$ km^2 per year in 2018 to $13.2 \cdot 10^3$ km^2 in 2021 due to the weakening of national policies for Amazonian protection. The 2019 Brazilian deforestation in Amazonia released about 559 Tg CO_2, according to estimates from the Brazilian Space Agency (Instituto Nacional de Pesquisas Espaciais – INPE), and deforestation is increasing carbon emissions over the last seven years (Brando et al., 2020). As the climate becomes hotter and dryer in the next few decades, the eCO_2 emissions from these fires (eCO_2 defined as fire-induced emissions of CO_2, CO, CH_4, N_2O, and NO_x) could reach 6.0 Pg in the 2050s, a 10-fold increase since 2019 (Brando et al., 2020).

The complex physical-chemical interaction seen in the Amazon basin includes the processes of rainfall formation, daily, seasonal, inter-annual cycles, cloud spatial organization, the mechanisms controlling cloud formation, including aerosols acting as condensation nuclei (CCN), i.e., the interaction between vegetation, boundary layer, clouds, and upper troposphere (Davidson and Artaxo, 2004). These processes are all nicely coupled, defining a stable climate that produces rainfall equivalent to about 2.3 meters over the $6.1 \cdot 10^6$ km^2 of Amazonas basin, equivalent to $14 \cdot 10^3$ km^3 of water each year. The trees return about 2/3 of this water to the atmosphere through evapotranspiration, crucial for precipitation downwind south of the Amazonian basin (Spracklen et al., 2012). However, these unique nonlinear complex mechanisms are being modified by human activities. Recently Nobre et al. (2019) show how the present stable environment can be disturbed and move to another state of equilibrium far from the present that abundantly produces fresh water, keeps the forest alive, and has an important role in the global atmospheric circulation and energy distribution.

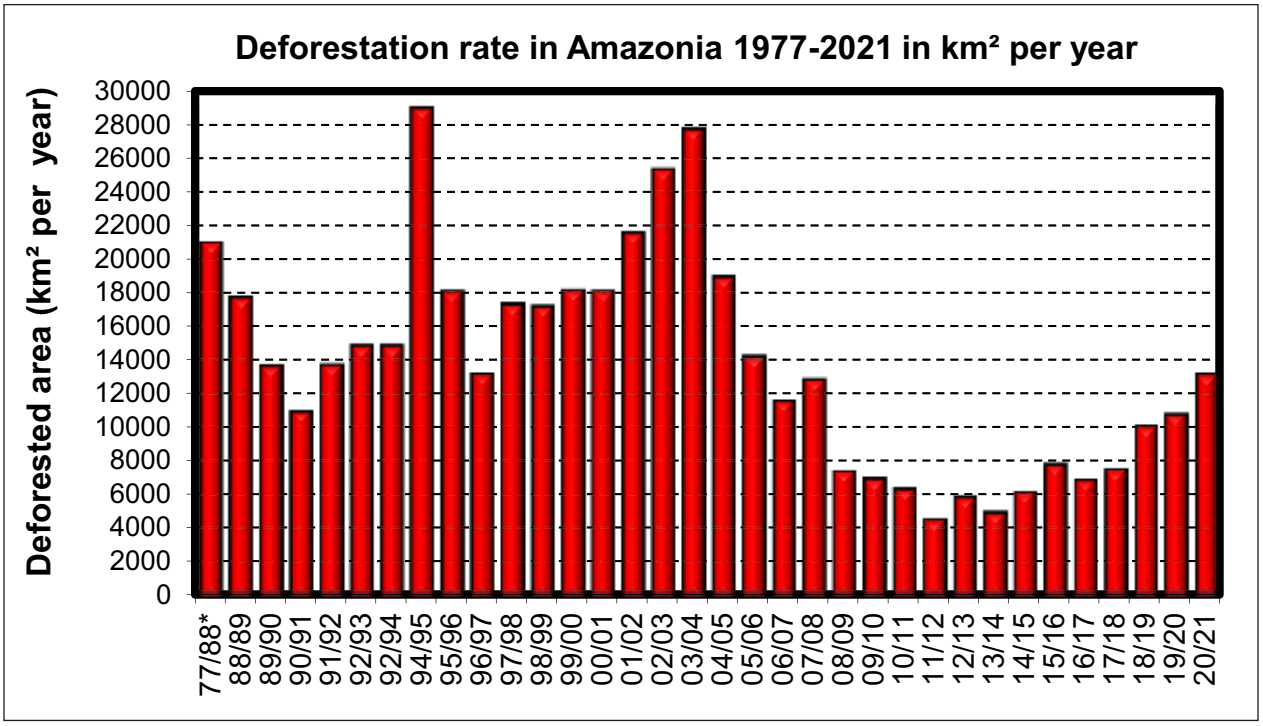

Figure 2.2 The annual rate of Brazilian Amazonian deforestation in km² per year from 1977 to 2021. The data from 77/88 are estimates derived from ground measurements. The remaining data are from the INPE/PRODES system that calculates deforestation areas based on extensive analysis of Landsat images. From: *http://www.obt.inpe.br/OBT/assuntos/programas/amazonia/prodes*.

Not adopting actions to control the removal of natural vegetation increases deforestation, causing greater changes in vegetation, greater changes in the hydrological cycle, and thermal control (Amaral e Silva et al., 2020).

Observations show climate change is already having an impact on forested regions (Mitchard, 2018). The hydrological cycle is changing in Amazonia. The Amazonas River discharge at Óbidos has increased by 15% from 1990 to 2013 (Gloor et al., 2013, 2015). Simultaneously, a recent systematic increase in Vapor Pressure Deficit over tropical South America is observed (Barkhordarian et al., 2019), indicating important changes in the Amazonian water cycle. The observed increase in tree mortality suggests decreased evapotranspiration, explaining less water vapor above the forest simultaneous with an increased river flow. However, analyses of Amazon run-off and gridded precipitation data suggest an intensification of the hydrological cycle over the past few decades with the wet season precipitation and peak river run-off (since 1980) as well as annual mean precipitation (since 1990) have increased, while dry season precipitation and minimum run-off have decreased. Also, the lengthening of the dry season by 15 days over the last ten years was observed in Southwestern Amazonia (Fu et al., 2013). This study highlights the potential mechanisms by which interactions between deforestation, land surface processes, atmospheric convection, biomass burning emissions, and climate change may alter the timing of wet season onset and provide a mechanistic framework for understanding how deforestation extends the dry season and enhances regional vulnerability to drought (Aragão et al., 2008).

2.3. BOREAL FORESTS

The boreal forest covers about $11{\cdot}10^6$ km^2 (Pan et al., 2011), i.e., ~30% of the global forests. The boreal forest is the world's largest terrestrial biome between 50°N to 70°N, covering ca. 15% of the Earth's terrestrial area in inland Alaska, Canada, Scotland, Fennoscandia (Sweden, Finland, Norway) and Russia, parts of the northern continental United States, northern Kazakhstan, and Japan. They are adapted to the mean annual temperatures from about –10 to 5°C and annual precipitation generally below 500 mm. Much of the boreal forest was recently glaciated (ca. 10 kyr ago). The retreat of glaciers left depressions in the topography that have been filled with water since then, creating an abundant network of lakes and bogs, typical throughout the boreal forest. Important for the carbon balance is the moderate precipitation, the low evaporative demand, and slow run-off from the wetlands results in the accumulation of peat, characteristic of boreal forest zone soils. In upland boreal forests, soils tend to be relatively young and nutrient-poor, formed via the podzolization process: the acidic reaction of decomposed litter causes leaching and moving of minerals to the top of the soils, resulting in an eluvial horizon just below the litter (Brassard and Chen, 2006). Boreal forests are also characterized by a low below-ground temperature. However, large differences are also seen here: in areas with abundant precipitation in winter, soils are covered with thick snowpack and only moderately frozen, whereas, in drier regions, frost penetrates to very deep layers. Permafrost forms in areas with a low mean annual temperature and very low

winter temperatures. Low soil temperatures hinder soil development and the ease with which plants can use their nutrients and have consequences on the ecosystem properties and carbon accumulation to the system.

The boreal zone is much less diverse in plant species than the tropical zone (Gauthier et al., 2015). The trees also remain moderate in height compared to tropical forests. Dominating species belong to evergreen Abies, Picea, and Pinus genera. However, in eastern parts of the Russian boreal zone, the deciduous Larix species form large stands (Soja et al., 2007). Also, a few broadleaved trees (Alnus, Betula, Populus) are represented either as subcanopy species or forming larger stands, particularly after disturbances like stand-replacing fires, windstorms, or clear cuts where most if not all older trees are removed from an area of forest. In the southern boreal forest stands, trees are forming closed canopies. In contrast, in the north, trees are smaller and sparsely situated, and more light penetrates to the ground level allowing abundant ground vegetation. The photosynthetic activity of deciduous broadleaved species is limited to the growing season from leaf budburst during spring to leaf shed during autumn.

Nevertheless, needles and leaves of evergreen trees are not shed after the first growing season but may remain active in the canopy for up to 10 years (Bäck et al., 1994; Dengel et al., 2013). The dark-colored needle-leaf trees are well adapted to cold winters and short growing seasons. They have the capacity for hardening to survive the winters and dehardening in spring to photosynthesize and grow as soon as temperatures allow. Most commonly also, the ground level (understory) species are evergreen: dwarf shrubs, mosses, and lichens. The diversity of soil organisms in the boreal forest can be high.

Boreal forest carbon stocks account for ~272 ± 23 Pg C (Pan et al., 2011). For centuries, many boreal forests in North America and Scandinavia have been actively managed for timber and other wood products. Widespread uses of the forest have historically included slash-and-burn cultivation, tar production, forest pasturage, shipbuilding, and iron mining. The onset of the forest industry in the 19th century further accelerated the disappearance of primeval forest cover. Wood removals from boreal forests are currently ca 0.4 Mm^3 annually (compared to tropical forests ca 1.5 Mm^3 annually (Köhl et al., 2015). Forest harvesting in boreal forests is nowadays often done as even-aged forestry involving clear-cut logging, i.e., removing whole stands and replanting the forest as a single species stand. This has severe consequences on carbon storage and biodiversity, and the logging residues, rich in carbon and crucial for many species depending on decaying wood-like woodpeckers and many fungi invertebrates, are collected and removed (Köhl et al., 2015). Most of the remaining natural and old-growth forests of boreal Fennoscandia are located at northern, high-altitude, and low-productivity sites.

With the largest predicted warming in high latitudes, the impacts of climate change in boreal and arctic ecosystems are largely seen in expanding the forested area to higher elevations and further north with longer growing seasons and milder winter climate, arctic greening (IPCC SRCCL, 2019). The species composition and extent of forests are likely to change. Entire forest types may disappear, while new assemblages of species may be established, hence new ecosystems (Settele et al., 2014). Northern terrestrial ecosystems are likely to change from tundra to boreal forests, although vegetative changes are slow and lag climatic change. The greening coincides with the migration of novel, previously more southerly tree species (e.g., oaks, elms) to the southern boreal areas and increases in the productivity of species possessing plasticity against climate extremes (Morin et al., 2008, Lindner et al., 2010). On the other hand, the forecasted and already observed changes in temperature and precipitation can make boreal ecosystems more prone to, e.g., drought stress, insect outbreaks, and fire. Further, warmer summer temperatures increase evaporation, allowing the drought-adapted grasses to push northward, especially in the continent's interior, which may lead to a gradual loss of the boreal forest at the southern ecotone. These changes may give even more global warming due to complex effects on forest biophysical properties and biogeochemical cycles from widespread tree mortality, deforestation, and forest dieback (Seidl et al., 2017; Aubin et al., 2018).

2.4. OBSERVATION SITES USED FOR THIS REVIEW

Observations are invaluable and necessary to achieve a basic understanding of the role forest ecosystems have in the climate system. Sites such as Amazon Tall Tower Observation site (ATTO), Zotino Tall Tower Observatory (ZOTTO), and observation networks such as the Large Scale Biosphere-Atmosphere Experiment in Amazonia (LBA), Aerosols, Clouds, and Trace gases Research Infrastructure (ACTRIS), Integrated Carbon Observation System (ICOS), eLTER (European Long-Term Ecosystem and socio-ecological Research Infrastructure), SMEAR II (Station to Measure Ecosystem-Atmosphere Relations in Hyytiälä), and other existing observing systems can track ongoing changes in a way that enables attribution of causes, predictions of recovery trajectories versus further decline, or understanding of the consequences for the maintenance or loss of forest services. These observational sites also provide observations to study key processes in the forest-climate interaction, such as positive and negative feedbacks and how forests respond to changes in precipitation, radiation, and temperature changes. Unfortunately, few sites have extensive and comprehensive atmospheric and ecosystem measurements, both in tropical and boreal forests. In Africa, only short intensive sampling campaigns were done in tropical forests, and no long-term observations

are available in the region. Similarly, in Southeast Asia forests such as Borneo, where the 2008 Oxidant and Particle Photochemical Processes (OP3) experiment was done, only short time experiments were performed (Hewitt et al., 2010).

In this review, based on extensive literature published over the last two decades, measurements from a few key sites stand out due to their long-term comprehensive observations: ATTO, ZOTTO, SMEAR II at Hyytiälä in Finland, but considerable information is coming from observations networks such as LBA, ACTRIS, ICOS, OP3, and other experiments such as Dynamics–Aerosol–Chemistry–Cloud Interactions in West Africa (DACCIWA).

The Amazon Tall Tower Observatory (ATTO) has been set up in a pristine rain forest region in the central Amazon Basin, about 150 km northeast of the city of Manaus. Two 80 m towers have been operated at the site since 2012, and a 325m tower has been in operation since 2017 (Andreae et al., 2015). The ATTO site is located at 130 m above sea level, with coordinates S 02° 08.752′, W 59°, 00.335′. ATTO is a joint scientific collaboration between Germany and Brazil, run by the Max Planck Institute, INPA (The Brazilian National Institute for Amazonian research), UEA (The State University of Amazonas), and several Brazilian research institutions. The towers are fully instrumented to continuously measure the vertical profile of aerosol properties, trace gases, and meteorological parameters and are mostly free from local and regional anthropogenic pollution. ATTO is situated in an ecological reservation with a primary tropical rain forest. Detailed info can be obtained at *https://www.attoproject.org/*.

The Zotino Tall Tower Observatory (ZOTTO) is a joint Russian-German project, with measurements beginning in 2006 (Heimann et al., 2008, 2014). ZOTTO has been established in a cooperation project between the German Max Planck Society and the V. I. Sukachev Institute of Forest, Krasnojarsk. The 305 m high tower is located in central Siberia at 60°47′ N, 89°21′ E, 20 km west of the Yenisei River and about 10 km from the village Zottino. The location was chosen to be in the center of the Siberian taiga on the eastern side of the West Siberian plain. Trace gas and aerosol measurements are being done since 2006. Details of the project can be found at *www.zottoproject.org*.

SMEAR is a set of sites for long-term observation of land-atmosphere interactions and is part of the ACTRIS and ICOS European observation networks. SMEAR II is the most well-developed station and is located in Hyytiälä, Southern Finland (61°51′ N, 24°17′ E, 181 m above sea level). The terrain around the station is representative of managed boreal coniferous forest. The 55-year-old Scots pine (Pinus sylvestris L.) dominated stand is homogenous for about 200 m in all directions, extending to the north for about 1.2 km. The largest city near the station is Tampere, ca. 60 km S-SW of the measurement site. The terrain is subject to modest height variation. The SMEAR II station includes measurement buildings, a 128-meter-high mast, several walk-in towers reaching the canopy height, and two mini-watersheds. Detailed information can be found in *http://www.atm.helsinki.fi/SMEAR/index.php/smear-ii*, Vesala et al. (1998), and Kulmala et al. (2001). The Pallas Global Atmosphere Watch (GAW) station is located in northern Finland (67°58′ N, 24°07′E; 565 m a.s.l.) on a treeless hill. The tree line about 100 m representing the northwestern edge of the Eurasian boreal forest.

2.5. TROPICAL FOREST CLIMATE AND METEOROLOGY

The connection of global climate and Amazon regional climate is mostly based on teleconnections processes carried out by tropical and equatorial large-scale waves (Avissar and Werth, 2005; Raupp and Silva Dias, 2010). Earlier work by Silva Dias et al. (1983) pointed out the importance of convection over large tropical areas, such as the Amazon, in the wet season. These quasi-permanent deep convection areas, called tropical heat sources, generate gravity waves that impact the global climate. In particular, the well-defined diurnal cycle of convective activity in the Amazon is fundamental in determining the impact on the global climate (Raupp and Silva Dias, 2009). On the other hand, global phenomena such as the El Niño/La Niña oscillation (ENSO) in the Pacific strongly impact the local climate. Marengo et al. (2013, 2016) show that both the ENSO and the sea surface temperature of the Northern tropical Atlantic affect droughts and floods in the Amazon. Sena et al. (2018) have shown that the ENSO is associated with a delayed onset and early demise of the rainy season in the Amazon, leading to a reduction of the wet season length (Fu et al., 2013). The intertropical convergence zone (ITCZ), a planetary-scale band of heavy precipitation close to the equator, is one of the main systems producing rainfall over the tropics. ITCZ migrates to the South (North) during Austral Summer (Austral Winter). Therefore, the rainfall variability in the tropics is associated with the ITCZ interannual (Donohoe et al., 2014) and intraseasonal variability (Tomaziello et al., 2016). ITCZ is also modulated by climate change (Byrne et al., 2018).

The seasonal variation of rainfall over the Amazon is quite well defined (Rao and Hada, 1990; Horel et al., 1989). The dry season is roughly from May to September in the Southeastern half of the area, while there is almost no dry season in the Northwest Amazon. The day-to-day weather in the Amazon region is affected by large scale features such as tropical Atlantic easterly waves (Diedhiou et al., 2010), remains of extratropical cold fronts coming from the South (Rickenbach et al., 2002, Siqueira et al., 2004), upper-level vortices (Kousky and Gan, 1981) and the evolution of the Bolivian High. On the mesoscale, squall lines (Cohen et al., 1995, Silva Dias et al., 2002, Alcantara et al., 2011) and organized convection (Nunes et al., 2016, Romatschke and Houze, 2010) have been

studied and mapped. The diurnal cycle of convective activity is very well defined but variable throughout the regions (Machado et al., 2002, 2004, Tanaka et al., 2014, Saraiva et al., 2016), with nighttime convective storms close to the Andes mountains (Nunes et al., 2016). Local circulations driven by the Amazonas River considerably impact spatial rainfall (Fitzjarrald et al., 2008, Silva Dias et al., 2004, Dos Santos et al., 2014). The diurnal cycle close to the rivers has a specific cycle pattern. Sometimes it can be in phase with the diurnal heating but sometimes, out of phase generating a bimodal daily rainfall distribution (Burleyson et al., 2016). Amazonian atmospheric circulation influences the South American Andes, impacting aerosol and trace gas concentrations at the high mountains at Chacaltaya, with detailed back trajectory calculations showing atmospheric transport from Amazonia to the Andes (Bianchi et al., 2021, Aliaga et al., 2021).

Rainfall in Amazonia has very different characteristics in the dry and wet seasons. Convective clouds during the dry season have a smaller size, the ratio between cloud and rainfall area is higher, and the rain rate is more intense than the convective clouds observed during the wet season (Machado et al., 2018, Cecchini et al., 2014). The convection is mainly of mesoscale, and the tropical squall lines are key drivers of the mesoscale system in Amazonas. Convection moves westward with an average speed of 12.9 m/s (Anselmo et al., 2019), and most of the rainfall is associated with mesoscale cloud clusters. Giangrande et al. (2017), using two years of data from the radar wind profiler installed at the Observations and Modelling of the Green Ocean Amazon (GoAmazon2014/15) site (T3), described the main convective pattern of the Amazon clouds: a) updrafts and downdrafts increase in magnitude with height to the midlevel; b) downdrafts are the most frequent at low levels and decrease monotonically with height, and c) 33% of the convective area fraction is associated with cumulus congestus having echo top smaller than 8 km. Cold fronts can impact central Amazonian weather and micrometeorological variables that affect atmospheric chemistry (Camarinha-Neto et al., 2021). Enhanced convective storms over the southern half of the Amazon in Austral Spring have been associated with a complex interplay between atmospheric thermodynamic conditions and the effect of aerosol on cloud microphysics, as discussed by Andreae et al. (2004) and Albrecht et al. (2011).

Deforestation and connected biomass burning in the Amazon also have large-scale climatic impacts besides local and regional effects. In a review, Silva Dias et al. (2009) concluded that considerable new insights have come from the logical induction that land-use change affects rainfall. It alters the features of the Amazon tropical heat source, which interacts with planetary-scale waves providing the global teleconnections impacting remote regions of Eurasia and North America. The connection between land use and rainfall was supported by Machado et al. (2018), showing that boundary layer, aerosol number concentration, and cloud microphysics characteristics vary between forest and deforested regions. Freitas et al. (2005, 2017) showed that the aerosol plume is advected to the West over the Andes mountains reaching the tropical Pacific and/or to the South reaching subtropical South America and the adjacent Atlantic Ocean during the dry season (Bourgeois et al., 2015). The plume impacts the radiation budget at the surface with a reduction of surface temperature, reducing the water vapor flux, which may reduce convective rainfall (Sena et al., 2013, 2015). Camponogara et al. (2014, 2018) indicated that the cloud microphysics and dynamics in the subtropical mesoscale convective systems in Southern South America are altered by biomass burning aerosol injection advected from Amazonia. Cecchini et al. (2016) showed that clouds over the Manaus pollution plume have a higher number and smaller cloud droplets than clouds outside the plume. Depending on large-scale features, this may translate into a reduction or increase in rainfall.

For this review, we define for Amazonia the dry season from the end of May, going to the end of September, and the wet season from November to March. April and the first weeks of May is the transition from wet to dry season, while October- beginning of November is the transition of dry-to-wet season. There could be minor variations on a year-to-year basis and according to large-scale met situations such as El Nino and La Nina (Andreae et al., 2015).

2.6. BOREAL FOREST CLIMATE AND METEOROLOGY

The Boreal Forest also referred to as taiga, is one of the world's largest land biomes, covering more than $15{\cdot}10^6$ km^2 in North America and Eurasia in a latitude band between approximately 45° and 70°N (Larsen, 1980, Bonan and Shugart, 1989, Williams et al., 2011). The extensive geographical coverage of the boreal forest gives rise to a large variation in meteorological conditions across the region. The marine influence varies greatly, from negligible in continental Asia and North America to significant in the coastal regions of the continents, including Scandinavia. The account given in the following is hence general, and variations apply not least meridionally as a function of distance from the ocean.

As a whole, the boreal forest regions have a subarctic climate, belonging to the Dfc, Dwc, Dsc, Dfd, Dwd, and Dsd zones according to the Köppen classification, i.e., continental subarctic or boreal climates (D) with varying winter severity (Köppen, 1884, Beck et al., 2018). This indicates a cold climate with large seasonal temperature variability. These climate types are almost exclusively found in the Northern Hemisphere due to the near

absence of continents at the corresponding Southern Hemisphere latitudes.

Over central Eurasia, the wintertime circulation is dominated by the semi-permanent anti cyclone referred to as the Siberian high, which is replaced by a low-pressure center in summer. The corresponding North American high is less pronounced and less persistent, but the variation in insolation over the year gives a large seasonal variation in temperature across the vast terrestrial regions of boreal forests. The cold winters are more pronounced in, e.g., Eastern Siberia and inner Alaska, where permafrost is continuous, whereas the more temperate regions further south or with more oceanic influence may have discontinuous permafrost (Zhang et al., 1999). Due to the high latitude, winter months are dark with polar night north of the Arctic circle, whereas in summer, days are long, and the midnight sun appears north of the Arctic circle.

Snow cover, freezing, and thawing of the ground affect the seasonal temperature variation of the surface. In winter, snow insulates the surface, moderating the surface temperature loss. During the fall, freezing of the ground releases energy required for thawing in the spring, which causes a lag in the system (Betts et al., 2001). During spring, there is no surface evaporation before the snow melts and the ground thaws, which typically gives low relative humidity and large sensible heat flux, resulting in a deep boundary layer. In the fall, the relative humidity is typically high, and the boundary layer is shallower (Betts et al., 2001).

Albedo over the boreal forests varies between vegetation types (grass, leaf trees, conifers) and shows a large seasonal variation. Due to snow cover in winter, the surface albedo can be nearly four times larger in winter than in summer (Betts and Ball, 1997). However, the most extensive seasonal changes in albedo are measured for the grass-covered surface. Although albedo is greater in winter than in summer for all vegetation types, in conifer-covered regions, the winter albedo is only moderately higher than the summer albedo (Betts and Ball, 1997). Similarly, the presence of trees moderates the surface albedo feedback to global warming, i.e., the reinforcement of warming through melting of ice and snow (Bonan et al., 1992, and references therein).

Precipitation is typically low (ranging between 200 and 1000 mm annually according to data from the Global Precipitation Climatology Project, GPCP) and falls mainly as rain during summer. Fog is common, and snow typically remains on the ground during winter. Precipitation generally exceeds evaporation in the regions of boreal forests.

Large parts of the boreal forest areas are dominated by westerly winds, with baroclinic disturbances on the polar front resulting in cyclones traveling in a general west-to-east direction following the large-scale Rossby wave pattern. The mid-latitude storm tracks, described in detail by, e.g., Chang et al., 2002, are most pronounced over the oceans where they transport heat and moisture northward, from the subtropical regions towards the polar regions, hence reducing the meridional temperature gradient. The cyclone activity gives rise to varying weather and a temperate climate, with precipitation largely associated with the frontal passages. Storm track activity has also been found to moderate continental temperatures in the mid-latitudes, with summer heat extremes and winter cold spells associated with low storm track activity (Lehmann and Coumou, 2015).

The storm track positions vary during the year, with the westerly wind maximum on average centered closer to the equator in winter and further poleward in summer. The seasonal migration of the fronts separating air masses contributes to seasonal variation in the boreal forest regions. In the summer, sub-tropical air masses can extend to higher latitudes and the polar front separating polar, and sub-tropical air masses affect the boreal forest regions, while this warmer air mass retreats equatorward during winter, and the boreal forest areas are rather affected by the Arctic front. Outbreaks of cold arctic air can then affect the boreal forest areas, and such events have also been associated with enhanced aerosol formation (e.g., Nilsson et al., 2001).

The large-scale circulation in the North Atlantic, and thereby the location of the maximum in westerlies, or storm track position over the Eurasian boreal forest region, is related to the North Atlantic Oscillation (NAO) (Hurrell,1995, Scaife et al., 2008). The NAO describes a mode of variability in pressure, which is measured as the normalized pressure difference between the Azores and Iceland. A large pressure difference results in a positive NAO index, which is associated with stronger westerlies in a more northerly track, transporting warm and moist air towards Europe and Asia. The positive NAO phase corresponds to warmer temperatures, more precipitation in the northern European part of the boreal forest region, and cooler temperatures over their eastern North American parts. A weaker pressure difference contrarily results in a negative NAO index with weaker and less well-organized storm tracks.

Boreal forests may be expected to be affected by climate change both because of their sensitivity to warming and because of Arctic amplification leading to large warming in the regions they cover (e.g., Chapman and Walsh, 1993, Bekryaev et al., 2010, Manabe and Wetherald, 1975, Holland and Bitz, 2003). For instance, with increasing temperatures, the permafrost distribution changes, and its total coverage is observed to be reducing (e.g., Romanovsky, 2010). The atmospheric circulation influencing the boreal forest regions is also sensitive to temperature changes. Climate models, as well as observations, have suggested that the position of the mid-latitude storm tracks and their associated clouds have shifted and will continue to shift poleward

as the climate warms (Yin, 2005, Bender et al., 2012), with implications for not only temperature but also the precipitation in the affected areas.

The seasons in the boreal forest zone in this review are usually defined according to the meteorological definitions of spring, summer, fall, and winter. However, the length of the different periods varies strongly from the southern to the northern boarder.

Although the topical and boreal forest regions feature several different cloud types, both convective and stratiform, the main difference is the dominance of deep convective cloudiness in the tropics and cloud systems and precipitation related to frontal passages in the tropics the boreal forest areas. Ice phase clouds are also present at lower altitudes in the boreal regions than in the tropics.

3. OBSERVATIONS OVER BOREAL AND TROPICAL FOREST ECOSYSTEMS

3.1. CHEMICAL COMPOSITION AND TYPES OF AEROSOLS IN BOREAL AND TROPICAL FORESTS

The chemical composition of aerosols is important because it reflects the sources, emissions, and atmospheric processes. The chemical composition affects aerosols' role in climate and their capacity to act as CCN via aerosol-cloud interactions (Boucher et al., 2013). Particularly their capacity to act as CCN depends on their size (Dusek et al., 2003), their chemical composition (Lambe et al., 2011, Schmale et al., 2018), and their hygroscopicity (Swietlicki et al., 2008), which are interdependent (e.g., Hong et al., 2015). Specifically, in biogenically dominated environments, the organic aerosol composition is an important factor determining their climatic impacts (Jimenez et al., 2009). Furthermore, the presence of certain key trace elements such as P, K, and S, even at very low concentrations, can enhance the CCN activity of primary and secondary organic aerosol (Pöhlker et al., 2012).

Aerosol chemical composition varies with particle size and season for both tropical and boreal forests. In general, the composition can be discussed in terms of the organic and inorganic components. In Amazonia, the two main aerosol sources are natural biogenic aerosol, which dominates in the wet season (December to July), and the biomass burning component in the dry season (August-November). Other aerosol sources are Sahara dust events that occur from February to May, when the ITCZ allows transport from Sahara to Amazonia (Ben-Ami et al., 2010, Moran-Zuloaga et al., 2018), sporadic urban air pollution from a few locations such as Manaus, Belem, Santarem, that have local or regional effects (Martin et al., 2010, Mouchel-Vallon et al., 2020). Recently, long-range transport of biomass burning and volcanic emissions from Africa to Central Amazonia has been documented (Saturno et al., 2018b, Holanda et al., 2020). In the boreal environment, the aerosol chemical composition is also dominated by biogenic organic compounds (e.g., Allan et al., 2006; Cavalli et al., 2006; Corrigan et al., 2013; Finessi et al., 2012; Kourtchev et al., 2013) with variable volatilities (e.g., Hong et al., 2017). Also, the contribution of biomass burning related aerosol particles, anthropogenic organic aerosols, and inorganic compounds are observed (e.g., Crippa et al., 2014; Äijälä et al., 2019; Heikkinen et al., 2020), which can become dominant during the winter season, when biogenic emissions are at a minimum (Äijälä et al., 2017). The anthropogenic influences can be highly localized or linked to long-range transport (e.g., Yttri et al., 2011, Liao et al., 2014, Corrigan et al., 2013, Äijälä et al., 2017, Boy et al., 2019).

The pristine aerosol life cycle is potentially prone to fundamental disruption. It would only require relatively minor emissions of anthropogenic SO_2 to provide enough H_2SO_4 vapor in the tropical PBL to enable homogeneous nucleation of aerosol particles and subsequent new particle formation and growth by uptake of organic vapors. Such new particle formation and increased SOA production have been observed in the urban plume from the city of Manaus (Wimmer et al., 2018; Shrivastava et al., 2019). As a result, CCN concentrations could increase significantly in the wet season, when the Amazonian atmosphere is most sensitive to perturbations, with important consequences for cloud and precipitation properties.

3.1.1. Mass balance of PM based on the main chemical species

The aerosol particles over the Amazon Basin are dominated by the carbonaceous fraction in the fine mode, accounting for 70–90% of PM_1 mass (Shilling et al., 2018; de Sá et al., 2017, 2019; Chen et al., 2009; Fuzzi et al., 2007). In the coarse mode, 60–85% of particle mass consists of carbonaceous aerosol (Gilardoni et al., 2011; Graham et al., 2003b; Formenti et al., 2001). As this component comprises mostly primary biogenic aerosol particles, it is frequently observed the presence of trace elements associated with vegetation such as K, P, S, and others (Arana et al., 2014). Small amounts of soil dust and some marine aerosol can also be observed in the coarse mode aerosol (Artaxo et al., 1988, 1990). Among the carbonaceous components, the organic fraction is the most abundant throughout both seasons and also the most studied due to the great complexity and variety of compounds it comprises (Tong et al., 2019, Mouchel-Vallon et al., 2020).

Large seasonal variations in the air concentrations of the main chemical components are found in the Amazon basin but not in their mass balance. For instance, although the submicron organic aerosol loading can vary widely between seasons (0.6 to 45 μg m^{-3}), the organic

fraction remains rather constant (70–90%) (Chen et al., 2009; Decesari et al., 2006). ***Figure 3.1.1*** shows the time series of PM_1 monthly average aerosol composition at the ATTO tower from January 2014 to October 2017. There is a strong dominance of organic aerosol and a clear seasonal behavior, with very low concentrations in the wet season (about 0.6–1.5 μg m^{-3}) and much higher concentrations in the dry season (about 5–12 μg m^{-3}) due to biomass burning emissions. Black carbon also has an important seasonal variability, with higher concentrations in the dry season.

The average PM_1 aerosol composition can be observed in ***Figure 3.1.2*** for the wet and dry seasons from 2014 to 2016. The total PM_1 aerosol loading varies from an average of 1.4 μg m^{-3} to 5.3 μg m^{-3}. Sulfate concentrations appear in low concentrations, as well as nitrate and NH_4. Note that the presented composition also includes long-range transport events from Africa for the wet season, which bring biomass burning and Sahara dust in episodic but in significant amounts. This can be observed from the equivalent black carbon (eBC) values that are quite high for an

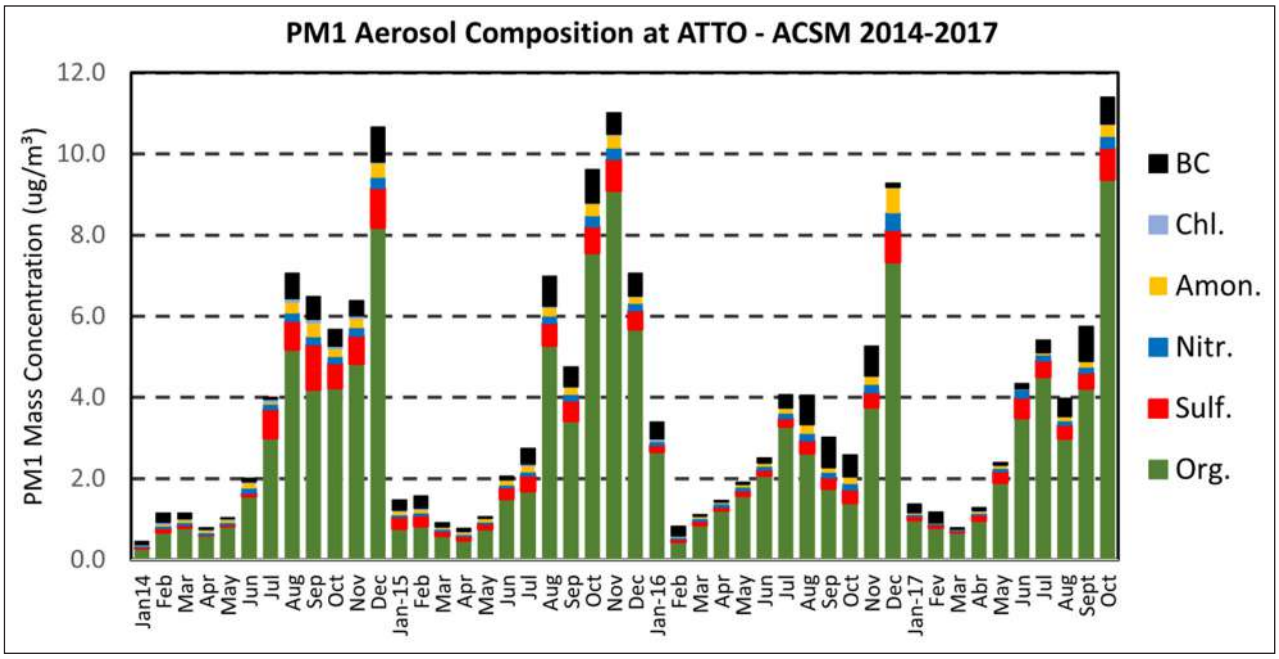

Figure 3.1.1 Time series of PM_1 monthly averaged aerosol composition in Central Amazonia (ATTO tower), from January 2014 to October 2017. Measurements were performed with an Aerodyne Aerosol Chemical Speciation Monitor (ACSM).

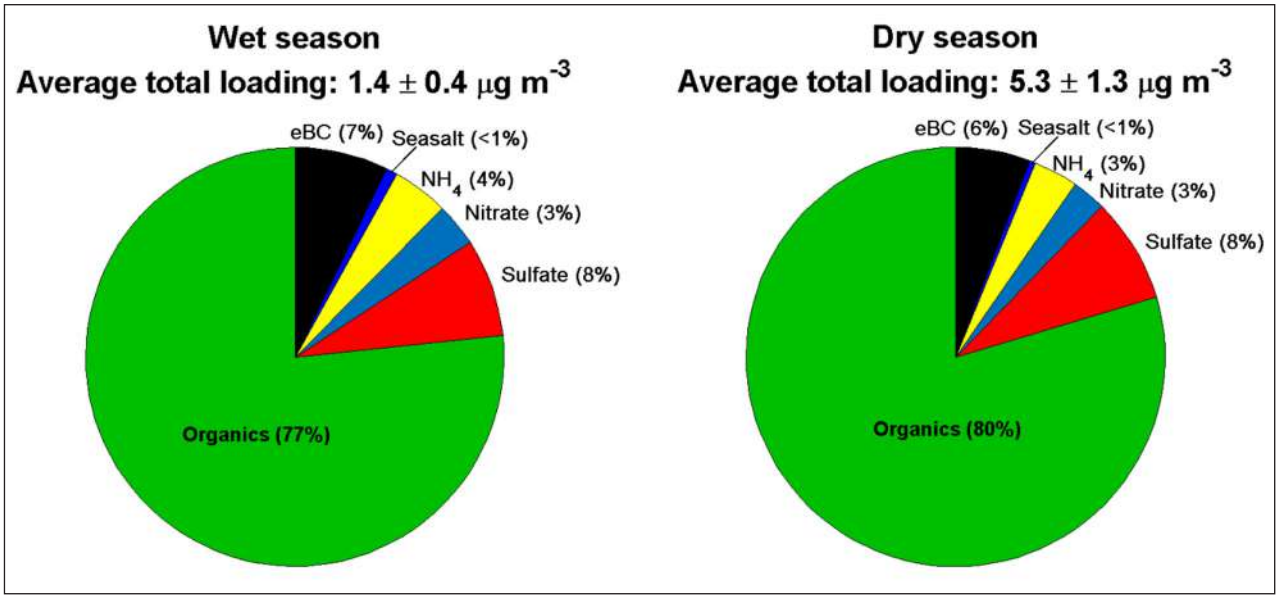

Figure 3.1.2 Average composition of PM_1 aerosol in the wet (left) and dry (right) seasons of central Amazonia at the ATTO tower (the same color coding as in figure 3.1.1). Measurements of PM_1 composition with an ACSM at the ATTO tower from January 2014 to December 2016. Measurements of eBC were obtained with a MAAP instrument.

aerosol that consists only of natural primary and secondary biogenic aerosol.

To remove the effects of long-range transport in the wet season, it is possible to carefully identify episodes of Sahara dust and biomass burning from Africa and remove these episodes from the data. This procedure is reported in Pöhlker et al. (2018), which shows lower concentrations than reported in ***Figure 3.1.2***. The average composition for an expanded data set from 2014 to 2016 at ATTO shows the following concentrations: Organics 0.848 ± 0.639 μ gm^{-3}, sulfate 0.058 ± 0.064 μ gm^{-3}; nitrate 0.042 ± 0.041 μ gm^{-3}; Ammonium 0.067 ± 0.025 μ gm^{-3}; eBC 0.035 ± 0.042 μ gm^{-3}. These concentrations are similar to the ones reported by Pöhlker et al. (2018) and are really low concentrations for a continental background site. Note the low eBC concentrations of 35 n gm^{-3}. ***Figure 3.1.3*** shows the Amazonian wet season PM1 aerosol composition under background conditions, with episodic long-range transport removed from the time series.

For the dry season in Amazonia, in terms of water-solubility character, measurements of water-soluble organic carbon (WSOC) in the Amazon forest show that on average, the WSOC represents 64% of the total carbon (TC) in the fine mode and 34% in the coarse mode (Decesari et al., 2006). In addition, larger content of WSOC is found during the daytime samples compared to the nighttime, which might be related to different combustion stages (smoldering vs. flaming fires in the dry season) or photochemical production of secondary organic aerosol (SOA) with different solubilities. Such processes affect the soluble/insoluble character of the fine aerosol particles (Decesari et al., 2006).

The comprehensive and long-term observations in Hyytiälä at SMEAR II (Hari and Kulmala, 2005) shows that the aerosol chemical composition measured at the boreal forest site in Hyytiälä, Southern Finland, is dominated by organic species all over the seasons, as shown in ***Figure 3.1.4***. (Allan et al., 2006; Äijälä et al., 2019; Heikkinen et al., 2020). The mean organic aerosol mass concentration is the highest in summer (July, August) and late winter (February) (Heikkinen et al., 2020). The winter peak is associated with anthropogenic inorganic components, while the summer maximum is driven by forest BVOC emissions. Its concentration depends on meteorological parameters such as ambient temperature, radiation, wind direction, and speed, with summer heatwaves causing strong positive anomalies (Heikkinen et al., 2020). ***Figure 3.1.4*** also shows seasonal variability of inorganic species and eBC, as well as the temperature dependence of important atmospheric components such as monoterpenes, CO, eBC, and organic aerosols.

In the boreal environment, on average, 20% of the aerosol is assumed to be non-volatile, and only half of the non-volatile mass could be explained by black carbon or crustal material, and a further investigation reveals the presence of non-volatile organics in the condensed phase (Häkkinen et al., 2012; Hong et al., 2014). The formation of this low-volatile organic aerosol can be explained by the condensation of highly oxygenated molecules (HOM) arising from the monoterpene oxidation in the gas phase (e.g., Yan et al., 2016; Mohr et al., 2017; Roldin et al., 2019,

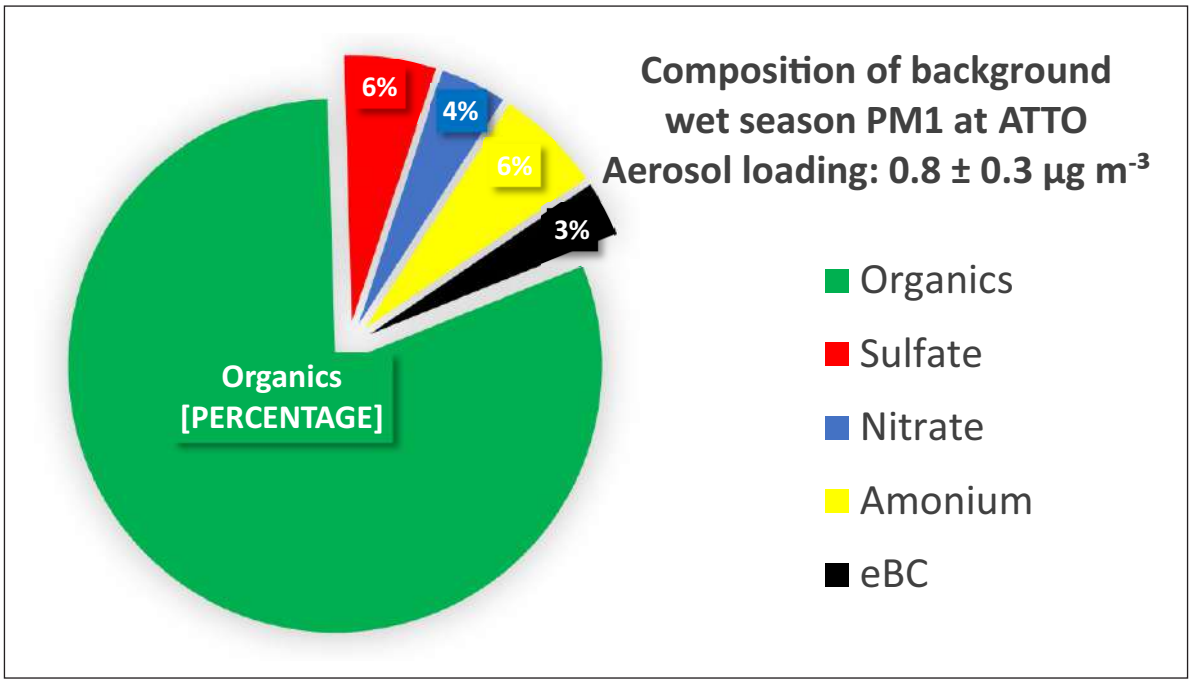

Figure 3.1.3 PM_1 composition for Amazonian wet season aerosol under background conditions, with episodic long-range transport removed from the time series. Measurements with an Aerodyne ACSM at the ATTO tower from January 2014 to December 2016. Measurements of eBC were obtained with a MAAP instrument.

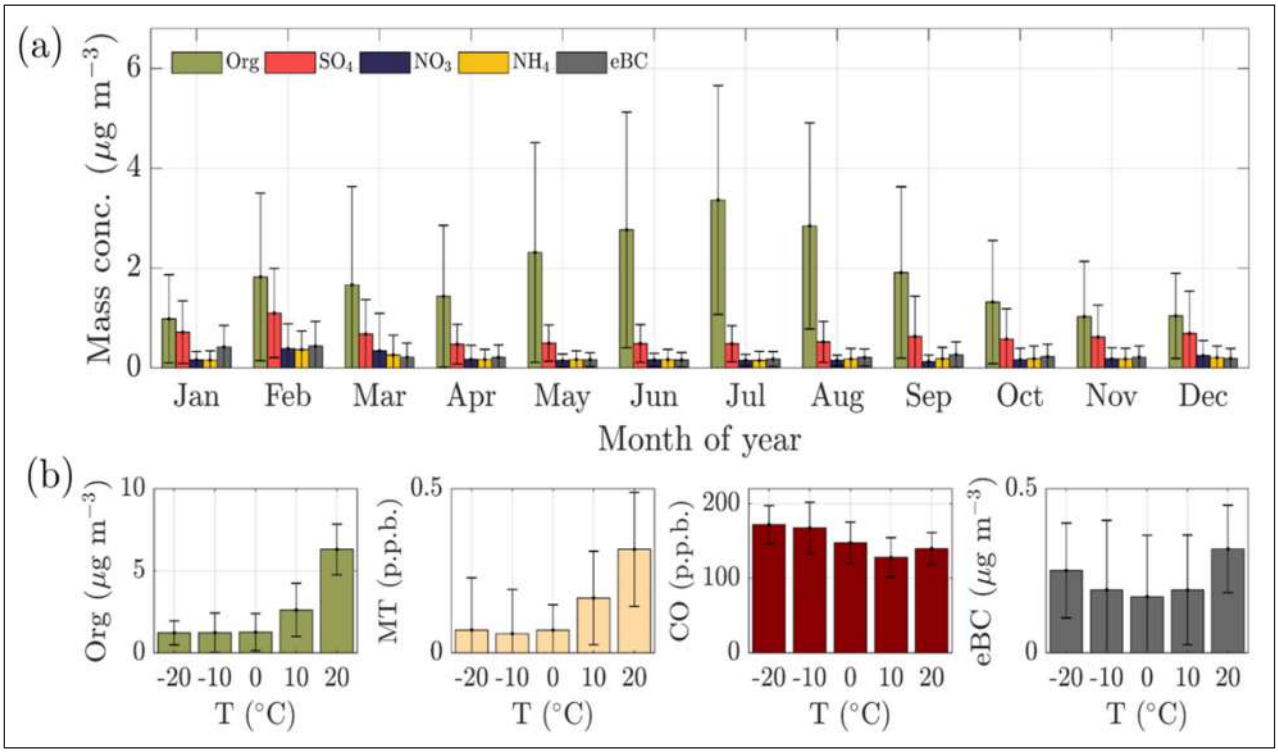

Figure 3.1.4 (a) PM_1 Monthly mean (± sdev) mass concentrations of organics (Org), sulfate (SO_4), nitrate (NO_3), ammonium (NH_4), and equivalent black carbon (eBC) recoded within the boreal forest canopy with an aerosol chemical speciation monitor (ACSM) and an aethalometer. **(b)** the mean (± sdev) concentrations of Org, monoterpenes (MT), carbon monoxide (CO), and eBC were recorded under different ambient temperatures (5°C bins). The measurement period at SMEAR II was 2012–2018. The data presented here are adapted from Heikkinen et al., 2019.

Tong et al., 2019), as well as their further oligomerization reactions within the particle phase (Riva et al., 2019) (see Section 3.1.5). A modeling study by Roldin et al. (2019) assigns 18% of OA to HOM-SOA. The other major component of the organic aerosol (OA) in the boreal forest is a semi-volatile oxygenated organic aerosol (SV-OOA) that is presumably the fresh SOA derived from terpene oxidation (e.g., Ebben et al., 2011b, Finessi et al., 2012; Crippa et al., 2014; Hong et al., 2017). The wide spectrum of observed aerosol volatilities can also be described by the carbon oxidation states that range between –1 and 1 (Kourtchev et al., 2013) and carbon-to-oxygen ratios (O:C) between 0.2 and 0.7 (Äijälä et al., 2017).

To contrast the observations in the boreal setting in Finland, we summarize results from Siberia, specifically from the ZOTTO tower (Heintzenberg et al., 2008) in ***Figure 3.1.5***. The data shows that biomass burning is the main source of carbonaceous aerosols in the summertime in Siberia, and also, the biogenic SOA is at the highest. ***Figure 3.1.5*** shows a time series 2010 to 2014 of PM_{10}, total carbonaceous material (TCM) (calculated as TCM = 1.8 × OC + EC) at the ZOTTO tower. The highest concentrations are observed in the spring and summer periods, with high temperatures and lower precipitation. The median PM_{10} (25^{th} and 75^{th} percentiles) is 7.9 (5.1–14.4) μg m^{-3} (Mikhailov et al., 2017). Based on the average composition for summer and wintertime at ZOTTO, there is an increase in the presence of elemental carbon and sulfate in the cold season, with non-sea-salt sulfate reaching a high value of 27% of $PM_{2.5}$ (Mikhailov et al., 2017). Organic aerosol has a dominant contribution in the summer with similar values as Amazonia (68% of $PM_{2.5}$). Even in the summer, sulfate is a high 19% of $PM_{2.5}$, and this is quite different from Amazonia, where sulfate contribution is typically much lower.

The average $PM_{2.5}$ aerosol composition at the ZOTTO tower from April 2010 to April 2014 is shown in ***Figure 3.1.6***. Similar to Amazonian aerosols, both sites have a large dominance of organics, but in Siberia, a much higher contribution from sulfate and NH_4 is present. Therefore, despite the Siberian site's remoteness and the very small concentrations observed in wintertime, this environment is affected by (diluted) anthropogenic emission products, and to a greater extent in winter than in summer, relatively to the biogenic sources. Finally, also higher crustal material and sea salt can be observed at ZOTTO compared to ATTO.

3.1.1.1. Black and brown carbon

In the Amazon, a component of carbonaceous aerosols consists of elemental carbon (EC, carbon component when thermo-optical measurements are used) or eBC when light absorption measurement techniques are involved (Martins et al., 1998, 2009, Schmid et al., 2006). The EC contribution is, on average, 5 to 20% of the total carbon (TC) in the wet and dry periods, respectively (Decesari et al., 2006). In terms of the aerosol modes, EC represents about 5% of the fine mode aerosol

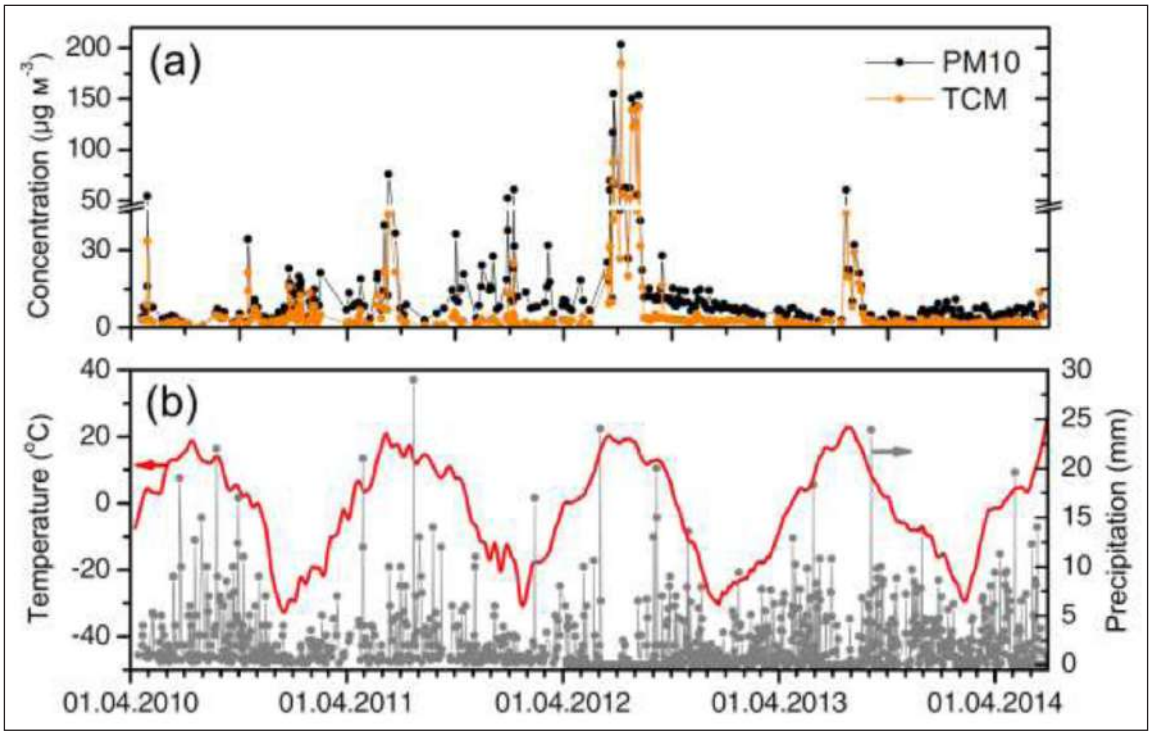

Figure 3.1.5 Seasonal and interannual variations in the PM_{10} aerosol mass and total carbonaceous material (TCM) concentrations at the ZOTTO tower from April 2010 to April 2014 **(a)** and of daily averaged meteorological parameters **(b)**: temperature – red line; precipitation – grey line and symbols.

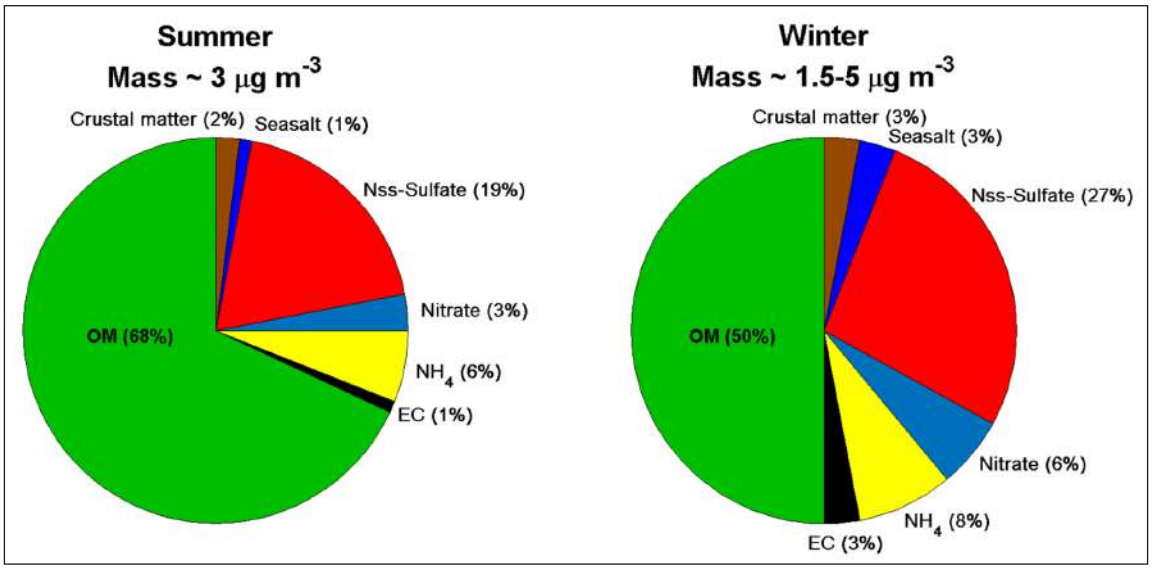

Figure 3.1.6 Average $PM_{2.5}$ aerosol composition at the ZOTTO tower for summer and wintertime. Details on the data can be found in Mikhailov et al., 2017.

loading. During the dry season, eBC concentrations are larger than the EC, and this is partially attributable to the presence of brown carbon (BrC) (Rizzo et al., 2010; Gilardoni et al., 2011). BrC aerosol consists of light-absorbing organic particulate matter with larger wavelength-dependent absorption as measured using the absorption Ångström exponent (AAE) (Andreae and Gelencsér 2006). The BrC fraction in Amazonia has been studied using in situ measurements (Saturno et al., 2018a) as well as remote sensing techniques (Wang et al., 2016). The in-situ measurements show that the BrC contribution was measured at 17%–29% (25th and 75th percentiles) of the total absorption coefficient at 370 nm. The BrC contribution increased to 27%–47% during fire events under El Niño related drought conditions from September to November 2015. The seasonality of the BrC fraction of the total absorption is on average 27% during the wet season and 22% during the dry season (Saturno et al., 2018a). Using a long-term sun photometer from the NASA Aerosol Robotic Network (AERONET) network and Aethalometer measurements, Wang et al., 2016 show that BrC represents a significant 10–18% of eBC

absorption at 370 nm, underlining the importance of BrC absorption at the wet and dry seasons in Amazonia.

The annual average concentration of BC at the SMEAR II boreal site at Hyytiälä is 320 ng m^{-3} (Hyvärinen et al., 2011) that represents 5–10% of the fine particulate matter concentration (Saarikoski et al., 2005; Hyvärinen et al., 2011). It is mainly transported from Central and Eastern Europe, and typically the highest loadings are associated with southerly winds (Hyvärinen et al., 2011). The observed BC is mainly attributed to long-range transported fossil fuel combustion, and only a minor fraction originates from biomass burning (Hyvärinen et al., 2011; Yttri et al., 2011). However, during specific episodes, biomass burning contributes significantly to the organic aerosol concentrations. For example, up to 25% of organic matter is associated with transported biomass burning emissions with organic carbonyl functional groups (41%) and alcohol groups (25%) in summer 2010 (Corrigan et al., 2013). Furthermore, during these biomass burning periods, BrC (Chakrabarty et al., 2016) can be dispersed into the boreal environment (Di Lorenzo et al., 2018). Normally, the highest eBC concentration is recorded during winter, but during heat waves, its concentration can increase due to wildfires (***Figure 3.1.4b***; Heikkinen et al., 2020).

3.1.1.2. Composition of the aerosol inorganic fraction

Sulfate is the dominant inorganic compound in the fine mode Amazonian aerosol in both seasons ranging from 4 to 26% of PM_1 (Chen et al., 2015; Gilardoni et al., 2011; Chen et al., 2009; Fuzzi et al., 2007, Maenhaut et al., 1999, Yamasoe et al., 2000). Measurements during the wet season indicate that sulfate is not fully neutralized, and, for this reason, the presence of ammonium bisulfate is suggested (Chen et al., 2015; Graham et al., 2003b). Most of the sulfate measured in the central Amazonian Basin is attributed to out-of-basin sources of marine-derived sulfate from the Atlantic Ocean and combustion-derived sulfate from Africa. Only a small fraction was attributed to in-basin biogenic sources, such as the oxidation of sulfur-containing gases (DMS and H_2S) emitted from the rainforest ecosystem (Andreae et al., 1990). In the coarse mode, it is shown that sulfate is relatively insignificant in terms of mass concentration, accounting for a low 1% on average (Gilardoni et al., 2011).

However, Saturno et al., 2018b analyzed the long-range transport of sulfur-rich particles from volcanic emissions, specifically aerosol particles from Nyamuragira volcano in Congo to Central Amazonia. They found that hourly mean sulfate mass concentrations in the submicron size range reached a very high value of 3.6 µg m^{-3} at the ATTO observatory under the volcanic influence, which is the highest value ever reported in the Amazon region. The long-range transported (LRT) air masses take, on average, 6–7 days to reach the central Amazonian Basin. Overall, this illustrates that African dust emissions, biomass burning, and volcanos influence the aerosol composition in Central Amazonia in an episodic manner.

Other inorganic ions, such as nitrate, ammonium, and chloride, account for less than 10% in the fine aerosol mass when added up and less than 5% in the coarse mode (Gilardoni et al., 2011; Chen et al., 2009; Fuzzi et al., 2007). The diel trends of sulfate, nitrate, ammonium, and chloride resemble similar behavior to the organics, with a minimum mass concentration in the morning (daybreak) and maximum in the afternoon, indicating aerosol mass production from the morning to the afternoon (Chen et al., 2015).

The inorganic fraction of aerosol particles at the boreal site mainly consists of ammonium sulfate (Makkonen et al., 2014; Äijälä et al., 2019; Heikkinen et al., 2020). Other minor inorganic components are water-soluble ions, such as chlorine, sodium, magnesium, and calcium, likely originating from marine sources and nitrates (Makkonen et al., 2014; Heikkinen et al., 2020). The interpretation of both particle and gas-phase data of low-volatile vapors hints towards a large fraction of the observed nitrates being organic (Makkonen et al., 2014; Yan et al., 2016; Kortelainen et al., 2017; Äijälä et al., 2019; Heikkinen et al., 2020). The inorganic fraction is typically the highest in winter and the lowest in summer (***Figure 3.1.3a***; Heikkinen et al., 2020). Interactions between the inorganic and organic fractions are shown with a combination of laboratory and atmospheric observations in the boreal environment (Riva et al., 2019), but further studies are required to address the consequences of these interactions.

3.1.2. Elemental composition of primary aerosol particles

The African mineral dust and smoke, marine, biomass burning, and biological particles are among the main identified types of primary aerosol particles in the Amazon (Arana et al., 2014; Martin et al., 2010; Graham et al., 2003b). The intrusion of air masses from Africa is more frequent during the wet season when the ITCZ is shifted to the south of the basin allowing for air masses from the North Hemisphere to reach the central Amazonian basin episodically (Moran-Zuloaga et al., 2018; Pöhlker et al., 2018). These air masses are rich in soil dust particles from the Sahara Desert (with Ca, Al, Si, Ti, Mn, Fe, and others) and smoke from the African savanna fires and occasional volcanic aerosol (Saturno et al., 2018b). As those air masses cross the Atlantic Ocean, also marine aerosol particles will reach the central Basin and contribute to the fine and coarse aerosol modes, characterized by the elements Na, Mg, Cl, and others (Andreae et al., 2015; Ben-Ami et al., 2010; Ansmann et al., 2009; Formenti et al., 2001; Artaxo and Hansson 1995). The incoming particles impact the coarse mode more clearly, with a sharp increase in coarse mass concentration up to 100 µg m^{-3} (Moran-Zuloaga et al., 2018; Pöhlker et al., 2019).

African smoke transport is also observed during the dry season when the ITCZ is shifted to the north. However, during these episodes, mass concentration changes were more evident in the fine than in the coarse aerosol mode (Moran-Zuloaga et al., 2018). Source apportionment results using trace elements, BC, and sulfate indicated the LRT aerosol (dust and marine) represents 18% of the coarse aerosol mode (Arana et al., 2014; Artaxo 2002).

3.1.3. Composition and properties of organic aerosol (OA)

Particulate organic matter includes primary organic aerosols (POA) and SOA, both contributed by biogenic and anthropogenic sources. Biogenic POA occurring in forest environments encompass pollen, spores, plant debris, and bacteria (see Sections 3.1.8 and 3.1.9). Forest fires represent intermittent, strong additional sources of POA that naturally take place in remote boreal forest areas (see Section 3.4.5). The secondary organic aerosol (SOA) refers to the gas-to-particle conversion of precursor vapors (Kulmala et al., 2014b). The vapors can either form new aerosol particles or condense onto existing aerosol particles. The former contributes significantly to the aerosol number budget (e.g., Merikanto et al., 2009, Kulmala et al., 2013a), and the latter contributes to the aerosol mass concentrations (Shrivastava et al., 2017). Here we concentrate on the SOA formation in terms of aerosol mass. The mechanisms in the production of SOA in the forests involve complex chemical reactions with BVOC, nitrogen oxides (NO_x), ozone (O_3), hydroxyl radical (OH•) and sulfur species (DMS, H_2S, and SO_2), gas-to-particle conversion followed by the processes of condensation of the low-vapor pressure gases and photooxidation (Martin et al., 2010). There are different pathways of SOA production depending on the BVOC that originates the process, such as isoprene, terpenes, or others (Yáñez-Serrano et al., 2020, Yee et al., 2020, Kesselmeier et al., 2000, Shrivastava et al., 2019). The major gas-phase BVOC is isoprene in Amazonia and monoterpenes in the boreal environment (see section 4.1.1).

In the last twenty years, detailed measurements of the POA and SOA in forest environments have been performed using off-line and online techniques and were able to provide a comprehensive understanding of its loading, chemical composition, and atmospheric processing (Soto-Garcia et al., 2011, Ebben et al., 2011a, 2012). Organic speciation by means of chromatographic-mass spectrometric techniques (GC/MS or LC/MS) led to the identification of the mean sources of POA and SOA in the two environments. In the Amazon, during the dry period, the fine aerosol mode is dominated by biomass burning tracers (anhydrosugars and phenolic compounds) and by dicarboxylic acids C3–C6 (DCA C3–C6) and oxalic acids, which are produced by extensive photochemical aging of the aerosol. In contrast, during the so-called wet period with intense precipitation, the aerosol is dominated by DCA C3–C6, followed by anhydrosugars, oxalic acid, and methyl-tetrols (2-methyl-tetrol and 2-methyl-erythritol). The 2-methyl-tetrols are of particular interest once they can be taken as markers of photooxidation of isoprene in low-NOx environments (Claeys et al., 2004, Allan et al., 2014, Schulz et al., 2018). In the coarse size fraction, both day and night time samples are dominated by sugars/sugar alcohol (62% and 78%, respectively), followed by short-chain carboxylic acids including hydroxyl-acids (30% and 4%) and fatty acids (7% and 18%) of biogenic origin (both primary and secondary) (Graham et al., 2003a). Examples of the identified sugars associated with biological material (spores, plant fragments) are trehalose, sucrose, glucose, and fructose, and sugar alcohols are glycerol, erythritol, arabitol, mannitol, and inositol. The composition also suggests that the short-chain carboxylic acids found in the daytime fine mode are largely associated with the biogenic SOA formation. Finally, fatty acids and alcohols, such as octacosanol, are typical organic tracers for plant waxes.

The detailed molecular speciation of OA in the boreal forest shows several analogies with those characteristics of the Amazon rainforest. Fatty acids and alcohols from plant waxes and anhydrosugars from wood burning are among the most common constituents of $PM_{2.5}$ (Alves et al., 2012). Methyl-tetrols and C5-alkenetriols are found in concentrations at ng m^{-3} levels in the middle of the summer when isoprene emissions are maximum (Kourtchev et al., 2005). The contribution of monoterpene oxidation products to SOA is much larger than the sesquiterpene, where the pinene skeleton (α– and β–pinene) is the most abundant monoterpene (Andreae et al., 2015). In addition, the monoterpene oxidation product concentrations in the central Amazonian Basin are in close agreement with the concentrations measured during summertime in the Boreal forest (Vestenius et al., 2014). However, monoterpene SOA tracers dominate over isoprene oxidation products in the boreal forest, especially in spring and fall.

To complement the organic speciation by GC/MS and LC/MS techniques, functional group analysis by NMR and FTIR spectroscopy has been used for organic source attribution (Graham et al., 2003a; Cavalli et al., 2006; Finessi et al., 2012; Corrigan et al., 2013). This approach led to the identification of SOA enriched with aliphatic amines, terpene SOA, and various classes of anthropogenic aerosols from biomass burning and fossil fuel combustion in the boreal forest. Source apportionment based on factor analysis and spectral fingerprints became more powerful and extensively used with the introduction of online aerosol mass spectrometry (AMS). The comprehensive AMS database acquired at the SMEAR-II station (Allan et al., 2006; Corrigan et al., 2013; Crippa et al., 2014; Äijälä et al., 2017; Äijälä et al., 2019) shows that the contribution of anthropogenic POA

to the total OA is usually low, below 16% (Crippa et al., 2014; Äijälä et al., 2019). This contrasts to the tropical forests, even if in wintertime, where the contribution from wood burning (BBOA) can be more significant. Most of the OA at the boreal forest site can be apportioned into two classes of oxidized organic aerosol (OOA), one with a lower oxygen content and semivolatile character (SV-OOA), and a second one represented by low-volatility oxygenated organic aerosol (LV-OOA) (e.g., Finessi et al., 2012; Crippa et al., 2014; Hong et al., 2017; Äijälä et al., 2019). While SV-OOA has certainly contributions from monoterpene oxidation products such as pinonic and pinic acids, the origin of LV-OOA has remained controversial for long: although possible contributions from long-range transport of anthropogenic aerosols are expected (Corrigan et al., 2013; Äijälä et al., 2019), the main source of low-volatility organic compounds in the boreal forest is now believed to be biogenic. Highly oxygenated multi-functionalized organic compounds are found in the early stages of monoterpene oxidation (Müller et al., 2012). At the same time, the fast formation of accretion products (dimers) can largely reduce the volatility of OA (Kenseth et al., 2018). In recent years, advanced high-resolution chemical ionization mass spectrometric techniques enabled the detection of medium-to-high molecular weight organic compounds exhibiting a high O/C ratio in the gas phase and ambient aerosols. It provides completely new insight into the processes driving the gas-to-particle conversion of SOA precursors. Extensive observations in the boreal forest showed that the formation of highly oxygenated molecules (HOMs) (Ehn et al., 2014, Bianchi et al., 2019) via auto-oxidation processes involving monoterpene oxidation products is one of the main drivers of both new particles (Kulmala et al., 2013a, Kerminen et al., 2018) and oxidized SOA (OOA) formation (Roldin et al., 2019). Monoterpene concentration increases as a function of temperature due to enhanced biogenic activity and emissions from the vegetation (***Figure 3.1.4b***, Paasonen et al., 2013). The observations provided by Kourtchev et al. (2016) and Daellenbach et al. (2019) at the SMEAR-II station show that in hot summer seasons, not only a larger amount of OOA is formed, but also a much greater proportion of accretion products (dimers) occur, due to the enhanced probability of RO_2 peroxy radical self-reactions at higher monoterpene concentrations levels. Overall, the most recent findings on OA composition in the boreal forest confirm a dominant contribution from monoterpene oxidation products with a high degree of overlap between the molecular composition determined in the lab and the field (about 70% of overlap in molecular formulas, according to Kourtchev et al., 2013).

In Amazonia, the AMS source apportionment analyses with the non-refractory PM_1 organic aerosol fraction have identified three chemical classes of SOA during the wet season. Those chemical classes differ in oxidation extent, OOA-1, OOA-2, and OOA-3, in decreasing order of oxidation (Chen et al., 2009, 2015). Where OOA-1 is consistent with aged SOA and the OOA-2 is produced by isoprene photooxidation. The OOA-3 resembles that of fresh biogenic SOA produced in the laboratory under relevant conditions of the Amazonian basin (Chen et al., 2015). With respect to their diel cycle, the last two OOAs presented maximum mass concentration in the afternoon, which agrees with SOA afternoon production, while OOA1 is rather constant over the day. The authors also concluded that most of the organic material composing submicron particles over the basin is derived from biogenic SOA production. The AMS observations in the Amazon confirm a primary role played by the oxidation of isoprene in the formation of SOA in this environment. Isoprene oxidation in relation to SOA mass formation is summarized in Shrivastava et al. 2017 and references therein. A particularly important oxidation pathway is related to the formation of isoprene epoxydiols (IEPOX), formed from the photooxidation of isoprene under low-NOx conditions, are proposed as precursors of SOA, so-called IEPOX-SOA (Clayes et al., 2004, González et al., 2014, Paulot et al., 2009; Surratt et al., 2010). Factor analysis of AMS datasets in environments impacted by isoprene oxidation is often able to detect and quantify one factor recovering the bulk IEPOX SOA chemical class (Hu et al., 2015). The time trend of the IEPOX-SOA AMS factor is found to correlate with the concentrations of C5-alkenetriols and 2-methyltetrols (Pearson correlation, $R>0.8$), which are markers of EPOXI-derived PM (de Sá et al., 2018; Lin et al., 2012; Surratt et al., 2010). The IEPOX-SOA contribution in the Amazon to the organic aerosol loading ranges between 17 to 34%, with larger contribution during the wet season (de Sá et al., 2017, 2018; Chen et al., 2015). Significant concentrations are also found in other tropical areas, like in Borneo (Robinson et al., 2011). It is important to note that this chemical class is not yet observed in the boreal forest, which relate to the fact that isoprene emissions in boreal forests are much lower than in the tropics.

The employment of high-resolution mass spectrometric techniques to the analysis of OOA in the Amazon basin shows that, in agreement with laboratory studies of isoprene oxidation, HOMs contribute to the biogenic SOA composition in this environment (Tong et al., 2019). A fraction of HOMs is also associated with accretion products. However, the contribution of HOM to total OA and their average molecular weight is smaller in the Amazon with respect to the boreal forest, which explains the difference in volatility. The lower average molecular weight of HOMs in the Amazon is a direct consequence of the lower carbon number of isoprene oxidation products and their accretion products (Heinritzi et al., 2020).

3.1.3.1. Anthropogenic influence on SOA production

The atmospheric chemistry of biogenic VOCs in a polluted atmosphere involves several non-linear processes and counteracting effects. Pollution generally increases the availability of oxidants (including NO_3 radicals at night) hence accelerating SOA formation (Jimenez et al., 2009). At the same time, the enhanced aerosol loadings drive the chemical equilibria of semi-volatile organic compounds (SVOC) partitioning toward the particulate phase and increase the kinetics of heterogenous uptake reactions, which are key in IEPOX SOA formation (Allan et al., 2006, 2014). On the other hand, increased NOx concentrations can reduce SOA yields for most biogenic VOCs. The net effect of pollution on biogenic SOA formation has been extensively debated in the scientific literature. Still, the most recent studies support an enhancement effect on SOA mass (Pye et al., 2019). Traditionally, the negative impact of NO_x on monoterpene SOA yield was explained by the fragmentation of alkoxy radicals formed by the RO_2 + NO reaction. However, Sarrafzadeh et al. (2016) showed that such an effect was only moderate and that the most important effect of NOx in depressing monoterpene SOA formation was due to the suppression of dimer formation. At the same time, the formation of organic nitrates via RO_2 + NO reactions and from night-time NO_3 radical chemistry partly compensates for the loss of accretion products.

Organic nitrates have been determined in ambient aerosol particles in the boreal forest in multiple studies. They are found in concentrations of up to 0.5 μg m^{-3} accounting for 22–35% of SOA mass at night at the SMEAR-II station (Lee et al., 2016, 2018). The diurnal trend in the concentrations typically shows an overnight accumulation with a peak around dawn. However, Bianchi et al. (2019) also report organic nitrate "factors" with characteristic daytime maxima. Hellén et al. 2018 studied the reactivity of several BVOC toward atmospheric oxidants on a monthly basis at SMEAR-II. They conclude that nighttime reactions with NO_3 could be a significant source of SOA, especially in the spring and fall months.

Urbanization is also a key issue in tropical areas. For example, about 80% of about 20 million people live in urban areas in the Brazilian Amazonia. Manaus is a metropolitan area with nearly 2 million people, with emissions from traffic, power plants, and industry, in the middle of a pristine central Amazon Forest (Martin et al., 2010, 2016). The research program 2014/15 examined the impact of the interactions of the Manaus emissions on the atmospheric chemistry downwind of the city (Martin et al., 2016, Machado et al., 2018, Kuhn et al., 2010, Mei et al., 2020). This is a globally important issue since forest regions in tropical Asia, Africa, and South America are all under pressure from growing urban areas. At the GoAmazon2014/15 site Manacapuru, the production of IEPOX-SOA is modulated by NO_y and sulfate (de Sá et al., 2017; Shrivastava et al., 2019). Under background conditions, PM_1 organic aerosol concentrations are about 1.0 μg m^{-3} (de Sá et al., 2017, 2018). When exposed to elevated NO_y concentrations from 0.5 to 2 ppb, SOA increases to 3.3 μg m^{-3}. This clearly shows the strong effect of urban pollution on SOA formed from forest emissions. Similar conclusions were obtained by Shilling et al. (2018) from aircraft measurements downwind of Manaus and Cirino et al. (2018) using gas and aerosol tracers to distinguish the impact of Manaus pollution. These studies show that as tropical regions become increasingly urbanized, we expect more SOA formation due to enhanced IEPOX and other organic aerosol components. Studies in Amazonia using an oxidation flow reactor (OFR) coupled with an aerosol mass spectrometer (AMS) shows a significant potential of SOA formation when the natural atmosphere is exposed to high OH concentrations (Palm et al., 2018). The amount of SOA formed in the OFR was very high, as much as 10 μg m^{-3}, depending on the amount of biogenic SOA precursor gases in ambient Amazonian air (Palm et al., 2018). Modeling the SOA production downwind of Manaus, as a result of interactions of BVOC with NOx from urban pollution, shows large production of ozone and SOA far from Manaus (Nascimento et al., 2021).

Figure 3.1.7 shows the impact of urban emissions on organic aerosol formation in central Amazonia for the wet season, measured during the GoAmazon 2014/15 experiment. The different meteorological situations are separated using fuzzy cluster analysis in 4 groups from background to polluted conditions. In the upper part, the large increase in secondary aerosols from Backd-1 to Pol-2 can be seen. The increase in SOA mass is from 1.2 to 3.3 μg m^{-3}. We can also observe the decrease in IEPOX-SOA from Bkgd-2 to Pol-2 condition, increasing medium (MO-OOA) and low (LO-OOA) oxidized organic aerosol components (de Sá et al., 2018).

Concerning the IEPOX-SOA production, the pollution emitted by Manaus is responsible for IEPOX-SOA suppression due to the elevated NO concentrations (de Sá et al., 2017). Curiously the suppressed IEPOX SOA is counteracted with the large increase in MO-OOA and LO-OOA (***Figure 3.1.7***). Moreover, the urban influence over the mass concentration and chemical composition of submicron aerosol particles in the central Amazonian basin was investigated, and a shift in the pathways of PM production under polluted conditions is proposed. PM production shifts from an HO_2-dominant to a NO-dominant state, affecting the concentration of several oxidants in the atmosphere. Such condition helps to speed up the oxidative processing of PM (de Sá et al., 2018, 2019).

Figure 3.1.8 shows for the dry season how the SOA, for each aerosol species and each PMF organic aerosol factor, changes the aerosol composition in conditions of impact and no impact of Manaus plume. The summed PM_1 mass concentrations for periods when the plume is influencing

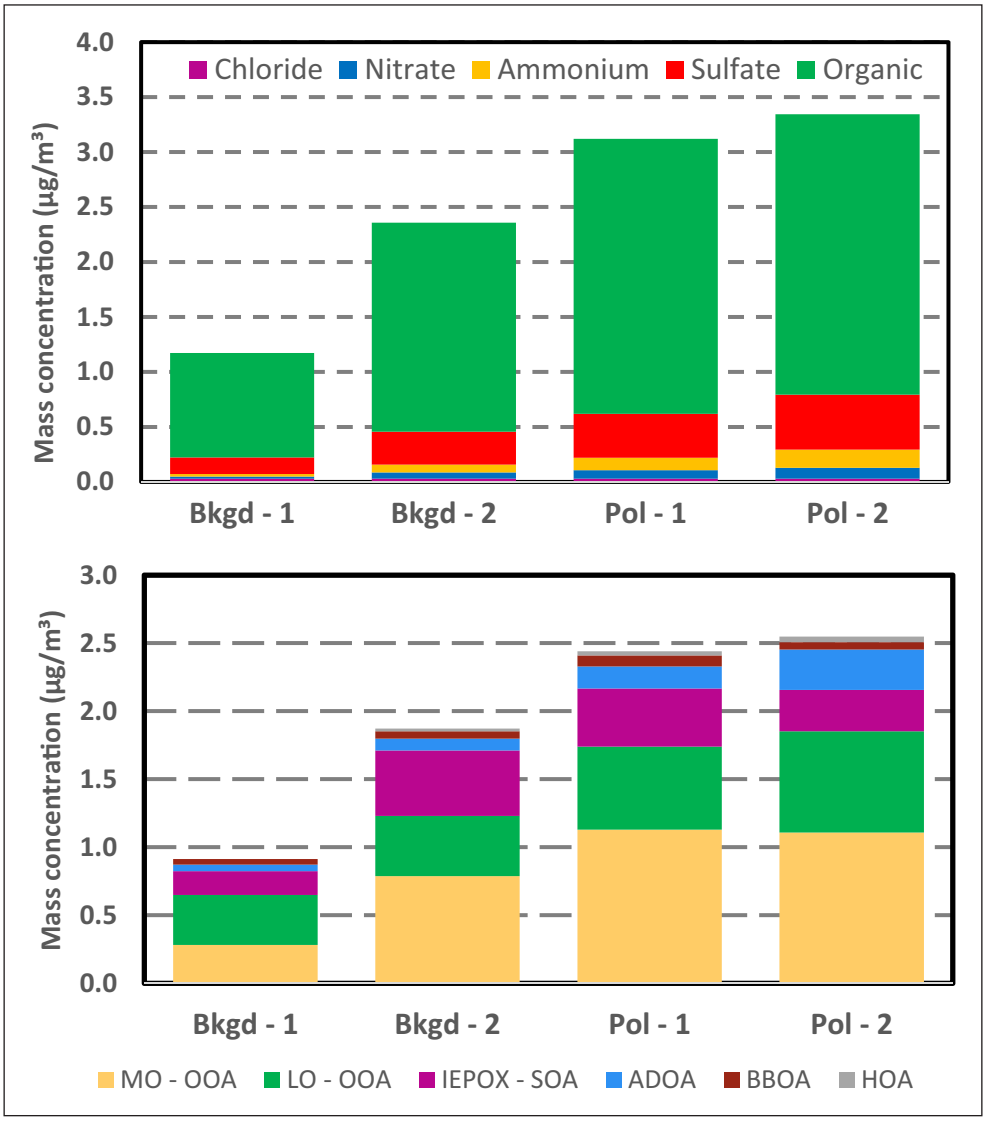

Figure 3.1.7 Increase in SOA formation from background to polluted conditions for the wet season in Central Amazonia, as measured at the GoAmazon2014/15 experiment. Urban air pollution from Manaus interacts with natural biogenic emissions producing significant amounts of SOA. Four meteorological conditions were separated using fuzzy cluster analysis in 4 groups, from background to polluted conditions. The increase in SOA mass due to pollution impact is very significant, with PM1 values around 1.2 µg/m³ going up to 3.3 µg/m³ under impact of Manaus pollution. From de Sá et al., 2018.

SOA production is 12.3 µg m^{-3}. This concentration is 33% higher than that representing the baseline cluster (9.2 µg m^{-3}). This result is based on a direct comparison of PM_1 mass concentrations between the ATTO background site and Manacapuru, the main experimental site of the GoAmazon experiment (Martin et al. 2016). Therefore, the overall effect of Manaus pollution is to add about 3 µg m^{-3} of SOA in the dry season. In the wet season, about 2 µg m^{-3} is added. The most significant component from the Positive Matrix Factorization analysis (PMF) is the MO-OOA due to the distance from Manaus to the Manacapuru site (70 km). Submicron aerosol particles were more oxidized downwind of Manaus, showing that aerosol undergoes oxidation during the transport. These results were confirmed by Shilling et al. (2018) using aircraft measurements in the vicinity of Manaus. The authors observed clear aging in the OA on the plume that was transported downwind of Manaus, that is, the oxidation state ($\overline{OS_c}$) increased from –0.6 to –0.45 during 4–5 h photochemical aging (Shilling et al., 2018). Although photochemical aging is clear, the observed Δorg/ΔCO is rather stable, which differs from most measurements in other parts of the globe that report a significant increase in Δorg/ΔCO for the first day of plume aging. Finally, the authors conclude that the SOA formation mechanisms in the vicinity of Manaus are likely different from other places, e.g., the USA. Moreover, the OA is more oxidized in the dry ($\overline{OS_c}$ = –0.02, O:C=0.78) than in the wet season ($\overline{OS_c}$ = –0.45, O:C=0.6). The average O:C ratio value in the wet season is higher than Chen et al. (2009) observed, ranging from 0.42 to 0.49 for in-basin and out-basin influence.

3.1.4. Mixing state and phase of aerosols

Atmospheric aerosols are complex mixtures of different chemical species, and individual particles exist in

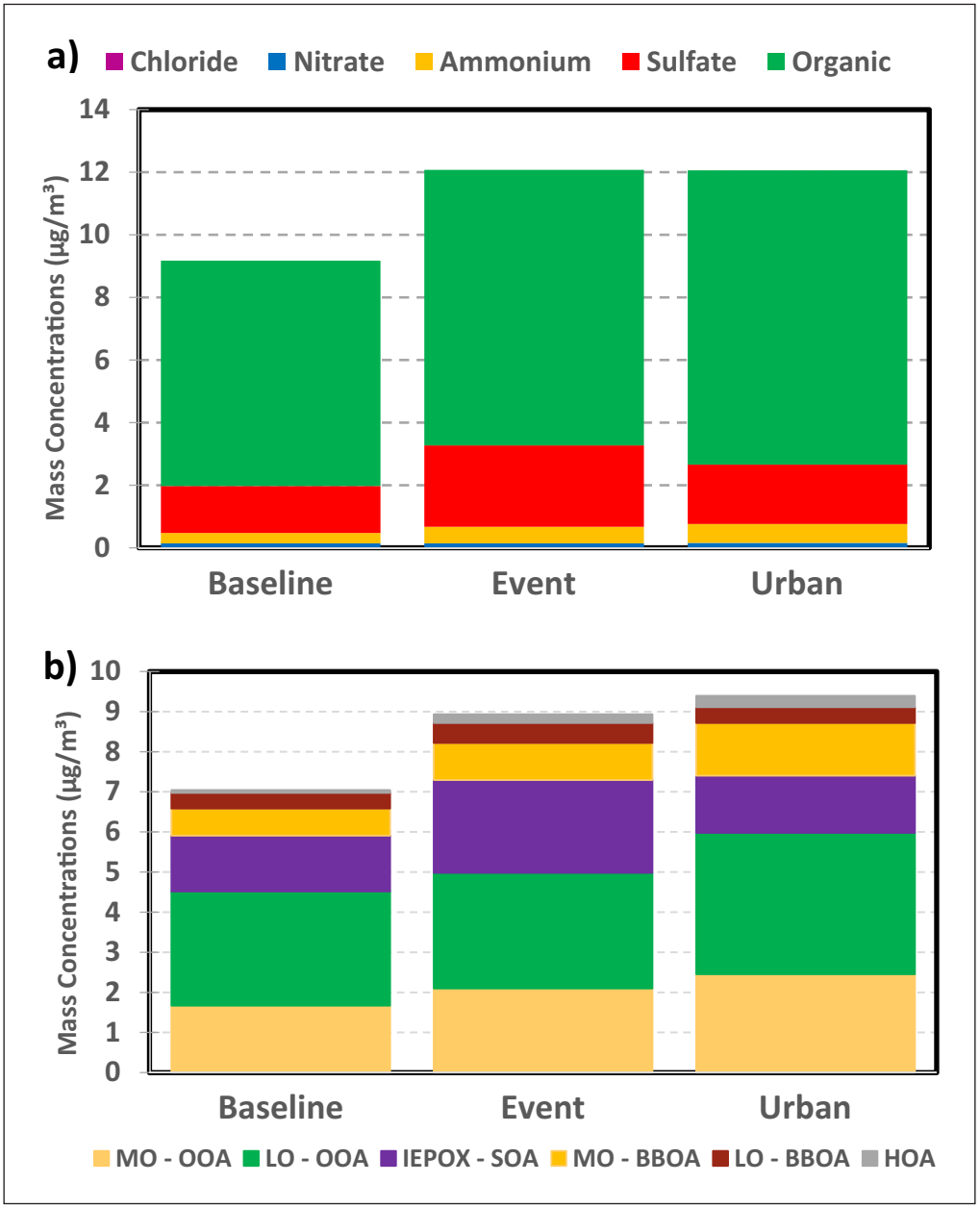

Figure 3.1.8 Dry season increase in SOA in Central Amazonia, for each species (Upper part) and each PMF organic aerosol factor (lower) when urban air pollution from Manaus interacts with biomass burning aerosols. Baseline represents conditions with no Manaus plume impact, and Event and Urban represent when the Manaus plume hits the site. It is possible to see an increase in PM1 from 8.5 µg/m³. to 12 µg/m³ (from de Sá et al., 2019).

many different shapes and morphologies. The particle population can be internally or externally mixed, indicating whether all the particles in an aerosol population have the same uniform chemical composition or the aerosol population is composed of different subpopulations with different chemical compositions (Swietlicki et al., 2008, Riemer et al., 2019). The mixing state (internally or externally) is key to many physicochemical properties, i.e., hygroscopicity, which can detect the mixing state. In Amazonia, X-ray micro spectroscopic measurements indicate that the internally mixed particles prevail over the externally during the transition from dry to wet season (Pöhlker et al., 2014, Adachi et al., 2020). Similar results are obtained by the combination of different spectra microscopy techniques that found similar mixing state indices (>0.8) for all samples analyzed, indicating the presence of highly (80–90%) internally mixed particles during the dry season (Fraund et al., 2017, Adachi et al., 2020).

In the boreal forest, the frequency of externally mixed particles increases with size in the size range of 10 to 150 nm mobility diameter aerosol particles (Hämeri et al., 2001). In addition, it is demonstrated that in the nucleation mode, externally mixed particles are mostly connected to air masses arriving from polluted areas (Väkevä et al., 2002). Industrial emissions and anthropogenic influence tend to increase the hygroscopicity during the transport within the boreal environment (Petäjä et al., 2005). In clean conditions, the biogenic aerosol in the boreal forest is typically internally mixed with low hygroscopic growth

factors (Ehn et al., 2007). The hygroscopicity has a clear diurnal cycle with a maximum at noon. This reflects the gas-phase concentrations of sulfuric acid and organic condensable vapors (Hong et al., 2014, 2015, see also 3.3).

Regarding the particulate phase (liquid or solid), measurements of submicrometer particulate matter show that it is primarily in liquid form during dry and wet seasons (Bateman et al., 2015, 2016, 2017). This is due to the soluble composition as well as the very high relative humidity. When it is above 70% (which is very frequent), more than 90% of the particles are in liquid form. Nevertheless, there is experimental evidence of the presence of SOA in an amorphous solid form in the Boreal forest (Virtanen et al., 2010).

3.2. PRIMARY BIOLOGICAL AEROSOL PARTICLES

Primary biological aerosol particles (PBAP), also called bioaerosols, are defined as solid or liquid airborne particles of biological origin, which are emitted directly from the biosphere into the atmosphere (Patade et al., 2021, Prass et al., 2021, Després et al., 2012; Fröhlich-Nowoisky et al., 2016). They represent a highly diverse particle mixture in terms of size (i.e., few nm up to hundreds of µm), morphology, taxonomy, and metabolic state, occurring in the atmosphere throughout the globe (Burrows et al., 2009a; 2009b; Fröhlich-Nowoisky et al., 2012; Huffman et al., 2010, 2020; Matthias-Maser et al., 2000). Bioaerosols typically comprise entire organisms such as bacteria, archaea, and algae, as well as reproductive units of the same. In addition, insect, and plant fragments, as well as pollen grains, fungal spores, and various further particle types, can be detected (Després et al., 2012). They are primarily emitted passively through mechanical momenta, such as air currents or rain splash (e.g., Joung et al., 2017), but also actively through humidity triggered spore discharge mechanisms (e.g., Webster and Weber, 2007; Turner and Webster, 1995; Trail et al., 2005), or a combination of both (e.g., Johansson et al., 2014; 2016). Once emitted, the atmospheric lifetime of PBAP depends on particle properties (i.e., size, density, hygroscopicity), their mixing state (e.g., their potential adhesion to other aerosol particles), as well as meteorological conditions (i.e., wind speed and precipitation), and typically ranges from a few minutes up to days (Heald and Spracklen, 2009; Burrows et al., 2009a, Löbs et al., 2020).

Bioaerosols are regarded as important factors in climatology, ecology, agriculture, and public health, with their role and relevance in these fields still being a matter of active research (Pöschl and Shiraiwa, 2015; Ekström et al., 2010, Bauer et al., 2003; Reinmuth-Selzle et al., 2017; Fröhlich-Nowoisky et al., 2015; Prenni et al., 2013, Schneider et al., 2011, Prass et al., 2021). In terms of atmospheric processes and relevance for the Earth's climate system, the ability of PBAP to act as (giant) CCN and ice nuclei (INP), as well as their interaction with chemical processes in the atmosphere, have been shown (Morris et al., 2004; 2011, Patade et al., 2021). Generally, bioaerosols are most abundant in the particle size distribution's coarse mode (>1 µm). As they occur in comparatively low abundance compared to other aerosol types, their relevance is still under lively debate (e.g., Möhler et al., 2007; Huffman et al., 2013; Delort et al., 2010; Fröhlich-Nowoisky et al., 2016). Bioaerosol analytics has remained challenging due to the highly complex and diverse particle properties. However, the establishment of new analytical methods, such as DNA analysis and real-time detection, have substantially increased our knowledge on PBAP composition and distribution in the atmosphere (e.g., Burrows et al., 2009b; Stanley et al., 2011; Fröhlich-Nowoisky et al., 2012; Huffman et al., 2013; Womack et al., 2015). In this context, online data based on single-particle autofluorescence detection provides information on the fraction of fluorescent aerosol particles (FAP), which is regarded as a reasonable proxy for the overall PBAP burden (e.g., Pöschl et al., 2010; Huffman et al., 2010; Savage et al., 2018). However, it is important to note that the large PBAP diversity imposes significant analytical challenges in terms of sound PBAP quantification (Prass et al., 2021). Accordingly, number and mass concentrations derived from different measurement techniques and sampling locations are comparable only within certain limits, and similarities and deviations must be evaluated carefully (Löbs et al., 2020). China et al., 2018 showed that fungal spores could be a source of sodium salt particles in Amazonia.

3.2.1. Primary biological aerosol particles in tropical forests

The number of studies that have investigated the properties and concentrations of bioaerosols in tropical forests, such as in Brazil, Malaysia, North-East Borneo, and Queensland, Australia, is still comparatively small (Graham et al., 2003a; 2003b; Gilbert and Reynolds, 2005; Gabey et al., 2010; 2011; Martin et al., 2010; Whitehead et al., 2010; 2016; Huffman et al., 2012; Andreae et al., 2015; Womack et al., 2015). Most of these studies have been conducted in the Amazon rain forest, which is a predestined ecosystem, to study periods of unperturbed tropical biosphere-atmosphere exchange. Generally, the Amazonian atmosphere is characterized by a pronounced seasonality, which is mostly driven by large variations in atmospheric circulation patterns and precipitation regimes at comparatively constant temperatures (Pöhlker et al., 2019). Similarly, the aerosol abundance and composition (biogenic vs. anthropogenic particles) are subject to large seasonal variations, finding its concentration minimum in the wet and it is maximum in the dry season (Saturno et al., 2018a; Moran-Zuloaga et al., 2018). Remarkably, the aerosol coarse mode, which comprises most of the PBAP mass (i.e., fungal spores,

pollen, fragments of a different kind), is comparatively constant throughout the year (Moran-Zuloaga et al., 2018), which suggests a weaker seasonality in the overall abundance of the PBAP population as compared to the accumulation mode aerosol.

Figure 3.2.1a shows the rather modest seasonal variability of the Amazonian aerosol coarse mode size distributions, according to Moran-Zuloaga et al. (2018). Furthermore, ***Figure 3.2.1b*** shows the abundance and relative fractions of fluorescent aerosol particles from all studies currently available from the Amazon region. This comparison of the total vs. fluorescent particle concentrations (NT vs. NF) emphasizes the following findings: The size distributions of all coarse mode measurements (total vs. fluorescent particles) generally agree quite well. However, the measurements of the fluorescent particle fractions, NF/NT, bear some inherent uncertainty due to instrumental differences (i.e., the ultra-violet aerodynamic particle sizer, UV-APS, vs. the wideband integrated bioaerosol sensor, WIBS) and strong size dependence of the fluorescence properties (Healy et al., 2014; Savage et al., 2017; Huffman et al., 2019). Pöschl et al. (2010) provide a comparison of actual PBAP fractions for particles >1 µm (number fraction of PBAP in total particles: NPBA/NT = ~80%; mass fraction of PBAP in total aerosol mass: MPBA/MT = ~85%) vs. the corresponding fluorescent fractions (NF/NT = ~40, MPBA/MT = ~64%), which helps to put the NF/NT results into perspective. In terms of particle size, all studies consistently report maxima of the total as well as fluorescent particle size distributions between 2 and 3 µm (e.g., Gabey et al., 2010; Pöschl et al., 2010; Huffman et al., 2012; Andreae et al., 2015; Whitehead et al., 2016).

In contrast to the rather weak seasonal variability, strong diurnal cycles in the abundance of fluorescent particles are observed (e.g., Gabey et al., 2010; Huffman et al., 2012; Whitehead et al., 2016). The total coarse mode aerosol shows distinct diurnal patterns when PBAP is predominant (Moran-Zuloaga et al., 2018).

Specifically, concentrations increase after sunset, reaching a maximum during the night, while concentration minima occur during the day (e.g., Gabey et al., 2010; Huffman et al., 2012; Whitehead et al., 2016). The diurnal variability appears to be driven by the interplay of boundary layer dynamics (i.e., convective dilution during the day vs. thermal stratification during the night) as well as characteristic bioparticle emission patterns. Here, the discharge processes of fungal spores may contribute to the diurnal changes, as fungi have been reported to emit spores in diurnal, pulsing patterns with maxima occurring during the night and minimum concentration during the day (Paulitz, 1996; Gilbert and Reynolds, 2005; China et al., 2018; Löbs et al., 2020).

Furthermore, the sampling height strongly influences the measured bioaerosol concentrations (Šantl-Temkiv et al., 2019). A strong vertical gradient in PBAP abundance was observed, ranging between 50 and 4000 L-1 below the canopy and between 50 and 400 L-1 above, in a tropical rain forest in Borneo, Malaysia (Gabey et al., 2010). Likewise, Gilbert and Reynolds (2005) observe spores to be 52-fold more abundant in the understory than in the canopy of a tropical rain forest in Australia. This vertical concentration gradient is defined by the in- and below-canopy character of the sources and the fact that larger size PBAP fractions are less prone to be transported to higher altitudes. The resulting comparatively low PBAP number concentrations at high altitudes (i.e., cloud base levels) are one reason for the ongoing debate on their role and relevance in aerosol-cloud interaction. Within a broader context, a recent study report PBAP concentrations in the troposphere and stratosphere and showed that cell concentrations at

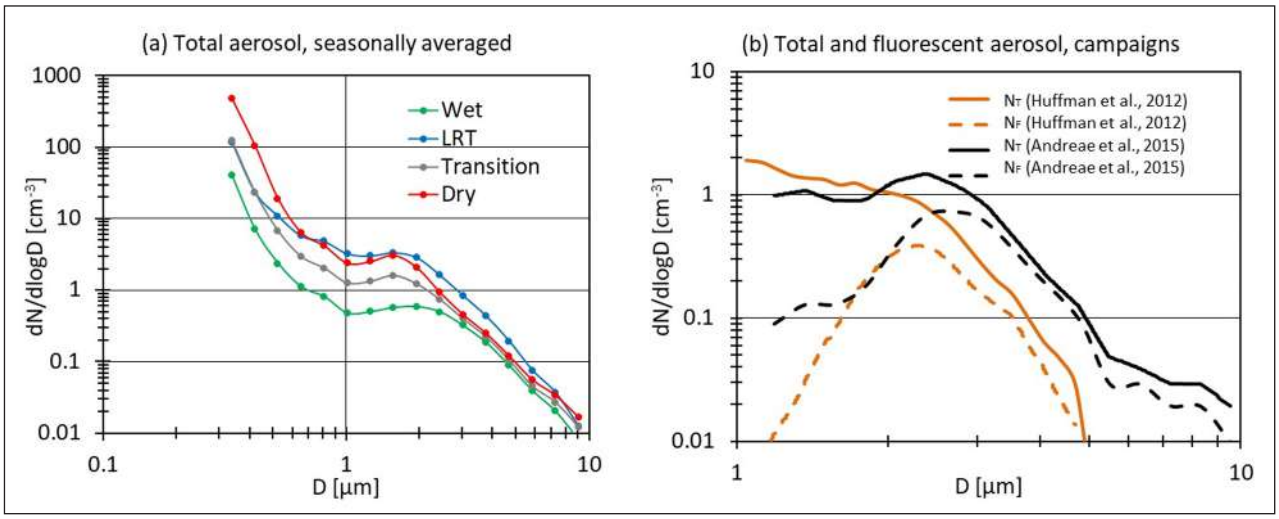

Figure 3.2.1 Amazonian aerosol number size distributions for the coarse and accumulation modes, dN/dlogD: **(a)** seasonal averages adapted from Moran-Zuloaga et al., 2018; **(b)** total (NT) and fluorescent (NF) particle distributions. In (a), "Wet" means wet season, "LRT" means African long-range transport periods, when Sahara dust is observed, "Transition" is the wet-to-dry transition season, and "Dry" are measurements from the dry season. Data from Moran-Zuloaga et al., 2018; Huffman et al., 2012 and Andreae et al., 2015.

altitudes between 3 and 29 km were highly similar and approximately threefold lower than those observed in the convective boundary layer (Bryan et al., 2019).

For tropical forests, only little is known about the bioaerosol composition. Until now, particle identification is limited to few microscopic and molecular genetic analyses, which identified fungal spores as a predominant fraction of primary biological particulate mass (Graham et al., 2003b; Elbert et al., 2007; Pöschl et al., 2010; Huffman et al., 2012; Womack et al., 2015). Recently, Souza et al. (2019) conducted a metagenomic DNA extraction and analysis on Amazonian aerosols samples and revealed that fungi and bacteria are a significant fraction of the organisms present in Amazonian bioaerosol. These organisms are known to disperse via cells and/or spores through the atmosphere. During the wet season, 35% of the coarse mode air particulate matter was found to be fungal spores in the Amazonian tropical rain forest region (Elbert et al., 2007). Moreover, a comparison of the studies by Graham et al. (2003b) and Huffman et al. (2012) suggest that fungi and/or fungal spores tend to dominate the bioparticle population.

3.2.2. Primary biological aerosol particles in boreal forests

The boreal forest is poor in species diversity and dominated by only a few main tree species. Most native boreal trees are wind-pollinated, and high pollen concentrations can be expected under favorable conditions. During the peak season, according to pollination phenology, up to 65 % of total PM may be of biological origin (Manninen et al., 2014). Despite their large size, bioaerosols, including pollen grains, are aerodynamically buoyant (Reponen et al., 2001; Després et al., 2012) and can be transported over long distances via wind dispersal. Therefore, their occurrence is not limited to the timing of local pollination (Gregory, 1978; Hjelmroos, 1991; Prospero, 2005; Sofiev et al., 2006; Hussein et al., 2013; Tack et al., 2014).

Speciation of annual patterns in PBAP was done in a boreal forest at the SMEAR II site (Manninen et al., 2014), and the two main particle groups – differing in their peak timing – are pollen grains and fungal spores. Due to strong seasonality in boreal vegetation activity, the highest concentrations of pollen in the atmosphere are recorded in late spring and early summer (Siljamo et al., 2008; Yli-Panula et al., 2009; Schumacher et al., 2013; Manninen et al., 2014), whereas spores dominate the concentrations in late summer and fall. Elevated abundances of bacteria and free amino acids (FAAs) are also observed during the local pollen season, as determined with molecular genetic analysis (DNA) and mass spectrometric techniques (Helin et al., 2017). In winter, the air is practically free of PBAP in boreal latitudes. The highest daily pollen number concentrations (*Betula* spp. and *Pinus* spp.) can exceed 10^4 and 10^3 grains m^{-3}, respectively, whereas those of spores can vary between 10^4–10^6 m^{-3}. Most fungal spores are identified as Basidiomycota and Ascomycota, with *Cladosporium* being particularly dominant (Helin et al., 2017). Pollen increases the measured PM mass during the pollen season. Still, their effect on total particle number is negligible. Fungal spores constitute the largest fraction of measured PBAP numbers (~99%), whereas pollen constitutes a higher relative mass fraction (~97%) of PBAP (Manninen et al., 2014).

Although the annual dynamics of pollen emission are fairly similar from year to year, their concentration levels can change significantly depending on meteorological conditions during the prevailing and previous growing season (Jones and Harrison, 2004; Manninen et al., 2014). Day-to-day variation in PBAP concentrations is large, temperature and humidity being the most important factors (Schumacher et al., 2013; Manninen et al., 2014). According to Manninen et al. (2014), the highest seasonal average PM mass concentrations are 6.5 μg m^{-3} and 1.7 μg m^{-3} in PM_1 and PM>10, respectively, with the highest PM concentrations peaking in spring and summer during pollen emission. While intermediate size ranges, $PM_{1–2.5}$ and $PM_{2.5–10}$ generally show lower concentrations.

The lowest FAA and total DNA concentrations are measured during winter and highest during late spring (Helin et al., 2017). The maximum amount of extracted DNA reach 48 ng m^{-3} (May–June) and the maximum FAA concentration 751 ng m^{-3} (late May, roughly similar in all size classes). However, bacterial, and fungal DNA reach their maximum levels (N_c = up to 4–6 *10^5 cells m^{-3}) in different seasons, with bacteria peaking in late spring and fungal DNA in late summer and autumn, corresponding to the spore maximum. Positive correlations are observed between PBAP component abundances with rainfall recorded before and during sampling as well as with rainfall recorded after sampling (Schumacher et al., 2013; Manninen et al., 2014).

A recent analysis of INP indicates that common epiphytic lichen spores or soredia may contribute to ice nucleation activity in a boreal environment (Proske, 2018). This has potentially significant consequences on the atmospheric processes and cloud properties over boreal regions.

3.2.3. Similarities and differences in tropical vs. boreal bioaerosol cycling

Tropical and boreal forests are characterized by different seasonal and vegetation patterns (see sections 1 and 2). Seasons in boreal forests are temperature driven, inducing spring, summer, fall, and winter, resulting in large differences in biological, specifically plant, activities. Tropical forests, in contrast, are characterized by seasonal changes in precipitation rates causing wet and dry seasons connected by transition periods (see section 2). These seasonal characteristics of tropical and boreal forests are reflected by differences in bioaerosol emission, composition, and properties across the biomes.

Still, also similarities can be found by comparing published data. For instance, it was shown that PBAP dominates the coarse mode mass concentrations in both forest systems, with boreal winter month as a notable exception (e.g., Pöschl et al., 2010; Huffman et al., 2012; Manninen et al., 2014). In terms of number concentrations, PBAP contributes significantly to the coarse mode in tropical forests (Pöschl et al., 2010) but only to a minor extent in boreal forests (Schumacher et al., 2013; Manninen et al., 2014). Furthermore, the seasonal patterns differ, as displayed in ***Figure 3.2.2***. Boreal forests show pronounced seasonal PBAP cycles ($N_{F,c}$ = 0.046 ± 0.048·10^6 m^{-3} in summer and 0.004 ± 0.005·10^6 m^{-3} in winter) during comparably constant total aerosol number values. As a result, number concentration ratios are highly variable (Schumacher et al., 2013). In tropical forests, in contrast, moderate seasonal changes in total aerosol number concentration are found ($N_{T,c}$ = 6.5 ± 5.3·10^6 m^{-3} during the wet season without dust intrusion and 71.9 ± 58.1·10^6 m^{-3} during dry season). It is assumed that they are driven by PBAP number concentration changes, as this particle type mainly constitutes the total aerosol number concentration (Moran-Zuloaga et al., 2018). PBAP ratios are found at constant high levels (e.g., Pöschl et al., 2010; Whitehead et al., 2016).

In terms of diurnal cycles, tropical and boreal forest systems display similar distinct pattern with the highest PBAP values during the night and decreasing concentration after sunrise (e.g., NF,c = 0.04·10^3 cm^{-3} at daytime and 0.15·10^3 cm^{-3} at night-time, Huffman et al., 2012, ***Figure 3.2.2***).

As emphasized by ***Figures 3.2.2*** and ***3.2.3***, FBAP number size distributions are comparable, showing distinct concentration peaks in size range from 2–3 µm, independent of forest type and season (***Figure 3.2.2***). Multiple studies suggest that fungal spore emissions cause this maximum. In general, mass concentration in tropical forests is dominated by fungal spore populations (Graham et al., 2003b; Elbert et al., 2007; Huffman et al., 2012; Womack et al., 2015). In boreal forests, number size distributions show a comparably long tail for larger particle diameters, especially during summer, indicating the presence of pollen grains (***Figure 3.2.4***). Pollen grains dominate the mass fraction up to 60% with respect to the total PM mass (and 5% for other PBAP) in the boreal forest (Manninen et al., 2014). Even though data displayed in ***Figures 3.2.2*** and ***3.2.1*** are achieved with an instrument of the same type, a direct comparison between the absolute numbers is possible only to a certain extent, as sampling conditions differ.

3.3. AEROSOL SIZE DISTRIBUTION

The complexity of sources and processes is reflected in the temporal and spatial variability, seasonality, and shapes of the aerosol size distribution in forest ecosystems. Size distribution is one of the critical properties in the effects of aerosols on climate, including radiative

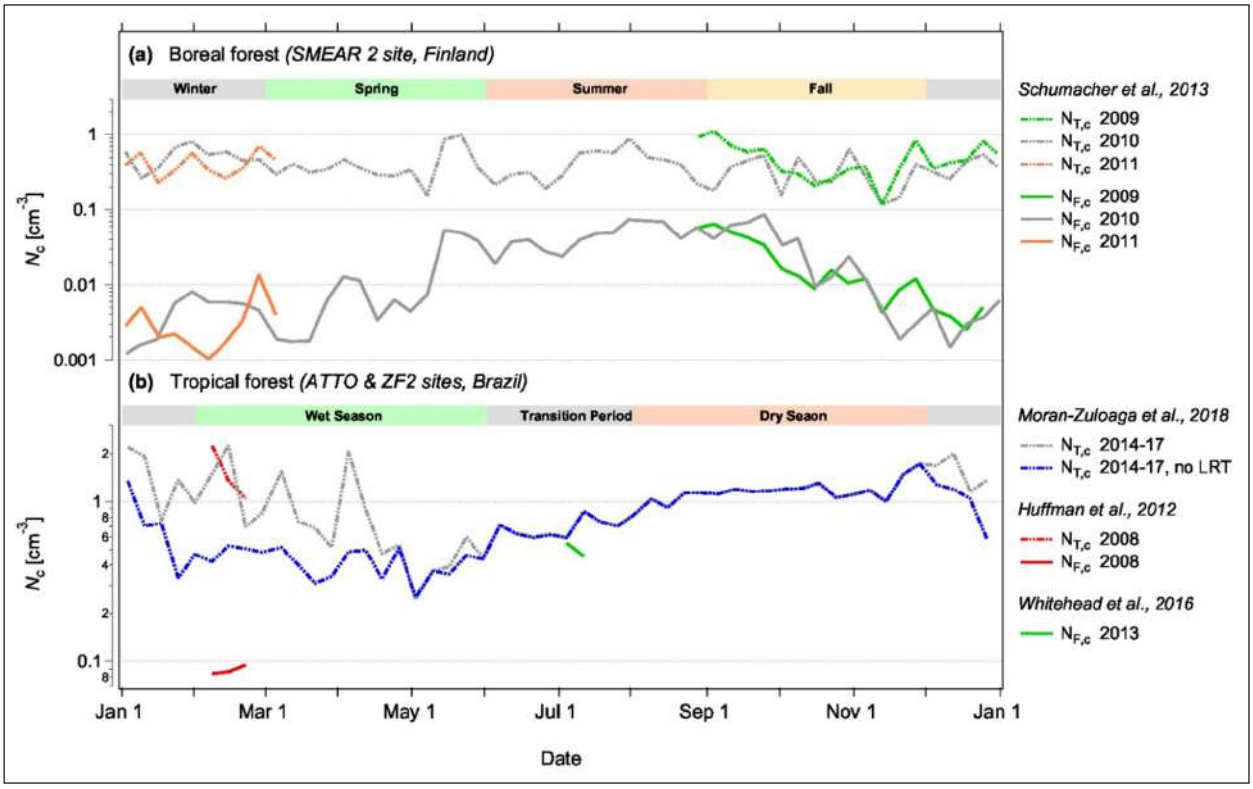

Figure 3.2.2 Seasonality in total ($N_{T,c}$) and fluorescent ($N_{F,c}$) coarse mode particle concentrations in tropical (Amazon) vs. boreal forest (Finland). The tropical forest data shown here has been adapted from Huffman et al. (2012), Whitehead et al. (2016), and Moran-Zuloaga et al. (2018). The boreal forest data has been adapted from Schumacher et al. (2013).

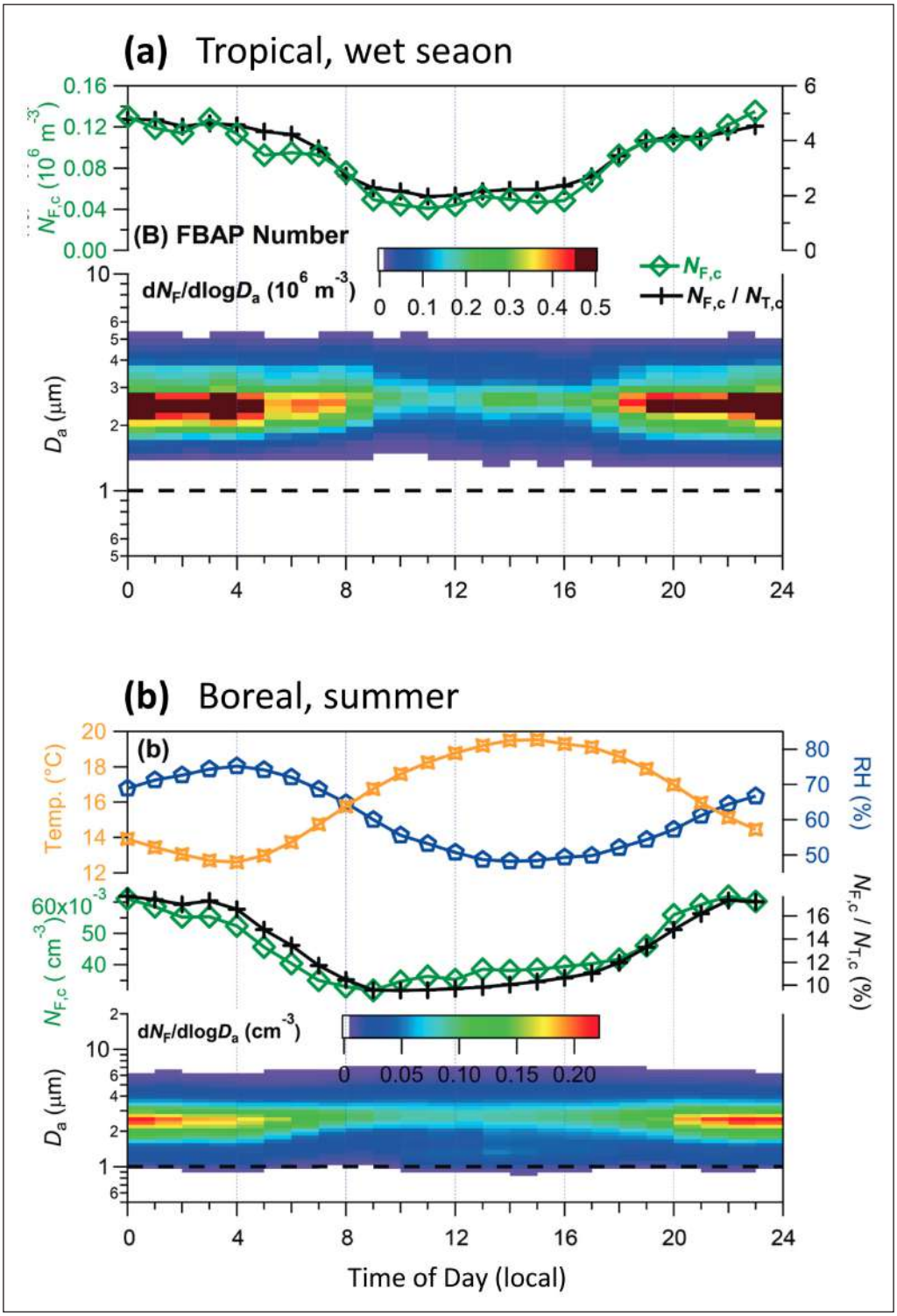

Figure 3.2.3 Characteristic diurnal cycles of temperature, number of PBAP and PBAP diameter in tropical (wet season) and boreal forests (summer) – both measured with the UV-APS and thus being comparable. Also shown is the percentage of the number of fluorescent particles ($N_{F,C}$) to the total number of coarse mode particles (N_{TC}). The lower part of both plots shows the diurnal variability of PBAP size distribution from 1 to 10 micrometers. The data has been adapted from Huffman et al. (2012) and Schumacher et al. (2013).

forcing and nucleation of cloud droplets (Boucher et al., 2013). Recently, there has been important progress in understanding the complex processes that regulate the shape of the size distribution in forested environments, including different secondary organic aerosol formation mechanisms and detailed measurements of the coarse mode aerosol size distribution that is mostly biogenic.

3.3.1 Aerosol size distribution in tropical forests

During the wet season, when pristine atmospheric conditions prevail, the coarse particle mode ($2.0 < D_p < 10$ µm) predominates, representing 60 to 80% of PM_{10} mass concentrations (***Table 3.3.1***). Source apportionment analysis indicates biogenic emissions as the main source of coarse mode aerosols in the wet season, followed by

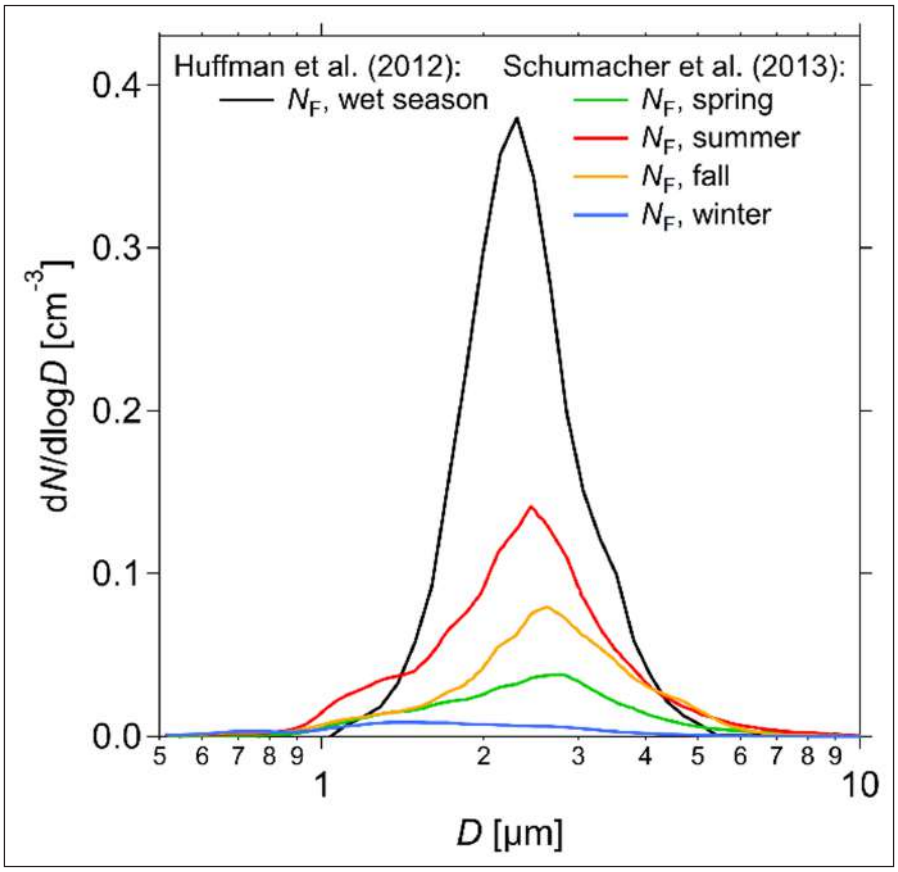

Figure 3.2.4 Characteristic size distributions, d*N*/dlog*D*, of fluorescent particles in tropical and boreal forests – both measured with the UV-APS and thus being comparable. The data has been adapted from Huffman et al. (2012) and Schumacher et al. (2013).

mineral dust and sea salt (Artaxo and Hansson, 1995; Echalar et al., 1998; Gilardoni et al., 2011; Pauliquevis et al., 2012; Pöhlker et al., 2012; Moran-Zuloaga et al., 2018). Observations at forest sites report higher concentrations of coarse mode particles during night-time at ground level, compared to measurements right above the canopy, as discussed in detail in section 3.1 (Artaxo et al., 2002; Artaxo and Hansson, 1995; Guyon et al., 2003; Rizzo et al., 2010). The authors suggest the influence of biogenic sources of coarse mode particles in the Amazon Forest at night, affecting the cycling of crucial ecosystem nutrients such as K and P.

The mass concentration and source apportionment of coarse mode particles are relatively constant throughout the year, indicating a persistent contribution of natural biogenic emissions in Amazonia (Andreae et al., 2015; Pauliquevis et al., 2012; Moran-Zuloaga et al., 2018). Disturbances in this steady behavior are caused by the intrusion of long-range transported African aerosols, acting as an external source of a mixture of different aerosol types: mineral dust, African biomass burning, and sea salt. The advection of African aerosols to the Amazon is frequent between January to April, causing a substantial increase in particle mass concentrations (up to 100 µgm^{-3}) (Moran-Zuloaga et al., 2018), and changes in aerosol optical properties (e.g., Baars et al., 2011, 2012; Saturno et al., 2018b). Moreover, the long-range transported aerosols can have a fertilizing effect in Amazonia over the long term due to the transport of P in dust aerosols and deposition in the forest (Swap et al., 1996, Formenti et al., 2001, Ben-Ami et al., 2010, Rizzolo et al., 2017).

Fine particle mode predominates during the dry season, representing 46 to 84% of PM_{10} mass concentrations (***Table 3.3.1***). That result and remote sensing measurements show that regional biomass burning emissions affect the whole Basin, even remote forest sites in Western and Central Amazonia (Sena and Artaxo, 2015). However, the impact of biomass burning emissions on fine particle concentrations is greatest at pasture and forest sites located in the so-called Arc of Deforestation in Amazonia, where fine particles represent more than 80% of the aerosol mass (Artaxo et al., 2002; Guyon et al., 2003). Source apportionment analysis indicates that the main source of fine mode particles is biomass burning emissions during the dry season and biogenic emissions during the wet season (Echalar et al., 1998; Pauliquevis et al., 2012). The concentration of fine mode particles is strongly influenced by the seasonal biomass burning emissions, increasing one order of magnitude from the wet to the dry season.

Strong seasonal variability is also evident in submicrometer particle number size distributions measurements in Amazonia. During the wet season, Aitken ($\sim 30 < D_p < 100$ nm) and accumulation ($\sim 100 < D_p < 600$ nm) modes have comparable contributions to the particle size

YEAR	SEASON	LANDSCAPE	SUB REGION	AIR MASSES	PM_{10} (μg/m³)	FPM (μg/m³)	CPM (μg/m³)	REFERENCE
1992–1995	Wet	Forest	AD	mostly clean	21.9	5.5	16.4	Echalar et al., 1998
1996–1998	Wet	Forest	AD	mostly clean	25.0	9.9	15.1	Maenhaut et al., 2002
1998–2002	Wet	Forest	CA	mostly clean	8.8	2.2	6.6	Pauliquevis et al., 2012
1999	Wet	Forest	AD	mostly clean	6.0	2.2	3.8	Guyon et al., 2003
2008–2012	Wet	Forest	CA	mostly clean	9.5	1.9	7.6	Arana et al., 2014
2009–2012	Wet	Forest	AD	mostly clean	8.7	1.8	6.9	Arana et al., 2014
1999	Wet	Pasture	AD	mostly clean	8.6	2.9	5.7	Artaxo et al., 2002
2014–2017	Wet	Forest	CA	mostly clean, dust episodes excluded	–	–	4.0	Moran-Zuloaga et al., 2018
2014–2017	Wet	Forest	CA	Dust episodes	–	–	11–39	Moran-Zuloaga et al., 2018
1992–1995	Dry	Forest	AD	aged and fresh biomass burning	81.0	47.0	34.0	Echalar et al., 1998
1996–1998	Dry	Forest	AD	aged and fresh biomass burning	100.0	63.0	37.0	Maenhaut et al., 2002
1996–1998	Dry	Forest	CA	aged biomass burning	13.4	6.2	7.2	Pauliquevis et al., 2012
1999	Dry	Forest	AD	aged biomass burning	40.1	33.5	6.6	Guyon et al., 2003
2004	Dry	Forest	CA	aged biomass burning	13.3	8.1	5.2	Rizzo et al., 2010
2008–2012	Dry	Forest	CA	aged biomass burning	7.8	3.4	4.4	Arana et al., 2014
1999	Dry	Pasture	AD	aged and fresh biomass burning	83.0	66.0	17.8	Artaxo et al., 2002
2009–2012	Dry	Pasture	AD	aged biomass burning	43.2	33.0	10.2	Arana et al., 2014
2014–2017	Dry	Forest	CA	aged and fresh biomass burning	–	–	6.5	Moran-Zuloaga et al., 2018

Table 3.3.1 Mean values for aerosol mass concentration observed at different sites in the Amazon Basin: PM_{10} (inhalable particle matter, Dp < 10 μm), FPM (fine particle mode, Dp < 2.0 μm), CPM (coarse particle mode (2.0 < Dp < 10 μm). Amazonian sub-regions: AD (Arc of Deforestation) and CA (Central Amazonia). At all forest sites, measurements reported here were taken above the canopy.

spectra at forest sites in Central Amazonia (***Figure 3.3.1*** and ***Table 3.3.2***). Aitken and accumulation modes are frequently separated by a pronounced Hoppel minimum (Hoppel et al., 1986), indicating the influence of aerosol in-cloud processing. Nucleation mode particles (D_p <~30 nm) are occasionally observed within the boundary layer but do not contribute significantly to particle number concentrations, at least with seasonal means. Wet season means particle number concentrations are in the range of 300–400 cm^{-3} at forest sites (Andreae et al., 2015; Martin e al., 2010; Rizzo e al., 2018; Zhou et al., 2002).

On the other hand, during the dry season, the submicrometer particle size spectrum is dominated by the accumulation mode (***Figure 3.3.1*** and ***Table 3.3.2***), resulting from regional biomass burning emissions (e.g., Andreae et al., 2015; Artaxo et al., 2013). Brito et al. (2014) report that the aging of regional biomass burning plumes, indicated by changes in the O:C ratio from 0.2 to 0.7, do not change the shape of particle size distributions, depicting either a single accumulation mode or a superposition of Aitken and accumulation modes. Total particle number concentrations typically increase 3 times from wet to dry season, with mean values in the range 1000–1400 cm^{-3} at forest sites in Central Amazonia (Andreae et al., 2015; Rissler et al., 2004; Rizzo et al., 2010, 2018) and in the range 5,700–10,000 cm^{-3} at sites in the Arc of Deforestation region (Artaxo et al., 2002; Brito et al., 2014; Rissler et al., 2006).

New particle formation and subsequent growth are rarely observed within the boundary layer in Amazonia (Andreae et al., 2015; Rissler et al., 2004, 2006; Rizzo et al., 2018; Zhou et al., 2002). Observations between 2008 and 2014 at a forest site in Amazonia report only 3% of new particle formation (NPF) event days (Rizzo et

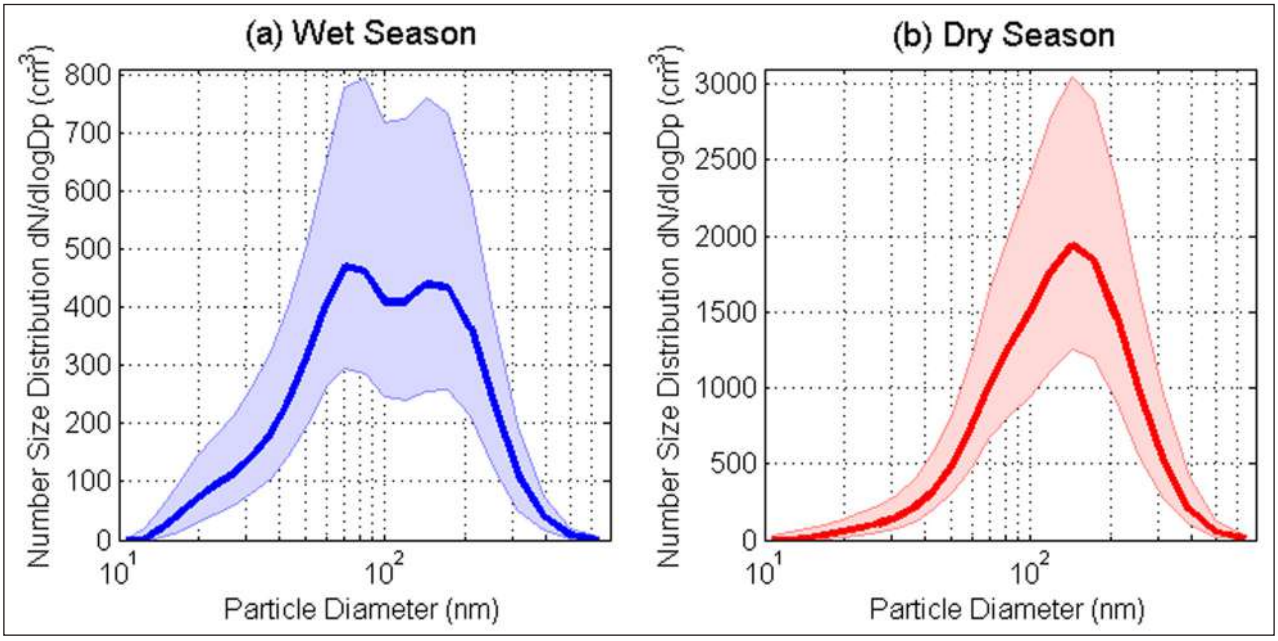

Figure 3.3.1 Median particle number size distributions at a forest site in Central Amazonia between 2008 and 2014 during the **(a)** wet and **(b)** dry season. Please note the different values in the Y-axis. Measurements were taken for dry aerosols under low RH conditions (30–40%) and 10 m above the canopy. Shadows represent the 25–75th percentile range. Data and analysis from Rizzo et al., 2018.

SEASON	LANDSCAPE	AIR MASSES	MODES	OCCURRENCE (%)	N (cm^{-3})	D_{pg} (nm)	σ_{pg}	REFERENCES
Wet	Forest	mostly clean	Accumulation	100	159–240	145–172	1.34–1.41	Pöhlker et al., 2016; Rissler et al., 2004; Rizzo et al., 2018; Zhou et al., 2002
			Aitken	92–100	167–475	67–70	1.34–1.50	
			Nucleation	18–79	40–191	17–25	1.31–1.50	
Wet-Dry transition	Forest	aged biomass burning	Accumulation	100	736	139	1.45	Rissler et al., 2004
			Aitken	100	304	68	1.32	
			Nucleation	55	276	15	1.29	
Dry	Forest	aged biomass burning	Accumulation	100	672–2670	144–179	1.48–1.51	Brito et al., 2014; Pöhlker et al., 2016; Rizzo et al., 2010, 2018
			Aitken	63–100	307–4071	71–98	1.35–1.78	
			Nucleation	19–38	6–948	14–33	1.60–2.50	
Dry	Pasture	fresh and aged biomass burning	Accumulation	–	5214	190	1.53	Rissler et al., 2006
			Aitken	–	5213	92	1.63	
			Nucleation	–	1090	12	1.82	
Dry-Wet transition	Pasture	aged biomass burning	Accumulation	–	785	128	1.66	Rissler et al., 2006
			Aitken	–	406	61	1.39	
			Nucleation	–	849	12	1.82	

Table 3.3.2 Ranges of reported mean values for submicrometer particle size distribution parameters in Amazonia for the aerosol modes: accumulation, Aitken, and nucleation (N: modal particle number concentration; D_{pg}: modal mean geometric diameter; σ_{pg}: modal geometric standard deviation). All measurements reported here were taken within the boundary layer and above the forest canopy.

al., 2018), a very low frequency compared to a boreal forest in Finland (24% of NPF event days, Dal Maso et al., 2005). At the remote boreal forest site, ZOTTO new particle formation events occurred only on 11 days in a 3-year period, suggesting that homogeneous nucleation with a subsequent condensational growth could not be the major process, maintaining the particle number concentration in the planetary boundary layer of the remote boreal forest area of Siberia (Wiedensohler et al., 2019). While NPF is uncommon, bursts of Aitken mode

particles without subsequent growth are observed in Amazonia during 28% of the measurement days, mostly in the wet season, both daytime and nighttime (Wang et al., 2016; Rizzo et al., 2018). The origin of such Aitken mode particle bursts is still unclear, and the absence of a clear diurnal pattern indicates that different processes may contribute to the observed particle bursts, such as vertical transport of particles (Wang et al., 2016), secondary aerosol formation, and primary biogenic emissions, such as the rupture of fungal spores (e.g., China et al., 2016).

Airborne observations in Amazonia have shown strong vertical gradients of particle number concentrations and submicrometer size distributions. Within the lower troposphere (less than 4 km), concentrations decrease with height. Within the upper troposphere (8 and 15 km), corresponding to the height of outflow of deep convective clouds, particle number concentrations can exceed boundary layer concentrations by one order of magnitude (Andreae et al., 2018; Krejci et al., 2003; Wang et al., 2016), showing a profusion of ultrafine particles (D_p < 90 nm). The origin of such particles is attributed to NPF driven by the upward transport of biogenic volatile organic compounds by deep convection (Andreae et al., 2018, Murphy et al., 2015). Sharp differences in the particle size distribution and chemical composition between the boundary layer and upper troposphere aerosols further support the occurrence of NPF, ruling out the convective transport of surface ultrafine particles as a source (Andreae et al., 2018). ***Figure 3.3.2*** illustrates the enhancement of Aitken mode particles as we move up from the boundary layer to the free troposphere. Enhancements on the accumulation mode above 10 km have also been reported, although less pronounced than the enhancement of ultrafine particles, with higher spatial variability (Glicker et., 2019; Andreae et al., 2018; Krejci et al., 2003; Schulz et al., 2018). This component is identified as isoprene-epoxydiol-derived secondary organic aerosol (IEPOX-SOA) (Schulz et al., 2018). The organic mass increase is accompanied by increased nitrate mass concentrations, most likely due to NO_x production by lightning. The authors also indicate that nitrate in the upper troposphere exists mainly in the form of organic nitrate. IEPOX-SOA and organic nitrates coincide with each other, indicating that IEPOX-SOA forms in the upper troposphere (UT) either on acidic nitrate particles forming organic nitrates derived from IEPOX or on already neutralized organic nitrate aerosol particles. Layers of enhanced accumulation mode particles in the upper troposphere can result from different processes, such as long-range transport, convective transport, and cloud processing.

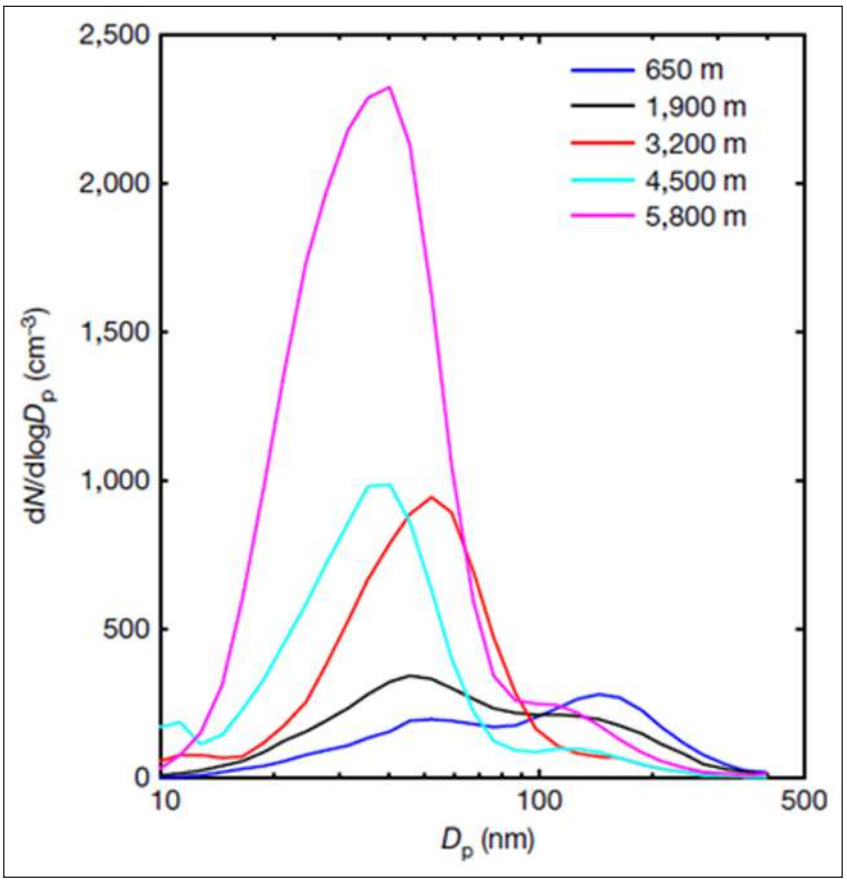

Figure 3.3.2 Airborne observations of submicrometer particle size distributions at five different altitudes above a forest area in Amazonia on 7 March 2014. Observations were taken on board the G-1 aircraft during the GoAmazon2014/15 experiment. Reproduced from Wang et al., 2016.

Observations and modeling studies indicate the downward transport of particles as an important source of submicrometer particles to the boundary layer at preserved forest sites in Amazonia (Rizzo et al., 2018; Wang et al., 2016, Krejci et al., 2003), and conceptual models have been proposed (see section 6.2). The downward transport of particles to the boundary layer can occur by convective downdraft events. The level of origin of convective downdrafts in Amazonia is typically in the range of 1.5–2.5 km (Betts et al., 2002; Schiro and Neelin, 2018). A hypothesis is that new particles formed in the outflow region of deep convective clouds (~10 km) are transported to the lower free troposphere by slow subsidence, growing to the Aitken mode by condensation and coagulation. Afterward, convective downdrafts during precipitation events would rapidly transport the Aitken mode particles into the boundary layer (Andreae et al., 2018; Wang et al., 2016). However, the precise mechanisms of new particle formation and growth at the free troposphere and the vertical transport of particles into the boundary layer are not completely understood and require more investigation.

In addition to the downward transport of Aitken mode particles to the boundary layer, observations and modeling studies indicate two other submicrometer particle sources in Amazonia: entrainment of accumulation mode particles, either from in-cloud processing or long-range transport; and primary emission of Aitken mode particles at night within the boundary layer (Rizzo et al., 2018). The mechanism for the latter particle source is still unclear but could be related to the rupture and wet discharge of fungal spores (China et al., 2016; Elbert et al., 2007) (see 3.2.1–3.2.4).

3.3.2. Boreal forests aerosol size distribution

The aerosol size distribution over the boreal region has been characterized in numerous studies. Still, the two longest aerosol time series over boreal forests reported here are from the Hyytiälä SMEAR II station (Station for Measuring Forest Ecosystem-Atmosphere Relations), Southern Finland (Kulmala et al., 2001; Vesala et al., 1998), and the ZOTTO tower (Heimann, 2008). In the Fenno-Scandinavia region, the average number concentration is highly dependent on geographical location; observations from stations further north on average yield higher integral number concentration than at stations located in the southern rim of the boreal region. For example, Tunved et al. (2003) report annual average number concentration of nucleation mode particles of 50–100 cm^{-3}, Aitken mode particles of ca 200 $cm^{-3,}$ and accumulation mode particle concentration of ~150 cm^{-3} at the two northern stations (~67°N) Värriö and Pallas (e.g. (Komppula et al., 2006; Dal Maso et al., 2007) to be compared with 300 cm^{-3} nucleation mode size particles, and 750 cm^{-3} and 290 cm^{-3} in Aitken and accumulation mode size range, respectively, at Hyytiälä. Even a little further south, and across the Baltic to the west, the annual average concentration for each of the three modes at the Swedish site Aspvreten (58°48′39.5″ N 17°23′54.8″ E) was reported to be 300, 1200 and 390 cm^{-3} in nucleation, Aitken, and accumulation mode size range.

By performing more detailed studies during both northerly transport and southerly transport across Fenno-Scandinavia, it has been concluded that the boreal region acts as a net source of particle number during southward transport of clean marine air (Tunved et al., 2006a; Vaananen et al., 2013; Tunved et al., 2006b), while acting as a sink when polluted air is transported northwards. During the southward transport, the forest plays an active role in particle formation and growth. During northerly transport, transport of air masses with a comparable high condensation sink leads to more rare nucleation events, and predominantly sink processes affect the aerosol size distribution, in particular wet deposition (Lehtinen et al., 2003).

These previous results highlight that anthropogenic sources play an important role in shaping the aerosol over the Fenno-Scandinavian parts of the boreal region. The "true" un-perturbed boreal signal can only be found in air masses transported over moderately unpopulated regions in the Northern parts. Heintzenberg et al. (2013) investigated potential source regions of air masses reaching ZOTTO through ten-day back trajectories for the period 2006–2011, which covered large parts of the Eurasian landmass. The back trajectories touched major anthropogenic source regions along the string of urban areas along the Trans-Siberian railway corridor and Siberian fire regions. Even Middle East midlatitude sources and possibly emissions from Northern China may be seen at times at ZOTTO (Heintzenberg et al., 2013). As over Fenno-Scandinavia, the least perturbed air masses can be expected during north to northeasterly wind flow.

In ***Figure 3.3.3***, the seasonal median and 25th–75th percentile ranges for size distributions observed at Hyytiälä (red) and ZOTTO (green) are shown. In general, the integral number concentration is much lower at ZOTTO compared to Hyytiälä. The median integral number observed at ZOTTO is 720 cm^{-3} (620–750 cm^{-3} as 25^{th}–75^{th} percentile range), and 1820 cm^{-3} (1360–2210 cm^{-3} as 25^{th}–75^{th} percentile range) at Hyytiälä. It is also clear from ***Figure 3.3.3*** that the largest difference in number concentration is found in the sub-100nm size range as well as the seasonal variation is much more pronounced at Hyytiälä; the period March–May has a bimodal structure, with a dominant Aitken mode and the average integral concentration is around 2220 cm^{-3}. During the summer (June–August), Hyytiälä observations on average give nearly mono-modal size distribution with an average concentration of 2160 cm^{-3}. The autumn period (September–November) exhibits an average of 1450 cm^{-3} with a distinct bimodal structure of the size distribution. Wintertime (December–February) is associated with the

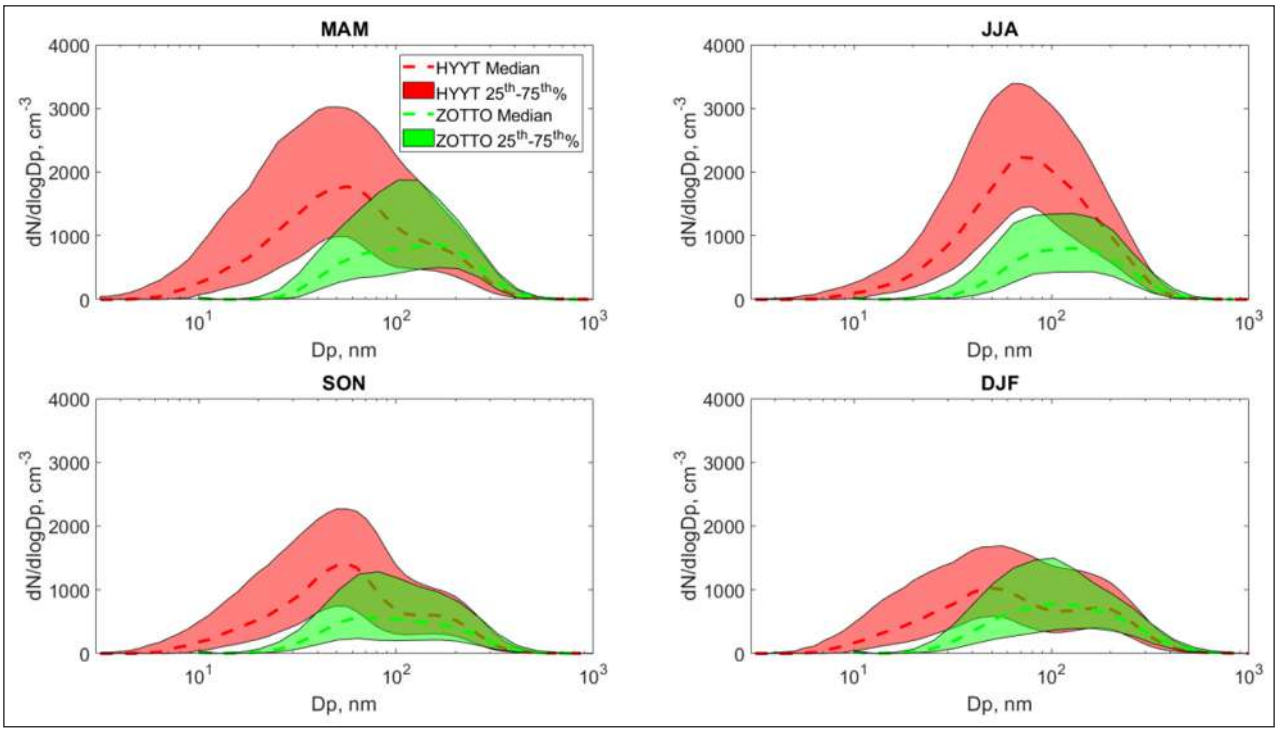

Figure 3.3.3 Particle number size distribution for boreal forest sites. Seasonal median and 25th–75th percentile ranges in the shaded areas of size distributions observed at Hyytiälä (HYYT) and ZOTTO 2006–2011 are shown. The timing of each analysis is coded as MAM: March–May; JJA: June–August; SON: September-October; DJF: December–February.

lowest number concentration, around 1260 cm^{-3}, and bimodal size distribution with almost equal fractions of accumulation mode and Aitken mode particles.

The seasonal behavior of ZOTTO aerosols is somewhat different. During the spring, the size distribution is as in Hyytiälä bimodal but dominated by accumulation mode-sized particles. The number concentration is on average 760 cm^{-3}, about one-third of the average integral number concentration observed at Hyytiälä. The summertime distribution is also more monomodal at ZOTTO as in the case for Hyytiälä, and integral number concentrations are substantially lower, about 750 cm^{-3}, but on average with a larger average size of the mode. Autumn size distributions at ZOTTO are again generally bimodal with integral number concentration around 530 cm^{-3}. The wintertime size distribution at ZOTTO is in contrast to Hyytiälä, almost monomodal on average. It is furthermore only marginally lower in integral number concentration compared to spring and summer periods. Fitted model parameters for both sizes per season are given in ***Tables 3.3.3*** and ***3.3.4*** for Hyytiälä and ZOTTO, respectively.

Hyytiälä and ZOTTO measurements on boreal aerosol size distributions were clustered in Wiedensohler et al., 2019, and a maximum number of eight clusters is judged to be enough to capture the variability of the aerosol number size distribution at the two boreal stations. The clustering is performed separately for each of the two boreal sites. The clustering revealed that about 10% of the measured size distribution in Hyytiälä was showing ongoing to recent NPF dominating the size distribution. At ZOTTO, only possible remains of NPF were found in about 1% (Wiedensohler et al., 2019). They found that new particle formation events in the boundary layer occurred only on 11 days in 3 years, suggesting that homogeneous nucleation with a subsequent condensational growth is not a major process in maintaining the particle number concentration in the planetary boundary layer at ZOTTO. However, as the lower size cut for the sampling system was 10 nm and growth rates can be expected to be low, there is a possibility that there is a larger fraction of interrupted events, which is classified as undefined. The number undefined found at ZOTTO was 83, i.e., a considerably larger fraction than found at Hyytiälä (Buenrostro Mazon et al., 2009) but still a much lower number. The ZOTTO distributions generally show much larger median sizes for submicrometer particles indicating aged aerosol. Investigating the occurrence of fires along the transport path showed that almost 30% of the distribution was influenced by smoke from forest fires at ZOTTO, while such influence was absent at Hyytiälä. Hyytiälä had influence from other sources, probably anthropogenic in more than 70% of the size distributions.

The difference in NPF at the two boreal sites is the most striking in the aerosol distribution at the two sites. The NPF at Hyytiälä is detected in clean air masses arriving from the Arctic Sea or very North Atlantic, often less than a day's transport away, while ZOTTO is located 1500 km from the Siberian coast in the central Siberia, and the sampling at ZOTTO is at 300-meter altitude while the aerosol in Hyytiälä is sampled just above the forest

MODE	DG-RANGE (μm)	# OBSERVATIONS	N (cm^{-3})	Dg (μm)	GSD
March-April-May					
Nuclei	0.001–0.025	9052	321	0.012	1.4
Aitken	0.025–0.07	6899	2131	0.044	1.6
Acc1	0.07–0.25	8953	854	0.148	1.6
Acc2	0.25–1.0	2620	10.4	0.403	1.5
June-July-August					
Nuclei	0.001–0.025	8269	111	0.013	1.4
Aitken	0.025–0.07	5790	1921	0.045	1.5
Acc1	0.07–0.25	8995	1742	0.138	1.5
Acc2	0.25–1.0	3593	7.4	0.419	1.4
September-October-November					
Nuclei	0.001–0.025	8203	167	0.013	1.4
Aitken	0.025–0.07	6665	1458	0.046	1.6
Acc1	0.07–0.25	7931	549	0.155	1.6
Acc2	0.25–1.0	2611	8.9	0.401	1.4
December-January-February					
Nuclei	0.001–0.025	8878	172	0.013	1.3
Aitken	0.025–0.07	7153	1175	0.045	1.6
Acc1	0.07–0.25	8913	763	0.159	1.6
Acc2	0.25–1.0	2187	20.1	0.375	1.5

Table 3.3.3 Statistical representation of modal parameters derived from fitting, per season, for Hyytiälä 2006–2011. Data presented as 50th percentile of fitted parameters. N represents the number of particles in the mode, Dg is the geometrical diameter, and GSD is the geometric standard deviation.

canopy. The NPF processes will be reviewed more in detail in section 4.4. The influence of forest fires is as well very different at the two sites, as well as the influence of other long-distance transported anthropogenic sources. This indicates that the composition of the boreal atmosphere is very variable due to the influence of various sources. Thus, it is difficult to exactly identify and quantify the natural emission of the boreal forest and thus its influence on the composition of the atmosphere and its function.

3.4. AEROSOL HYGROSCOPIC PROPERTIES AND CCN ACTIVATION

The hygroscopic properties of aerosol constituents govern the water content of atmospheric aerosol particles and the role these particles can play in cloud droplet formation. Most particles take up water at relative humidity (RH) below 100%, which has consequences for various chemical processes taking place in the atmosphere and the light scattering and absorption by atmospheric aerosol, thus affecting climate directly. Hygroscopicity influences which particle forms cloud droplets, thus affecting the radiative properties of clouds and hence influencing climate indirectly (Spracklen et al., 2008; Rosenfeld et al., 2014; Freud et al., 2008a, 2008b, Pöhlker et al., 2016, 2018).

The capacity of a given particle to take up water at subsaturated conditions or act as CCN depends on the chemical composition and size of the particle and is usually described by equilibrium thermodynamics (see, e.g., Köhler, 1936; Rissler et al., 2006; Petters and Kreidenweis, 2007). In many cases, these standard approaches are enough when combined with the aerosol composition and size distribution knowledge. However, more detailed theories are warranted if there are, e.g., significant particle-phase chemistry, phase separation, or transport processes taking place (McFiggans et al., 2006). There is also evidence that in some conditions, aerosol particles' hygroscopic growth and CCN behavior can depend on the saturation ratio of other vapors than water present in the system (e.g., Topping et al., 2012; Murphy et al., 2015). Furthermore, atmospheric aerosol particles mostly consist of complex mixtures of organic and inorganic compounds in various physical phases ranging from completely dry particles or highly concentrated solutions to very dilute aqueous solutions, depending on the RH.

The water uptake by individual aerosol particles at subsaturated conditions is often quantified using the

MODE	DG-RANGE (μM)	# OBSERVATIONS	N(cm^{-3})	Dg(μm)	GSD
March-April-May					
Nuclei	0.001–0.025	2034	5.6	0.013	1.2
Aitken	0.025–0.07	6641	229	0.045	1.3
Acc1	0.07–0.25	9255	716	0.144	1.5
Acc2	0.25–1.0	1936	76.3	0.299	1.3
June-July-August					
Nuclei	0.001–0.025	3210	4.9	0.014	1.3
Aitken	0.025–0.07	6255	142	0.042	1.3
Acc1	0.07–0.25	9522	691	0.14	1.5
Acc2	0.25–1.0	2950	37.4	0.345	1.4
September-October-November					
Nuclei	0.001–0.025	4459	5.1	0.014	1.2
Aitken	0.025–0.07	9928	250	0.045	1.4
Acc1	0.07–0.25	12566	534	0.144	1.5
Acc2	0.25–1.0	2772	17	0.345	1.4
December-January-February					
Nuclei	0.001–0.025	2087	5.7	0.011	1.2
Aitken	0.025–0.07	4999	238	0.044	1.4
Acc1	0.07–0.25	6767	817	0.137	1.6
Acc2	0.25–1.0	1162	168	0.293	1.5

Table 3.3.4 Statistical representation of modal parameters derived from fitting per season at the ZOTTO tower 2006–2011. Data presented as 50th of fitted parameters.

hygroscopic diameter growth factor (Gf), defined as the ratio between the wet particle diameter at a given RH (< 100%) and the dry diameter of the particle at RH ≈ 5–10%. The Gf can be measured directly by the Hygroscopic Tandem Differential Mobility Analyzer (H-TDMA) technique, which has been applied in various environments all over the globe, including tropical and boreal forests (Swietlicki 2008; Schmale et al., 2018). Cloud Condensation Nucleus Counters (CCNC) measure the number of particles that have grown to activated cloud droplets at a certain supersaturation, often in the range of approximately 0.1 to 1% (Roberts et al., 2002; Rose et al., 2008).

3.4.1. Hygroscopicity parameter κ in boreal and tropical environments

To parameterize and compare measurements of Gf and CCN, a commonly used conceptual model is based on the realization that, to a first-order approximation, the hygroscopic growth and CCN activation of aerosol particles is determined by the number of soluble ions or molecules per dry particle volume, often denoted by the hygroscopicity parameter κ. For a fully soluble particle, κ can be approximated by $\kappa \approx i_s \cdot \rho_s / M_s \cdot M_w / \rho_w$, where i_s stands for the van't Hoff factor of the solute, ρs, and M_s is the density and molar mass of the solute, and ρ_w and M_w are the density and molar mass of water, respectively (Petters and Kreidenweis, 2007, Rose et al., 2010). We notice that kappa is related to the physicochemically well-defined and well-established van't Hoff factor of the solute (i_s) rather than a purely stoichiometric dissociation coefficient or "number of ions" (ν). Usually, the hygroscopicity parameter κ refers to the volume of aerosol particles and components, but it can also be applied on a mass basis (Mikhailov et al., 2013). In principle, measurements of the subsaturated particle growth (using, e.g., an H-TDMA) and the supersaturated particle growth (using a CCNC) can be used to quantify κ for a given aerosol particle population – or the other way around, if κ and the aerosol distribution are known, hygroscopic growth and CCN activation can be predicted (for instance Gunthe et al., 2009, Rissler et al., 2010). ***Figure 3.4.1*** presents a compilation of hygroscopic properties of atmospheric aerosols from tropical rainforest air (AMAZE) and rural boreal air (SPB), with three different hygroscopic regimes identified.

Limitations to such a simplified approach include the variability in κ over the range of RH as a result, e.g. (i) solution non-ideality effects including solubility limitations (Reutter et al., 2009, Riipinen et al., 2015;

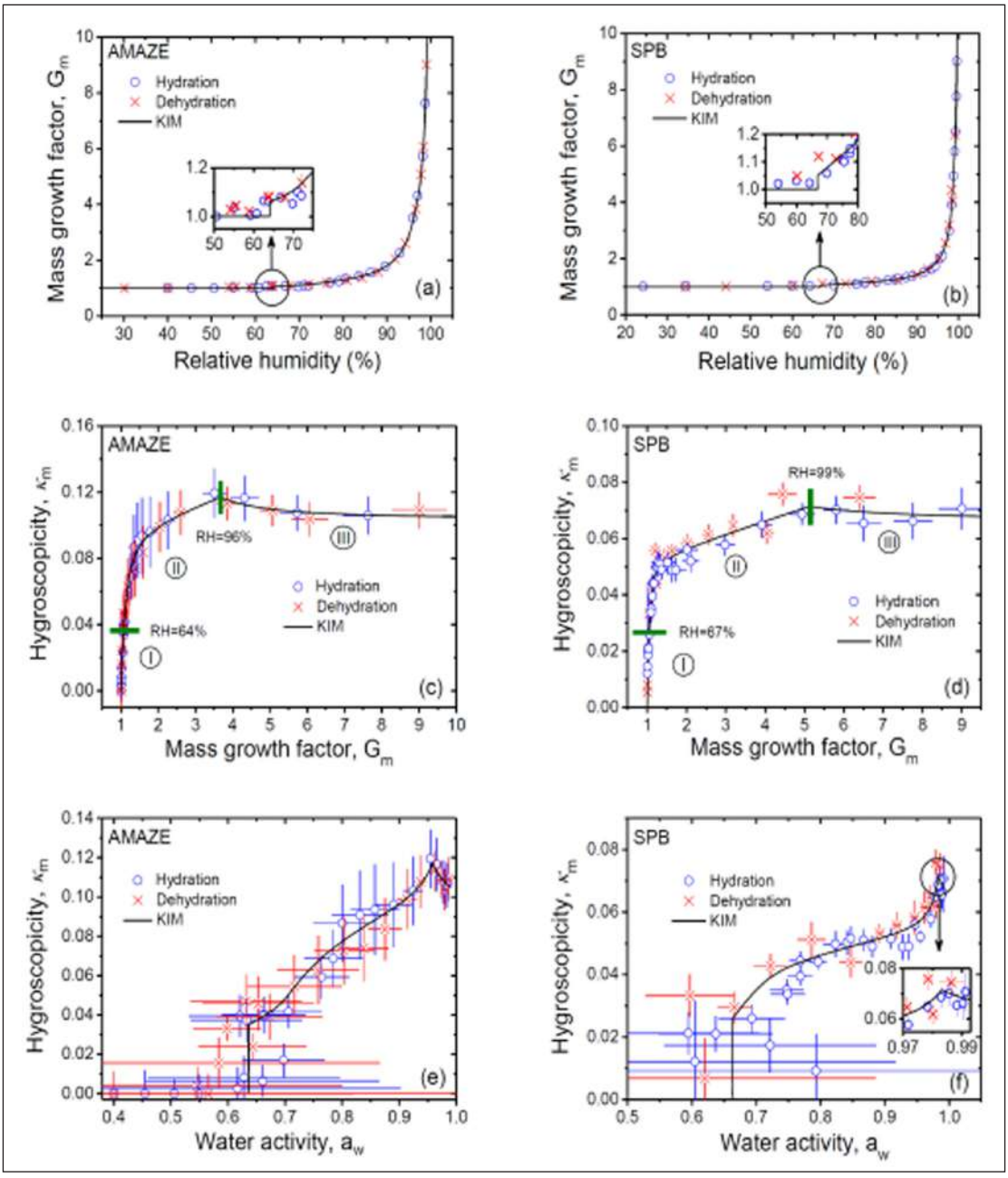

Figure 3.4.1 Hygroscopic properties of atmospheric aerosols from tropical rainforest air (AMAZE) and rural boreal air (SPB). Three different hygroscopic regimes are identified: (I) a quasi-eutonic deliquescence and efflorescence regime at low-humidity where substances are just partly dissolved and also exist in a non-dissolved phase; (II) a gradual deliquescence and efflorescence regime at intermediate humidity where solutes undergo gradual dissolution or solidification in the aqueous phase; and (III) a dilute regime at high humidity where the solutes are fully dissolved. **(a, b)** mass growth factors (Gm) were observed as a function of relative humidity compared to a mass-based κ interaction model (KIM) they developed; **(c, d)** κ_m calculated as a function of mass growth factor and **(e, f)** κ_m plotted against water activity. The data points and error bars (mean value ±standard deviation) are from FDHA experiments of hydration (blue circles) and dehydration (red crosses). The black lines are fits of κ_m – interaction model (KIM). From Mikhailov et al., 2013.

Rastak et al., 2017); (ii) surface-to-bulk partitioning of surface-active compounds (e.g., Ruehl et al., 2016; Ovadnevaite et al., 2017); (iii) condensation and evaporation of gas-phase compounds (e.g., Topping et al., 2012); (iv) kinetic effects related to particle-phase transport processes (e.g., Shiraiwa et al., 2017). Indeed, differences in the κ values measured for the same aerosol in sub- vs. supersaturated conditions have been reported, specifically when it comes to the complex organic fraction (Zhang et al., 2017). Also, field studies on tropical and boreal forests report lower κ values at subsaturated than supersaturated conditions (***Figure 3.4.1*** and, e.g., Cerully et al., 2011; Zhao et al., 2016; Paramonov et al., 2013; Whitehead et al., 2016, Mikhailov et al., 2015). This is probably caused by the gradual dissolution of a multitude of poorly water-soluble compounds as RH increases (e.g., Rastak et al., 2017, ***Figure 3.4.1***). With these limitations in mind, these observations of κ values suggest that the

aerosol in the tropical forest environments is generally more hygroscopic than in the boreal zone. However, the differences are relatively small (***Figure 3.4.1***), especially compared with the variability in the other relevant parameters (e.g., aerosol size).

Several studies report different hygroscopic properties of the aerosol particles for the boreal forest, as listed in ***Table 3.4.1***. Cerully et al. (2011) report HTDMA-derived κ values that were generally 30% lower than the CCNC values. A later study by Hong et al. (2014) report observations from

CAMPAIGN, LOCATION, YEAR	INSTRUMENT, TECHNIQUE	SEASON, TIME PERIOD	*S* [%]	D_a [nm]	κ_{CCN}	N_{CCN} [cm^{-3}]	*D* [nm]	κ_{HTDMA}	REFERENCE
Tropical forests									
AMAZE-08, observational tower (TT34), Amazon, Brazil, 2008	Size resolved CCN	wet season, 14 February –12 March 2008,	0.10 0.19 0.28 0.46 0.82	199 128 105 83 55	0.2 0.2 0.17 0.12 0.13	41 90 114 141 194	–	–	Gunthe et al., 2011, Martin et al., 2010
OP3 project, Global Atmospheric Watch (GAW) station, tropical rainforest in Borneo, Malaysia, 2008	Size resolved CCN, HTDMA	3 July –20 July 2008	0.63 0.56 0.51 0.48 0.47 0.43 0.26 0.25 0.18 0.18	65 74 84 96 110 129 148 171 199 224	0,13 0,1 0,09 0,07 0,05 0,04 0,05 0,6 0,06 0,06	–	32 53 104 155 208 259	0,20 0,17 0,21 0,24 0,27 0,30	Irwin et al., 2011
observational tower (TT34), Amazon, Brazil, 2013	Size resolved CCN, HTDMA	transition season, 4–28 July 2013	0.15 0.26 0.47 0.8 1.13	152 105 78 56 45	0.18 0.18 0.13 0.12 0.12	87 161 212 248 268	45 69 102 154 249	0.09 0.09 0.12 0.15 0.17	Whitehead et al., 2016
GoAmazon2014/5, ATTO, Amazon, Brazil, 2014–2015	Size resolved CCN	Annual average, March 2014–February 2015	0.11 0.15 0.2 0.24 0.29 0.47 0.61 0.74 0.92 1.1	172 136 117 105 98 77 63 57 49 43	0.22 0.22 0.21 0.19 0.17 0.13 0.14 0.13 0.13 0.13	275 457 571 652 719 883 900 941 987 1013	–	–	Pöhlker et al., 2016
Boreal forests									
SMEAR II station, Hyytiälä, Finland, 2007	Size resolved CCN, CFSTGC and HTDMA	Spring, 25 March–15 May 2007	1.1 0.61 0.36	40 60 80	0.2 0.29 0.22	–	30 50	0.15 0.14	Cerully et al., 2011
SMEAR II station, Hyytiälä, Finland, 2008–2009	Size resolved CCN, HTDMA	Summer, July 2008–June 2009	0.1 0.2 0.4 0.6 1	– – – – –	– – – – –	169 346 546 678 894	–	–	Sihto et al., 2011
SMEAR II station, Hyytiälä, Finland, 2009–2012	Size resolved CCN	Annual average, January 2009–April 2012	0.1 0.2 0.4 0.6 1	174 114 88 73 57	0.26 0.23 0.13 0.1 0.07	–	–	–	Paramonov et al., 2013
HUMPPA-COPEC, SMEAR II station, Hyytiälä, Finland, 2010	Size resolved CCN, VH-TDMA	Summer, 12 July–12 August 2010	0.09 0.22 0.48 0.74 1.26	41 55 70 102 203	0.12 0.14 0.17 0.28 0.22	–	50 75 110	0.12 0.12 0.15	Hong et al., 2014

Table 3.4.1 Summary of hygroscopicity observations at tropical and boreal sites. S, D_a, $\kappa_{CCN,}$ and N_{CCN} are the set supersaturation, observed activation diameter, calculated κ, and the number of activated particles as measured with the CCNC. For the HTDMA measurements, set diameter D and calculated κ from the measured growth factor.

the year 2010 and also yielded higher values for CCNC-derived than HTDMA-derived κ, although with lower κ for supersaturated conditions than reported by Cerully et al. but with a lower difference between supersaturated and subsaturated κ. The difference to Cerully et al. (2011) is probably due to a greater biogenic SOA contribution in the summer period (see 3.4.2 below). Sihto et al. (2011) report an average GF-derived κ of 0.18, which agrees well with what was derived with the CCNC. Paramonov et al. (2013) report 29 months of hygroscopicity and size-resolved CCN data from Hyytiälä. These CCN data correspond to a bimodal κ distribution with κ for Aitken mode particles of ~ 0.1 and κ for Aitken mode particles ~ 0.25. This is a possible indication of the addition of soluble material by cloud processing (see 3.4.2 and Hong et al., 2015). The range of hygroscopicity values reported for the SMEAR II site at Hyytiälä and the difference between sub- and supersaturated conditions are generally in line with laboratory studies conducted with biogenic SOA (e.g., Pajunoja et al., 2015; Rastak et al., 2017 and references therein), which is indeed a dominant component of the aerosol particles in the boreal forest (see 3.1).

Size-resolved CCN measurements in the Amazon were conducted during the AMAZE-08 campaign (***Table 3.4.1***.; Gunthe et al., 2009; Martin et al., 2010a). The observed κ values ranged between 0.13 and 0.20 (***Table 3.3.1***). Whitehead et al. (2016) reported κ derived from CCNC data ranged from 0.12 to 0.18 in excellent agreement with values derived from subsaturated measurements, ranging from 0.09 to 0.17. These agree well with measurements in the Amazon (e.g., Gunthe et al., 2009, Whitehead et al., 2016) but are lower than similar measurements in the Bornean rainforest (0.17 to 0.37 at 90% RH, Irwin et al., 2011). Results from size-segregated CCN measured over one year at the ATTO site (Pöhlker et al., 2016) show the κ values at this site to be rather constant the range of 0.13 to 0.22, despite the large differences in the aerosol particle number concentrations (NCN) in the wet (NCN ~ 320 cm^{-3}) vs. the dry (NCN ~ 1500 cm^{-3}) seasons, no substantial diurnal patterns of aerosol hygroscopic properties were found by Pöhlker et al., (2016). No significant CCN-inactive fraction was found for a supersaturation S > 0.11% during all seasons except the biomass burning season. This is probably due to the dominance of organics in the aerosol composition during both the wet and the dry season. The key features and contrast between pristine and polluted conditions in the Amazon rainforest are discussed in detail by Pöhlker et al., 2018. During the GoAmazon2014/5 campaign size-resolved CCN measurements at the T3 site, 60 km downwind of the city Manaus have shown a constant hygroscopicity of the organic component of the aerosol (κ_{OA}) of 0.15 and a high O:C ratio of 0.8 under background conditions (Thalman et al., 2017).

Irwin et al. (2011) report on sub- and supersaturated measurements in Borneo, Malaysia, from March to July 2008, where the CCNC-derived κ decrease with particle size from 0.20 (Aitken mode) to 0.05 (accumulation mode) – in contrast with the other environments discussed. On the other hand, κ derived from the HTDMA data shows an increase in particle diameter (from 0.2 to 0.3 between the Aitken and accumulation modes). All in all, the reported values observed in the various field studies are relatively similar, being generally of the order of 0.1 with considerable variation caused by, e.g., variability in the chemical composition and the origin of the particle population (see 3.4.2 and 3.4.3). However, while values also clearly below 0.1 have been reported for the boreal forest, such observations are scarce for the tropical rainforest. In both boreal and tropical forests, the biogenic organic component dominates the aerosol hygroscopicity (see section 3.1). To understand the factors controlling the hygroscopicity and CCN activity in these environments, the properties (e.g., the origin and the oxidation state) of the organic molecules and the mass fraction of the inorganic material present need to be known.

3.4.2. Influence of aerosol composition on hygroscopicity

Numerous studies report considerably smaller κ values for most organic aerosol (OA) compounds compared to common inorganic aerosol (IA) substances. Observed hygroscopicities of OA are generally in the range κ_{OA} = 0.03–0.2 (Zhao et al., 2016; Cerully et al., 2011, Dusek et al., 2010; Gunthe et al., 2009, Jurányi et al., 2009; Rose et al., 2010, 2011; Topping et al. 2011), compared to, e.g., κ_{AS} of about 0.6 for ammonium sulfate and κ_{NaCl} of about 1.1 for sodium chloride (e.g., Petters and Kreidenweis, 2007). While the average hygroscopicity values reported for the boreal and tropical sites (see Sect. 3.4.1) are generally in line with organic aerosol hygroscopicity, even small amounts of inorganic compounds can significantly increase particle hygroscopicity during periods of significant anthropogenic influence, or, as Paramonov et al. (2013) suggest, as a signature of cloud processing. Schmale et al. 2018 relate the observed organic-to-inorganic mass ratio (denoted as OA/IA) to κ values derived from observed chemical compositions at a variety of sites, including the SMEAR II site at Hyytiälä and ATTO (see ***Figure 3.4.2***), illustrating the importance of knowing not only the inorganic contribution to the aerosol composition but also its composition, e.g., Mace Head, Ireland (MHD) having a strong influence of sea salt, Hyytiälä, (SMEAR II) of ammonium sulfate and ATTO, Amazon (ATT) of sulfuric acid.

The average hygroscopicity values Cerully et al. (2011), Sihto et al. (2011), and Hong et al. (2014), as well as Pöhlker et al. (2016, 2018), report is generally in line with expected κ values for organics with various levels of oxidation (Jimenez et al., 2009; Pajunoja et al., 2015 and references therein). Furthermore, Cerully et al.

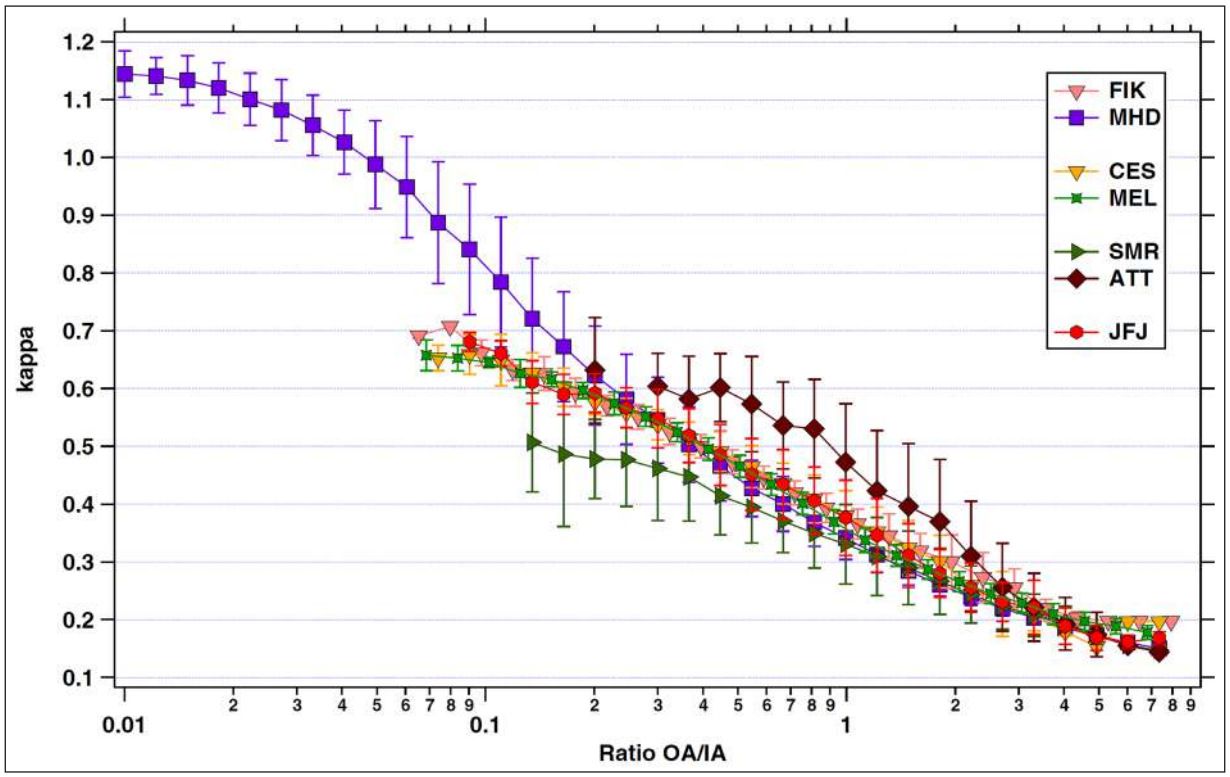

Figure 3.4.2 Relationship of the composition-derived hygroscopicity parameter κ to the binned and averaged ratio of organic (OA) to inorganic (IA) aerosol components (Schmale et al., 2018) for seven different measurements sites: FIK = Finokalia, Crete; MHD = Mace Head, Ireland; MEL = Melpitz, Germany; SMR = Hyytiälä, Finland; ATT = ATTO tower, Amazon; JFJ = Jungfraujoch, Switzerland. Note that the asymptotic-like approach of the curves towards 0.1 is due to the assumption of $\kappa_{OA} = 0.1$.

(2011) report diurnal trends of κ showing a minimum at sunrise and a maximum in the late afternoon, co-varying with inorganic mass fraction and the AMS m/z 44 organic mass fractions related to oxidized organic molecules. For the tropical forest, Thalman et al. (2017) report lower hygroscopicity of the organic mass fraction in aerosols influenced by urban pollution compared to background conditions (κ_{OA} ~ 0.11–0.14 vs. 0.13–0.17, respectively), explained by the lower contribution of highly oxygenated organic compounds (based on the fraction of m/z 44 and O:C ratio from AMS). Therefore, the role of the organic fraction in dominating the hygroscopic properties and CCN activation of aerosol particles in these two environments is well established.

Several factors are proposed as an explanation to the small κ_{OA} values as compared to those for the common inorganics, including (i) Organic substances, are often non-polar or only slightly polar, which leads to low solubility in water; (ii) Molecular weights are often larger for organic compared to inorganic compounds; (iii) Organic salts and acids are weak electrolytes and acids and show weak dissociation into ions; (iv) Oligomerization of organic compounds may occur in the particle phase; (v) Gas-to-particle partitioning for semi-volatile organic compounds may result in loss of soluble material lost from particles; (vi) Highly viscous particles may limit diffusion within particles of, for instance, ozone, leading to a reduction in oxidation rates (see, e.g., Topping et al., 2011 and references therein). All these factors reduce the number of water-soluble molecules and ions in the aerosol particles, thus limiting hygroscopic growth and CCN activation. Furthermore, organic aerosol hygroscopicity tends to be confined to a relatively narrow range around values of the order of 0.1 at atmospheric RHs, due to, e.g., a relatively small variation in the molecular properties of the relevant organic compounds (see, e.g., Topping et al., 2011; Cerully et al., 2015; Riipinen et al., 2015). However, some variability arises from the differences in the identities and properties of the organic molecules present in the particles. A growing understanding of the mechanisms behind the influence of the organic component on hygroscopicity and CCN activation has developed during recent years with the use of complex multi-parameter ion and molecule interaction models (Mikhailov et al., 2013, Pajunoja et al., 2015, Rastak et al., 2017).

An obvious difference between the boreal and the tropical forest aerosol is the dominant precursor vapors for the secondary aerosol component: monoterpenes (MT) dominate the VOC species emitted from the boreal forests. In contrast, isoprene (ISP) dominates the tropical environment (see Sect. 4.1). The SOA resulting from oxidation of these BVOC shows low but slightly different κ_{OA} values, which are only readily observable under controlled laboratory conditions. Pajunoja et al. (2015) conducted flow reactor experiments to examine pure SOA particles formed by OH and/or O_3 oxidation of ISP and MT and determined κ_{SOA} at sub- and supersaturated

conditions. At subsaturated conditions (RH < 95%), MT-SOA show lower κ values than ISP-SOA, 0.10 and 0.14, respectively. Both SOA types show an increase in κ_{SOA} with an increased degree of oxidation and increasing RH – although the latter effect is less pronounced for ISP-SOA than MT-SOA. However, it should be noted that these experiments are done for pure SOA, where an aqueous phase is often nearly absent at low RHs. This is not typical for atmospheric forest aerosols, where small amounts of IA can cause particles to contain water also at low RHs. The differences in κ_{SOA} values for MT-SOA and ISP-SOA are considerably smaller at supersaturation, conditions at which both MT-SOA and ISP-SOA are nearly completely soluble (Pajunoja et al. 2015; Rastak et al. 2017). For comparison, smog chamber experiments on anthropogenic SOA from toluene and xylene compounds with OH doses equivalent to 1–4 days of OH exposure in the atmosphere yielded κ_{SOA} values of around 0.1 (Zhao et al. 2016).

3.4.3. Influence of size-dependent chemistry on the hygroscopicity

For the boreal and Amazonian Forest environments, κ is found to be size-dependent, with Aitken mode κ being lower than that of the accumulation mode particles (Gunthe et al., 2009; Paramonov et al., 2013; Pöhlker et al., 2016; Pöhlker et al., 2018). This is likely caused by, e.g., in-cloud processing of activated aerosol particles, with more secondary inorganic compounds (sulfates and nitrates) in the larger size accumulation mode range. Since tropical and boreal forest environments are often limited in the availability of gas-phase sulfur and nitrogen compounds as compared with the organics, the difference between the Aitken and accumulation mode κs, however, relatively small, with the exception of pollution episodes (e.g., Thalman et al., 2017). Nucleation mode particle composition and hygroscopicity are expected to be governed by the condensable vapors present at the measurement sites, similarly to the Aitken mode. In contrast, the accumulation mode is often more aged and reflects more long distant anthropogenic sources as seen in particles 100 nm and larger for Hyytiälä in ***Figure 3.4.3***. If urban emissions are impacting, they will subsequently affect the hygroscopic properties for all size ranges (Thalman et al., 2017).

As discussed above, the chemical composition gives rise to differences in the hygroscopic growth factors and thus CCN activities of natural boreal and tropical aerosol particles. However, these differences are probably relatively small in the context of aerosol-climate interactions, as compared with, e.g., the uncertainty in the overall OA budget (see 3.1) or its impacts on aerosol size distribution (e.g., Rastak et al., 2017, see 3.3 and 4.4). As pointed out, the fraction of inorganic salts strongly affects the hygroscopicity of the aerosol, which is particularly noticeable in the accumulation mode particles for anthropogenic affected aerosols.

However, as discussed in sections 4.4 and 6, the new particle formation in the upper troposphere subsiding into the boundary layer include a natural chemical and physical transformation, i.e., aging producing a boundary layer aerosol of oxidized condensable compounds that most likely is more hygroscopic (Andreae et al., 2018). Similar nucleation and particle growth might be an important natural source for the boundary layer aerosol in the continental boreal regions (e.g., Section 4.4). The natural continental boreal aerosol and its interaction with clouds might be similar to the Amazon during warm summer. However, further research is warranted in comparing the chain of processes leading from emission

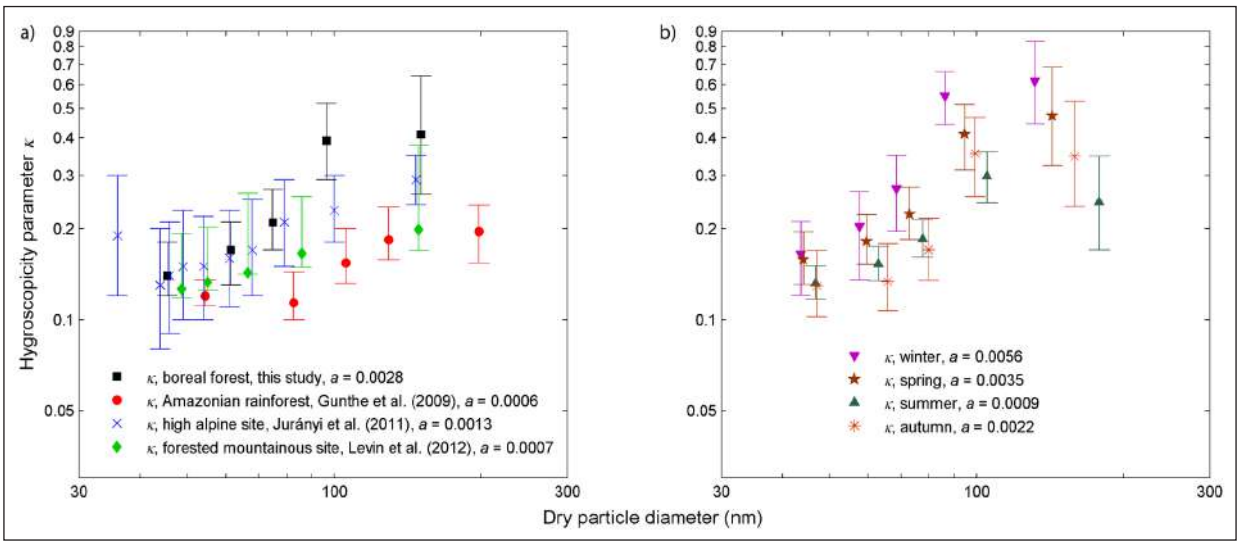

Figure 3.4.3 Relationship between dry particle diameter and κ for boreal and tropical forests, as well as the seasonality of κ for Hyytiälä. In **(a)**, we can observe the comparison among sites; in **(b)**, we can see the comparison among seasons for Hyytiäla. Both panels show the median values, with error bars being 25th and 75th percentiles. Legend entries also indicate the slope of the linear regression y = ax + b fit. Figure from Paramonov et al., 2013).

from the boreal and tropical biota to changes in aerosol loadings, cloud properties, and climate.

3.4.4. Aerosol hygroscopic properties in boreal and tropical forests

Aerosol hygroscopic properties are strongly dependent on the chemical composition and particle size. Typically, inorganic compounds are strongly hygroscopic, while organics are less hygroscopic. The SOA in Amazon is mainly isoprene driven, giving an SOA slightly less hygroscopic than the boreal monoterpene driven SOA. Despite small differences, they can have a small but significant effect on the radiation balance. The main influence on hygroscopicity is due to the influence of inorganic compounds as sulfates, which are often of anthropogenic origin, thus influencing forested areas within the range from major source areas.

A natural aging process that might affect the hygroscopic properties of the natural aerosol in both the tropical and the boreal is the processing of clouds and subsequent new particle formation and growth in the subsiding air providing an aged boundary layer aerosol.

3.5. AEROSOL OPTICAL PROPERTIES

Many of the aerosol impacts in the ecosystem depend on the aerosol optical properties (AOP), including aerosol light scattering (σ_{sp}) and aerosol light absorption (σ_{ap}) at a certain wavelength, and single scattering albedo (SSA, defined as the ratio of σ_{sp} to total aerosol extinction, $\sigma_{ext} = \sigma_{sp} + \sigma_{ap}$). The radiation budget and changes in surface temperature are directly influenced by the amount of radiation scattered and absorbed by the aerosol particles in the atmosphere. The SSA, which represents the absorbing properties of an aerosol population, is one of the most important parameters in determining the direct aerosol radiative forcing (Takemura et al., 2002). Recent advances in instrumentation with higher spectral resolution allow a more comprehensive aerosol characterization in terms of their optical properties. The mass concentration of BC, the most important absorbing aerosol species, can be derived from the absorption measurements by assuming an appropriate mass absorption cross-section (MAC). Moreover, the optical properties are also linked to aerosol size distribution and composition. For example, the wavelength dependency of the scattering and absorption coefficients expressed as scattering Ångström exponent (SAE) and absorption Ångström exponent (AAE), respectively, can be closely related to the aerosol size distribution and emission sources (e.g., diesel or biomass burning). These quantities are also often used to estimate the contribution of the BrC (see section 3.1.1.1) to total aerosol absorption (Wang et al., 2016, Saturno et al., 2018a, de Sá et al., 2019). Continuous remote sensing and in-situ measurements at key sites in forested areas show a strong seasonality in the optical properties from tropical and boreal forests that influences ecosystem functioning. Aerosol absorption may change the vertical temperature profile and convection and cloud properties and thus precipitation patterns (Koch and Del Genio., 2010). Recent modeling studies of the SOA optical properties downwind of Manaus, as a result of interactions of BVOC with NOx from urban pollution, show large production of scattering SOA, with an SSA varying from 0.91 close to Manaus to 0.98 160 Km downwind of Manaus (Nascimento et al., 2021).

3.5.1. Aerosol optical properties (AOPs): interannual variability

Measurements of AOPs in Amazonia started in the 1990s when the first AERONET sun-photometers began to operate in Southern Amazonia. In the same decade, the Brazilian LBA project (Keller et al., 2004) started its operations, and, since then, many intensive and long-term experiments have been conducted in Amazonia. Between 1999 and 2007, in-situ measurements of aerosol optical properties were still scarce and limited to short-term intensive experiments, most of them conducted at Amazonian pasture sites. Continuous monitoring of in-situ aerosol optical properties started in 2008 at two forest sites in Central Amazon (Rizzo et al., 2013, Saturno et al., 2018a, Holanda et al., 2020). The long-term measurements revealed a defined seasonal trend in atmospheric conditions, oscillating between biogenic and biomass burning-dominated states. Thus, aerosol scattering, and absorption coefficients increase by one order of magnitude from the wet to dry season (***Figure 3.5.1***). Long-range transport of aerosols from Africa (e.g., mineral dust and smoke in the wet season, as well as biomass burning from central Africa in the dry season) are also often observed in central Amazon, with significant impacts in the AOPs (e.g., Swap et al., 1992, Rizzo et al., 2013, Moran-Zuloaga et al., 2018, Saturno 2018a, Holanda et al., 2020). The highest aerosol loadings are observed at anthropic landscapes during the dry season, mostly in the region of the *arc of deforestation* where the regional biomass burning emissions are more intense, resulting in σ_{sp} ~10^2 Mm^{-1} and σ_{ap} ~10^1 Mm^{-1}, while the aerosol optical depth at 550 nm (AOD_{550nm}) can be as high as 4 (Artaxo et al., 2013). For a detailed presentation and discussion on biomass burning and its effect on AOD and the ecosystem, see section 4.5.

The descriptive statistics of selected extensive (scattering and absorption coefficient: σ_{sp} and σ_{ap}) and intensive (SAE, backscatter fraction: BSF, SSA, and AAAE) aerosol optical state parameters observed in the boreal forest are presented in ***Tables 3.5.1*** and ***3.5.2***. The results for the green wavelength (550–574 nm) are shown. The mean and medians of σ_{sp} and σ_{ap} are the highest at the SMEAR II site at Hyytiälä, while at ZOTTO, it is ~1–3 Mm^{-1} lower. The lowest is found at Pallas, approximately 40–50% of observed at SMEAR II (***Table 3.5.1***). Even though located in a background area, the results show that SMEAR

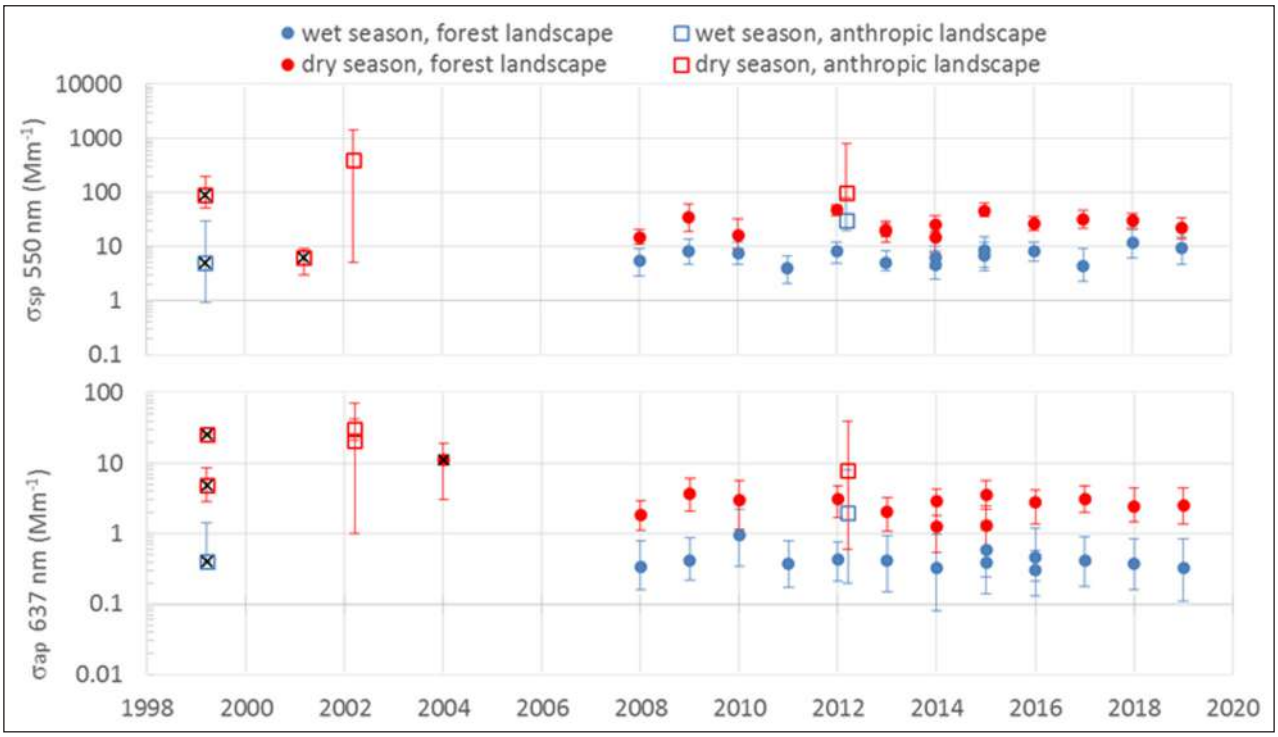

Figure 3.5.1 Reported ranges for particle light scattering (σ_{sp}) and absorption (σ_{ap}) in the Amazon Basin, during the wet and dry seasons, at a forest and anthropic landscapes (arc of deforestation). This compilation integrates results from intensive and long-term field experiments using different platforms (ground-based and airborne). Data points refer to medians and interquartile ranges. Scattering coefficients were measured at 550 nm. Absorption coefficients were calculated at wavelengths ranging from 370 to 565 nm from 1999 to 2004 and at 637 nm from 2008 onwards. Most measurements were taken under dry conditions (RH < 40%), except for the data points marked in the figure as 'X.' References: Artaxo et al., 2013; Chand et al., 2006; Guyon et al., 2003; Kuhn et al., 2010; Rizzo et al., 2011, 2013; Saturno et al., 2018a.

REF.	SITE	LAT	LON	PERIOD		σ_{sp} MEAN ± STD	σ_{sp} MEDIAN	σ_{ap} MEAN ± STD	σ_{ap} MEDIAN
1	SMEAR II	61° 51′ N,	24° 17′ E	2006–2009		18 ± 20	12	2.2 ± 2.4	1.5
2				2006–2015		17 ± 19	11		
3				2006–2017		15 ± 17	10	2.2 ± 2.5	1.4
4	Pallas	67° 58′ N	24°07′ E	2001–2010		7.8 ± 9.6	4.4	0.74 ± 1.1	0.35
2				2000–2015		7.9 ± 16	4.3		
5	ZOTTO	61°N	89°E	2006–2011	50 m	15 ± 18	11	1.87 ± 2.54	1.15
				2006–2011	300 m	14 ± 16	10	1.74 ± 2.4	1.02

Table 3.5.1 Descriptive statistics of extensive aerosol optical properties scattering and absorption coefficient (σ_{sp} and σ_{ap}) at SMEAR II, Pallas, and ZOTTO at λ = 550 nm. At the ZOTTO tower, σ_{ap} was measured at λ = 574 nm.

References: 1) Virkkula et al., 2011; 2) Pandolfi et al., 2018; 3) Luoma et al., 2019; 4) Lihavainen et al., 2015; 5) Chi et al., 2013.

II is closer to anthropogenic sources than both Pallas and ZOTTO and more exposed to long-range transport of air pollutants. Besides anthropogenic sources, SMEAR II is also influenced by maritime air masses (Zieger et al., 2015). The mean and medians of SAE at all sites are in the range of ~1.8 to ~1.9, suggesting that the shapes of size distributions are not very different. On the other hand, BSF is the lowest at ZOTTO, ~0.11, and the highest at SMEAR II, ~0.15. Since BSF is roughly inversely related to particle size, this result suggests that the mean size of particle size distributions is somewhat smaller at SMEAR II than at ZOTTO. The SSA is the highest, 0.91 at Pallas and the lowest ~0.87 at SMEAR II and 0.88 at ZOTTO. The differences in SSA are not large but still reasonable: PALLAS is furthest away from black carbon sources and often receives air masses from the sea. It should be kept in mind that the SSA is measured and here given at dry conditions (usually RH < 30–40%). At the same time, the

REF.	SITE	PERIOD		SAE MEAN ± STD	MEDIAN	BSF MEAN ± STD	MEDIAN	SSA MEAN ± STD	MEDIAN	AAE MEAN ± STD	MEDIAN
1	SMEAR II	2006–2009		1.7 ± 0.5	1.8	0.14 ± 0.03	0.14	0.88 ± 0.07	0.89	1.4* ± 0.3	1.4
2		2006–2015		1.8 ± 0.5	1.84	0.15 ± 0.03	0.147				
3		2006–2017		1.8 ± 0.6	1.88	0.15 ± 0.03	0.15	0.86 ± 0.08	0.87	0.94 ± 0.41	0.98
4	Pallas	2001–2010		1.7 ± 0.7	1.8	0.13 ± 0.03	0.12	0.92 ± 0.06	0.91	1.1 ± 0.6	1.1
2		2000–2015		1.63 ± 0.67	1.78	0.132 ± 0.04	0.125				
5	ZOTTO	2006–2011	50 m	1.84 ± 0.47	1.89	0.112 ± 0.01		0.88 ± 0.08	0.88		
		2006–2011	300 m	1.85 ± 0.49	1.9	0.117 ± 0.01		0.88 ± 0.88	0.88		

Table 3.5.2 Descriptive statistics of intensive aerosol optical properties scattering Ångström exponent (SAE) backscatter fraction (BSF), single-scattering albedo (SSA), and absorption Ångström exponent (AAE) at SMEAR II, Pallas, and ZOTTO. SAE was calculated for the wavelength range λ = 450 – 700 nm, BSF at λ = 550 nm, SSA at λ = 550 for SMEAR II and Pallas and at λ = 574 nm for ZOTTO. The AAE was calculated over the Aethalometer wavelength range λ = 370 – 950 nm.

References: 1) Virkkula et al., 2011; 2) Pandolfi et al., 2018; 3) Luoma et al., 2019; 4) Lihavainen et al., 2015; 5) Chi et al., 2013.

*) Virkkula et al. (2011) calculated σ_{ap} with the algorithm of Arnott et al. (2005) that yields higher AAE than the algorithm of Collaud Coen et al. (2010) used by Luoma et al. (2019).

ambient SSA and climatically more relevant SSA are higher due to the uptake of atmospheric water (see, e.g., Fig 10c in Zieger et al., 2010). The AOP observations agree well with the chemistry and size distribution observed (see 3.1. and 3.3), even though the size distributions at Hyytiälä have a much stronger influence of smaller particles than ZOTTO. That is not reflected in the scattering as those small particles scatter considerably less, i.e., scattering is strongly dependent on particles in a limited size range.

3.5.2. Seasonal cycles of aerosol optical properties

The sources and transport mechanisms vary significantly with the seasons of the tropical and boreal forests. Additionally, precipitation patterns and the impact of biomass burning, and long-range transport change the AOP significantly. ***Figure 3.5.2*** shows the scattering Ångström exponent (SAE), absorption Ångström exponent (AAE), and single scattering albedo (SSA) in the Amazon Basin, during the wet and dry seasons, at a forest and anthropic landscapes.

Mean σ_{sp} at λ = 550 nm in Amazonia is 22 ± 25 Mm^{-1} averaging for all data from 2012 to 2017 and 7.5 ± 9.3 Mm^{-1} and 33 ± 25 Mm^{-1} in the wet and dry seasons, respectively (Saturno et al., 2018a). For σ_{ap} at λ = 637 nm, the respective numbers are 2.1 ± 2.2 Mm^{-1} in all data and 0.68 ± 0.91 Mm^{-1} and 4.0 ± 2.2 Mm^{-1} in the wet and dry seasons. SSA at 500 nm in Amazonia typically ranges between 0.85 and 0.96, but lower values have been reported under the influence of fresh biomass burning emissions. Plume-wise events of long-range transport of dust and biomass burning aerosols from Africa also have an impact on particle optical properties during the wet season in Amazonia, in a way that SSA may reach down to low values of 0.82 during such events in the wet season, and 0.85 in the dry season (Rizzo et al., 2013; Rizzolo et al., 2017; Saturno et al., 2018a; Holanda et al., 2020).

During the wet season, when coarse mode biogenic particle emissions predominate, SAE is typically lower than 1.5, increasing to the range 1.5–2.0 during the dry season when there is an input of fine mode particles from biomass burning emissions (***Figure 3.5.2***). There are few reports on the spectral dependency of absorption in Amazonia, with AAE typically ranging between 1 and 2, showing high variability during the dry season. Saturno et al. (2018a) report increased AAE values in air masses impacted by the transport of aged biomass burning smoke from southern Amazonia.

To compare the seasonal cycles of σ_{sp}, σ_{ap} and SSA in the two types of forests, observations from the three boreal stations and ATTO are shown in ***Figure 3.5.3***. We use seasonal data from SMEAR II given by Virkkula et al. (2011), i.e., 3-month averages of the whole data. For Pallas, the highest and lowest monthly averages are based on all data and those classified by back trajectories to continental air masses as given by Lihavainen et al. (2015). For ZOTTO, the seasonal averages of polluted and clean air masses after a source classification as given by Chi et al. (2013) and for ATTO averages for the dry and wet season are presented by Saturno et al. (2018a).

Despite the methodological differences, some obvious similarities and differences can be observed. At SMEAR II, the highest σ_{sp} and σ_{ap} are observed in winter, the lowest σ_{sp} in autumn but the lowest σ_{ap} in summer. Consequently, the SSA is the highest in summer and the lowest in autumn and winter. The usual explanation for this kind of seasonal cycle is low BC emissions during the summer season. The seasonal cycles are very similar in

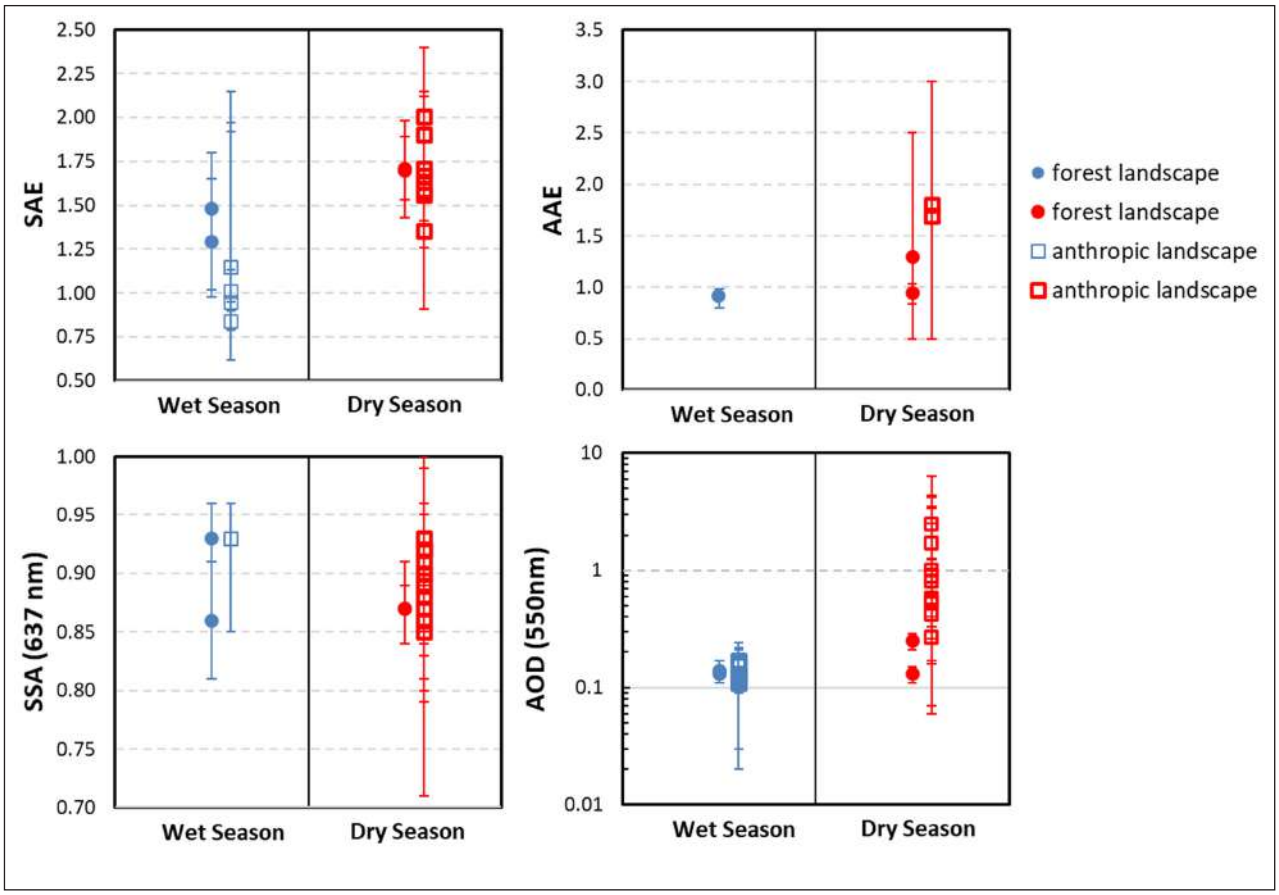

Figure 3.5.2 Reported ranges for scattering Ångström exponent (SAE), absorption Ångström exponent (AAE), and single scattering albedo (SSA) in the Amazon Basin, during the wet and dry seasons, at a forest and anthropic landscapes (arc of deforestation). This is a compilation of results from intensive and long-term field experiments using different platforms (ground-based, airborne, remote sensing). Data points refer to averages or medians. SAE, AAE, and SSA values are given at dry conditions, with measurements made at 30–40% RH. References: Artaxo et al., 2013; Chand et al., 2006; Guyon et al., 2003; Kuhn et al., 2010; Marenco et al., 2016; Pérez-Ramírez et al., 2017; Reid et al., 1999; Rizzo et al., 2011, 2013; Saturno et al., 2018a; Schafer et al., 2008; Sena et al., 2013.

the ZOTTO data classified into the polluted air masses. Clearly, different cycles are found at Pallas and in the clean air masses at ZOTTO: The highest σ_{sp} is observed in summer. In summer σ_{ap} is the lowest – like at all sites – leading to the highest SSA in summer.

At ATTO, the seasonal averages of both scattering and absorption coefficients are close to the ZOTTO clean season averages, and the dry season averages are higher than the winter averages of polluted air masses at ZOTTO and at SMEAR II. The dry-season SSA average at ATTO is at the same level as the winter-season averages at all boreal sites and the wet-season average at the same level as the summer-season averages at the boreal sites.

The reason for the σ_{sp} summer maximum at the boreal sites is emissions from biogenic sources. Tunved et al. (2006b) show that as air masses get transported from the sea to both Pallas and to SMEAR II, the mass of newly formed particles grows significantly and linearly as a function of transport time over land due to the condensation of biogenic emissions from the forest. This growth resulted in an increased σ_{sp} (Lihavainen et al., 2009, ***Figure 3.5.4a***). SAE also grows as a function of transport time from the sea (***Figure 3.5.4b***) due to the increasing dominance of new particles and the decreasing number of large sea-salt particles transporting time from the sea.

The average AOD at λ = 500 nm is 0.12 ± 0.04 and 0.08 ± 0.02 at SMEAR II in southern Finland and Sodankylä in northern Finland, respectively (Aaltonen et al., 2012). It is worth noting that these are in the range of the above-presented values of AOD in Amazonia during the wet season but lower than those in the dry season.

3.5.3. Trends of aerosol optical properties

Trends of scattering, backscattering, BSF, and SAE are analyzed by Pandolfi et al. (2018) for several European sites, including Pallas and SMEAR II. In that analysis, no absorption data is discussed. Luoma et al. (2019) present a detailed trend analysis for SMEAR II aerosol optical properties, including scattering and absorption data.

For σ_{sp}, Pandolfi et al. (2018) observed statistically significant decreasing trends of –0.225 Mm^{-1} a^{-1} at Pallas for the period 2000–2010, but for the period 2000–2015, the trend is positive but statistically not significant. For SMEAR II the trend calculated by Pandolfi et al. (2018) is statistically significantly decreasing by –0.588 Mm^{-1} a^{-1} in 2006–2015. Luoma et al. (2019) also get a statistically significant decreasing trend of –0.34 Mm^{-1} a^{-1} in 2006–2017 at SMEAR II, so the scattering

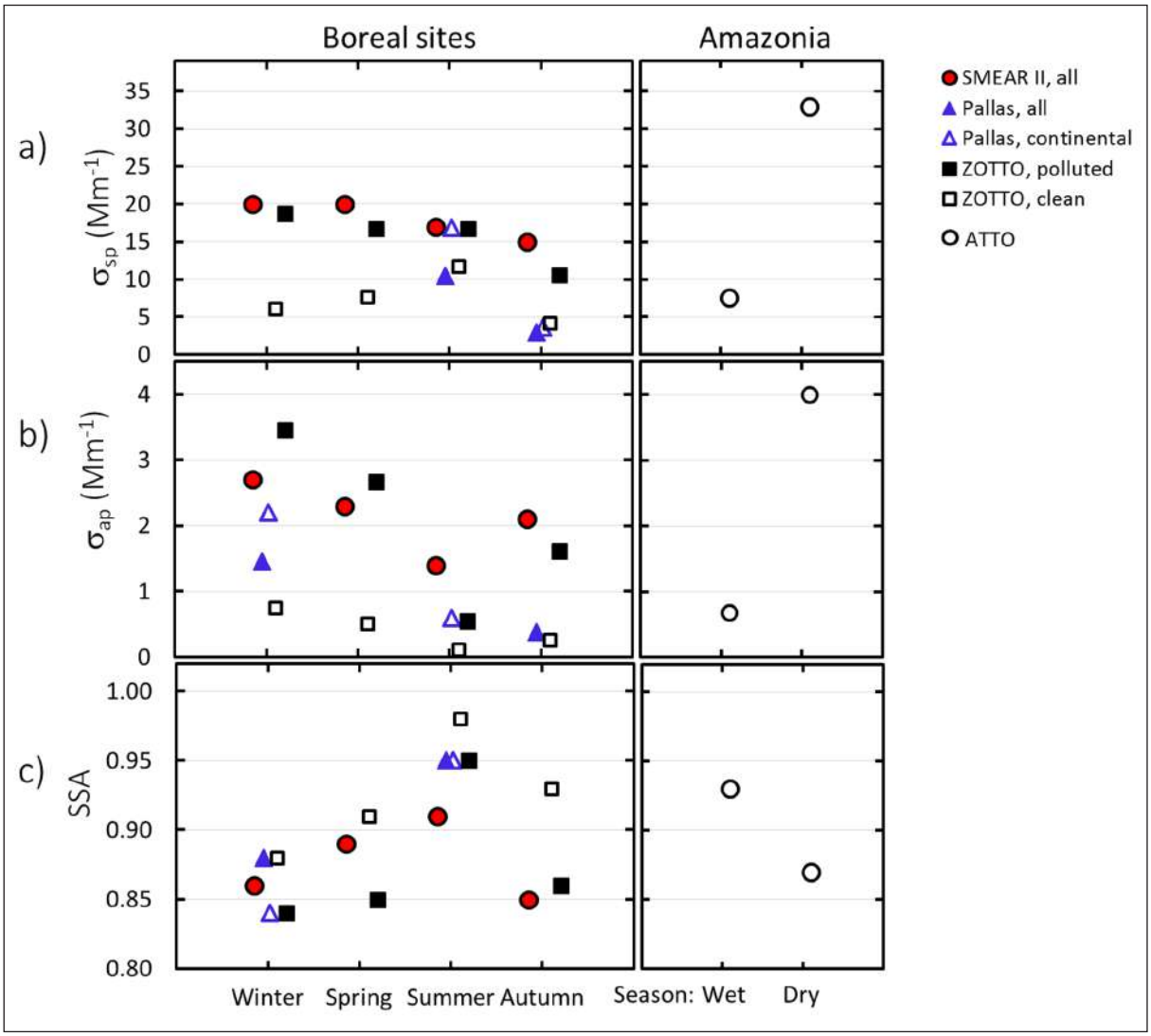

Figure 3.5.3 Seasonal variations of σ_{sp} and σ_{ap} and SSA at the boreal forest sites SMEAR II, Pallas, and ZOTTO and at the Amazonian site ATTO. All σ_{sp} are calculated at λ = 550 nm, at SMEAR II and Pallas, with $\sigma_{ap,}$ and SSA are at λ = 550 nm. At ZOTO σ_{ap} and SSA are at λ = 574 nm and at ATTO σ_{ap} and SSA are at λ = 637 nm. The figure was prepared from the results presented for SMEAR II by Virkkula et al. (2011), for Pallas by Lihavainen et al. (2015), for ZOTTO by Chi et al. (2013), and for the Amazonian site ATTO by Saturno et al. (2018a). For Pallas, Lihavainen et al. (2015) reported as numbers the highest and lowest monthly averages of the annual cycle of all data and of continental air masses. For ZOTTO, Chi et al. (2013) presented the seasonal averages of σ_{sp} and σ_{ap} and SSA in polluted and clean air masses, and for ATTO, Saturno et al. (2018a) presented averages of σ_{sp} and σ_{ap} and SSA for the dry and wet seasons.

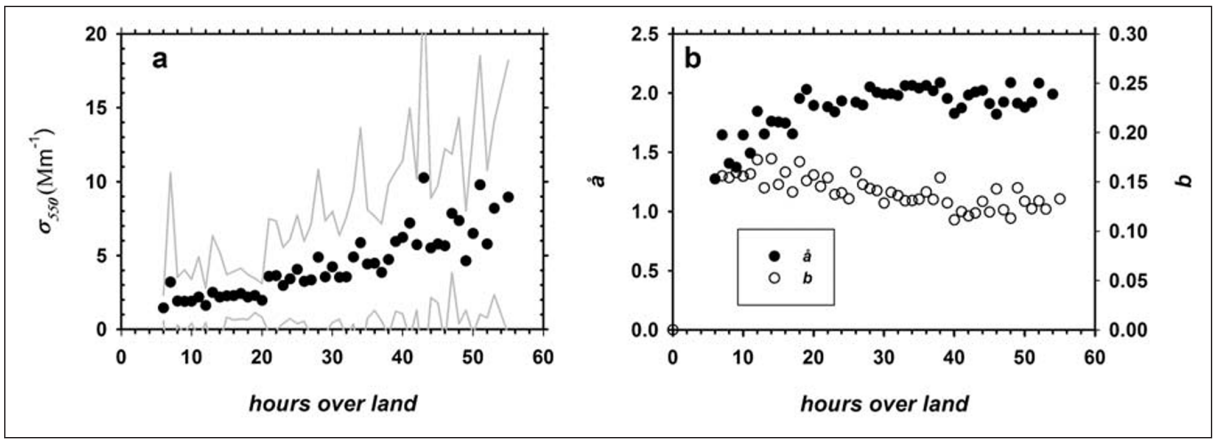

Figure 3.5.4 (a) Scattering coefficient σ_{550}, measured at 550 nm. The gray lines represent ± standard deviation. **(b)** Ångström exponent, å, calculated based on values of σ at 450 and 550 nm, along with the backscattering fraction, b. The data cover the days of year 120–270 during the period 2000–2006. All quantities have been plotted as a function of the time the air masses have spent over land prior to arriving at the measurement site. From Lihavainen et al. (2009).

coefficient is decreasing in the western part of the Eurasian boreal forest. The trend of σ_{ap} at SMEAR II in the same period is –0.095 Mm^{-1} a^{-1}, stronger than that of σ_{sp}, and consequently, the trend of single-scattering albedo (SSA) is statistically significantly positive, 0.0034 a^{-1} (Luoma et al., 2019). The decreasing trends of scattering and absorption are very likely indicative of decreasing influence of anthropogenic emissions and the increasing trend of SSA, indicating that the contribution emissions containing black carbon are decreasing even faster.

The trend of SAE at Pallas is negative, –0.019 /year in 2000–2015 (Pandolfi et al., 2018), suggesting that the particle size distributions are dominated by larger particles towards the end of the period than in the beginning. On the other hand, BSF increased at Pallas by 0.0007 a^{-1} in the same period (Pandolfi et al., 2018), which indicates a shift towards smaller particles. For SMEAR II, the trends of both SAE and BSF are positive, presented both by Pandolfi et al. (2018) and by Luoma et al. (2019) for the periods 2006–2015 and 2006–2017, respectively, indicating a shift towards smaller particles consistently. Further support to this trend is given by Luoma et al. (2019), who also show that the geometric mean diameter and the volume diameter decreased in 2006–2017 by 0.09 nm a^{-1} and 1.73 nm a^{-1}, respectively.

Chi et al. (2013) do not present trends in the AOP data measured at ZOTTO. The data should be further analyzed to find out possible trends also in central Siberia. Saturno et al. (2018a) present the longest time series of AOP measured in situ in the Amazon Forest (2008–2017), but long-term trends are not discussed. A clear interannual variability on AOP is mostly related to variability in synoptic conditions, as discussed in section 4.4.1. However, trends along this 9-year period of observations in the Amazon are not clear, suggesting that, in the long term, the optical characteristics of the aerosol population in the Amazon are rather constant, in spite of the intense seasonal variation described in section 4.4.

3.5.4. The influence of relative humidity on aerosol optical properties

The ability of particles to take up atmospheric water termed hygroscopicity (see Sect. 3.4), directly affects their optical properties due to a change in particle size and refractive index. Especially, particle light scattering is strongly dependent on ambient RH. The particle light absorption coefficient is influenced by humidity as well. However, its overall effect on the particle light extinction and single scattering albedo is small for most aerosol types due to the dominance of the RH-effect on particle light scattering and the dominance of light scattering itself (Nessler et al., 2005). Long-term monitoring sites have therefore agreed to conduct aerosol measurements generally at dry conditions (RH < 40%; WMO/GAW 2016) to keep aerosol measurements comparable. However, the consideration of the water uptake effect on particle light scattering is important for direct radiative effect calculations and the evaluation of remote sensing retrievals (Zieger et al., 2011, 2013).

The particle light scattering enhancement factor, *f*(RH), is defined as the ratio of wet to dry particle light scattering coefficient. It is commonly used to quantify the change in light scattering due to water uptake. *f*(RH) depends on both the particle's chemical composition and size distribution (and wavelength λ, which is omitted here for simplicity reasons). It has been extensively studied across the globe (for an overview, see, e.g., Zieger et al. (2013) or Titos et al. (2016) and references therein) but only sparsely for boreal regions. Zieger et al. (2015) used a humidified nephelometer system during a three-month campaign at Hyytiälä, Finland. They found values of *f*(RH) of 1.63 ± 0.22 at RH = 85% and λ = 525 nm (mean ± standard deviation), which can be regarded as generally lower compared to other sites. In the Amazon, humidified nephelometer measurements are performed during the GoAmazon2014/15 campaign (Martin et al., 2016). Similar values compared to Hyytiälä are found with 1.3 ± 0.1 and 1.4 ± 0.2 for PM_{10} and PM_1, respectively, for RH = 85% and λ = 550 nm (Burgos et al., 2019). The dominance of organic substances, generally known to have a low hygroscopicity, mainly explains the low observed values of *f*(RH) in boreal regions. In Hyytiälä, increased f(RH) values are correlated with the increased influence of maritime airmasses transporting more hygroscopic sea spray particles to the site (see ***Figure 5*** in Zieger et al., 2015).

Figure 3.5.5 shows the optical hygroscopicity parameter γ versus the organic mass fraction measured by aerosol mass spectrometry and filter-based absorption techniques for SMEAR II. The parameter γ is commonly used to parametrize the magnitude and RH-dependency of *f*(RH) in a simplified form using the equation $f(RH)=a(1-RH)^{-\gamma}$ (where $a \approx 1$). The magnitude of *f*(RH) and the organic mass fraction are almost linearly correlated for boreal aerosol encountered at Hyytiälä. These observations are also in line with inorganic-dominated continental aerosol performed with a similar experimental set-up in Melpitz, Germany. In turn, the linear dependency shown in ***Figure 3.5.5*** can be used to predict *f*(RH) if no humidified nephelometer measurements are available (Zieger et al., 2015).

3.5.5. Aerosol optical depth (AOD)in the tropical and boreal regions

In situ remote sensing networks such as the NASA AERONET and satellite observations of aerosol properties using several sensors and satellite platforms such as Cloud-Aerosol Lidar with Orthogonal Polarization (Caliop), Moderate Resolution Imaging Spectroradiometer (MODIS), Multi-angle Imaging SpectroRadiometer (MISR), Along Track Scanning Radiometer (ATSR) and other sensors allow monitoring of aerosol concentrations

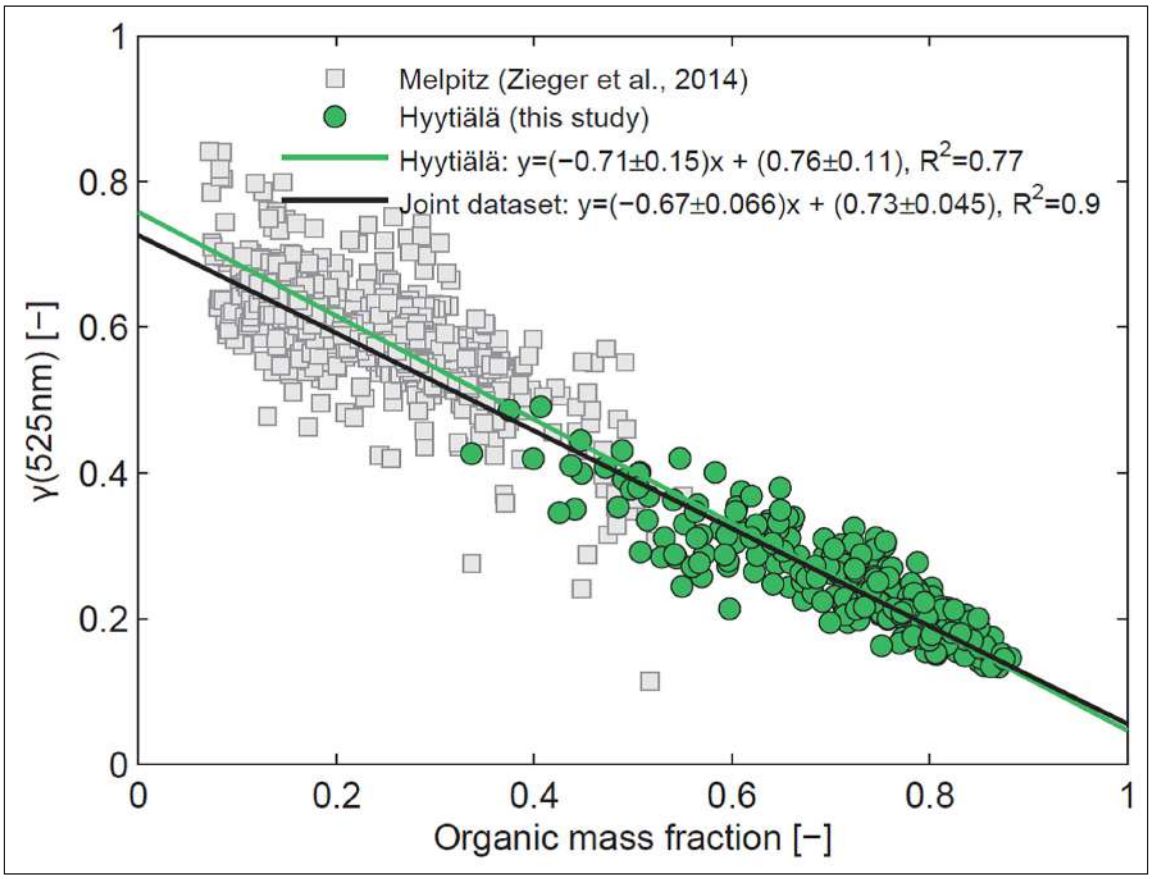

Figure 3.5.5 The optical hygroscopicity parameter γ versus the organic mass fraction for boreal aerosol measured in Hyytiäla, Finland (green points). The grey squares show γ in more inorganic dominated aerosol in Melpitz, Germany, during wintertime (Zieger et al., 2014). γ describes the magnitude of the scattering of enhancement factor *f*(RH), where $f(RH)=\alpha(1\text{-}RH)^{-\gamma}$. Figure taken from Zieger et al. (2015).

over forests. However, the high cloud cover over tropical forests during the wet season makes remote sensing of aerosols difficult. However, remote sensing products are very important when monitoring biomass burning emissions and their long-range transport, with daily global maps of the spatial distribution of properties of biomass burning aerosols. AOD measures the total amount of optically active aerosol in the whole atmospheric column. ***Figure 3.5.6*** shows the time series of AOD at several AERONET sites in Amazonia from 2000 to 2020. The figure shows the strong seasonality of AOD, with very low values in the wet season (typically 0.1 at 500 nm) to very high values in the dry season, with AOD up to 6 at 500 nm. It is possible to observe the decrease in AOD with the decrease in deforestation after 2007 (***Figure 3.5.6***).

The use of satellites for the retrieval of aerosol properties over the boreal forest is constrained by the availability of light at high latitudes during the winter months and the low solar zenith angles in spring and autumn, as well the high surface reflectance over snow and ice in these seasons. In addition, aerosol retrieval is only possible in clear sky conditions. As a result, satellite-retrieved aerosol data are available for only part of the year, e.g., over Finland, typically from April to October, depending on latitude. A somewhat longer time series is available from ground-based sun photometer measurements, but also here, the light availability is a severe limitation, and large gaps occur. This is clearly illustrated from the overview of sun photometer measurements of AOD (at 500 nm) in Finland, with five sites from Helsinki in the south to Sodankylä in the north within the polar circle (Aaltonen et al., 2012). The AOD across Finland is very low with values which on average are around 0.1, and Ångström exponents of 1.4. Similar values are also observed in Scandinavia (Toledano et al., 2012). Higher AOD values are ascribed to the transport of polluted air from Central Europe and biomass burning aerosol from Russian forest fires, as concluded from the cluster analysis (Aaltonen et al., 2012). The AOD time series and especially the multi-annual monthly means of the AOD in Finland and Scandinavia (Toledano et al., 2012) show distinct seasonal patterns that vary with latitude. Where the observations at the highest latitudes show a spring peak due to Arctic haze and very low AOD (0.06) in summer, in southern Fennoscandia, a spring peak (0.15) coincides with snow melt and agricultural burning, with a second maximum in summer related to anthropogenic emissions, dry weather, and forest fires.

Many AERONET monitoring stations are in operation in boreal forests, but in areas such as Siberia with frequent forest fires in the summer, the number of stations is

sparse. ***Figure 3.5.7*** shows the time series of aerosols from 2005 to 2018 for 3 AERONET stations over Eurasian Boreal forests: Yakutsk, Yekaterinburg, and Tomsk. The yearly impact of biomass-burning aerosols is very clear, as well the large year-to-year variability. High values with AOD at 500 nm larger than three were observed almost every year during the last 13 years.

AOD over the Canadian Arctic shows that forest fires also in the Canadian boreal forest are very important in terms of impact on aerosol optical properties. ***Figure 3.5.8*** shows the time series of AOD at 500 nm from 1997 to 2018 for 4 sites in the Canadian boreal forest region. AOD values larger than 2 are observed for more than half of these years.

Figures 3.5.6 to ***3.5.8*** show that during the last five years, the AOD over Amazonas, Canada, and Russia has the highest values in the range 3–4. This indicates that biomass burning affects all these areas similarly

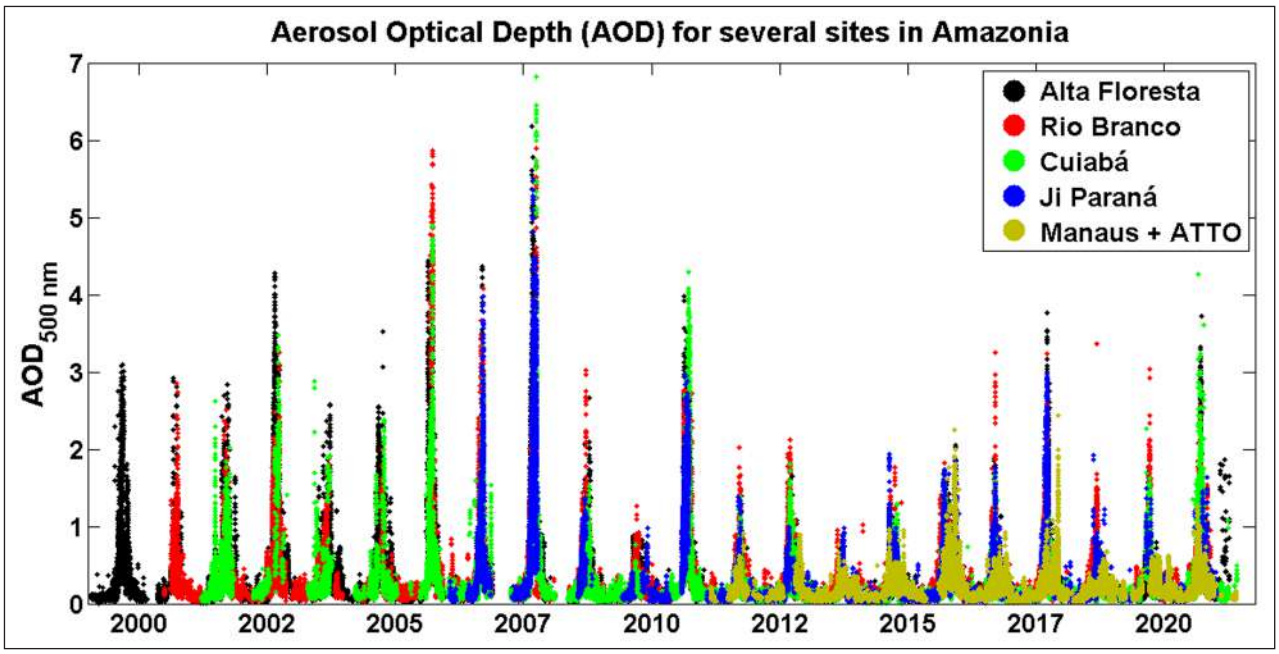

Figure 3.5.6 Time series of aerosol optical depth (AOD) at 500 nm for several sites in Amazonia from 2000 to 2020 measured with AERONET sun photometers.

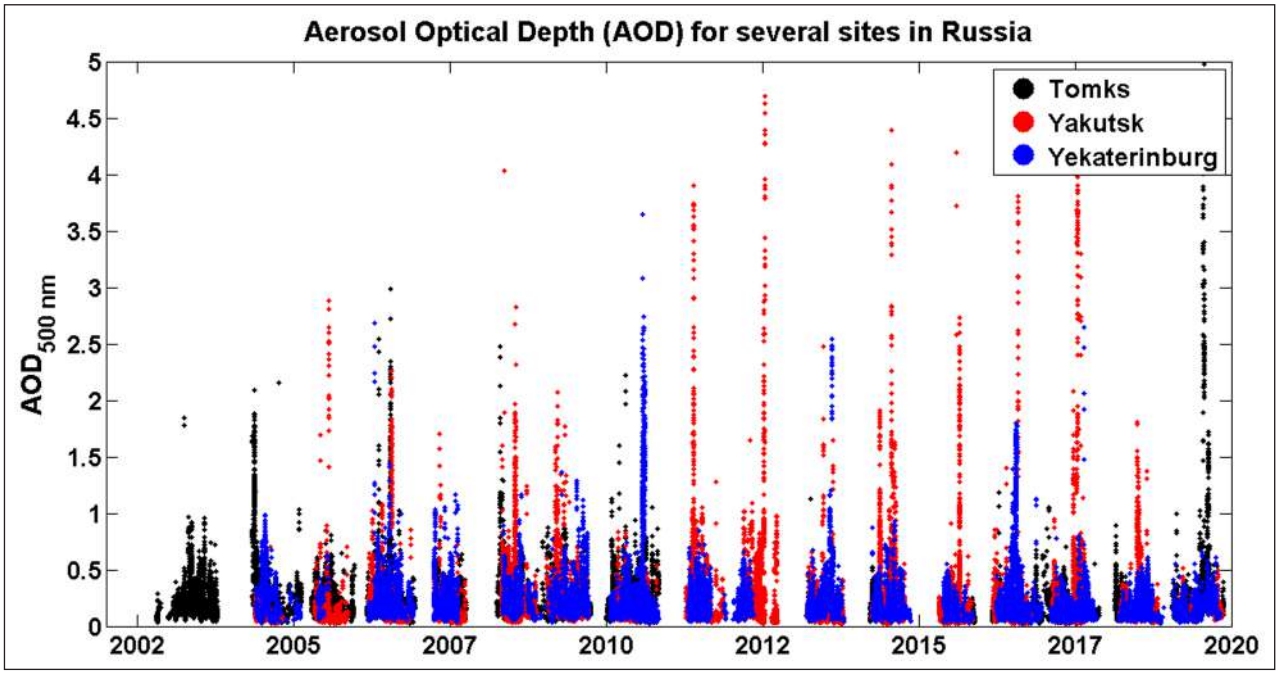

Figure 3.5.7 Time series of aerosol optical depth at 500 nm from 2004 to 2019 for 3 AERONET stations over Eurasian Boreal forests: Yakutsk, Yekaterinburg, and Tomsk.

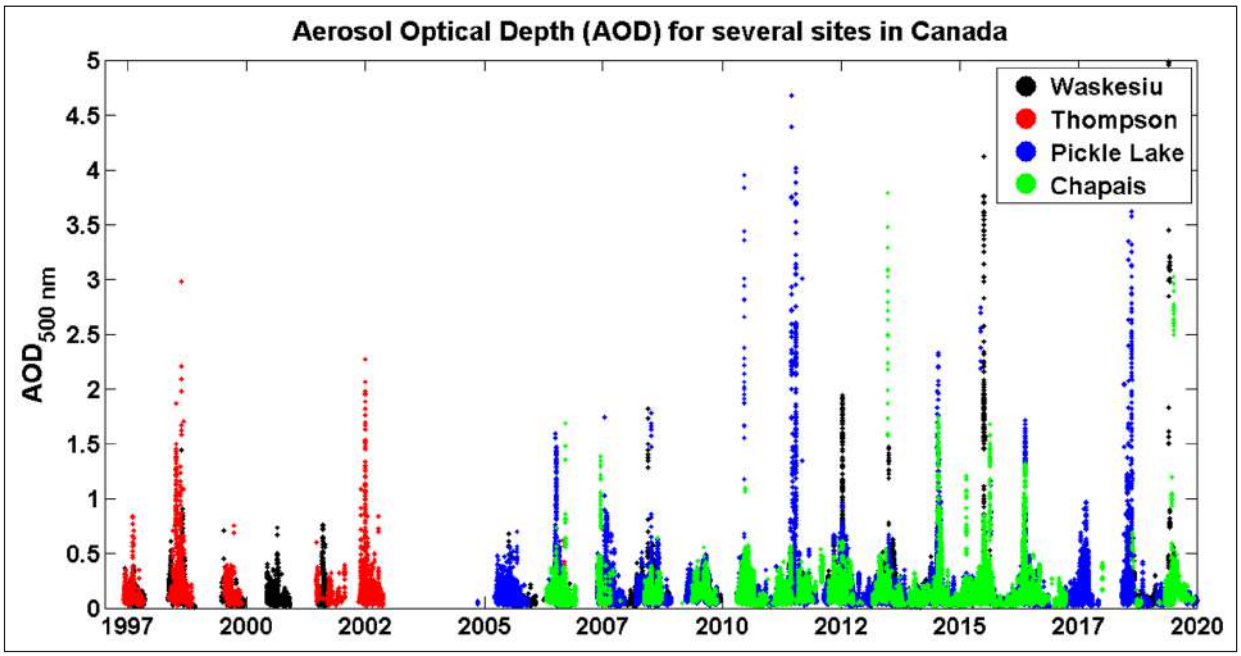

Figure 3.5.8 Time series of Aerosol Optical Depth at 500nm from 1997 to 2019 for 4 AERONET sites in the Canadian boreal forest region: Waskesiu, Thompson, Pickle Lake, and Chapais.

regarding aerosol concentrations and affects the aerosol burden, which in turn changes both the direct and indirect aerosol climate forcing.

This analysis shows that biomass burning aerosol emissions are the main driver for increased AOD over boreal and tropical forests, changing the radiation balance, affecting cloud development and precipitation.

4. ECOSYSTEM – ATMOSPHERE INTERACTION PROCESSES

4.1. EMISSIONS OF BIOGENIC VOLATILE ORGANIC COMPOUNDS

The emission of BVOCs by forests impacts atmospheric chemistry and aerosol formation (Yáñez-Serrano et al., 2020, Peñuelas et al., 2010). BVOCs play important roles at the cellular, foliar, ecosystem, and atmospheric levels. The role of BVOCs in SOA formation and growth has been extensively studied in boreal areas, showing a strong contribution to the SOA growth processes in the boundary layer (e.g., Tunved et al., 2006b; Yli-Juuti et al., 2011). In the Amazon, recent findings show that the emissions of BVOCs can be the starting point of aerosol formation in the upper atmosphere, where they produce particles that are oxidized, reducing their volatility, and transported back to the lower atmosphere where it populates the lower atmosphere (Andreae et al., 2018).

While tropical rainforests are exceptionally diverse in their tree species composition, boreal forests are composed of relatively few, mainly coniferous, tree species. The BVOC emission from the tropical rainforest is dominated by isoprene (Alves et al., 2016). Coniferous boreal species are typically monoterpene emitters with significantly lower isoprene emissions (Rinne et al., 2009). Isoprene emissions in many parts of the boreal zone originate either as minor emissions from dominant species, such as Norway spruce, or higher emission from non-dominant trees or shrubs (aspen, willows). Wetlands, a significant part of the landcover mosaic in boreal regions, are mainly isoprene emitting ecosystems. In both regions, ecosystems also emit a wide range of other compounds, including sesquiterpenes, methanol, and carbonyls.

4.1.1. Tropical and boreal BVOC emissions studies

The first BVOC studies outside of temperate regions were conducted in the tropics in the 1960s and demonstrated that isoprene and alpha-pinene were abundant in the emissions of tropical trees and the surrounding atmosphere (Rasmussen 1970). Aircraft campaigns in the late 1970s demonstrated that these BVOCs were present at ppb levels in the tropical forest atmosphere in Amazonia (Crutzen et al., 1985) and Malaysia (Cronn and Nutmagal 1982) and that isoprene was the dominant BVOC. Isoprene is typically present in the tropical forest atmosphere at mixing ratios ranging from 1 to 6 ppbv. Total monoterpene mixing ratios tend to be around 10 to 15% of the isoprene mixing ratio (Alves et al., 2016). The early recognition of the potential importance of tropical forest BVOC for atmospheric chemistry motivated a series of investigations of tropical BVOC sources, sinks, and atmospheric impacts, including the 1985 ABLE 2A study in Amazonia (Zimmerman et al., 1988) and the 1986/1988 DECAFE study in the Congo. From 1996 to 2004, the Large-scale Biosphere-Atmosphere Experiment in Amazonia (LBA) included more than a dozen Amazonian BVOC studies. Additional neotropical

studies were conducted in the Guyana highlands and central America during that time (Keller and Lerdau 1999, Crutzen et al., 2000, Geron et al., 2002). In contrast, our quantitative knowledge of African tropical forest BVOC is limited to the 1996 EXPRESSO study in the Congo Basin (Guenther et al., 1999) and the 2006 AMMA study in west Africa (Saxton et al., 2007). Our understanding of BVOC from southeast Asian tropical forests is limited to the extensive observations characterizing BVOC emissions and impacts during the 2008 OP3 project in Borneo (Hewitt et al., 2010) and studies in southern China (Baker et al., 2005, Geron et al., 2006). The scientific community has continued to advance BVOC understanding in Amazonia in recent years (e.g., Alves et al., 2018, Bourtsoukidis et al., 2018, Jardine et al., 2017, Martin et al., 2017, Yáñez-Serrano et al., 2015, 2018a, 2020, Weber et al., 2021) but studies have been lacking for other tropical forests.

The early work on BVOC emissions from boreal forest includes studies by Isidorov et al. (1985) and Janson (1993) in Eurasia, the BOREAS project in North America (Sharkey et al., 1997; Zhu et al., 1999), and the BIPHOREP project in Europe (Laurila et al., 1999). These works generally show lower VOC emissions and concentrations than in the tropics. The monoterpene landscape emission is usually dominating over isoprene (Lindfors et al., 2000). Typical concentrations of both the isoprene and monoterpenes are below 1 ppb. Also, boreal VOC emission studies show considerable variation in the VOC emission spectrum by vegetation type. Many studies in the boreal region have been conducted in the European part of the taiga, with vast Siberian taiga remaining virtually unstudied, with few exceptions (Kajos et al., 2013).

A global model of BVOC developed in the early 1990s (Guenther et al., 1995) estimated that tropical forests were responsible for about half of the global total BVOC emission even though they covered less than 15% of the whole land surface. The boreal forest, covering about 10% of the total land surface, is estimated to contribute about 2.5% of isoprene and 5.7% of monoterpene emissions (Guenther et al., 2012). Of the 22 BVOC field studies used to parameterize the Guenther et al., 1995 model, only the 1985 ABLE 2A results (Zimmerman et al., 1988) represent the tropical forests. This single study was the basis for tropical forest BVOC emission estimates in most modeling studies for at least the following decade. Four of the 22 BVOC studies synthesized by Guenther et al. (1995) included some boreal forest observations. A more recent synthesis of BVOC emissions data consists of 168 studies reporting temperate vegetation, 45 for tropical vegetation, and 40 for boreal vegetation (Guenther, 2013).

4.1.2. Emissions by BVOC compound group

4.1.2.1 Isoprene

In addition to the significant spatial variations, isoprene emissions also vary across several orders of magnitude over a day and throughout the year (Yáñez-Serrano et al., 2020). Isoprene emission from boreal ecosystems follows light and temperature relations that are similar to other ecosystems (Guenther et al., 2013). Keller and Lerdau (1999) reported that the isoprene emission response of tropical trees to temperature and light does not follow the behavior represented in models based on temperate plants' observations. For example, isoprene emissions continue to increase with solar radiation even at very high levels as a Photosynthetic Photon Flux Density (PPFD) of more than 1500 $\mu mol\ m^{-2}\ s^{-1}$. It remains unclear whether this difference is a characteristic of tropical plants or because of the high temperature and light environment of the upper canopy sun leaves they investigated. Canopy scale measurements demonstrate that existing models can generally predict isoprene emission variations at tropical sites and show that isoprene diurnal behavior is similar in tropical forests like other landscapes (e.g., Karl et al., 2007, 2009).

In contrast, seasonal variations in tropical forest isoprene emissions differ from those observed in temperate and boreal regions (Barkley et al., 2009). Emissions of isoprene in the dry season appear to be higher than expected, even when accounting for the higher light and temperature in the dry season (Alves et al., 2016). Although tropical rainforests have previously been assumed to have generally constant Leaf Area Index (LAI) throughout the year, phenological and LAI variations can have an essential role in controlling the high seasonal variations in the tropics (Alves et al., 2018).

Regional variations in isoprene concentrations within the Amazon are similar to the differences between tropical forests in different continents (Greenberg et al., 2004). Attempts to assign and extrapolate plant species-level emission capacities have shown some progress (e.g., Harley et al., 2004). The discovery of hyper-dominant trees in the Amazon forests (Fauset et al., 2015) has stimulated efforts to characterize species-level isoprene emissions and relate isoprene to other plant traits that could be used to quantify regional distributions (Taylor et al., 2018). A distinct feature of most tropical rainforests is the lowland (floodplain) and upland (Terre Firme) landscapes with characteristic species composition and soil environment, resulting in differences in isoprene emission. Aircraft flux measurements reveal that isoprene emissions from upland landscapes are considerably higher than lowland emissions, but the process responsible for this is still unknown (Gu et al., 2017).

In boreal landscapes, the most dominant tree species are not high isoprene emitters (Rinne et al., 2009 and references therein). However, Norway spruce in the European boreal zone emits both isoprene and monoterpenes (Hakola et al., 2017). As Norway spruce is one of the dominant tree species, it contributes to isoprene emissions from these areas (Tarvainen et al.,

2007). The high isoprene emitting tree species in boreal regions are typically non-dominant species, such as deciduous broadleaved willows and aspen (Hakola et al., 1998, Rinne et al., 2009). Even though the biomass of these species is often relatively small, and the trees may be in a sub-canopy position, their high emission renders them a significant source of isoprene in these regions (Tarvainen et al., 2007). In addition, wetland vegetation can contribute significantly to the isoprene emission from boreal regions (Haapanala et al., 2006; Holst et al., 2010; Tarvainen et al., 2007).

4.1.2.2. Monoterpenes

Monoterpene emission from boreal coniferous trees originates from two parallel emission pathways (Ghirardo et al., 2010). They can be emitted directly from synthesis as de novo emission or large specialized storage structures as evaporative emission. The monoterpene emission from some broadleaved species, such as birches, originate totally from synthesis as de novo emission. In a forest ecosystem, most monoterpenes originate from the foliage of trees, but in coniferous forests, tree trunks and soils are sources of monoterpenes (Vanhatalo et al., 2015, Aaltonen et al. 2013).

The evaporative emission of monoterpenes can be described by temperature-dependent algorithms (Tingey et al., 1980; Guenther et al., 1991), and the de novo emission can be described by light and temperature-dependent algorithm, similar to the isoprene emission algorithm (Schuh et al., 1997, Dindorf et al., 2006). Thus, for the coniferous trees in which the two emission pathways are present, a parallel algorithm can be formulated as $E = E_{evap.} + E_{de\ novo}$. By defining fraction of emission originating as de novo synthesis, f, this equation can be written as

$$E = E_0\left(fC_LC_T + (1-f)\gamma\right)$$

Where E_0 is the overall emission potential, the f parameter is practically the same as the light-dependent fraction used in some emission models, C_L is the light-dependent term, C_T is the temperature-dependent term. For species with fully de novo monoterpene emission f = 1 and the algorithm simplify to an isoprene-like emission algorithm. If f = 0, the algorithm reduces to the classical Tingey-Guenther monoterpene emission algorithm.

The de novo fraction of monoterpene emission varies between tree species and within the growing season. The broadleaved deciduous monoterpene emitters, such as birches and oaks with more than an order of magnitude smaller monoterpene storage than conifers, typically have a de novo fraction of 1 (Ghirardo et al., 2010). For conifers, the derived de novo fractions have ranged from 0.1 to 0.9. Typically, ecosystem-scale flux measurements by micrometeorological methods at boreal coniferous forest sites show values around 0.4–0.6, with large uncertainties (Taipale et al., 2011; Rantala et al., 2015). De novo fraction is typically higher at the beginning of the growing season, according to both branch and ecosystem-scale data. Especially during monoterpene emission bursts in early spring, the emission can be of entire de novo origin (Aalto et al., 2015; Rantala et al., 2015).

The evaporative monoterpene emission from coniferous trees, which is not dependent on PPFD, leads to significant nocturnal monoterpene emission. This, coupled with a stable nocturnal boundary layer, leads to nocturnal atmospheric monoterpene mixing ratios higher than daytime mixing ratios (Rinne et al., 2005; Hakola et al., 2012). This contrasts with tropical rainforests, where mixing ratios are lower at night (Zimmermann et al., 1988; Yáñez-Serrano et al., 2015).

The relationship between monoterpene synthesis, storage, and emission is very complex and, in evergreens, varies with needle age. The monoterpene synthase activity shows significant variations between growing seasons and is highest in young, developing needles. However, monoterpene storage does not change much with needle aging and does not seem to have a close relationship with emission. (Vanhatalo et al., 2018).

A typical feature of monoterpene emission from coniferous trees is the intra-species chemo-diversity, i.e., the tree-to-tree variation of emitted monoterpene mixture within tree species (Bäck et al., 2012; Hakola et al., 2017). This is also reflected by the diversity of monoterpene synthase activities between trees of the same species (Vanhatalo et al., 2018). The monoterpene emission from different individual Scots pine trees varies from being dominated by α-pinene via different mixtures of α-, β-pinene, and Δ^3-carene, to being Δ^3-carene dominated (Bäck et al., 2012). Also, Norway's spruce shows similar chemo diversity (Hakola et al., 2017). Ecosystem scale micrometeorological measurements show the monoterpene emission from a Scots pine forest to be dominated by α-pinene, with Δ^3-carene being the second and β-pinene third (Rinne et al., 2000), reflecting the higher abundance of α-pinene emitters at the stand.

An interesting characteristic of tropical forest sites in Amazonia and Southeast Asia is that monoterpene emissions tend to be highly light-dependent, similar to some Mediterranean oak woodlands but in contrast to most temperate and boreal forest landscapes (Rinne et al., 2002; Kuhn et al., 2002; Karl et al., 2004; Pugh et al., 2010). Thus, the monoterpene emissions in the tropical rainforest have a de novo fraction near unity, and the emission originates directly from biosynthesis. The quantitative understanding of monoterpenes required for their representation in air quality and climate models is challenging in tropical rainforests due to the diversity of compounds and sources and the extreme variability in their temporal and spatial patterns. Some tree species have high monoterpene emissions while others emit

rates of several orders of magnitude lower, and each tree species has a unique fingerprint of chemical composition. As a result, characterizing monoterpene emissions is especially challenging in tropical forests because of the high species diversity, complicating monoterpene emissions diversity at a plant species level.

4.1.2.3. Sesquiterpenes

Most boreal monoterpene emitting tree species also emit sesquiterpenes (Hakola et al., 2006; 2017; Haapanala et al., 2009; Rinne et al., 2009). During a major part of the growing season, their emission from coniferous trees is often an order of magnitude lower than monoterpenes. Sesquiterpene emission from coniferous tree species is typically highest in the late summer when it can even surpass the monoterpene emissions (Hakola et al., 2006; 2017). Also, birch species may have stress-related sesquiterpene emission surpassing their monoterpene emission (Hakola et al., 2001; Haapanala et al., 2009). While monoterpene emission from birch responds rapidly to changes in light conditions, sesquiterpene emission is not affected (Hakola et al., 2001). This may indicate different emission pathways of these compounds, in addition to their different biosynthetic pathways (Jardine et al., 2014). Sesquiterpene emissions from tropical forests do not follow the diurnal pattern of isoprene and monoterpenes and instead are relatively constant throughout day and night and are thought to be dominated by emissions from soil organisms (Bourtsoukidis et al., 2018).

4.1.2.4. Non-terpenoids

In addition to terpenoids discussed above, the tropical and boreal forests also emit non-terpenoid compounds, especially methanol, acetone, and acetaldehyde in particular during the spring, at the new foliage flushing and growth period (Janson et al., 1999; Rinne et al., 2007; Rantala et al., 2015, Aalto et al. 2014, Karl et al., 2004). Our understanding of their emission processes and our ability to model these emissions are lower than for terpenoid emissions. Also, more significant aldehydes (C_4-C_{10}) have been measured in Norway spruce emissions (Hakola et al., 2017). These emissions reached the level of monoterpene emissions during late summer. Acetaldehyde and other oxygenated VOC emissions can be elevated in response to flooding. As a result, their emissions are potentially higher in flooded tropical lowlands, although it appears that plants that are routinely flooded may not exhibit this emission behavior (Kesselmeier et al., 2009).

Virtually all vegetation emits methanol. Its emission can be related to growth via cell wall expansion (Nemecek-Marshall et al., 1995; Hüve et al., 2007, Aalto et al., 2014) or decay of vegetation (Warneke et al., 2002). Methanol is also deposited on ecosystems, and this deposition seems to be connected to wet surfaces (Holst et al., 2010; Rantala et al., 2015; Schallhart et al., 2018).

While many western hemisphere pines emit large amounts of 2-methyl-3-buten-2-ol (MBO), the emission from Scots pine, the major pine in the European boreal zone, is very small (Tarvainen et al., 2005; Hakola et al., 2006).

4.1.3. VOC soil emissions

In addition to trees and other vascular vegetation, soils also emit VOCs. VOCs can be produced by understory vegetation, roots, decomposition processes, soil microbes, and vegetative litter concentrated in the organic soil layer in the soil and below-canopy layer. The litter decomposition strongly dominates boreal forest soil emissions, and thus the timing and emission rates correlate with the litter production of dominant species (Aaltonen et al., 2013). Soil emissions are often closely linked to soil moisture and temperature. Most tropical forest BVOC is primarily emitted from trees' foliage, but soil microbes can be a major source of some compounds, including sesquiterpenes (Bourtsoukidis et al., 2018). Methanol is often a dominant component of soil emissions (Penuelas et al., 2014).

4.1.4. Disturbances, land-use change, and global change influencing BVOCs

BVOC emission changes have important implications for global atmospheric chemistry (Weber et al., 2021). Model predictions of future BVOC emissions are uncertain in all landscapes, especially in the relatively understudied and highly diverse tropical forests. Plant species composition, total leaf area, solar radiation, temperature, soil moisture, and CO_2 concentrations are expected to lead to significant changes in BVOC emissions (Sindelarova et al., 2014). Conversion of tropical forests to pasture and cropland can substantially decrease emissions of isoprene and monoterpenes (Guenther et al., 2012). Isoprene responses to soil moisture and CO_2 concentration have not yet been investigated in tropical landscapes, so models have assumed that tropical forests respond similarly to temperate vegetation (Guenther et al., 2012). Jardine et al. (2015a) report elevated emissions of stress-induced BVOC, including C6 oxygenated VOC, in response to drought and high temperatures in the Amazon Basin. Relatively high emissions of ocimenes, highly reactive monoterpenes were also observed in response to high temperatures (Jardine et al., 2017). This behavior is not unique to tropical forests and has previously been observed in Mediterranean oak trees (Staudt and Bertin, 1998). BVOC emission deviations driven by changes in species composition within tropical forests are likely to determine future BVOC. Still, there are currently no quantitative approaches for estimating these changes. Taylor et al. (2018) have recently shown that the fraction of isoprene emitters within a landscape is correlated with

average temperature and dry season length at a location and speculated on the ecological basis for this finding. A better understanding of these relationships can inform how tropical forest BVOC emissions will respond to species composition change related to a changing climate (Weber et al., 2021).

It has long been known that wounding enhances monoterpene emission from monoterpene storing tree species (Juuti et al., 1990). Mechanical wounding by herbivorous insects leads to elevated emissions from monoterpene storing trees, while the effect on de novo emission is less clear (Ghimire et al., 2013). Physical disturbance of *Betula pubescens* leaves also causes very high emissions of cis-3-hexen-ol, cis-3-hexenylacetate, 2-hexenal, and 1-hexenol (Hakola, 2001). However, monoterpene emissions from this de-novo monoterpene emitter are not affected.

Ecosystem scale flux data from a clear-cut commercial shows high monoterpene fluxes that can contribute 10% to the monoterpene emissions in heavily managed North European boreal regions (Haapanala et al., 2012). Locally, forestry operations can lead to enhanced monoterpene mixing ratios (Räisänen et al., 2008).

These studies clearly show that BVOC emissions are highly sensitive to land-use change, climate change, and other disturbances. Still, our limited understanding of the processes controlling the specific responses makes it difficult to quantitatively compare and contrast the response of tropical and boreal ecosystems to global change. The role of these disturbances in determining emission variations should be a priority for future research efforts. Yáñez-Serrano et al., 2020 show a decreasing trend of isoprene in Amazonia during the wet season, most likely due to forest biomass loss and an increasing trend of the sesquiterpene to isoprene ratio during the dry season suggest increasing temperature stress-induced emissions due to climate change. ***Figure 4.1.3*** shows satellite-based isoprene flux estimates from 2005 to 2014 in Amazonia, derived from formaldehyde columns in the wet season, measured by the satellite-borne OMI spectrometer. It is possible to observe a decreasing trend of isoprene in the wet season of -0.42% per year. Similar results are observed from modeled isoprene fluxes. The decrease of isoprene fluxes during the wet season can be partly attributed to significant and rapid changes in land cover (Acosta Navarro et al., 2014). Also, forest degradation due to deforestation (Bullock et al., 2020) can be associated with this effect.

4.1.5. Modeling BVOC emissions

The studies of tropical and boreal BVOC emission distributions and processes described in this section are integrated into global BVOC emission models used as inputs to numerical chemistry and transport models (Muller et al., 2008, Arneth et al., 2007, Guenther et al., 2006). The accuracy of BVOC emission model predictions for boreal and tropical regions can be assessed by comparing the canopy, landscape, and global scale field observations. Emission models and canopy scale observations tend to agree within ~25% when site-specific parameters are used in boreal and tropical landscapes (Rinne et al., 2007, Karl et al., 2007, Unger et al., 2013). Aircraft flux observations, including direct eddy covariance measurements and indirect inverse modeling estimates, indicate that BVOC emission model estimates for boreal and tropical (Greenberg et al., 1999, Spirig et al., 2004, Karl et al., 2007) regions are within a factor of two of observations across regional scales. Satellite-based estimates of formaldehyde distributions have been used to characterize regional isoprene emissions in tropical and boreal regions. They typically are within a factor of two of BVOC emission model estimates (Barkley et al., 2011, Stavrakou et al., 2009, Marais et al., 2012). Stavrakou et al. (2018) report the global distribution of isoprene emission trends for 2005 to 2015 and report that satellite-based estimates generally agree with

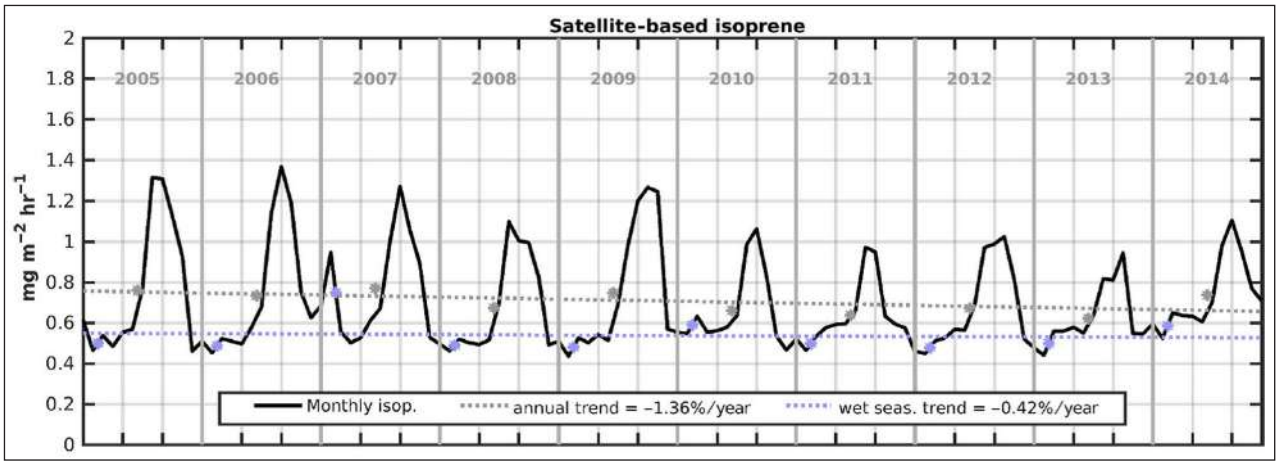

Figure 4.1.3 Wet season satellite-based isoprene flux estimates from 2005 to 2014 in Amazonia, derived from OMI formaldehyde columns. A decreasing trend of –0.42% per year for isoprene fluxes was observed during the wet season. Figure from Yáñez-Serrano et al., 2020.

model estimates of emission responses to environmental change. While these results demonstrate some success in improving BVOC emission models during the past several decades, substantial uncertainties remain, especially for emission variability, stress-induced emissions, and climate and land cover changes (Weber et al., 2021).

4.2. TRACE GAS CONCENTRATIONS AND EMISSIONS

Forest emissions and the forest-atmosphere trace gas exchange influence the concentration of many atmospheric species such as CO_2, CH_4, CO, SO_2, NO_X, and O_3. Photosynthesis and respiration control the concentrations and fluxes of CO_2 over any forest. CH_4 is also a critical gas because of its importance for the global radiation balance and its role in key processes that link soil-plant-atmosphere compartments. CH_4 is emitted in large quantities in flooded forests in Amazonia (Miller et al., 2007, Beck et al., 2012). Reactive trace gases such as NO_X and O_3 mediated by OH control many oxidation pathways in the atmosphere. O_3 deposition over forests in an increasing global O_3 concentrations framework affects CO_2 exchange and Net Primary Productivity (NPP) (Ainsworth et al., 2012, Schultz et al., 2017, Pacifico et al., 2015, Pugh et al., 2019b). SO_2 is important for the formation of new particles through atmospheric oxidation, even at very low concentrations (see sections 3.3 and 4.4). NO_X emissions and deposition affect the nitrogen cycle by fertilizing N-depleted ecosystems, and NO_x is important for the isoprene oxidation pathways that produce significant amounts of SOA in tropical forests (de Sá et al., 2018, 2019, Liu et al., 2016, 2018, Yingjun et al., 2016, 2018).

In the tropics, continuous and accurate in-situ concentration measurements of trace gases, such as CO_2, CH_4, CO, O_3, NO_X, SO_2, are still scarce – foremost because of the complex environmental and logistical conditions that make the continuous operation of complex scientific equipment at a remote site challenging and expensive. In Amazonia, essentially all measurements done until a few years ago were either campaign-based or long-term CO_2 flux measurements, providing highly relevant information on the amplitudes of daily and seasonal variations of trace gas concentrations as part of the "bottom-up" approach (e.g., Andreae et al., 2002; Araújo et al., 2002; Querino et al., 2011; Oliveira et al., 2018; Saleska et al., 2003). Extending the spatial coverage for carbon flux estimates, since the year 2000 and with some interruptions, bi-weekly to monthly airborne vertical profiles were flown at heights from 300 up to 7300 m a.g.l. at several locations throughout the Amazon basin (Gatti et al., 2010). Several trace gas species were measured, including CO_2, CH_4, and CO (Basso et al., 2016; Gatti et al., 2014; Miller et al., 2007). Other large airborne and ground-based measurement campaigns, during which at least part of the abovementioned gas species was measured, including the 2008/2009 BARCA campaigns (e.g., Andreae et al., 2012; Lloyd et al., 2007, Beck et al., 2013), the 2014 ACRIDICON-CHUVA campaign (Wendisch et al., 2016, Machado et al., 2018, Schulz et al., 2018, Mei et al., 2020), SAMBBA (Morgan et al., 2020, Hodgson et al., 2017, 2018, Darbyshire et al., 2019) and the GoAmazon2014/5 campaign (Martin et al., 2016).

In the boreal forest region, trace gas concentrations are continuously measured at several sites as part of air quality monitoring (e.g., Anttila and Tuovinen, 2010). More comprehensive measurements are conducted in fewer locations. In Finland, measurements of trace gases are performed since the 1990s at two boreal forest sites: in Hyytiälä (Lyubovtseva et al., 2005) and Värriö in Finnish Lapland (Ruuskanen et al., 2003). In addition to ground-based measurements, airborne measurement campaigns have been organized to measure the vertical profiles of trace gases in these locations, for instance, in connection with wildfire plumes (Leino et al., 2014).

The ZOTTO site (Heimann et al., 2014) is one of the measurement sites of the EUROSIBERIAN CARBONFLUX and "Terrestrial Carbon Observing Programme—Siberia (TCOS-Siberia)" projects (Heimann 2002). Before constructing the 304 m tall ZOTTO tower, most studies focused on eddy covariance flux measurements (Lloyd et al., 2002a; Shibistova et al., 2002; Röser et al., 2002; Kurbatova et al., 2002). From 1998 until 2005 also regular vertical aircraft profiles up to 3,000 m above the ground level recorded temperature, humidity, CO_2 concentration, and stable isotopic composition, as well as concentrations of CH_4, CO, H_2, and N_2O (Lloyd et al., 2002; Levin et al., 2002) over the ZOTTO site. High-precision measurements of trace gases and aerosols started at the ZOTTO tower in 2006 (e.g., Kozlova et al., 2008; Kozlova and Manning, 2009; Vivchar et al., 2009; Winderlich et al., 2010).

Regionally, trace gas concentration and aerosols measurements were conducted during ground-based campaigns, for example, during the "Trans-Siberian Observations Into the Chemistry of the Atmosphere" (TROICA) project in a mobile lab traveling on the Trans-Siberian railroad (TROICA; e.g., Oberlander et al., 2002; Tarasova et al., 2006). Also, vertical aircraft profiles were conducted either during campaigns on a regional scale such as YAK-AEROSIB (Paris et al., 2008, 2010) or locally at some of the Japan–Russia Siberian Tall Tower Inland Observation Network (JR-STATION) of towers (e.g., Sasakawa et al., 2010, 2013; Saeki et al., 2013).

4.2.1. Emissions of the trace gases CO_2, CH_4, and CO

Local and regional factors influence the seasonal variation of atmospheric trace gas concentrations by these gas species' ecosystem processes and their reactivity. Even in locations where the seasonal variations of some environmental drivers can be minimal (e.g., the length of day close to the equator), due to other factors such

as variations of the cloud cover intensity, frequency and intensity of precipitation or biomass burning events, the position of the ITCZ, etc., the background concentrations of most trace gases vary on seasonal (wet and dry season) and yearly scales (e.g., ENSO conditions-dependent). As for a major part of Amazonia, the trade winds dominate the long-range transport of trace gases. It is important to note that even with its height of 325 m a.g.l. and its accordingly large fetch area, the ATTO tall tower footprint is strongly biased towards the NE-E-SE sectors (e.g., Pöhlker et al., 2019). No large-scale biomass burning, land-use change, or small cities are within the footprint of the ATTO tower.

In contrast to tropics, boreal regions exhibit a substantial seasonal variation in environmental variables, such as solar radiation and temperature. This largely determines the seasonal cycle of trace gas concentrations by affecting their sources and sinks, including emissions from vegetation, atmospheric oxidation, dilution due to boundary layer mixing, and wet and dry deposition. In addition, trace gas concentrations are affected by seasonal variation in the emissions from different pollutant sources, which are often higher in winter (e.g., Shtabkin et al., 2016). Furthermore, forest fires occurring in summer and long-range transport from polluted regions affect trace gas concentration levels in the boreal region.

4.2.2. Concentrations of the trace gases CO_2, CH_4, and CO

The mole fraction of CO_2 in boreal forests exhibits a strong seasonal cycle (amplitude 18–24 ppm) due to variations in the uptake of CO_2 by the vegetation, reaching the highest values in midwinter and lowest in late summer (Kilkki et al., 2015). The diurnal variation is largest in summer (3–20 ppm) and smallest in winter (0–3 ppm). The general trend follows the global increase of CO_2 of about 2 ppm/year. In 2017 the mole fraction in Pallas, northern Finland, was 415 ppm in winter and 390 ppm in summer. Locally the concentrations vary depending on local fluxes and air mass history (Kilkki et al., 2015). The concentration of CH_4 is also increasing steadily. CH_4 concentration of 1,950 ppb was observed in Pallas in 2017. Forest regrowth plays an important role in global carbon sink dynamics. Pugh et al., 2018 found that it is not possible to understand the current global terrestrial carbon sink without accounting for the sizeable sink due to forest demography. They also imply that a large portion of the current terrestrial carbon sink is strictly transient. Tropical forest fragmentation results in habitat and biodiversity loss and increased carbon emissions (Hansen et al., 2020).

At ZOTTO, the CO_2 seasonal cycle amplitude in the period from 2007–2015 was reported to be mostly between 25 and 30 ppm (Kozlova et al., 2008; Winderlich et al., 2010; Timokhina et al., 2018), which is higher than for many other continental sites at which the marine atmospheric influence is more pronounced (Winderlich et al., 2010). The annual CO_2 growth rate is highly variable for the same period, with a mean value of 2.34 ppm/year (Timokhina et al., 2018). CH_4 has an almost flat baseline, on which concentration spikes occur throughout the year. At the same time, in summer, they can be mostly attributed to biotic activity (mainly in the nearby bogs) and forest fires. The origin of the winter concentration spikes remains unclear (Winderlich et al., 2010, 2014).

In Amazonia, while the CO_2 and CH_4 growth rates at ATTO are comparable to global growth rates, the monthly-averaged absolute concentrations are typical for air masses under the influence of the Northern and Southern Hemisphere (NH and SH, respectively) that impacts in different seasons the air sampled at ATTO. The CH_4 concentration is constantly about 50 ppb higher than for background sites influenced exclusively by SH air masses and only little (up to 20 ppb) below values of NH background sites. During austral summer (wet season), this is due to the ITCZ being at the southern border of Amazonia, south of ATTO, which is mostly influenced by NH air masses (see Andreae et al., 2015). In austral winter (dry season), when ATTO is in the SH atmosphere, the CH_4 concentrations remain high due to enhancements from local to regional CH_4 sources: wetlands, diffusion, and ebullition from rivers and reservoirs (e.g., Sawakuchi et al., 2014; Wilson et al., 2016), sided by tree-mediated soil (Pangala et al., 2017) and biomass burning emissions (e.g., Andreae et al., 2012). For CO_2, the temporal evolution of its concentration is in line with the NH/SH alternation described above and increased uptake in the Amazon compared to both NH and SH during the wet season, when the concentration at ATTO is lower than for both (see Andreae et al., 2015).

CO exhibits a seasonal cycle in boreal forests, with the highest concentrations in winter (January–February) and the lowest in late summer (July–August). At the ZOTTO site, the seasonal averages of background CO concentrations range from ca. 90 ppb to 160 ppb (Chi et al., 2013). The diurnal variation of CO concentration is typically weak in remote boreal forests (Chi et al., 2013). In Finnish boreal forests, CO concentration has decreased considerably during the last decades due to combustion emission reductions (Anttila and Tuovinen, 2010). The average summertime CO concentration in Hyytiälä is ca. 120 ppb (Leino et al., 2014).

In Amazonia, the diurnal variation of CO_2, CH_4, and CO (monthly averages) is influenced by the air intake height, time of day and year, biological activity, and other environmental drivers. Generally, CO_2 and CO accumulate in the nighttime with a positive gradient with height (up to about 100 ppm and 20 ppb, respectively). During the daytime, they are mainly vertically mixed (Gatti et al., 2021). CO displays relatively stable concentrations around 120 ppb in the wet season and on average about

50 ppb higher during the dry season; the occasional larger and shorter CO peaks are related to biomass burning and can – depending on the event's proximity – have an amplitude of several 100 ppb (Andreae et al., 2012, Gatti et al., 2021). The diurnal variation of CH_4 is similar to the one of CO_2 but less pronounced; with up to 40 ppb, it is largest from August to October and lowest in the period November – April with up to ~ 10 ppb. In contrast to CO_2, during the nighttime of the months' May to October, the CH_4 profile displays a negative gradient with height, which suggests above canopy CH_4 advection from most likely local sources (i.e., wetlands/water bodies), followed by homogenization by vertical mixing after sunrise (Botía et al., 2020).

4.2.3. Concentrations of the trace gases O_3, NOx, and SO_2

For both wet and dry seasons at the ATTO site, the diurnal variation of O_3 concentrations shows a similar pattern, increasing from the morning to peak around 14:00 LT and subsequent decrease due to deposition and chemical reactions. The difference is that in the dry season (Aug–Sep 2013), the maximum values of ~ 12 ppb are about 4 ppb larger than those in the wet season (Feb 2014) (Andreae et al., 2015). A similar observation was made by Bela et al. (2015) when they measured O_3 concentrations of <20 ppb to the west and north in both seasons and all investigated regions of the Amazon basin during the wet-to-dry transition season. In contrast, they observed elevated O_3 concentrations of 40–60 ppb to the east and south of Manaus in the dry-to-wet transition when biomass-burning O_3 precursors were present. Oliveira et al. (2018) have concluded that intermittent turbulence may produce very large fluxes and affect concentrations of CO_2 and O_3 from near the stable boundary layer top down to the middle of the canopy. Paralovo et al. (2019) report measurements in a semi-urban environment in the Amazon region, concentrations of nitrogen dioxide (NO_2): 0.10–23 and 0.30–6.1 μg m^{-3}, sulfur dioxide (SO2): 0.12–3.7 and 0.14–15 μg m^{-3}, and ozone (O_3) 1.4–14 and 1.0–40 μg m^{-3}, during the wet (March–April 2014) and dry season (August–October 2014), respectively.

The concentration of O_3 has a clear seasonal cycle in boreal forests, with the highest concentrations in spring (March–May) and the lowest concentrations in late autumn (October–November) (Lyubovtseva et al., 2005; Chen et al., 2018). In Hyytiälä, monthly mean O_3 concentrations range from ca. 20 ppb to 40 ppb. At ZOTTO, in the period 2007–2012, monthly mean O_3 concentrations range from ~ 15 to ~ 50 ppb, with the maximum in April and a flat minimum from September to January (Moiseenko et al., 2018). At many boreal forest sites, an increasing trend is seen in the spring-time maximum concentrations of O_3 (Karlsson et al., 2007). The diurnal pattern of O_3 exhibits a maximum in the late afternoon and a minimum in the early morning in boreal forests (Lyubovtseva et al., 2005).

In pristine tropical rainforests, the level of NO_x ($NO_x \equiv NO + NO_2$) is very low as anthropogenic sources are absent. Furthermore, the NO (nitric oxide) emitted by soils reacts with O_3 to NO_2 (nitrogen dioxide) inside the canopy, while NO_2 photolysis is low due to the shading of the canopy. Within the high and dense rain forest canopy, the produced NO_2 deposit on leaves, reducing the contribution to the nitrogen oxide levels above the canopy (~ 70% reduction (Jacob and Wofsy, 1990)), as O_3 formation in remote tropical regions are generally NO_x-limited (VOCs are not limiting factor in these environments). The amount of NO_x escaping the canopy, produced by lighting, transported from anthropogenic sources, and biomass burning will determine the levels of O_3 being photochemically produced. In the absence of strong sources, Jacob and Wofsy (1990) show that O_3 is photochemically produced from soil NO_x just above the canopy, but photochemical destruction in the remainder of the boundary layer, therefore having a minor net effect in pristine conditions. A modeling study (Scott et al., 2018a) also show that over the pristine rainforest, the direct reaction of O_3 with BVOCs outcompetes its formation involving BVOCs and NO_x due to NOx-limited conditions.

The NO_x concentration in boreal forests has a maximum in winter (December–February) and a minimum in summer (June–August) due to the seasonal variation of radiation and differences in long-range transport in different seasons. In Hyytiälä, the monthly means of NO_x concentration vary between ca. 0.5 and 3.5 ppb (Lyubovtseva et al., 2005). On a daily scale, NO_x concentration is the lowest during daytime and the highest at night. In Finnish boreal forests, NO_X concentrations have declined at the rate of ~3–4%/year during the last decades (Anttila and Tuovinen, 2010). Vivchar et al. (2009) report NO_x concentrations at ZOTTO for March to August 2007 to be from <0.11 to 7.63 ppb, with a median value of 0.37 ppb.

SO_2 is relatively low in boreal forests. The median concentration during 1997–2012 in Hyytiälä was 0.17 ppb (Nieminen et al., 2014). There is a clear seasonal cycle with the highest concentrations in winter (January–February) and the lowest in summer (May–October). A decreasing trend is seen in SO_2 mixing ratios over the boreal forest region, mainly due to air quality measures (Anttila & Tuovinen, 2010). In Hyytiälä, the trend is –1.6%/year, and an even faster decrease are observed in Värriö, Finnish Lapland, which is affected by Russian industrial activities (Kyrö et al., 2014).

H_2SO_4 is produced in the atmosphere by the oxidation of SO_2. The main gas-phase oxidant is OH, although other oxidants, like Criegee intermediates, might also play a role (Mauldin et al., 2012). The long-term trends in H_2SO_4 concentrations have been investigated using an

H_2SO_4 proxy based on its sinks and sources (Petäjä et al., 2009). The median molecular concentration of H_2SO_4 in Hyytiälä during 1997–2012 was $8.1 \cdot 10^5$ cm^{-3} (Nieminen et al., 2014). The H_2SO_4 proxy has a strong seasonal variation with the highest concentrations in winter (Jan–March) and the lowest during the summer, although a smaller secondary maximum is observed in autumn. The decrease in SO_2 is also reflected in decreasing H_2SO_4 concentrations of –1.4%/year (Nieminen et al., 2014).

Based on trajectory analysis, high NO_x and SO_2 concentrations in Finnish boreal forests are associated with air arriving from Eastern Europe, especially over Baltic countries, and St. Petersburg, pointing towards the importance of long-range transport of anthropogenic emissions (Riuttanen et al., 2013). In addition, elevated trace gas concentrations are linked to forest fires. Eastern European wildfires have been found to increase CO concentration over Finland by 50–160%. Elevated levels of CO_2, SO_2, O_3, and NO_x have also been observed in wildfire plumes (Leino et al., 2014), and emissions, as well as air quality issues, could be expected to increase (Carvalho et al., 2011).

4.2.4. Land atmosphere exchange of CO_2, CH_4, and H_2O in forests

Boreal forests store one-third of the global terrestrial carbon pool and play a significant role in global carbon and water cycles and climate (Bonan, 2008, Savage et al., 1997). Forests exchange large amounts of carbon dioxide (CO_2) via photosynthesis and decomposition in the boreal region. Methane (CH_4), as the second most important greenhouse gas after CO_2, is emitted from methanogenic organisms living in soil, biomass, plant litter, and woody debris under anoxic conditions in boreal forests (Keppler et al., 2006; Mukhin and Voronin, 2008). Meanwhile, it is consumed by methanotrophic microbial communities on the forest floor (Lohila et al., 2011). The water vapor (H_2O) flux from boreal forests to the atmosphere, also called evapotranspiration (ET), is a vital component of the terrestrial energy and water cycle (Jung et al., 2010). It is the second-largest component of the hydrological cycle after precipitation (Oki and Kanae, 2006; Trenberth et al., 2007). Several studies have shown that the impact of deforestation on rainfall depends on the deforested area (Chambers and Artaxo, 2017).

Boreal forest ecosystems have been identified as a sink for atmospheric CO_2 (Baldocchi et al., 2018; Luyssaert et al., 2007), with a mean (± standard deviation, SD) annual net ecosystem exchange (NEE) of –84 ± 110 g C m^{-2} a^{-1} (***Figure 4.2.1a***). They are commonly a sink for CH_4 with the forest floor of upland boreal forests providing a mean net uptake rate of about –0.27 ± 0.36 g C-CH_4 m^{-2} a^{-1} (***Figure 4.2.1b***) (Ni and Groffman, 2018). Meanwhile, boreal trees are recently identified as an additional significant but small source of CH_4 corresponding to ~1% of the forest floor uptake (Machacova et al., 2016). In terms of ET magnitude, roughly two-thirds of the annual precipitation in boreal forests is returned to the atmosphere via ET, accounting for approximately 10% of global ET (Schlesinger and Jasechko, 2014). The annual amount of incoming precipitation is often more significant than the amount of water lost via ET, resulting in an overall positive water balance for these ecosystems. The inter-annual variability of CO_2, CH_4, and H_2O fluxes in the boreal forests is relatively smaller compared to temperate and tropical forests. It is generally attributed

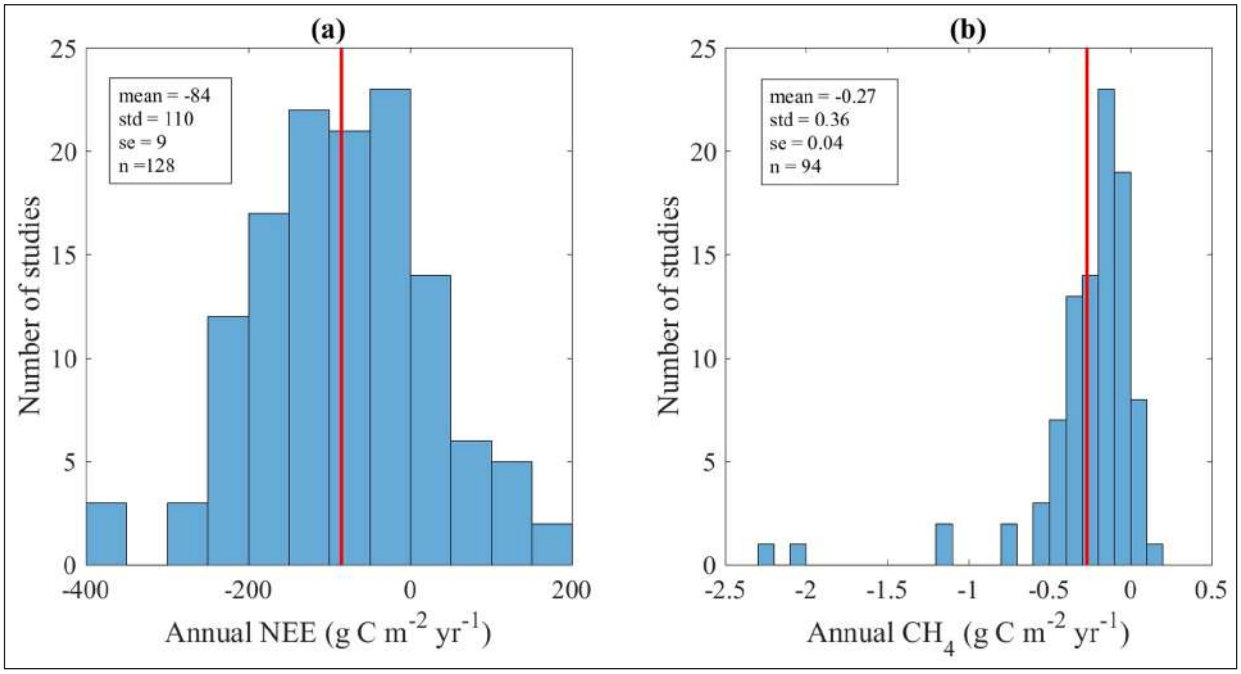

Figure 4.2.1 Histograms of annual net ecosystem exchanges of CO_2 and CH_4 in boreal forests from 1990 to 2015. **(a)** annual NEE flux data collected from a literature synthesis. **(b)** Annual CH_4 data were compiled based on Ni and Groffman (2018).

to the variations of incoming radiation, air temperature, precipitation, atmospheric demand for vapor, and soil temperature and moisture (Baldocchi et al., 2018; Law et al., 2008; Sundqvist et al., 2015; Williams et al., 2012).

Tropical forests are a central component of the Earth system, critically regulating many processes in the global climate by their considerable contribution to global land surface ET and cycling more CO_2 than any other biome (Gloor et al., 2012, Friedlingstein et al., 2019). It seems all components of the carbon balance are substantially larger in the tropics compared to other biomes (Malhi et al., 1999). Overall, tropical forests account for gross primary productivity (GPP) of about 41 Pg (~33% of the global GPP) of carbon per year (Pg C a^{-1}), with an additional 31 Pg C a^{-1} (~25% of the global GPP) taken up by tropical savannas and grasslands (Beer et al., 2010). Above-ground carbon storage in tropical forests is about 190 Pg (Saatchi et al., 2011), about 34% of the storage in terrestrial ecosystems.

Given the importance of the forests in the global carbon and water cycles, concerns about climate change and human disturbances effects in these forests have stimulated renewed interest in and created an unprecedented demand for information about their structure and functioning, both in pristine conditions and subject to disturbances such as forest management, deforestation, and land degradation. While intact tropical forests are estimated to be Earth's largest continental carbon sink (Pan et al., 2011; Phillips et al., 2009, Ometto et al., 2005), the stability of this sink is susceptible to a warming climate and disturbance processes (Lenton et al., 2008). Recent work based on long-term biomass plot monitoring provides evidence that the forest carbon sink is declining (Brienen et al., 2015, section 4.2.6). However, because plot networks sample only a small fraction of vast regions over a limited period, disturbances at timescales of decades or longer may not be sampled, potentially leading to overestimates of biomass increase (Chambers et al., 2009; Davidson et al., 2012; Lloyd et al., 2009).

Because of the total metabolic activity and of the large extension of tropical and boreal forests, a small but systematic bias in an eddy covariance flux estimate of 8 g C m^{-2} a^{-1} would propagate to more than 2 Pg C a^{-1} at the global scale, which illustrates the accuracy requirements of flux data for estimating global annual means (Jung et al., 2011). For CO_2, CH_4, and H_2O data to be suitable for inverse modeling ("top-down" approach), measurements must be continuous and well-calibrated, representing part of the relatively well mixed planetary boundary layer conditions during daytime and the residual layer during nighttime. This condition can be attained with the help of tall towers (e.g., Winderlich et al., 2010). In the boreal region, such towers are available, e.g., the 150 m tall tower within the research infrastructure ICOS (e.g., Chi et al., 2019). Since 2012, continuous and vertically resolved measurements of O_3, H_2O, CO_2, CH_4, and CO (the latter three species also as high accuracy measurements) are available from an 80 m-tall tower at the ATTO site (Andreae et al., 2015 or see section 2). The 325 m-tall tower increases the regional representativeness of ATTO measurements, further closing the gap between ground-based and airborne in-situ and remote sensing observations and providing an Amazon-wide unique research platform (Andreae et al., 2015).

4.2.5. Geographical and seasonal variability for CO_2, CH_4, and H_2O in boreal forests

The boreal biome is characterized by strong seasonality in incoming solar radiation with snow and soil frost during the winter. While the seasonal pattern of the incoming radiation is dependent on latitude, the seasonality in air temperature, snow, and soil frost varies geographically and temporally. Given this, CO_2, CH_4, and H_2O fluxes in boreal forests have very strong seasonal variations.

During the spring and autumn transition seasons, specific weather conditions are particularly important in controlling the seasonal and annual carbon and water fluxes. More specifically, the boreal spring is often characterized by high incoming solar radiation while the soil still is frozen, delaying ecosystem GPP until the soil frost thaw and also contributing typical season pattern of a lagged ecosystem respiration R_{eco} to GPP (Baldocchi et al., 2018). Many studies have demonstrated that earlier and warmer springs increased the boreal forest carbon sink strength significantly (e.g., Barr et al., 2002; Dunn et al., 2007; Kljun et al., 2007; Pulliainen et al., 2017). In contrast, the autumn period in the boreal regions is characterized by diminishing incoming solar radiation reducing the potential for photosynthesis. At the same time, soil, and air temperatures above zero degrees promote both autotrophic and heterotrophic respiration. These conditions usually lead to net CO_2 emissions during autumn periods (Öquist et al., 2014).

During the summer period, which is commonly characterized by sufficient incoming radiation and relatively high temperature, the CO_2 sink strength of boreal forests may be further determined by water availability but with varying responses across forest stands (e.g., Law et al., 2001). In comparison, the net CH_4 uptake rates are generally highest during the summer due to higher temperatures and drier soils. Forest soils may also periodically act as net CH_4 sources, e.g., during water-logged conditions (Lohila et al., 2016). In addition, during the snow-free growing season, ET is a major water loss pathway in boreal forests and can often exceed the amount of incoming precipitation (Sarkkola et al., 2013; Wang et al., 2017).

During the long winters with low incoming radiation, frozen soils, and precipitation in the form of snow, ecosystems are sources of CO_2 and CH_4 for approximately four-five months (Nov–Feb) (Treat et al., 2015; Zona et

al., 2016) and have reduced tree transpiration which otherwise is a major flux component of ET (Jasechko et al., 2013). However, the winter ecosystem respiration has been inferred to be declining over recent decades due to decreased snowpack, which might enhance the CO_2 sink strength in boreal forests (Yu et al., 2016). Despite reduced transpiration during the winter months, trees in boreal forests can intercept a large amount of snow in their canopies, which in turn can be directly lost back to the atmosphere during the process of sublimation and/or evaporative water losses. Previous studies in seasonally snow-covered ecosystems have shown that water losses via snow interception ranges represent, on average, ca. 20% of wintertime precipitation (Kozii et al., 2017). Moreover, the boreal ecosystems are experiencing rapid climatic changes (Chapin et al., 2005; IPCC, 2014), and even slight alterations in the timing and magnitude of precipitation could lead to a negative water balance and enhanced water stress for tree growth in boreal forests (Barber et al., 2000; Ma et al., 2012; Peng et al., 2011).

Besides the biophysical controls (i.e., weather conditions), forest management practices such as fertilization, drainage, and thinning/clearcutting also significantly alter the boreal forest CO_2, CH_4, and H_2O fluxes. As boreal forests are severely nutrient-limited, adding fertilizers can increase the CO_2 uptake, i.e., biomass production, by up to 25–30% (Bergh et al., 2014; Lim et al., 2015) but meanwhile suppress the CH_4 uptake rates by the forest floor (Maljanen et al., 2006). In certain parts of the boreal region, drainage of wet soils is a common practice to enhance tree growth. There is still significant uncertainty regarding the net effect on the carbon and greenhouse gases (GHG) balances from the increased decomposition of drained peat and increased carbon uptake in the vegetation (Lohila et al., 2011; Minkkinen et al., 2018; Sikstrom and Hokka, 2016). Thinning and clearcutting mainly introduce spatial variability within the forest stands, creating various carbon source and sink locations following each harvest operation and forest regeneration sequence. Specifically, recent clear-cut areas usually act as sources of CO_2 and CH_4 (Coursolle et al., 2012; Lee et al., 2002; Strömgren et al., 2016; Sundqvist et al., 2015). There is currently a scientific debate on the effects on the forest carbon exchange from the two different forest biomass extraction practices, clear-cut and continuous cover forest, with the latter being promoted to reduce GHG emissions associated with clear-cutting (Lundmark et al., 2016).

Given the important role trees play in ET (Jasechko et al., 2013), the continuous cover forest has been suggested as a way to reduce soil moisture in boreal forests to enhance tree growth while at the same time minimize the negative effects of enhancing GHG emissions as a result of ditching/drainage (Stenberg et al., 2018).

Natural disturbances, such as wildfires, droughts, and insects, are identified as important drivers of the boreal forest carbon and water balances in some boreal regions, i.e., mostly North America and Siberia (e.g., Amiro, 2001; Williams et al., 2016). Fires cause significant instantaneous carbon losses to the atmosphere and enhance water stress in the ecosystem, while the post-fire recovery might lead to enhanced CO_2 and CH_4 uptake (Bond-Lamberty et al., 2007; Köster et al., 2017; Yue et al., 2016).

Boreal forests generally have a positive water balance and act as a net sink for atmospheric CO_2 and CH_4 at the ecosystem scale. However, their annual fluxes vary significantly with individual forest stands depending on forest age, nutrient availability, and local climate conditions (Barber et al., 2000). Given the complexity and heterogeneity of boreal forests, there are still gaps in estimating the carbon and water budgets, especially upscaling to larger spatial scales. At the global scale, the highest rates of warming in northern latitude (IPCC, 2013) will result in a progressive lengthening of the growing season due to earlier springs and delayed autumns (Bunn et al., 2007; Richardson et al., 2013). Boreal forests may also be experiencing a wetter condition in Europe and Asia but drier in parts of North America (Greve et al., 2014). Such changes can have cascading effects on the carbon and water cycles in these ecosystems (Forkel et al., 2016), resulting in greater water limitation for plant growth in the dry areas (Barber et al., 2000). With increasing temperatures, there is a corresponding lengthening of the evaporative period leading to greater snow sublimation (Kozii et al., 2017) and, in turn, potentially enhanced soil water deficit over the early and middle portion of the growing season (Barnett et al., 2005; Jepsen et al., 2012), which may affect the carbon budget by reducing CO_2 uptake. Additionally, temporal shifts to earlier snowmelt when evaporative demand is low and trees are still dormant will result in more water being lost as runoff, thereby reducing soil moisture in the later part of the growing season (Barnett et al., 2005). Such changes in the hydrological cycle may help explain the current widespread pattern of reduced productivity (Barber et al., 2000; Ma et al., 2012) and increased tree mortality (Peng et al., 2011) in North American boreal forests.

4.2.6. Exchange of CO_2, CH_4, and H_2O in tropical forests

General questions about how tropical forests exchange carbon and other trace gases with the atmosphere, variability from seasonal to interannual scales, and how changes in land use affect carbon balance are currently being addressed for all tropical regions (Ciais et al., 2011; Gloor et al., 2012; Grace et al., 2014; Patra et al., 2013; Valentini et al., 2014). Most studies and efforts are focused on the Amazon region, largely because of

strong institutional developments and international collaboration projects stimulated during extensive experiments such as the LBA research program (Keller et al., 2004, Oliveira et al., 2007). One of the legacies of the LBA program was the establishment of a network of eddy flux towers in the Amazon that provides important knowledge about the characteristics of energy, water, and carbon fluxes throughout the region (Araújo et al., 2002; Borma et al., 2009; Saleska et al., 2003; von Randow et al., 2004). While terrestrial surface models have historically represented the Amazon ecosystem undergoing water stress, predicting declines in evapotranspiration and photosynthesis during the dry season, measurements in the Amazon towers seem to show a very little decline and even a slight increase in evapotranspiration and photosynthesis (related to greater availability of solar radiation) in the dry season (Restrepo-Coupe et al., 2013). However, towers in the southern part of the Amazon, with semi-deciduous forests or transition areas to the savanna and towers in deforested areas show evident declines in the fluxes during the dry season and signs of water stress, also related to a more intense dry season in these places (da Rocha et al., 2009; von Randow et al., 2004). Inundated tropical forests are underrepresented in analyses of the global carbon cycle and constitute 80% of the surface area of aquatic environments in the lowland Amazon basin. The CO_2 flux from the water in the flooded forest is about half of the net primary production of the forest estimated from the literature (Amaral et al., 2020).

von Randow et al. (2013) analyzed general relationships between annual fluxes of carbon and water with climate variables, as measured at the Amazonian LBA forest towers and as an ensemble means of model simulations. Data from 13 site-years of Net Ecosystem Exchange (NEE) of carbon against annual total precipitation (*P*) and a combined dryness index ($D = R_n / \lambda P$, where λ = 2.45 MJ / kg is the latent heat of vaporization and R_n is the net radiation), are presented in ***Figure 4.2.2***. In general terms, sites with low annual rainfall have lower C uptake than sites with high precipitation; dry years may result in a carbon source to the atmosphere (Gatti et al., 2014; Saleska et al., 2003; Zeri et al., 2014). This results in a pattern of higher net uptake at sites/years with higher annual rainfall or less D, which is partially captured by the models (von Randow et al., 2013, Silva Camila et al., 2018).

These estimates, performed at *Terra Firme* intact forests of the Brazilian Amazon, are corroborated by permanent plot measurements throughout the whole region, resulting in about 0.3 Pg C of carbon taken up per year in the undisturbed forest for non-drought years. Conversely, deforestation emitted about 0.24 Pg C per year in 2010 (Aragão et al., 2014). During drought years, carbon emissions increased by approximately twofold [0.46 Pg C per year], and drought-related carbon emissions from tree mortality and forest fires during extreme drought events become critically important, contributing to 48% of the total Brazilian Amazonia emissions. Several studies also show that clouds and precipitation are closely linked to carbon dynamics in tropical forests. Analysis of future warming and enhanced CO_2 on the vegetation-cloud interaction shows high sensitivity of tropical forests to enhanced CO_2. With elevations in CO_2, plant transpiration is reduced due to stomatal closure, resulting in reduced latent- and increased sensible heat fluxes. Elevations in temperature yielded opposite results with reduced sensible and increased latent heat fluxes, which reduced the turbulent kinetic energy and buoyancy rates, thereby negatively impacting cloud formation (Sikma et al., 2019).

Long-term analysis of 321 plots over Amazonia reveals that the net aboveground biomass, productivity,

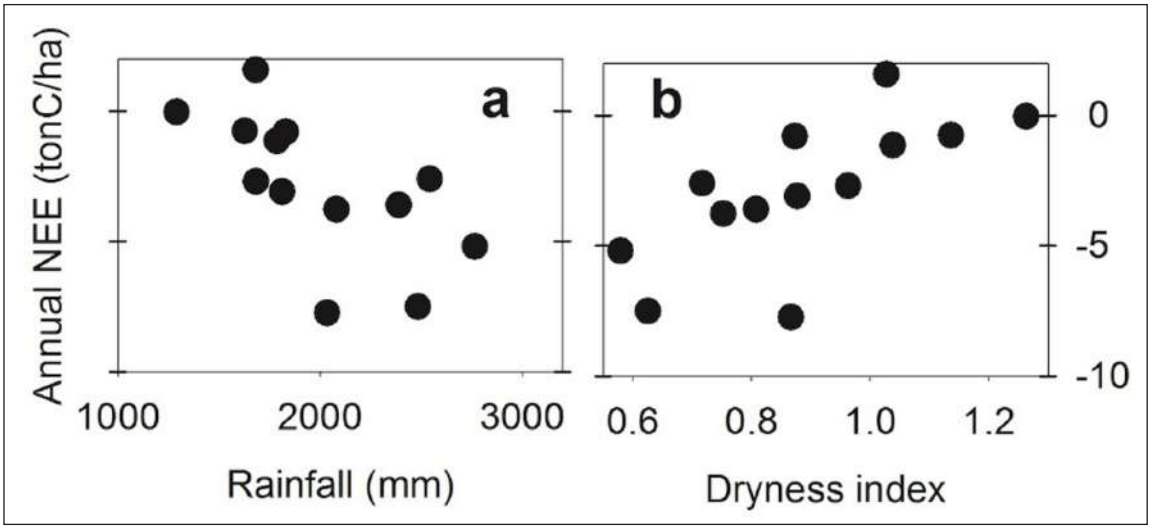

Figure 4.2.2 Annual Net Ecosystem Exchange (NEE) of carbon measured in Amazon flux towers at pristine forests, in the period 1999–2006, compared to measured rainfall and dryness index. Figure adapted from von Randow et al. (2013) (minus sign represents net carbon uptake by the forest here).

and mortality show clear trends (Brienen et al., 2015). The most important is the large increase in tree mortality attributed to an increase in climate extremes, particularly the droughts of 2005 and 2010. Rates of the net increase in above-ground biomass declined by one-third during the past decade compared to the 1990s. The observed decline of the Amazon sink diverges markedly from the recent increase in terrestrial carbon uptake at the global scale, driven mainly by boreal forests.

Figure 4.2.3 shows long-term (1985 to 2020) measurements of net biomass change, productivity, and biomass mortality in Amazonia. It shows remarkable changes in the carbon allocation in Amazonia, with an increase in biomass mortality, possibly by an increase in climate extremes or increasing temperatures (Brienen et al., 2015).

Hubau et al., 2020 analyzed structurally intact tropical forests from Africa and Amazonia from 1985 to 2014. The carbon sink in live aboveground biomass in intact African tropical forests has been stable for the three decades to 2015, at 66 g C m^{-2} a^{-1}, in contrast to the long-term decline in Amazonian forests. The difference is primarily driven by carbon losses from tree mortality (similar to Brienen's analysis in ***Figure 4.2.3***), with no detectable multi-decadal trend in Africa and a long-term increase in mortality in Amazonia. Both continents show increasing tree growth, consistent with the expected net effect of rising atmospheric CO_2 and air temperature. A model including carbon dioxide, temperature, drought, and forest dynamics accounting for the observed trends indicates a long-term future decline in the African sink.

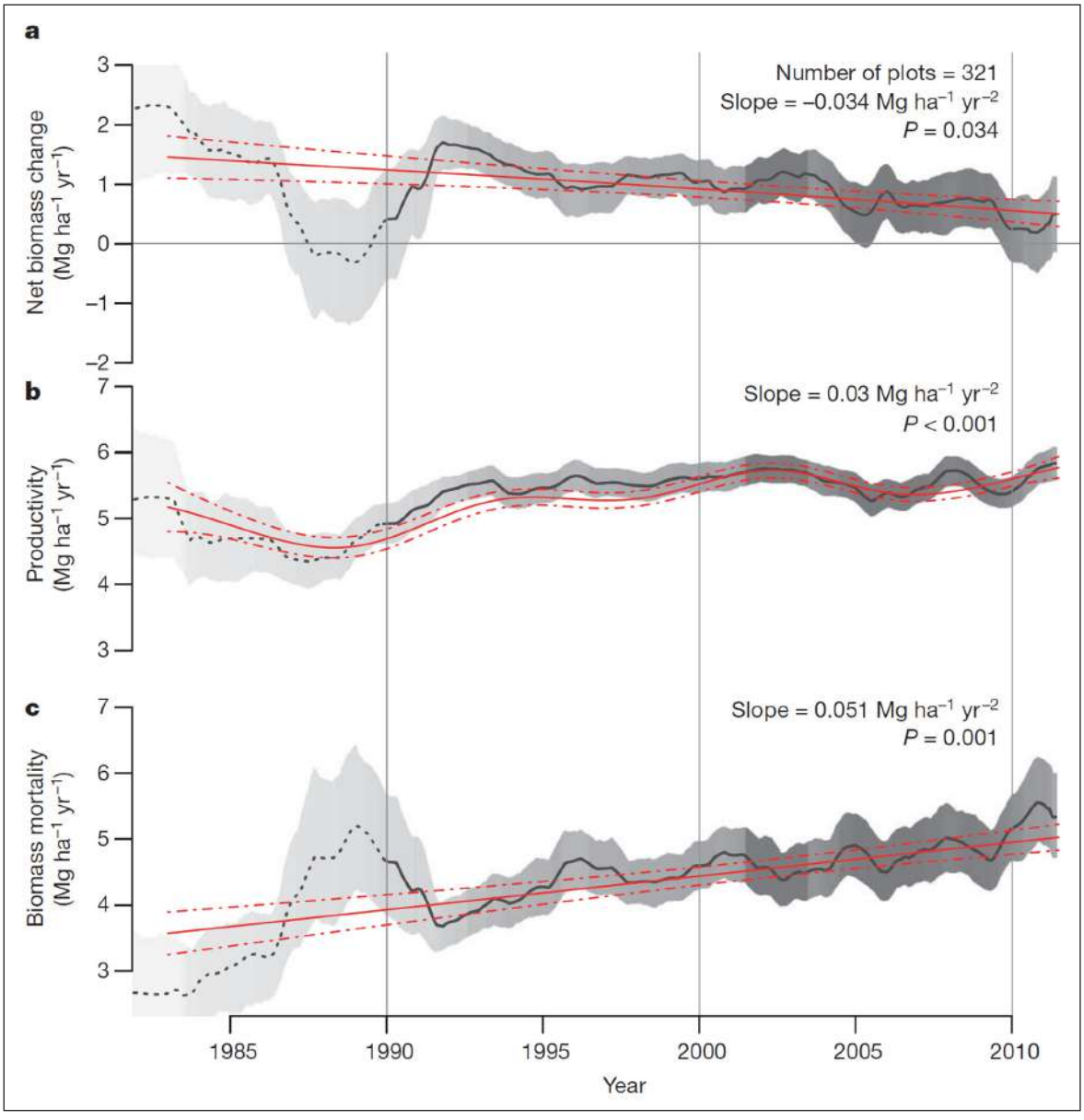

Figure 4.2.3 Time series of net biomass change, productivity, and biomass mortality from 1985 to 2010 in Amazonia, showing an increase in tree mortality that brings the net biomass change close to zero in recent years. Shading corresponds to the number of plots included in the calculation of the mean, varying from 25 plots in 1983 (light grey) to a maximum of 204 plots in 2003 (dark grey). Figure from Brienen et al., 2015.

In contrast to African tropical forests, the Amazonian sink continues to weaken rapidly (Mitchard et al., 2018). Tree mortality is the main difference for the two tropical forests, with a much higher mortality increase in Amazonia. Given that the global terrestrial carbon sink is increasing in size, independent observations indicate greater recent carbon uptake into the Northern Hemisphere landmass (Friedlingstein et al., 2019). Mitchard, 2018 details the impact of climate change on the tropical forest carbon cycle and shows that in the near future, tropical forests are likely to become a carbon source, owing to continued forest loss and the effect of climate change on the ability of the remaining forests to capture excess atmospheric carbon dioxide.

Recent works using several techniques such as remote sensing, forest inventory plots, atmospheric inversions, and modeling shows that Amazonia could already be a carbon source, at least for parts of the basin (Gatti et al., 2021, Qin et al., 2021, Mitchard et al., 2018). Qin et al. calculates the above-ground biomass (AGB) and indicates that forest degradation has become the largest process driving carbon loss in Amazonia. They show that during the period 2010–2019, the Brazilian Amazon had a cumulative gross loss of 4.45 Pg C against a gross gain of 3.78 Pg C, resulting in a net AGB loss of 0.67 Pg C. Forest degradation (73%) contributed three times more to the gross AGB loss than deforestation (27%), given that the areal extent of degradation exceeds that of deforestation. Gatti et al., 2021 analyzed 590 vertical aircraft profiles from 2010 to 2018 with high precision CO_2 and CO measurements. They show that in the Eastern Amazonia region, the carbon lost by deforestation was 0.20 PgC y^{-1}. Forest degradation lost 0.11 PgC y^{-1}, resulting in a total carbon loss in the region of 0.31 PgC y^{-1}. They explored

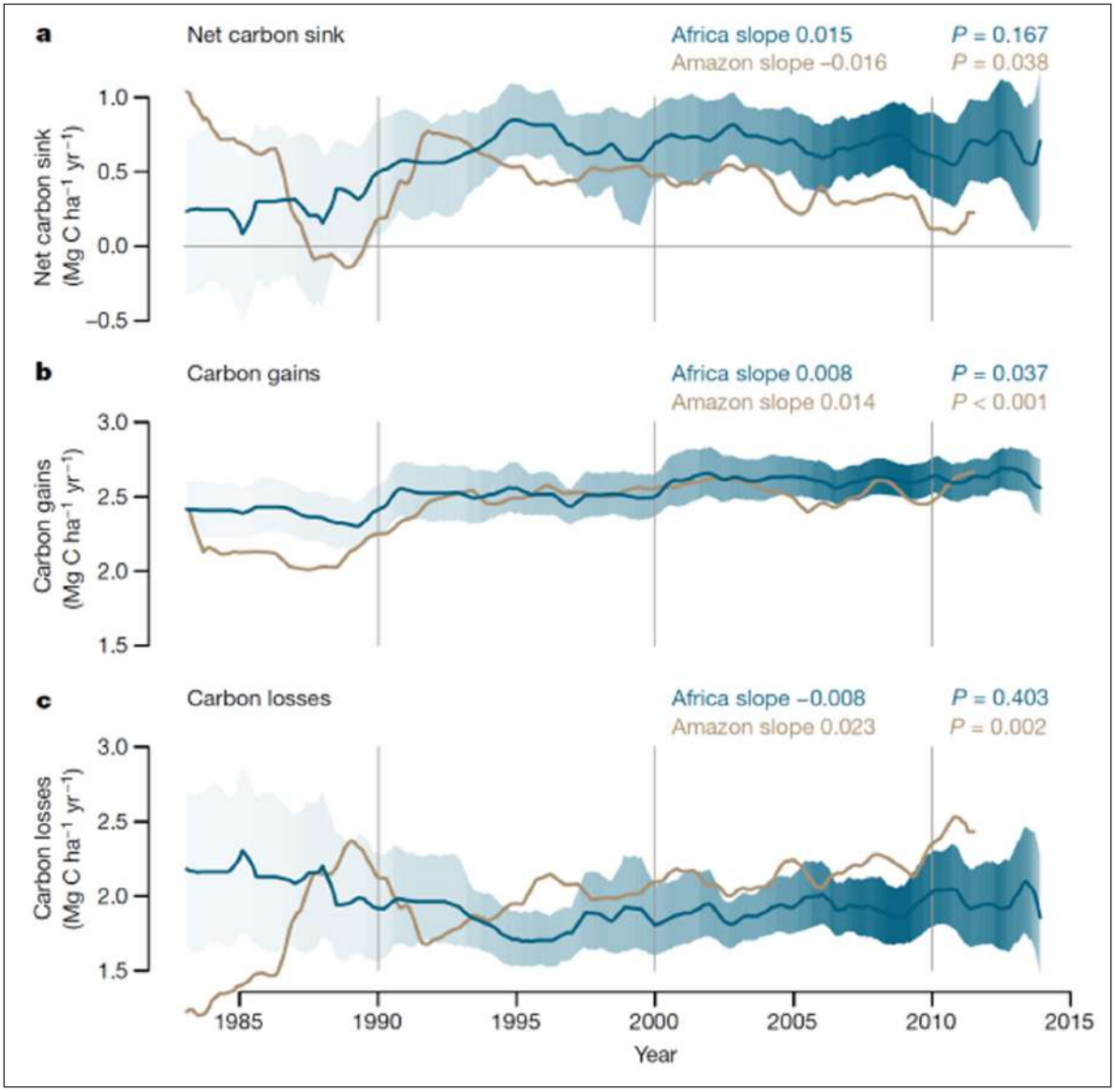

Figure 4.2.4 Long-term carbon dynamics of structurally intact old-growth tropical forests in Africa and Amazonia from 1985 to 2014. In **(a)** Trends in net aboveground live biomass carbon. In **(b)**, the carbon gains to the system from wood production. In **(c)**, carbon losses from the system from tree mortality. Shading corresponds to the 95% CI, with darker shading indicating a greater number of plots monitored in that year (the lightest shading indicates the minimum 25 plots monitored). Figure from Hubau et al., 2020.

the effect of climate change and deforestation trends on carbon emissions and found that the intensification of the dry season and an increase in deforestation seem to promote ecosystem stress, increase in fire occurrence, and higher carbon emissions in the Eastern Amazon. They also report an increase in tree mortality as a result of climate change, with higher temperature, increases in climate extremes, and lower precipitation, consistent with Brienen et al., 2015 and Hubau et al., 2020. This is consistent with the Brazilian Annual Land Use and Land Cover Mapping Project (MapBiomas Amazonia 2.0) and long-term inventories based on carbon stock estimates. Deforestation and climate change affect carbon sinks, and both vary geographically over the Amazon region.

Overall, these studies indicates that the Amazon could be acting as a carbon source (losses to the atmosphere) of 0.30 ± 0.20 Pg C y^{-1}, where mean fire emissions represent 0.39 ± 0.20 Pg C y^{-1} and a mean forest uptake represents –0.20 ± 0.15 Pg C y^{-1} (Gatti et al. 2014; Feng et al. 2017; Baccini et al. 2017; Assis et al. 2020; Gatti et al. 2021, van der Laan-Luijkx et al. 2015; Alden et al. 2016).

Considering methane fluxes before agricultural intensification and industrialization, wetland emissions likely account for most global budgets, with strong contributions from Amazonia. Natural wetland variability may control the interannual variability of CH_4 flux to the atmosphere (Gedney et al., 2004). Tropical wetlands, including areas of peat deposits with very high (and potentially vulnerable) carbon stocks, cover vast areas in tropical forest regions (Page et al., 2011). Studies of wetland areas during the LBA revealed that about 20% of the Amazon basin, especially at the end of the wet seasons, has wetland character and may contribute 5% of global CH_4 emissions (Hess et al., 2003; Melack et al., 2004). And it is important to highlight that these processes may still shift in response to changes in the water cycle and Amazonian landscape resulting from changes in climate and land use.

Based on satellite observations of atmospheric column-averaged methane for the 2010 drought and subsequent 2011 wet year, Saito et al. (2016) conclude that there are indications of an increase in atmospheric CH_4 over the southern Amazon region during the 2010 drought compared to the 2011 wet year. They attribute this increase to emissions from biomass burning driven by intense drought, combined with carbon monoxide, which shows seasonal variations corresponding to methane. Similarly, van der Laan-Luijkx et al. (2015) find by way of numerical analysis, combining CO_2/CO aircraft vertical profile measurements, satellite observations of CO, a burned area, and fire hot spots, that the hydrological cycle will be an important driver of future changes in Amazonian carbon exchange. Based on 13 years of regularly measured CH_4 aircraft profiles above the eastern Brazilian Amazon, Basso et al. (2016) find that CH_4 fluxes are highest at the beginning of the wet season and during the dry season. Using a CO:CH_4 emission factor estimated from the profile data, they estimated a contribution of biomass burning to be around 15% to the total flux in the dry season, indicating that biogenic emissions dominate the CH_4 flux. Considering its spatial heterogeneity, it is clear that more observation sites are needed for a better understanding of CO_2 and CH_4 fluxes over Amazonia (e.g., Molina et al., 2015).

Tropical forests also play a critical role in controlling the emission of nitrous oxide (N_2O) and methane (CH_4), two other key greenhouse gases, and also influence exchanges of organic compounds, including isoprene, monoterpenes, sesquiterpenes, and a wide range of oxygenated compounds collectively known as BVOCs (Yáñez-Serrano et al., 2020, Yee et al., 2020). These oxygenated compounds indirectly influence climate through atmospheric chemical reactions that generate or remove ozone or consume hydroxyl radical (OH), the main sink for CH_4. Thus, the interplay between their atmospheric distributions determines the lifetime of this strong greenhouse gas. Estimates of emission of N_2O in broadleaf forests and woody savannas are over 1.6 Tg of N_2O, the vast majority coming from the tropics. This amount equals the sum of all other cover types combined (Zhuang et al., 2012). Forests are one of the largest sources of N_2O emissions, with the highest contribution from tropical forests due to high nitrogen turnover. A recent systematic literature survey for Brazil also revealed the highest N_2O fluxes for Amazonian and Atlantic rain forests (Meurer et al., 2016).

The above-presented observations clearly show how climate change and then not only temperature and precipitation but also periodicity strongly affect both the boreal and tropical forests such that not only the H_2O fluxes but also the CO_2 and CH_4 fluxes are affected such that it can change from a sink to a source of greenhouse gases.

Although the understanding of tropical forests is improving, their representation in Earth System Models lags significantly behind that of temperate and boreal forests, as evidenced by, for example, the wide variation in estimates of tropical forest productivity (Beer et al., 2010) and large uncertainty. In addition to the need to better understand the functioning and seasonality of the metabolism of tropical vegetation, there is still little understanding of how these processes act in an integrated way to affect the interannual variability of fluxes and how possible global environmental change will impact this variability. By combining information from different sources of data (such as flux towers, long-term forest plots, and aircraft measurements) and process-based land biosphere models, we can improve our knowledge about the functioning of the ecosystems, interactions with the climate and identify missing mechanisms in the models that would improve the simulations of the Earth system.

Achieving the 1.5–2.0°C temperature targets of the Paris climate agreement require substantial and fast reductions in emissions of greenhouse gases (GHGs) but also requires increasing removals of GHGs from the atmosphere (Griscom et al., 2017; Rogelj et al., 2018). Reforestation is a potentially large-scale method for removing CO_2 and storing it in the biomass and soils of ecosystems. Tropical forests are critical to this removal of atmospheric CO_2. It appears probable that as the intact forest sink declines in size, tropical forests are in the process of switching from being approximately neutral to be a net source of carbon (Mitchard, 2018). This decline is caused by the combination of a decrease in the area of intact forests as well as an increase in temperatures and drought frequencies. With both forest loss and climate change likely to accelerate over the 21st century, tropical forests are likely to release ever more carbon, which will make limiting global warming to less than 2°C above pre-industrial levels challenging (Le Quéré et al., 2016). The ecosystem services such as water vapor processing could also be affected.

Large scale implementation in tropical forests of mechanisms such as REDD+ (defined as "reducing emissions from deforestation and forest degradation, and the role of conservation, sustainable management of forests and enhancement of forest carbon stocks in developing countries") can certainly play an important role in carbon exchange in tropical areas. However, only if the financial mechanisms to support REDD+ are set in place.

4.3. PROCESSES AFFECTING TRACE GAS AND AEROSOL CONCENTRATIONS

Terrestrial ecosystems are linked to the atmosphere via vertical momentum fluxes, sensible and latent heat, and fluxes of atmospheric constituents (Ramsay et al., 2020, 2021). The forest canopy is an essential feature of the biosphere-atmosphere interactions in tropical rainforests (Blundo et al., 2021). As the canopy bottom is mainly decoupled from the air aloft, the dense and tall rainforest can exert control on the residence times and turbulent transport of how plant emitted gases are released above the forest canopy (Bakwin et al., 1990; Fitzjarrald et al., 1988; Gerken et al., 2017; Santana et al., 2018). The whole canopy is predominantly decoupled from the air aloft during the nighttime, except for periods with bursts of intermittent turbulence (Freire et al., 2017). In this way, BVOCs are trapped within the canopy, and only a minor amount can escape to the free atmosphere, enhancing the within canopy reactions. For instance, 50–70% loss of O_3 within-canopy is attributed to the ozonolysis of highly reactive sesquiterpenes (Bourtsoukidis et al., 2018; Jardine et al., 2011b; Yee et al., 2018). Similarly, forest vegetation is a significant source of BVOC over boreal forests, where the forest floor adds importance to BVOC exchange in the biosphere-atmosphere interface (Zhou et al., 2017).

4.3.1. Atmospheric reactivity and oxidation capacity

The tropical atmosphere is considered a strong photoreactor due to the high insolation, strong BVOC emissions, high ambient temperatures, and relative humidity, which favor oxidation processes (Andreae, 2001a). In boreal forests, chemical reactions are primarily driven by a strong seasonality due to substantial temperature and solar radiation among seasons.

The major oxidants in the atmosphere are the OH (during daytime) and NO_3 (during nighttime) radicals, as well as O_3 (daytime and nighttime). The intense sunlight and high humidity levels persisting in tropical regions result in the rapid production of OH from the reaction of O(1D) atoms (originating from O_3 photolysis) with water vapor. The OH radical is closely related to hydroperoxy radicals (HO_2) formed from the reaction of the OH radical and VOCs. Some of the BVOCs are exceptionally reactive with these radicals (e.g., isoprene dominates vegetation emission and is highly reactive towards OH (Nölscher et al., 2016)), monoterpenes and sesquiterpenes are highly reactive towards O_3 (Jardine et al., 2015b, 2011b; Yáñez-Serrano et al., 2018a, 2018b; Yee et al., 2018), leading to large amounts of oxidation products contributing to SOA formation. Particularly in Amazonia, it has been estimated that isoprene oxidation contributes 50% to biogenic SOA (Shrivastava et al., 2019). The contribution from other BVOCs to aerosol loading in the tropical rainforest is more difficult to estimate. Still, it has been suggested that monoterpenes contribute 45% to biogenic SOA, and sesquiterpenes (SQTs) contribute 0.4–5% to biogenic SOA (Shrivastava et al., 2019; Yee et al., 2018, 2020). In contrast, monoterpene emissions, which dominate in the boreal forest (Hakola et al., 2012), have been major SOA formation players. Monoterpenes can be rapidly oxidized, e.g., via autoxidation, to form highly oxygenated molecules (HOM), the low volatility of which is crucial for new particle formation and growth of new particles in the boreal forest (Bianchi et al., 2019, Mohr et al., 2017).

The atmospheric reactivity can be accessed via OH reactivity, a measured parameter that expresses the amount of atmospherically present reactants towards OH. The reactants toward OH (i.e., BVOCs, NOx, CH_4, etc.) are usually measured independently, and the OH reactivity can be theoretically calculated by summing up the individual reaction rates. Due to the short lifetime of these radicals, measurements, and comprehensive understanding of OH production and consumption in forests are still scarce and potentially prone to interferences. The difference in the values between the directly measured and calculated OH reactivity is termed "missing OH reactivity" and expresses the unknown reactants in the atmosphere. The missing OH reactivity in tropical and boreal forests is several tens of percent, depending on seasons (Yang et al., 2016). The

characteristics of OH reactivity is different for the different forest types. In tropical forests, total OH reactivity was up to 2 times higher than in the boreal forest (Yang et al., 2016), mainly due to the higher amounts of BVOCs emitted by the vegetation.

In central Amazon, total OH reactivity is highly variable with the time of day (maximum during noon due to strong biogenic emissions) and along the seasons, being lower during the wet season (10 s^{-1}; missing OH reactivity from 5 to 15%) and higher during the dry season (62 s^{-1}; missing OH reactivity up to 79%). Overall, the less oxidative atmosphere, the relatively high deposition of oxidation products on wet surfaces, and possible enhanced leaf surface microbial could explain the missing reactivity in the wet season. During the dry season, there are higher oxidant concentrations and a higher impact of transport from polluted areas, which increase the reactivity and oxidation capacity of the atmosphere, as seen in the isoprene-to-isoprene oxidation products ratio (Yáñez-Serrano et al., 2015). However, the increased missing OH reactivity during this season indicates a hitherto gap of knowledge on trace gas reactivity towards OH during the dry season (Nölscher et al., 2016). As an outlook, diterpenes are pointed out to possibly be unmeasured compounds that could be of importance both in the tropics and in the boreal forest (Yee et al., 2018, Yañez-Serrano et al., 2018a). Nonetheless, the OH and HO_2 radicals in Guyana and Borneo tropical atmosphere have been measured to be much higher than predicted by box models (MacKenzie et al., 2011; Martinez et al., 2010), as HO_2 with isoprene peroxy radicals were able to recycle OH, sustaining the oxidative capacity of the atmosphere (Lelieveld et al., 2008; Stickler et al., 2007).

In boreal forests, OH reactivity is lower than in the tropics and mainly driven by monoterpene emissions instead of isoprene (Hakola et al., 2012, Yang et al., 2016). As a consequence, less distinct diurnal patterns are observed. To our knowledge, there is a lack of wintertime OH reactivity measurements from the boreal forest. Presumably, it will be to the lowest limit due to the much lower BVOC emissions following the lower atmospheric temperatures (Hakola et al., 2012). However, similar to Amazonia during the wet season, the missing OH reactivity is exceptionally high, with percentages of up to ~60% (Yang et al., 2016, Praplan et al., 2019). This indicates that better identification of oxidized BVOC and reactive compounds from emissions sources other than vegetation (e.g., soil) is needed.

The ratio of VOC to NO_x highly affects the photochemistry of any forested atmosphere (MacKenzie et al., 2011) as the HO_2 and NO pathways for oxidation depend on this ratio (Liu et al., 2016). In general, atmospheric oxidation processes of BVOC proceed via the attack of an oxidant (O_3, OH, or NO_3 radicals), which leads to the formation of peroxyradicals. These can react with themselves, which leads to stable products and the termination of the reaction chain, or with NO, which recycles radicals. Within these reaction cycles, products of different volatilities are formed, thus largely influencing SOA production. One important example is isoprene. When reacting with OH, it produces isoprene peroxy radicals (ISOPOO). These radicals can further react with HO_2 forming isoprene hydroxyhydroperoxides (ISOPOOH), or they can react with NO to largely produce methyl vinyl ketone and methacrolein (Liu et al., 2016). This has further effects on SOA production as increased NO_x concentrations suppress isoprene epoxydiols-derived secondary organic aerosol (IEPOX-SOA) production (de Sá et al., 2017; Schulz et al., 2018).

The VOC/NOx ratio in the boreal forest is determinant for forming new particles and their growth. It has been shown that NPF can largely be suppressed at high NOx conditions due to the reduced formation of HOM, which are key parameters in NPF (Lehtipalo et al., 2018). At the same time, NOx leads to the formation of a large fraction of highly functionalized organonitrates, which can contribute to high mass concentrations and are thus of increased importance for SOA production (Kortelainen et al., 2017).

4.3.2. Ozone in the forest atmosphere and canopies

Above the pristine tropical rainforest, ozone budgets are mainly controlled by transport from aloft and deposition to the canopy with little net influence from photochemistry (Jacob and Wofsy, 1990). Therefore, strong sources of surface ozone are downdrafts of convective storms (Dias-Junior et al., 2017; Gerken et al., 2016). The transport of ozone and ozone precursors (i.e., NOx and VOCs) from polluted areas and biomass burning regions is especially important during the dry season (Pope et al., 2020, Kuhn et al., 2010, Longo et al., 1999, Bela et al., 2015; Pacifico et al., 2015) and significantly alters the oxidation capacity of the atmosphere (Wei et al., 2019; Yee et al., 2018, 2020) For the European boreal forests, polluted regions act as a sink for O_3 in winter, and as a source in spring when photochemical activities start to become important (Kulmala et al., 2000). Given the importance of O_3 in BVOC oxidation, HOM formation, and subsequent new particle formation, changes in O_3 concentration will have large influences on the fate of BVOC emissions in the boreal forest.

Ozone provides physiological and biochemical damages to plants (Fuhrer et al., 1997, Schultz et al., 2017). Plant damage due to O_3 is widely assessed using an empirical concentration approach based on the accumulated O_3 exposure above a threshold concentration, typically 40 ppb, as a metric for O_3 dose. Inside the leaf, ozone can damage the lipid membranes of the cells and increases the production of reactive oxidative species (ROS) (Pinto et al., 2010; Scandalios, 1993). As such, ozone can also trigger BVOC emissions due to plant stress. For instance,

enhanced sesquiterpene emissions are reported after ozone stress for Brazilian tropical tree species *Croton floribundus* when exposed to high ozone levels (Bison et al., 2018), while the same observation with the same 40 ppb of O_3 threshold has been reported for Norway Spruce (*Picea abies*), which is highly abundant in boreal forests (Bourtsoukidis et al., 2012). For the Amazon, further investigations are essential to evaluate better the impact of ozone exposure on species that are acclimated to small O_3 concentrations. The production of this phytotoxic compound is increased during the burning season (Andreae et al., 2015; Pacifico et al., 2015; Rummel et al., 2007) and within urban plumes (Wei et al., 2019). In addition, ozone damage or oxidative stress can decrease net primary productivity (Pacifico et al., 2015) and alter the carbon cycle. The ozone damage is species-dependent. In a highly biodiverse ecosystem, it is difficult to quantify the total effect of the high O_3 exposure and the potential impact on plant species competition.

4.3.3. Influence of atmospheric transport on trace gas processing

The atmospheric processing in tropical rainforests is influenced by the seasonal movements in the ITCZ and trade winds (see section 2.1). These are the effects of the large-scale circulation in the tropics. During the wet season of the Amazon rainforest, air arrive predominantly from the northeast over a clean fetch region covered with pristine rain forest (Pöhlker et al., 2019). During this period, long-range transport from the Atlantic and Africa brings episodes of marine aerosol, Saharan dust, and smoke from fires in West Africa (Formenti et al., 2001, 2008, Holanda et al., 2020), and possibly even pollution from North America and Europe, but frequent rain events also contribute to the cleaning of the air. On the other hand, wind directions change to easterly and south-easterly fetch regions during the dry season, receiving considerable pollution from biomass burning regions and human activities in North-eastern Brazil (Andreae et al., 2015, Pöhlker et al., 2019).

The boreal forest influences mesoscale weather systems: Pielke and Vidale (1995) show that the position of the boreal forest influences the position of the polar front (which since the 1960s was believed to be vice versa) due to weaker albedo compared to the tundra. Whereas the strong seasonal variation in temperature largely governs BVOC emissions and reactivity in the boreal forest, solar radiation, and snow cover (Hakola et al., 2003), the transport of air plays an important role in the atmospheric processing of trace gases. Kulmala et al. (2000) identified 5 major air mass sectors for the boreal forest in Finland based on back trajectory calculations: the Arctic Ocean, Russia northeast, Russia southeast, the Kola peninsula, and Central Europe (including Great Britain). In winter and summer, air masses are coming most frequently from the Central European sector while in spring from the Arctic sector. The cleanliness of Arctic air influences the high frequency of NPF events in the boundary layer in spring in Fennoscandia (Kulmala et al., 2000) and thus plays an essential role in the fate of oxygenated BVOC (Lutz et al., 2019). Like the Eurasian continent, the boreal forest on the American continent can be influenced by marine and continental air (Gibson et al., 2013).

Besides the contribution of mesoscale transport, vertical transport in the planetary boundary layer additionally contributes to physical-chemical processes (Andreae et al., 2001). In the tropical forest, the BVOC species brought up by deep convection are converted into condensable species in the upper troposphere, resulting in newly formed aerosol particles. As such, downward mixing and transport from the upper troposphere can be a source of aerosol particles and CCN to the planetary boundary layer (Andreae et al., 2018). For instance, in the case of isoprene, it has been shown that significant SOA formation by isoprene oxidation products occurs in the upper troposphere (Schulz et al., 2018).

4.3.4. Trace gas deposition processes

Sink processes for trace gases comprise wet deposition and dry deposition (removal at surfaces), stomatal uptake, and, for VOCs, atmospheric oxidation until CO_2 is released as an end product. Oxidation generally increases water solubility and, therefore, removal by rain or by wet surfaces. The relative importance of dry versus wet deposition also depends on the amount and frequency of rain. Therefore, this process is of special importance during the wet season and rain events, as observed in a general decrease in trace gas concentrations (Yáñez-Serrano et al., 2020). Dry deposition depends on turbulent transport, the species' chemical properties, and the nature of the surface itself. The dry deposition of several VOCs may be underestimated in the tropical rainforest (Karl et al., 2004). Vegetation can also be a sink of trace gases via stomata uptake. For some compounds, particularly oxygenated BVOC, this process can be bi-directional. It depends on the gradient of the compound between the inside of the leaf and the ambient air concentration. The ambient concentration at which the flux is reversed is the so-called compensation point. In the tropics, this has been demonstrated for aldehydes (such as acetaldehyde (Rottenberger et al., 2004)) and acids that include formic and acetic acid (Jardine et al., 2011a). For the boreal forests, it has been shown that the majority of the emitted gases are transported out of the canopy and removed by chemical reactions and that bi-directional exchange can play an important role for in-canopy concentrations of smaller molecules such as acetaldehyde, methanol, acetone, or formaldehyde (Zhou et al., 2017). Production and transport from above the canopy generally compensate for dry deposition in the boreal forest.

4.3.5. Aerosol fluxes over forests

Two components are important in aerosol fluxes over forests: primary biogenic aerosol particles (PBAP) and secondary organic aerosol (SOA). Some observations of upward fluxes of submicron particles from forests have hinted that biogenic SOA may be formed quickly in forest canopies. Therefore, forests occasionally act as a net particle source (Buzorius et al., 1998). The dry deposition velocity of aerosol particles depends on particle size, friction velocity, and stability parameters. Buzorius et al., 1998 have done measurements over boreal forests (Hyytiälä) and derived deposition velocities from –15 to 10 mm s^{-1}. Usually, the fluxes were downwards, but episodes with flux directed upward were registered too.

In Amazonia, total particle flux and chemically resolved aerosol particle flux measurements were done in detail for fine mode particles in size range of 70–800 nm measured with AMS (Farmer et al., 2013, Ahlm et al., 2009, 2010, Nemitz et al., 2013). In the wet season, 60% of the particle fluxes pointed downward, which is a similar fraction to what has been observed over boreal forests. The net deposition flux prevailed even in the absolute cleanest atmospheric conditions during the campaign. Upward particle fluxes often appeared in the morning hours and seem largely to be an effect of entrainment fluxes into a growing mixed layer rather than primary aerosol emissions. In general, the number of primary aerosol particles within the footprint area of the measurements was small, possibly because the measured particle number fluxes mostly reflect particles less than approximately 200 nm (Ahlm et al., 2009). These are particle number fluxes, so as the PBAP are mostly in the coarse mode, they can contribute significantly to the mass flux, although they are not important in terms of number fluxes (Ahlm et al., 2009). In the Amazonian dry season, early in the morning, there was an upward particle flux peak associated with the emission of primary biogenic particles from the rain forest. Emitted particles may be stored within the canopy during stable conditions at nighttime, similarly to CO_2, and be released from the canopy when conditions become more turbulent in the morning (Ahlm et al., 2010). Particle transfer velocities peak around noon or in the early afternoon at values of 1–2 mm $s^{-1,}$ both in the dry and wet seasons.

Chemically resolved particle fluxes were determined by eddy covariance analysis using an Aerodyne High-Resolution Aerosol Mass Spectrometer (HR-AMS) (Farmer et al., 2013). Biosphere–atmosphere fluxes of different chemical components are affected by within-canopy chemistry, vertical gradients in gas-particle partitioning due to canopy temperature gradients, emission of primary biological aerosol particles, and wet and dry deposition. The oxygenated organic components representing regionally aged aerosol are deposited, while components of fresh SOA are emitted. The wet deposition was estimated to be an order of magnitude larger than dry deposition during AMAZE-08 (Farmer et al., 2013). Inorganic trace species fluxes were determined in Amazonia at the ATTO tower, including NH_3, SO_2, NO_3^-, Cl^-, SO_4^{2-}, NH_4^+ and they show high deposition rates for NO_3 and Cl^-, while aerosol components show average surface deposition rates of 2.8 mm s–1 for SO_4^{2-} and NH_4^+ (Ramsay et al., 2020, 2021).

Over boreal forests, Buzorius et al., 2000 measured in general downward fluxes, with typical normalized flux values in the range of 0.1–10 mm s^{-1}. When nucleation occurs, high values of deposition velocities of up to 40 mm s^{-1} were observed. Occasional upward fluxes are associated with new particle formation.

4.4. NEW PARTICLE FORMATION OVER FORESTS

The boreal forest environment was the first place where the large-scale formation of new atmospheric aerosol particles and subsequent growth of these particles to larger sizes, often termed regional new particle formation (NPF), was observed, and reported in the scientific literature (Mäkelä et al., 1997). During the past couple of decades, atmospheric NPF was measured at more than 10 ground-level sites in the boreal forest zone (see Kerminen et al., 2018, and references therein). The average particle formation rates associated with the observed NPF events are found to vary between about 0.1 and 1 cm^{-3} s^{-1} among the different sites, and the corresponding particle growth rates vary from about 0.5 to 5 nm h^{-1}. The annual frequency of NPF events varies between about 10 and 30%. The lowest frequencies are seen typically at the northern edge of the boreal forest zone and in the Siberian part of this region. A very high NPF frequency (25 events in 22 days) was observed in June 2019 at two remote forest sites in the temperate/boreal transition zone in western Canada (Andreae et al., 2019). In contrast, exceptionally low NPF event frequencies (<2%) and associated particle growth rates (<0.1 cm^{-3} s^{-1}) are reported in central Siberia based on long-term measurements conducted at the ZOTTO tower (Wiedensohler et al., 2019). The NPF event frequency tends to have a spring maximum, sometimes another maximum in late summer or autumn, while being typically very low during the wintertime (Dal Maso et al., 2007, 2008; Dal Maso and Sogacheva, 2007; Kristensson et al., 2008; Asmi et al., 2011; Nieminen et al., 2014; Kyrö et al., 2014).

Relatively little is known about the vertical profile of NPF over boreal forests. Aircraft measurements conducted around the SMEAR II station at Hyytiälä, Finland, show that NPF occurs throughout the mixed boundary layer during the daytime in this environment (O'Dowd et al., 2009; Schobesberger et al., 2013). Later measurements around the same site support this view and indicate occasional NPF in the free troposphere (Leino et al., 2019). When regional NPF is detected at the ground level, the largest concentrations of sub-3

nm particles are observed just above the forest canopy, which suggests that emissions from the forest itself are central to the occurrence of NPF in this region (Leino et al., 2019). Consistent with the findings around the SMEAR II station, the measurements made at the ZOTTO Tower in Siberia found, on average, slightly higher particle number concentration at the 50-m height compared with the 300-m height, while the shape of the particle number size distributions was very similar between these two heights (Heintzenberg et al., 2011).

Unlike at many other terrestrial locations around the globe, particles around 3 nm and their continuous growth to larger diameters have hardly ever been observed in the Amazon basin under natural or near-natural conditions, suggesting new particle formation is very rare in the Amazonian boundary layer (Andreae et al., 2015; Martin et al., 2010; Rizzo et al., 2013, 2018; Wimmer et al., 2018). The smallest particles observed usually have diameters ranging from 10 to 20 nm. Due to the scarcity of continuous particle growth, very few studies have been on particle growth rates. During an investigation in central Amazonia, limited measurements indicate a growth rate of 5 nm h−1 for the Aitken mode particles (Zhou et al., 2002). Wimmer et al. (2018) reported 8 NPF and growth events during the dry season of 2014 at an open pasture site regularly influenced by a Manaus pollution plume. They found that the growth rate of newly formed particles increased with increasing particle size, varying between 3 and 20 nm h^{-1} in the 7–20 nm size range.

In contrast to ground sites, airborne observations over the Amazon Basin showed high aerosol particle concentrations in the upper troposphere (UT) between the 8 and 15-km altitudes, with particle number densities frequently exceeding those in the boundary layer by 1 or 2 orders of magnitude (Andreae et al., 2018) (see section 6). These particles are attributed to new particle formation from ground-based emissions of VOCs transported aloft by convection and producing new particles at high concentrations. Aerosol mass spectrometer measurements show that these particles are mostly organic, with very low sulfate and nitrate (Schulz et a., 2018). Aircraft measurements above Suriname in Northern Amazonia observed enhanced ultrafine number concentrations in regions of cloud outflow at high altitude (***Figure 4.4.1***), suggesting nucleation (Krejci et al., 2003, 2005). These observations are in broad agreement with observations of cloud outflow regions from other locations worldwide (Clarke et al., 1999; Clarke et al., 1998; Perry and Hobbs, 1994).

Several studies identify sulfuric acid (H_2SO_4), low-volatile organic compounds, and bases (ammonia or amines) as the main gaseous precursors for atmospheric NPF (Kulmala et al., 2014b). In the boreal forest environment, NPF and subsequent particle growth are found to be tied strongly with both H_2SO_4 and low-volatile organic compounds, the latter becoming increasingly more important when the particles grow in size (Kulmala et al., 2013a; Ehn et al., 2014; Dada et al., 2017). The observed particle formation rates can be predicted relatively well using empirical relations where this formation rate is proportional to some combination of H_2SO_4 and low-volatile organic compound concentrations to the power 1 or 2 (Paasonen et al., 2010). Laboratory experiments and observations at the SMEAR II station suggest that not only H_2SO_4 and organic compounds but also ammonia, nitrogen oxides, and ions influence the NPF characteristics in the boreal forest environment (Lehtipalo et al., 2018; Yan et al., 2018). However, the relative roles of these constituents in NPF are likely to vary considerably in both time and space in this environment.

The Amazon Basin has weak sulfur sources, leading to SO_2 concentration typically around 20–30 ppt (Andreae and Andreae, 1988; Andreae et al., 1990). In comparison, SO_2 concentrations observed in the boreal forest environment are often several times higher than these values. In Hyytiälä, for example, the median SO_2 concentration is close to 200 ppt on NPF event days and around 500 ppt on non-event days. The low SO_2 concentration suggests correspondingly low gas-phase H_2SO_4 concentrations, although no direct measurements in the Amazon Basin have been reported. Model simulation suggests that H_2SO_4 concentrations in the Amazon Basin are too low for particle formation to occur near the surface because preexisting particles should scavenge any incipient molecular clusters before they grow into new particles (Spracklen et al., 2006). An alternative mechanism to the H_2SO_4 pathway, namely ion-mediated nucleation, is by modeling found to be an unimportant source of nuclei over the Basin (Yu et al., 2008). In addition to the low H_2SO_4 concentration, the absence of NPF near the surface may be related to biogenic emissions from the tropical rainforest. There is evidence suggesting that high isoprene emissions may suppress NPF even when there are sufficient amounts of monoterpenes (i.e., precursors of low-volatility organic compounds) in the air. However, the underlying mechanism for this suppression remains unclear (Kanawade et al., 2011).

Given the low temperature and existing surface area, the outflow region in the upper troposphere over the Amazon Basin provides an ideal environment for new particle formation to occur (Kulmala et al., 2006; Lee et al., 2004; Twohy et al., 2002). However, the mechanism for NPF at high altitudes is not well understood, mainly due to a lack of direct measurements of gas-phase precursors and the composition of critical clusters. As organic-rich boundary-layer air can be efficiently pumped into UT by convective systems, the new particles at high altitudes are likely formed by homogeneous nucleation of oxidized organic compounds (Ekman et al., 2008; Kulmala et al., 2006; Murphy et al., 2015). Studies

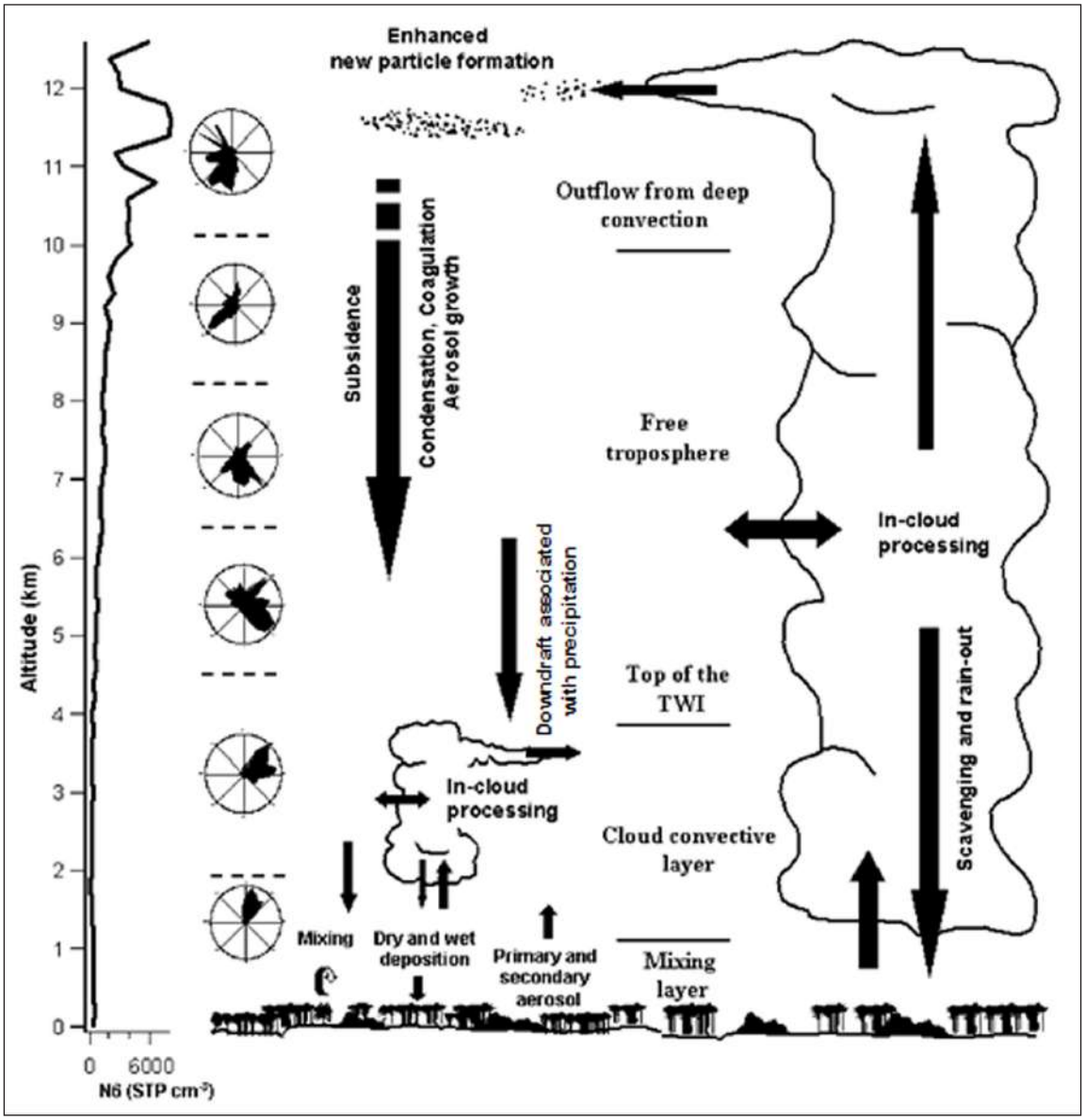

Figure 4.4.1 Schematic diagram showing processes producing fine particles due to convective cloud outflow above Suriname in Northern Amazonia, with enhanced ultrafine number concentrations in regions of cloud outflow, suggesting nucleation (Adapted from Krejci et al., 2003).

have shown that highly oxygenated organic molecules can nucleate to form particles even in the absence of H_2SO_4, especially in the UT (Bianchi et al., 2016; Kirkby et al., 2016). Co-nucleation of H_2SO_4 and oxidized organic molecules is also possible (Metzger et al., 2010; Riccobono et al., 2014). The importance of ions produced from cosmic radiation in this nucleation process remains unclear (Bianchi et al., 2016; Kirkby et al., 2016; Lee et al., 2003; Yu et al., 2008).

One of the most important consequences of atmospheric NPF outside urban regions is its ability to enhance the concentrations of aerosol particles capable of acting as cloud condensation nuclei, CCN (e.g., Merikanto et al., 2009; Kerminen et al., 2012). Increased CCN concentrations modify cloud microphysical properties, including the cloud droplet number concentration and effective radius, cloud albedo, the vertical extent of the cloud, and cloud precipitation properties (e.g., Rosenfeld et al., 2014). Based on long-term aerosol measurements, the formation of CCN associated with atmospheric NPF has been investigated at two sites located in the boreal forest: the SMEAR II at Hyytiälä (Sihto et al., 2011) and the Pallas station located at the northern edge of the boreal forest zone (Asmi et al., 2011). Depending on the assumed water vapor supersaturation, atmospheric NPF was estimated to enhance, on average, CCN concentrations by factors of 0.7–1.1 and 1.5–3.8 at SMEAR II and Pallas, respectively, when comparing the situation before an NPF event and the situation when then particles formed during this event had grown to larger sizes (50–100 nm). Global modeling studies give support for an important role of NPF in affecting CCN concentrations over boreal forests, especially during the summertime when biogenic emissions from the forest are at their highest (e.g., Spracklen et al., 2008; Spracklen et al., 2010, Kulmala et al., 2011, Makkonen et al., 2012).

Over the Amazon basin, the particles formed at high altitudes can grow into the Aitken mode in the upper free troposphere. Measurements show that the composition of the free-tropospheric aerosol is dominated by organic compounds, indicating the particle growth is mainly driven by the condensation of organic species (Andreae et al., 2018). This conclusion is also supported by modeling studies (Ekman et al., 2008; Murphy et al., 2015, Zhu et al., 2019). The grown particles are transported towards the lower troposphere by subsidence under the prevailing high pressure over the Amazon basin and downdrafts associated with deep convective systems. A recent study showed that the downdrafts could efficiently bring free troposphere air with a high concentration of Aiken mode particles into the boundary layer. This process represents a major source of particles and, therefore, CCN in the boundary layer under natural conditions, due to the absence of boundary layer new particle formation and anthropogenic emission (Wang et al., 2016). In the boundary layer, Aitken mode particles continue to grow into the accumulation mode by condensation of the organics due to biogenic emissions and become efficient CCN (Chen et al., 2009; Pöhlker et al., 2012, 2016; Pöschl et al., 2010).

A few studies have estimated the radiative effects of secondary organic aerosol (SOA) and CCN formation following NPF in the western part of the boreal forest zone. Analyses of atmospheric observations suggest that the resulting direct radiative effect is unlikely to exceed –1 W m^{-2} during the summertime, whereas the corresponding indirect radiative effect might be as high as –3 to –7 W m^{-2} (Kurtén et al., 2003; Kerminen et al., 2005; Lihavainen et al., 2009). A similar, relatively high estimate for the indirect radiative effect was obtained by Spracklen et al. (2008) using global model simulations. In a warming climate, these radiative effects might even be higher because both CCN and SOA formation associated with NPF appear to be sensitive to the extent of monoterpene emissions and thereby to the ambient temperature (Kulmala et al., 2004a; Tunved et al., 2006b, Liao et al., 2011, 2014). A few studies have estimated the corresponding feedback parameter over boreal forests, being close to –0.1 W m^{-2} K^{-1} for the feedback caused by direct radiative effect (Lihavainen et al., 2015) and between about –0.1 and –0.8 W m^{-2} K^{-1} for the feedback generated by indirect radiative effect (Paasonen et al., 2013).

4.5. BIOMASS BURNING EMISSIONS AND AEROSOL OPTICAL PROPERTIES

Biomass burning is one of the main drivers in the changes in atmospheric composition (Jia et al., 2019, Darbyshire et al., 2019). Fires have been a natural component of ecosystem functioning, especially in savannah in Africa and Cerrado in Central Brazil (Bowman et al., 2011a, Scott, 2000). Presently, a significant 3% of the Earth's land surface burns annually, affecting both energy and matter exchanges between the land and atmosphere. Climate is a major determinant of fire regimes through its control of fire weather, as well as through its interaction with fuel availability and flammability (Archibald et al., 2013) at the global (Krawchuk and Moritz, 2011), regional (Pausas and Paula, 2012) and local landscape (Mondal and Sukumar, 2016) scales. Humans are the main cause of fire ignition, with lightning playing a secondary role globally (Bowman et al., 2011; Harrison et al., 2010), although lightning has been responsible for large fires in boreal forests (Veraverbeke et al., 2017). Humans also influence fires by land-use change in tropical regions and increased fire risk in temperate zones. Climate change is also increasing in determining wildfire regimes, with future climate variability expected to enhance the risk and severity of wildfires in many biomes, and it is possible to observe that fire seasons are lengthening for temperate and boreal regions, and this trend should continue in a warmer world (Flannigan et al., 2009, Wotton et al., 2017). Fire weather seasons have lengthened globally between 1979 and 2013. While drought remains the dominant driver of fire emissions, there has recently been increased fire activity in some tropical and temperate regions during regular to wetter than average years due to warmer temperatures that increase vegetation flammability. The boreal zone is also experiencing more extensive and more frequent fires, increasing under a warmer climate.

Climate variability and extreme climatic events such as severe drought, especially those associated with the El Niño Southern Oscillation (ENSO), play a major role in the fire upsurges in the Asian tropical forests (Huijnen et al., 2016) as well as in the Amazon. Fire emissions in tropical forests increased significantly during El Niño years compared to La Niña years due to reductions in precipitation and terrestrial water storage (Chen et al., 2017). The expansion of agriculture and deforestation in the humid tropics has also made these regions more vulnerable to drought-driven fires (Davidson et al., 2012; Brando et al., 2014, Andreae et al., 2002). Even when deforestation rates were overall declining, as in the Brazilian Amazon during 2003–2015, fire incidence increased by 36% during the 2015 drought (Aragão et al., 2018).

Tropical forest degradation can be an important component of CO_2 emissions (Assis et al., 2020). Forest degradation is widespread worldwide due to multiple factors such as unsustainable logging, agriculture, invasive species, fire, fuelwood gathering, and livestock grazing. Several recent works show that tropical forest edges are important for carbon emissions and critical for forest degradation (Silva Junior et al., 2021). Nearly 20% of tropical forests are within 100 m of a non-forest edge due to rapid deforestation for agriculture. The Malaysian Borneo observed declines in carbon, averaging 22% along forest edges (Ordway and Asner, 2020).

Figure 4.5.1 shows the tropical primary forest loss from 2002 to 2020. It is possible to observe a sharp increase in 2016 and 2017. Countries that are responsible for most of the humid tropical primary forest loss are Brazil, the Democratic Republic of Congo, Bolivia, Indonesia, Peru, and Colombia. Important to emphasize that only 6 countries are responsible for more than 75% of tropical deforestation. Commodity-driven deforestation was the leading cause of tree cover loss (in primary and secondary forests) in Latin America and Southeast Asia while shifting agriculture dominates in tropical Africa. The resulting carbon emissions from this primary forest loss are calculated as 2.64 Gt CO_2 (World Resources Institute, WRI, 2021) (*https://research.wri.org/gfr/forest-pulse*).

Emissions from wildfires and biomass burning are a significant source of greenhouse gases (CO_2, CH_4, N_2O), carbon monoxide (CO), carbonaceous aerosols, and an array of other gases, including non-methane volatile organic compounds (NMVOC) (Akagi et al., 2011; Van Der Werf et al., 2010). In terms of CO_2 emissions, the whole Agriculture, Forestry, and Other Land Use (AFOLU) sector was a net emission of 5.5 ± 2.6 Pg CO_2 a^{-1} for 2008–2017, approximately 14% of total anthropogenic CO_2 emissions (Le Quéré et al., 2018). Satellite-based estimates of CO_2 emissions from loss of tropical forests during 2000–2010 agree with the modeled emissions: 4.8 Pg CO_2 a^{-1} (Tyukavina et al., 2015), 3.0 Pg CO_2 a^{-1} (Harris et al., 2015), 3.2 Pg CO_2 a^{-1} (Achard et al., 2014) and 1.6 Pg CO_2 a^{-1} (Baccini et al., 2017). Biomass burning is responsible for approximately 0.7 Tg N_2O-N a^{-1} (0.5–1.7 Tg N_2O-N a^{-1}) or 11% of total gross anthropogenic emissions due to the release of N_2O from the oxidation of organic nitrogen in biomass (van der Werf et al., 2010). The largest global source of BC aerosols is the open burning of forests, savannah, and agricultural lands with emissions of about 2.7 Tg a^{-1} in the year 2000 (Bond et al., 2013). Fire emissions during 1997–2016 are dominated by savanna (65.3%), followed by tropical forest (15.1%), boreal forest (7.4%), temperate forest (2.3%), peatland (3.7%), and agricultural waste burning (6.3%) (van der Werf et al., 2017).

In terms of emissions, biomass burning is a major global source of carbonaceous aerosols (Bowman et al., 2011; Roos et al., 2014, Harrison et al., 2010; Reddington et al., 2016, 2019; Artaxo et al., 2013, Mahowald et al., 2005). Biomass burning is responsible for very high ground-based aerosol concentrations in Amazonia (de Oliveira et al., 2020, Gonçalves et al., 2018, Palácios et al., 2020) that has significant health effects (de Oliveira et al., 2018, 2020, Butt et al., 2020). Knowledge of past fire dynamics has improved through new satellite observations, new fire proxies' datasets (Marlon et al., 2016; van Marle et al., 2017). A new historic biomass burning emissions dataset from 1750 has been developed, with a revised version of OC emissions (Van Marle et al., 2017), and it shows, in general, reduced trends compared to the emissions derived by (Lamarque et al., 2010) for the Coupled Model Intercomparison Project version 5 (CMIP5). Recent global emissions pathways (Hoesly et al., 2018) estimate global BC emissions in 2015 at 9.8 Tg BC a^{-1}, while global OC emissions are 35 Tg OC a^{-1}.

Compared with the past two millennia, there was a decrease in biomass burning during the 20th century, as inferred from charcoal sedimentary records (Doerr and Santín 2016). However, it has increased in the last 4–5

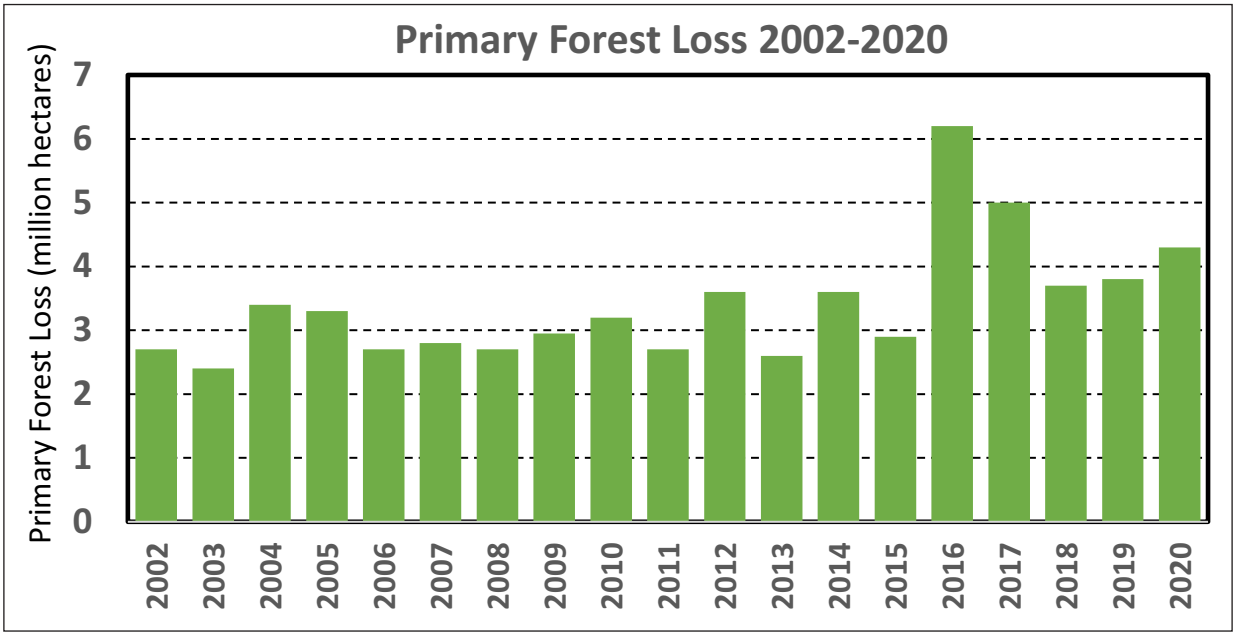

Figure 4.5.1 Tropical primary forest loss 2002–2020 in million hectares per year. The countries responsible for most tropical deforestation is Brazil, the Democratic Republic of Congo, Bolivia, Indonesia, Peru, and Colombia. Data source: World Resources Institute, WRI 2021, (*https://research.wri.org/gfr/forest-pulse*).

decades (Marlon et al., 2016). Trends in the land area burnt do vary regionally (Giglio et al., 2013). Northern Hemisphere Africa has experienced a decrease in fires since 2000, while Southern Hemisphere Africa has increased during the same period. Australia experienced a decline of about $5.5 \cdot 10^4$ km^2 a^{-1} (–10.7% a^{-1}) during 2001–2011, followed by an upsurge in 2011 that exceeded the annual area burned in the previous 14 years. An analysis using the Global Fire Emissions Database v.4 (GFED4s) (Randerson et al., 2015) concludes that the net reduction in the land area burnt globally during 1998–2015 is –24.3 ± 8.8% (–1.35 ± 0.49% a^{-1}) (Andela et al., 2017). However, most declines have come from grasslands, savannas, and other non-forest land cover types (Andela et al., 2017). Significant increases in forest area burned are observed in boreal North America (Abatzoglou and Williams 2016; Ansmann et al., 2018) and boreal Siberia (Ponomarev et al., 2016) in recent years. The 2017 and 2018 fires in British Columbia, Canada, are the largest ever recorded since the 1950s, with $1.2 \cdot 10^4$ km^2 and $1.4 \cdot 10^4$ km^2 of forest burnt, respectively (Hanes et al., 2019). The 2019 fires in Amazonia are the most substantial in the last ten years, with an increase of 69% over 2018, mainly in Brazil and Bolivia.

There is emerging evidence that recent regional surges in wildland fires are driven by changing weather extremes, indicating geographical shifts in fire proneness (Jolly et al., 2015). Fire weather season is already lengthened by 18.7% globally between 1979 and 2013, with statistically significant increases across 25.3% but decreases only across 10.7% of Earth's land surface covered with vegetation; even sharper changes have been observed during the second half of this period (Jolly et al., 2015). Correspondingly, the global area experiencing a long fire weather season has increased by 3.1% per annum or 108% over the period 1979–2013. Fire frequencies projected for 2050 conditions increase globally, relative to 2000 levels, where changes in fire meteorology play the most important role in the enhanced global wildfires, followed by land cover changes, lightning activities, and land use, while changes in population density exhibit the opposite effects (IPCC SRCCL 2019).

However, the climate is only one driver of a complex set of environmental, ecological, and human factors influencing fire regimes (Bowman et al., 2011). While these factors lead to complex projections of future burnt area and fire emissions, human exposure to wildland fires could still increase because of population expansion into areas already at high risk of fires (Knorr et al., 2016). Climate change and land-use change play an increasing role in determining wildfire regimes, with future climate variability expected to enhance the risk and severity of wildfires in tropical rainforests and boreal forests (IPCC SRCCL, section 2, 2019). The global land area burned has declined in recent decades, mainly due to less burning in grasslands and savannas.

Regional biomass burning aerosols can be transported over long distances, influencing atmospheric conditions even in the most remote regions. Synoptic scenarios impact the intensity of biomass burning activities, causing the large observed interannual variability on AOPs. For example, Saturno et al. (2018a) reported higher scattering and absorption coefficients in Amazonia during El Niño events, associated with precipitation anomalies and increased biomass burning emissions.

One way to express the absorption of solar radiation by the aerosol column is through Absorption Aerosol Optical Depth (AAOD), which is now a regular AERONET product (Wang et al., 2016). The aerosol loading expressed as AOD and AAOD correlate well with the number of fires and deforestation (Morgan et al., 2019, 2020). The drastically increased number of fires during the drought spells 2010 and 2012 shows a similar increase in AOD and AAOD these years.

Time series of satellite retrieved AOD (at 550 nm) over Alaska from 1995 to 2011 are shown in ***Figure 4.5.2***. The AOD was retrieved using the Aerosol Dual-View retrieval algorithm (Kolmonen et al., 2016; Sogacheva et al., 2017) with the entire mission data (1995–2011) from the European Space Agency Along-Track Scanning Radiometers ATSR-2 and AATSR (together ATSR). ***Figure 4.5.2*** shows the time series of the monthly mean AOD for each of the months, May-September. Also shown are monthly sums of ATSR-derived fire counts (Mota et al., 2006; available from *http://due.esrin.esa.int/page_wfa.php*) and forest fire aerosol emissions inverted from MODIS data using the System for Integrated modeling of atmospheric composition, SILAM (Sofiev et al., 2009; Soares et al., 2015; available from *http://silam.fmi.fi/thredds/catalog_IS4FIRES.html*). ***Figure 4.5.2*** shows the substantial variation of the AOD over Alaska with year-to-year variations each month, tracing both the fire counts and forest fire aerosol emissions. The fire counts and emissions are obtained using methods independent from the AOD retrieval. Note that MODIS data and thus forest fire aerosol emissions with this platform are available from 2000. ***Figure 4.5.2*** shows AOD smaller than 0.05 occurring in September and peak AOD occurring during the summer months coinciding with forest fires and associated biomass burning aerosol emissions. These peak AOD values do not exceed 0.4, close to the lower AOD values in dry season Amazonia. However, it should be kept in mind that these are monthly mean values, i.e., daily peaks as observed from AERONET may be substantially higher. Comparison with the yearly AOD550 shows that the AOD over Alaska in the summer months is low compared to Amazonia. However, it is important to note that forest fires, natural and anthropogenic, are the dominating source of aerosols during the dry summer period in both the tropics and the boreal regions. They act together with the enhanced BVOC emissions during summer, with both increasing concentrations of organic

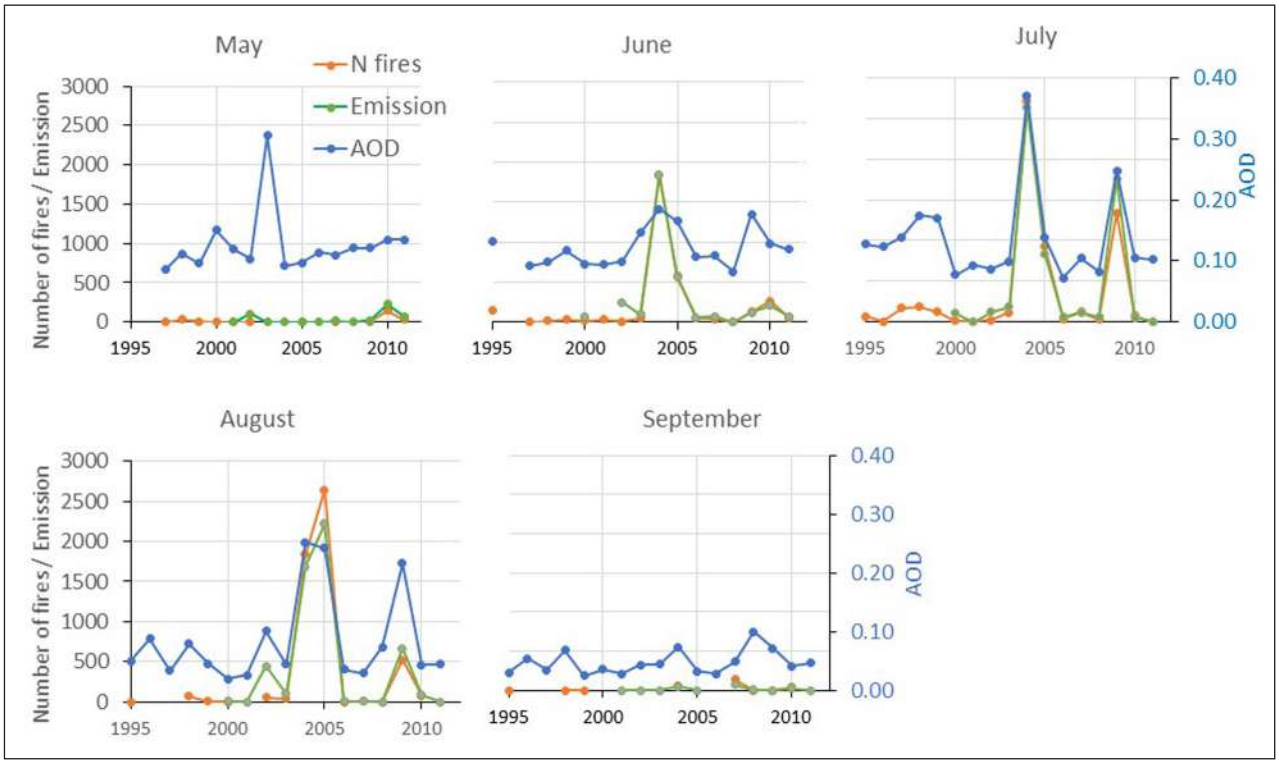

Figure 4.5.2 Time series of monthly mean AOD at 550 nm over Alaska retrieved from ATSR data using FMI's ADV v2.31 aerosol retrieval algorithm (blue, right axis)). The data are grouped for each month (May-September), showing the AOD variation for each of these months from 1995 until 2011. Also shown are the coincident monthly sums (left axis) of the ATSR-derived fire counts (red) and the fire emissions (green).

aerosols. BVOC dominates in periods of low biomass burning, but when the fires start, they dominate the aerosol population.

Submicron aerosol particles from biomass burning are significantly dominated by the carbonaceous fraction (Fuzzi et al., 2007; Decesari et al., 2006). Among the organic compounds, the anhydrosugars, such as galactosan, mannosan, and levoglucosan, are commonly used as tracers for biomass burning emission (Simoneit et al., 1999). Measurements in the west and the central Amazonian basin indicate that levoglucosan is the dominant anhydrosugar (88–96%) (Decesari et al., 2006; Graham et al., 2003b). Decesari et al. (2006) identified a class of organic compounds composed mainly of aromatic acids, aldehydes, and anhydrosugars during the dry season. They related it to the pyrogenic origin, which accounted for 55% of the total speciated compounds. Moreover, in the central Amazonian Basin, Gilardoni et al. (2011) identified that 44% of the fine total carbon mass was assigned to biomass burning emissions in the dry season. Other well-known biomass burning tracers, such as potassium-to-ammonium ratio and oxalic acid, have been found and associated with biomass burning in the fine mode during the dry season (Falkovich et al., 2005; Graham et al., 2002). Phosphorus, a key nutrient in tropical forests, can also be mobilized by biomass burning (Mahowald et al., 2005, Okin et al., 2004). In addition, malic acid was shown to track levoglucosan mass concentrations closely during the dry season in the fine aerosol mode. This fact suggests a similar aerosol formation process for both tracers. This happens through condensation of low-volatile organic gases emitted during deforestation fires or formed by photooxidation of biogenic emissions (Claeys et al., 2010).

In Hyytiälä, at the SMEAR II station, long-range transport of biomass burning aerosol contributes to summertime aerosols during hot and dry summers (Corrigan et al., 2013; Heikkinen et al., 2020). Evidence of such is visualized in ***Figure 3.1.4b***, where eBC and CO concentrations are elevated when the ambient temperature is at the highest (daily mean above 20°C). Airborne biomass-burning organic aerosol (BBOA) measurements from Canadian boreal forest fires reveal highly contrasting properties for plumes of different ages (Jolleys et al., 2015). The aging of BBOA is analyzed using AMS, looking at the ratio of f_{44}/f_{60}. In general, f_{60} is considered a fragment of levoglucosan and f_{44} a tracer for aged organic aerosols. Fires in Finland were analyzed by Corrigan et al., 2013, showing the impact of 4–5 days of transport from fires in Russia and Ukraine where the biomass burning factor contributed to a high 25% of OM on average, and up to 62% of OM during three periods of transported biomass burning emission. Large-scale aircraft observations on the biomass burning aerosol in the boreal environment were analyzed in several studies showing a high impact of biomass burning in the boreal summer (Leino et al., 2014; Pirjola et al., 2015, Virkkula 2014a; Virkkula et al., 2014b).

4.6. DIRECT AEROSOL RADIATIVE EFFECT AND IMPACTS ON THE ECOSYSTEM

The high loading of aerosols from biomass burning impacts the aerosol direct radiative effect (DRE) over large areas in tropical and boreal forests (Palácios et al., 2020, Liu et al., 2020, Procópio et al., 2003, Eck et al., 2003). The geographical distribution of DRE follows the sources and transport of biomass burning aerosols, as shown in ***Figure 4.6.1***. Some areas in Amazonia have a high average top of the atmosphere (TOA) aerosol radiative effect of –12 w/m³, i.e., a strong cooling effect induced over the Amazonia due to increased biomass burning aerosol loading. Note that the effect is negative, so the cooling effect from organic scattering aerosols dominates over black carbon.

The aerosol loading changes the radiation balance at TOA, at the surface (SUR), and in the atmosphere (ATM). ***Figure 4.6.2*** shows the monthly mean variation of short-wave aerosol radiative forcing (SWARF) averaged for 24 h at TOA (green), SUR (blue), and ATM (red) for the period 2011–2017 for the AERONET Manaus/Embrapa site, at (2.8942 °S, 59.9718 °W). The AOD components and aerosol microphysical properties derived from AERONET were used in a radiative transfer code to derive the different radiative effect components. It is possible to observe that the average monthly surface radiative effect (SUR 24 h) can be as high as –36 Wm^{-2} in the dry season, showing substantial effects of biomass burning aerosols on cooling the surface and heating the atmosphere (ATM) (Palácios et al., 2020).

Clouds and aerosols influence the flux of photosynthetic active radiation (PAR) that is critical for the photosynthetic process and carbon assimilation by the forests, as well as the ratio of diffuse to direct radiation (Rap et al., 2015, Procópio et al., 2004, Liu et al., 2020).

Park et al., 2018 analyzing ZOTTO data, showed that the diffuse radiation fertilization effect caused by smoke from wildfires and clouds enhanced net ecosystem productivity by less than 10% in boreal forests. Light intensity, canopy structure, and leaf area index determine the strength of the diffuse radiation fertilization effect. This effect is more substantial in tropical forests compared to boreal because the leaf area index is much higher, and tropical forests have a more closed canopy, in addition to stronger light intensity.

On the other hand, in Amazonia, a more significant effect of aerosols can be observed on the Net Ecosystem Exchange (NEE) that expresses the net carbon flux to the ecosystem (Malavelle et al., 2019). Analysis was performed continuously from 1999 to 2009 in Manaus and from 1999 to 2002 in Rondônia. In Rondônia (Jarú Biological Reserve), a 29% increase in carbon uptake (NEE) was observed when the AOD ranged from 0.10 to 1.5 at 550 nm. In Manaus (LBA ZF2 tower), the aerosol effect on NEE accounted for a significant 20% increase in NEE. High aerosol loading (AOD above 3 at 550 nm) or high cloud cover leads to reductions in solar flux and substantial decreases in photosynthesis until NEE approaches zero for AOD above 3–4 (Cirino et al., 2014).

Figure 4.6.3 shows the effect of aerosols on NEE for dry and wet seasons in Rondônia, where NEE is calculated as a function of the Relative Irradiance (RI) (Cirino et al., 2014). A clean atmosphere is associated with a RI of

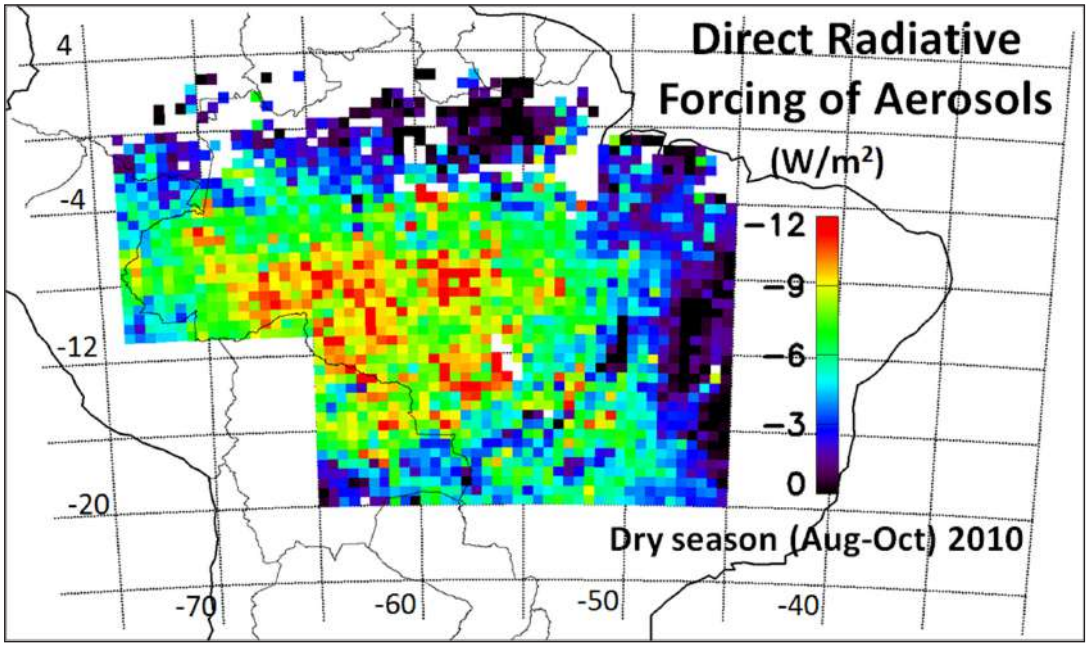

Figure 4.6.1 Average spatial distribution of the direct radiative forcing (DRF) of biomass burning aerosols in Amazonia during the dry season of 2010. Radiation flux at the TOA was measured by the CERES (Clouds and the Earth's Radiant Energy System) sensor, and aerosol was determined using the MODIS sensor. The average forcing is negative, so the cooling effect from organic scattering aerosols dominates over the warming from black carbon emissions.

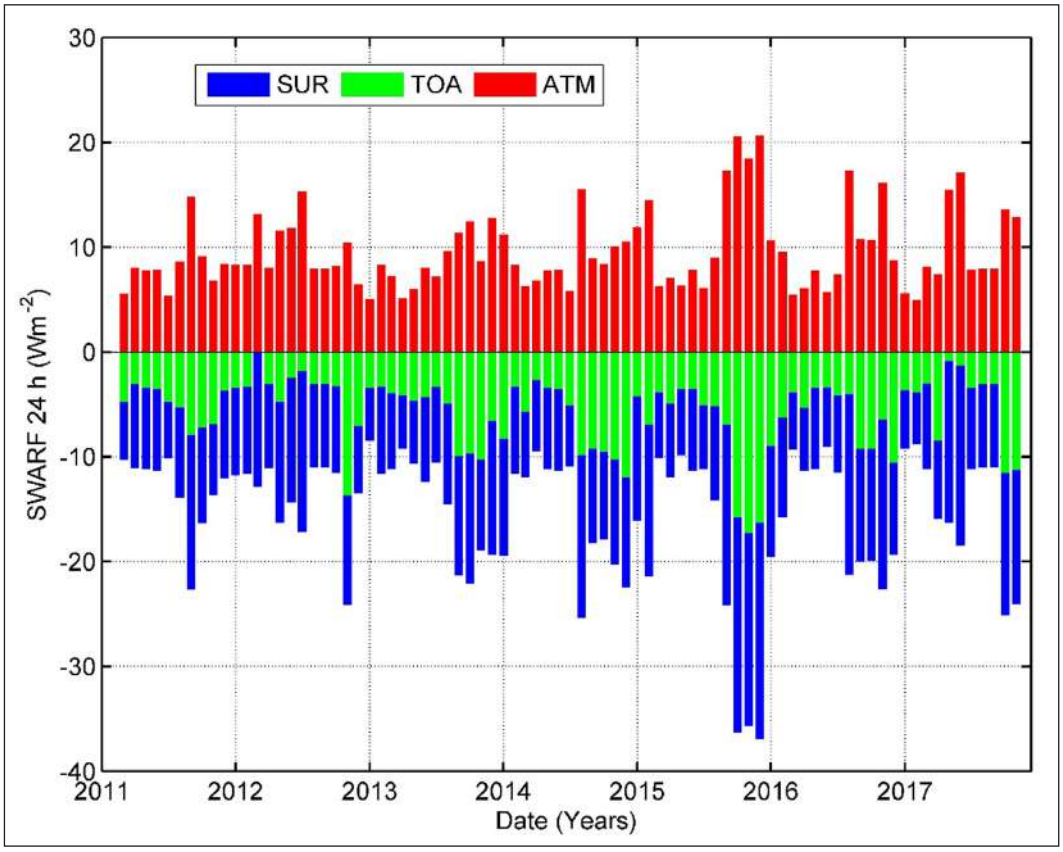

Figure 4.6.2 Monthly mean variation of short-wave aerosol radiative forcing (SWARF) averaged over 24 h at the top of the atmosphere TOA (green), surface SUR (blue), and within the atmosphere ATM (red) for the period 2011–2017 in Central Amazonia. Data from the Manaus/EMBRAPA AERONET site (Palácios et al., 2020).

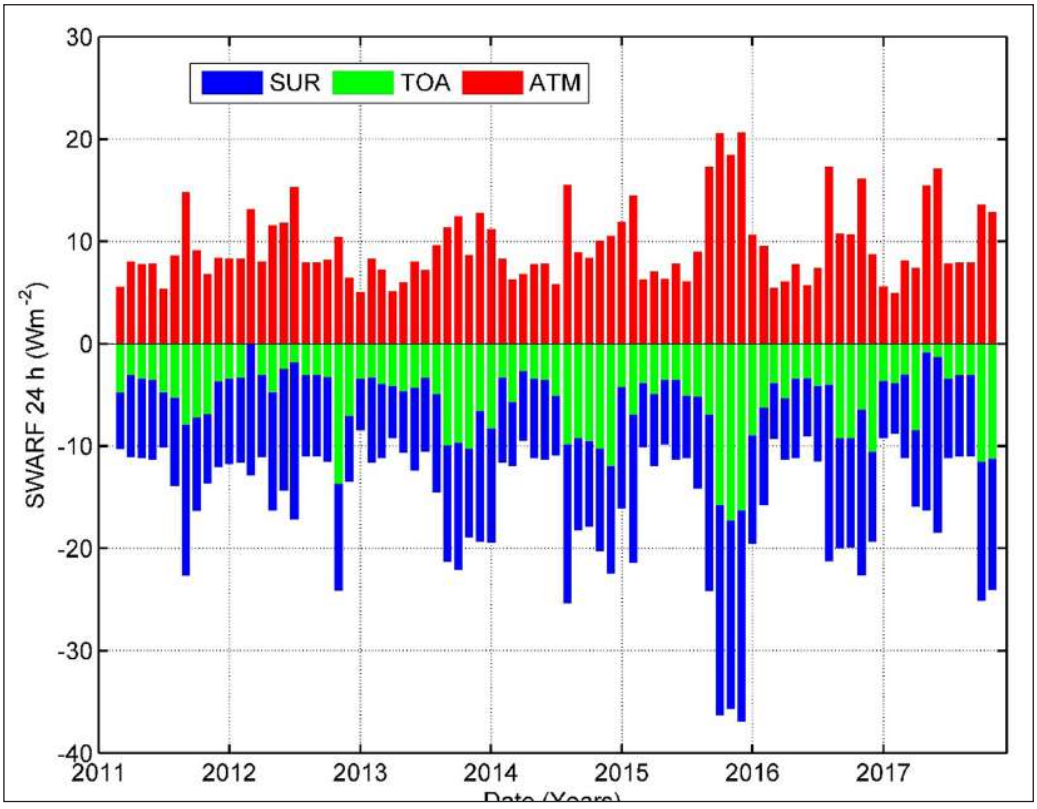

Figure 4.6.3 Effects of aerosols on carbon uptake by the Amazonian Forest expressed as NEE for dry and wet seasons in an LBA tower in Rondônia (Rebio Jarú). A relative irradiance of 1.0 corresponds to an atmosphere with background aerosols (AOD = 0.05). At increasing biomass burning aerosol loadings, the relative irradiance decreases. Analysis from Cirino et al., 2014.

1, which corresponds to AOD = 0.05 at 500 nm. As we increase the atmospheric aerosol loading, RI decreases. A RI of about 0.7 corresponds to an AOD at 500 nm of about 1.1. That is where the increase in NEE due to increasing diffuse to direct radiation starts to saturate. As the total radiation flux decrease with an increased aerosol concentration cause an increase in diffuse radiation the NEE decreases. It will reach values close to zero for high amounts of aerosols in the atmosphere.

Large-scale modeling studies show similar results in terms of strong aerosol effects on carbon uptake for Amazonia. Simulations with 3 times the BB (3xBBA) aerosol emissions of 2012 (***Figure 4.6.4***) show large-scale increases of 20–40% in diffuse radiation, gross and net primary production (GPP and NPP), especially in the August peak of the biomass burning season. This phenomenon is attributed to the increase in diffuse radiation by the aerosol loading and consequent more extensive radiation penetration into the forest canopy (Rap et al., 2015).

A significant number of studies on aerosol radiative effects from biomass burning in Africa focus on savannah fires, and only a few include measurements from tropical African forests. A modeling study used the Atmosphere Model version 5 (CAM5) and showed an average radiative forcing (RF) of –2 Wm^{-2} and a single scattering albedo at the wavelength 550 nm (SSA_{550}) of 0.92 in tropical Africa (Brown et al., 2021). Several AERONET sites in tropical and subtropical Africa reports large increases in AOD as a result of biomass burning emissions in Africa (Adesina et al., 2015, Boiyo et al., 2018, 2019). Long-term AOD_{500} measurements show an annual average of 0.23, with a mixture of sources (desert dust, biomass burning, and urban-industrial) (Boiyo et al., 2018). They also measured an average SSA_{440} of 0.89 and an average TOA aerosol radiative effect of –21.3 Wm^{-2} during the biomass burning season in July and –8.01 Wm^{-2} in November (Boiyo et al., 2018). Simeon et al., 2021 reports satellite observations and numerical simulations on the Southeast Atlantic region

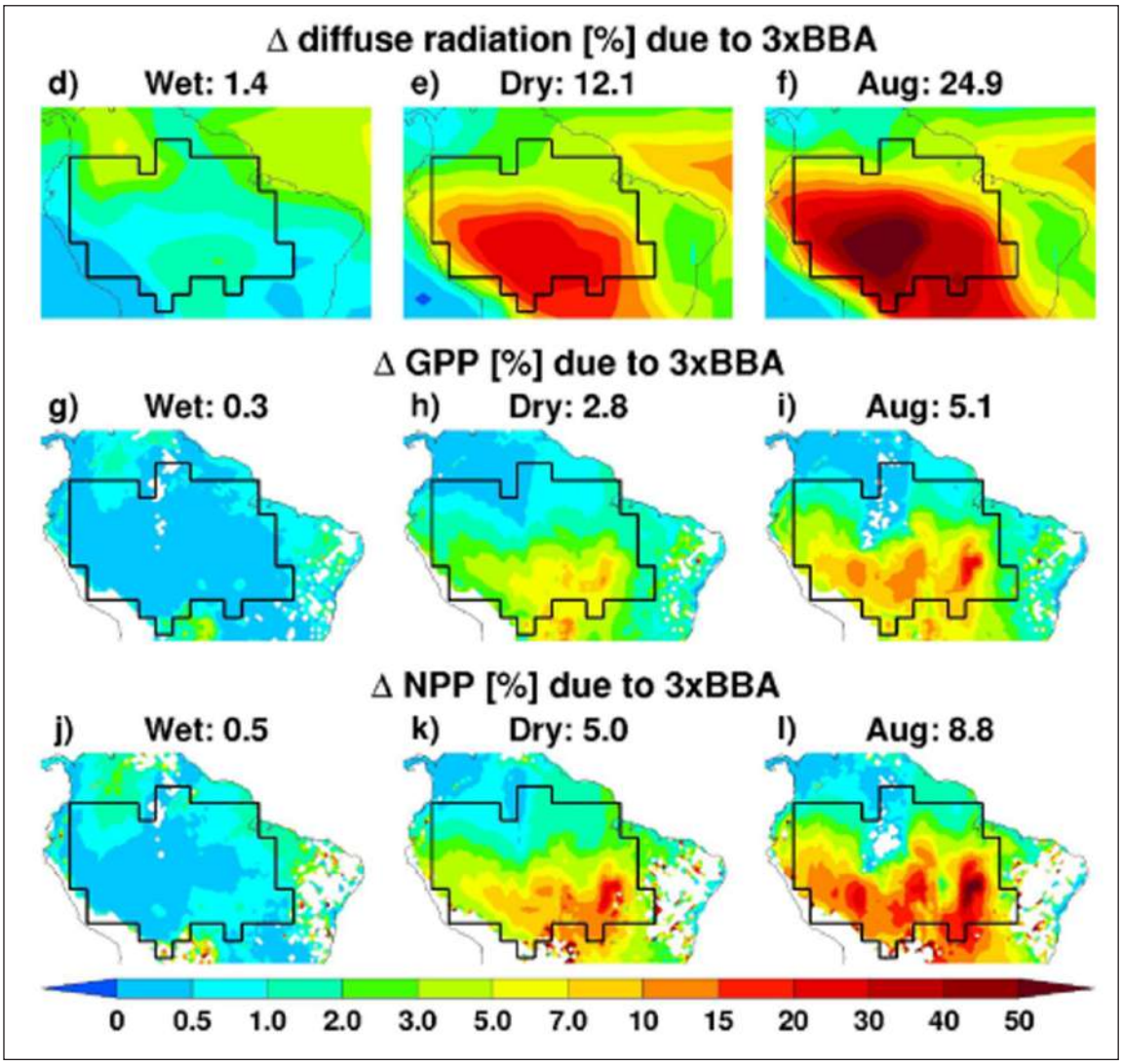

Figure 4.6.4 Modeled 1998–2007 mean percentage changes in **(d, e, f)** diffuse radiation, **(g, h, i)** GPP, and **(j, k, l)** NPP during the wet (defined here as of December to May) season, dry (June to November) season and August due to biomass burning aerosol (BBA) emissions. For details, see Rap et al., 2015.

influenced by African biomass burning. They observed some contribution from BrC, on the order of 3%, and an SSA_{550} of 0.84, a pretty absorbing aerosol. SSA retrieved from POLDER-3 shows an SSA of 0.85 at 565 nm. The BC/OC mass ratio influences SSA. African BBA plumes' values depend on the different types of burned vegetation in Africa (extratropical forests, tropical forests, savannahs, grasslands, or crop residues). These carbonaceous aerosol mixing ratios can be highly variable, ranging from 0.06 to 0.33 for BBA plumes (Simeon et al., 2021), affecting the aerosol radiative effect. Abel et al., 2005 using data collected by CIMEL sunphotometers from the NASA AERONET network and global climate models (GCM), showed that the net regional direct effect of the biomass smoke is −3.1 to −3.6 Wm^{-2} at the top of the atmosphere, and −14.4 to −17.0 Wm^{-2} at the surface, a strong effect. Aerosols from African biomass burning pollute the tropical South Atlantic significantly. Measurements made by the US Department of Energy Atmospheric Radiation Measurement (DoE ARM) Mobile Facility at Ascension Island showed an SSA_{500} of 0.78 to 0.83. An AOD_{500} of 0.4–0.7 when aerosol from biomass burning emissions in Africa impacted Ascension Island in June–October 2016–2017 (Zuidema et al., 2018).

A few studies analyze the radiative effect of aerosols emitted by North America and Northeast Asia boreal forests (Stocks et al., 1998, Spracklen et al., 2008). Randerson et al. (2006) used observations of the radiation balance over a chronosequence of forest fire burn scars combined with climate model analysis indicating that the radiative effect of mature boreal forest compared with the forest over an 80-year fire cycle was a warming of $2.3Wm^{-2}$.

In addition to the direct radiative effect analyzed in this section, aerosol-cloud interactions are very important for tropical and boreal forests. Both are the main uncertainties in the global radiative effect and have important impacts on future climate predictions (Boucher et al., 2013).

5. AEROSOL-CLOUD-PRECIPITATION INTERACTIONS

Aerosol-cloud interactions remain the most significant uncertainty in understanding anthropogenic perturbations to the climate system (Boucher et al., 2013). In this section, aerosol-cloud interactions will be reviewed, focusing on tropical and boreal forests. We will follow a process-based approach, tracing aerosol-cloud interactions from the micro- to the mesoscale. Forested areas are often characterized by distinct aerosol regimes: a clean regime dominated by a low concentration of organic aerosols forming from natural biogenic emissions and a polluted regime associated with aerosol emissions from wildfires and anthropogenic pollution. Perturbations to the global radiation balance are strongly associated with fire emissions (see sections 4.5–4.6).

5.1. THE COMPLEX MECHANISMS OF CLOUD-AEROSOL-PRECIPITATION-RADIATION INTERACTIONS

Many aerosol-cloud radiation interactions are nonlinear and critically important to climate. Aerosol particles scatter and absorb solar radiation and therefore reduce the incoming solar radiation at the surface ("dimming") (Ramanathan et al., 2001; Stephens et al., 2012, Liu et al., 2021). In addition, absorbing aerosols, notably black carbon from fire emissions, provides a diabatic heating term that increases atmospheric temperature and, therefore, reduces relative humidity as given by the Clausius-Clapeiron relationship. These "semi-direct" aerosol effects have been hypothesized to reduce cloud amount (Ackerman et al., 2000; Hansen et al., 1997; Koren et al., 2004). However, the associated modulation of temperature and humidity profiles also affects atmospheric stability and is sensitive to the height of the layer of absorbing aerosol (Koch and Del Genio, 2010, Hodgson et al., 2017). Absorbing aerosol layers above subtropical subsidence regions can also sharpen the inversion strength and increase the cover of stratocumulus clouds (Brioude et al., 2009; Johnson et al., 2004). This topic is also closely associated with carbon stocks in tropical forests due to the high sensitivity of the carbon cycle with temperature, clouds, and precipitation (Sikma et al., 2019).

5.2. AEROSOL-CLOUD INTERACTIONS MEDIATED VIA CHANGES IN CCN

Aerosols of suitable size and composition act as CCN at a given supersaturation SS (%). The number of CCN that is activated into cloud droplets is primarily determined by the number of CCN (condensation on CCN acts as a sink of supersaturation) as well as the updraft velocity (associated cooling reduces the saturation vapor pressure and therefore increases supersaturation) (McFiggans et al., 2006). Cloud droplet number concentrations in forested areas vary considerably between pristine, biogenically dominated, and polluted, fire-dominated conditions (Andreae et al., 2004; Roberts et al., 2001, Martins et al., 2011). There exists robust evidence that forest fires increase CCN and the number of activated cloud droplets (Andreae et al., 2004). The propagation of this perturbation in droplet numbers at cloud formation through cloud microphysical processes is more challenging to assess and, therefore, less certain. For the assumption of constant liquid water content, increased droplet numbers will directly translate into reducing cloud droplet radii, increasing cloud albedo, and exerting a negative (cooling) radiative effect on the top-of-atmosphere radiation balance (Twomey, 1974). Enhanced numbers of droplets with reduced size reduce the efficiency of droplets to grow to precipitable

size, which has been hypothesized to increase global cloud amount (Albrecht, 1989). This suppression of the warm rain formation mechanism via auto-conversion is also confirmed by theory (Khairoutdinov and Kogan, 2000), observations (Andreae et al., 2004), and modeling (Heikenfeld et al., 2019). However, it should be noted that reductions in droplet size also affect evaporation-entrainment feedbacks (Jiang et al., 2006), which could buffer the overall effect (Stevens and Feingold, 2009) so that the overall impact on precipitation could be small (Seifert et al., 2015, Toll et al., 2019). Although CCN affects the formation of liquid droplets, the associated perturbations also propagate to the mixed-phase convective clouds and ice cloud microphysics, affecting ice crystal number, mass, and morphology (Heikenfeld et al., 2019; White et al., 2017, Khain et al., 2005, Lynn et al., 2005, ***Figure 5.1***).

For deep convective clouds, if warm-phase precipitation is delayed until the freezing level, it has been hypothesized that the additional release of the latent heat of freezing leads to "convective invigoration" (Andreae et al., 2004, Rosenfeld, 2008). However, the importance of this mechanism is not entirely undisputed (e.g., Grant and van den Heever, 2015). Purely microphysical effects through an increase in the lifetime of anvil-cloud ice due to a larger number, smaller freezing droplets leading to smaller ice crystals with lower fall velocities could provide a complementary explanation for the "convective invigoration" (Fan et al., 2013; Grabowski, 2015; Grabowski and Morrison, 2016).

Observations from the recent ACRIDICON-CHUVA campaign in Amazonia provide evidence for aerosol effects on convective cloud microphysics. There exists a strong seasonal variability in tropical forests, with a distinct monsoon type rainy season and a dry season with more isolated and intense rainfall, as discussed in section 2. The monsoon type has a larger contribution of warm rain and deep convective clouds with moderate vertical velocity. The dry season has very intense deep convective clouds, more lighting, and graupel-hail particles (Machado et al., 2018; Ribaud et al., 2019). It is undoubtedly very different for the wet season due to the high amount of specific humidity (about 20 g/kg) and the typical ocean droplet size distribution behavior (the so-called green ocean). These features associated with the nearly pristine condition favor the development of warm rain with a short life cycle. Machado et al. (2018) show significantly different aerosol number concentrations between the seasons in Amazonas. The dry season has nearly three times more aerosols than the wet season (see section 3.3). Of course, the thermodynamic environment is also very different, resulting in very different cloud types and complicating the causal attribution of observed cloud variations to aerosol effects. For the wet season and low rain rates, primarily associated with warm cloud processes, the cleaner cases have a larger mean raindrop diameter than the most polluted events. For high rain rates, mostly related to deep convection, larger mean raindrop diameters are observed for the most polluted events, agreeing with the proposed cloud invigoration mechanism (Machado et al., 2018). Fan et al. (2018) suggest (based on the analysis of 17 convective events and cloud-resolving modeling) that the depletion of cloud water through precipitation in low aerosol environments can lead to high supersaturations and subsequent activation of small aerosol particles into cloud droplets (Ekman et al., 2011). This enhances condensation and latent heat release with the subsequent invigoration of convection. Cecchini et al. (2017) compare aircraft measurements of hydrometeor's shape (ice or liquid) for growing convective cumulus in polluted and pristine environments in Amazonia. They find a rapid increase in the fraction of ice particles above the melting layer for pristine clouds, while for polluted clouds, significant fractions of liquid droplets existed until –18°C. Another difference among cloud droplets from pristine and polluted environments is the vertical distribution of the cloud droplet number concentration. Wendisch et al. (2016) show a homogeneous cloud number concentration distribution with height in a polluted

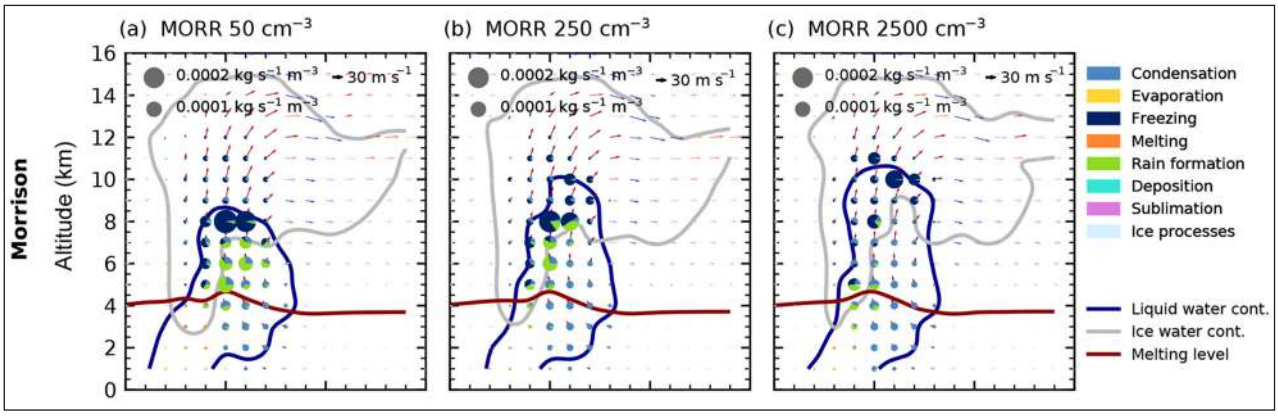

Figure 5.1 Illustration of the propagation of aerosol perturbations (idealized through prescribed cloud droplet number concentrations of 50 cm^{-3}, 250 cm^{-3}, and 2500 cm^{-3}) through mixed-phase cloud microphysics in a single-supercell convective cloud. With increasing droplet number concentrations, the warm rain formation is shut down while the freezing level increases (Heikenfeld et al., 2019).

environment and a significant decrease in cloud droplet number concentration for pristine clouds, consistent with the onset of collision/coalescence processes.

However, it should be noted that the uncertainties associated with mixed- and ice-cloud microphysics remain significant and can easily exceed the magnitude of model-simulated effects (White et al., 2017). There exists a need for robust observational constraints on the underlying microphysical processes. Another important factor to consider is that aerosol-cloud interactions are two-way interactions: not only do aerosols affect clouds, clouds and precipitation are also critical regulators of aerosols. Convective up and downdrafts are a key source of aerosol (precursors) (Krejci et al., 2003). Wang et al. (2016) show an increase of nanoparticles just after the onset of rain. Gerken et al. (2016) find a large increase in ozone concentration during convective raining events. They suggest that convective clouds bring gas and ultrafine aerosols from the upper troposphere by the downdrafts. Andreae et al. (2018) find a very high concentration of these ultrafine aerosols (up to 66000 cm^{-3}) around 8–12 km (see 4.4 and 6). They suggest a conceptual model where new aerosol particles are formed by biogenic volatile organic material brought up by the convective updrafts. Subsequently, these aerosols are transported by downdrafts of convective clouds to the surface and increased by the condensation of biogenic volatile organic compound oxidation products. At the same time, precipitation is also the main removal mechanism for aerosols, particularly for soluble aerosols suitable to act as CCN (Textor et al., 2006). This strong coupling between observable aerosol, cloud, and precipitation properties and the existence of many confounding factors makes it difficult to establish causality from purely observational studies (Gryspeerdt et al., 2014, 2015, Toledo Machado et al., 2021).

5.3. AEROSOL-CLOUD INTERACTIONS MEDIATED VIA CHANGES IN ICE NUCLEI PARTICLES (INP)

In addition to CCN, ice-nucleating particles (INP) can perturb cloud microphysics (Schrod et al., 2020). Both locally bioaerosol emitted (e.g., fungal spores, bacteria, plant fragments) and advected (e.g., soil dust) aerosols contribute to the forest budget of INP (Prenni et al., 2009). While global measurements seem to indicate a limited contribution of biogenic aerosols to the overall abundance of INP, they can be of much greater importance in source regions with large biological activity. However, the availability of measurements of INP is limited, so that is not yet possible to quantify their relative contributions. Model simulations suggest a limited role of INP on convective dynamics but highlight their role in regulating ice concentrations in convective anvils (Fan et al., 2010, Philips et al., 2005).

Recent field campaigns in Amazon provide detailed measurements of cloud microphysics. Using HALO aircraft measurements based on a stereoscopic particle imager, Wendisch et al. (2016) show different ice particle habits of cold cloud tops for in situ cirrus and an anvil outflow over the Amazon. In situ cirrus is typically composed of small ice particles, bullet rosettes, and bullet rosette aggregates; contrarily, anvil outflows were mainly composed of plates and aggregates. These cloud-top features represented the Amazonian deep convective cloud during polluted conditions. These differences in observed ice crystal habits are probably related to the different formation altitudes, microphysical processes, and strong vertical transport. Wendisch et al. (2016) suggest that these plate-like ice crystals, found in the cirrus outflow, were formed, and grown by heterogeneous nucleation on solid aerosol particles and grown in the warmer parts of the cloud. Ribaud et al. (2019) describe the convective and stratiform clouds ice microphysical properties over Brazil using a dual-polarization radar. Stratiform clouds typically have ice crystals, wet snow, aggregates, and clouds in the dry and wet seasons with very similar ice classification. The only observed difference is related to the higher levels of wet snow and aggregates found during the dry season. For the convective clouds, some differences were observed between dry and wet season clouds. The wet season convective clouds are composed of ice crystals, low-density graupel, and aggregates. The dry season has an additional ice spice, the high-density graupel. Those differences are related to the more intense convective clouds and the CCN concentration during the dry season. Jäkel et al. (2017) employed an imaging spectroradiometer during ACRIDICON-CHUVA to measure the side spectral reflectivity of deep convective clouds to assess the cloud phase. They found different mixed-phase upper (glaciation layer) and lower boundaries between moderate and polluted atmospheric conditions. Polluted clouds have a higher upper and lower boundary of the mixed-phase layer when compared with the moderate clouds. Albrecht et al. (2011) used the ground lightning network and radar data to discuss the deep convective cloud's behavior in Amazonas during the TRMM-LBA field campaign. They found no significant difference between thunderstorms and showers in terms of atmospheric pollution during the dry season. However, during the wet season, cloud-to-ground lightning is predominant during periods of higher aerosol concentration.

Due to the difficulty of observing ice cloud microphysics in convective clouds and the strong co-variability of CCN and INP that complicate the attribution, there is limited observational evidence on the effect of INP on convective cloud microphysics.

5.4. CLIMATE EFFECTS OF AEROSOL-CLOUD INTERACTIONS

Currently, there exists a disconnect between primarily processed-based and limited area studies of the impact

of forest aerosols on convective clouds and the regional and larger-scale climate impacts. A key reason is the current global and regional climate models that, due to limitations in the parameterization of convective clouds, do not typically include convective cloud microphysics and hence lack the ability to represent the majority of the effects proposed to be of importance for the impact of forest aerosols on clouds and climate. However, both recent development of advanced aerosol-aware convection parameterizations (Gettelman et al., 2015; Kipling et al., 2017; Labbouz et al., 2018), as well as the increasing availability of (near) global cloud-resolving modeling (Satoh et al., 2008), will help to close this gap in a medium to long-term perspective. Meanwhile, it is worth reiterating the importance of scales for aerosol-cloud interactions. While many process-based studies focus on a single or a limited number of clouds, for which limited budgetary constraints exist, it is not clear that the results from such studies apply to a cloud-field, on a regional or even on a global scale, for which moisture and energy budgets are of crucial importance (Allen and Ingram, 2002; Muller and O'Gorman, 2011). Such budgetary constraints may be the underlying mechanism of the concept of "buffering" (Stevens and Feingold, 2009). It is important for the global radiation balance to recall that the cooling/warming direct radiative effects of scattering/absorption from biomass burning aerosol approximately cancel each other (Myhre et al., 2013; Stocker et al., 2013). However, because both scattering and absorbing forest aerosols can act as CCN, and because the net aerosol effective radiative forcing from aerosol-cloud interactions is negative (Boucher et al., 2013), the net radiative effect of forest aerosol on the global radiation balance is likely to be negative but highly uncertain due to the above-mentioned limitations in global climate models used to quantify these effects. Future work should employ large-domain and global Large Eddy Simulation/Cloud Resolving Models (LES/CRM) simulations with prognostic aerosol parameters to facilitate comparison with observations and facilitate the interpretation of observed aerosol-cloud relationships, and ultimately provide more robust assessments of the effect of forest aerosols on clouds and climate.

From several studies, it is possible to observe that aerosol-cloud interactions (ACI) tend to saturate at high aerosol loading. In contrast, the strength of aerosol-radiation interaction (ARI) increases and plays a more important role in highly polluted episodes and regions. This should hold not only for biomass-burning aerosols over the Amazon but also for other light-absorbing aerosols. The importance of ARI at high aerosol loading highlights the need for accurately characterizing aerosol optical properties to investigate aerosol effects on clouds, precipitation, and climate (Liu et al., 2020, Gouveia et al., 2017).

6. ECOSYSTEM-ATMOSPHERE FEEDBACKS AND DRIVERS OF CHANGES

The preceding sections clearly show that tropical and boreal forests play a major role in key biogeochemical, atmospheric, and climatic issues up to the planetary scale. Tropical forests are one of the largest carbon reservoirs among terrestrial ecosystems. The forest ecosystems work through a complex nonlinear network of many different processes, with positive and negative feedbacks. For instance, deforestation is linked to reduced evaporation and increasing local temperatures, and these effects induce a further increase in land use, increasing forest degradation. Forest cover loss—if sufficiently extensive—can result in changes in local climate that, in turn, can degrade the forest and turn it more susceptible to fires (Feng et al., 2021, Junior et al., 2021). Degraded forests in Amazonia currently occupy an area larger than that which has been deforested (Matricard et al., 2020, Vancutsem et al., 2021), and this is important feedback (Malhi et al., 2009)

Several recent studies show that carbon cycling is changing in Amazonia (Brienen et al., 2015, Brando et al., 2019, 2015, Saatchi et al., 2021. A few decades ago, Amazonia was removing carbon from the atmosphere at a rate of about 50 g m^{-2} a^{-1} (Ometto et al., 2005, Araujo et al., 2002, Chambers et al., 2001). Recent works show that the intensification in tree mortality due to increased frequency and intensity of droughts brought the carbon balance of undisturbed forests close to neutral (Brienen et al., 2015, see also section 4.2.6). Future temperature and precipitation changes, in addition to increases in climate extremes, will bring additional stress (Lovejoy and Nobre, 2018, 2019, Nobre et al., 2019, Aguiar et al., 2016). This will most likely change the emissions and atmospheric processes that have been discussed in previous sections, especially if global climate change is aggravated regionally by deforestation (Hoffmann et al., 2003). Biomass-burning emissions can also change with new governmental policies in many countries and are major drivers for boreal and tropical atmospheric composition (Andreae, 1991, see also section 4.5). Higher temperatures for boreal forests could mean more insect infestations, changing albedo during wintertime, and produce other biophysical and climatic effects (Lappalainen et al., 2016). The boreal forest faces other challenges, with changing practices in forestry, changing climate resulting in changing temperature, growing season, precipitation, and changing biodiversity, which in turn changes the feedback processes. Climate change and rising CO_2 are altering the behavior of land plants in ways that influence how much biomass they produce relative to how much water they need for growth (Brando et al., 2019, Brienen et al., 2015, Saatchi et al., 2021). Plants have also become substantially more efficient

at fixing carbon per unit of water lost, which is possible because of the beneficial effects of elevated atmospheric CO_2. This result implies that, on a global scale, land plants have regulated their stomatal conductance to allow the CO_2 partial pressure within stomatal cavities and their intrinsic water use efficiency to increase in nearly constant proportion to the rise in atmospheric CO_2 concentration (Keeling et al., 2017).

In addition to the effects of climate change in tropical regions, land-use change, and urbanization are rapidly increasing, generating strong impacts in the ecosystem processes. Climate change in the tropics is expected to not only increase temperatures but also further alter precipitation patterns, as more frequent and intense droughts are combined with elevated temperatures that are already being observed (Stark et al., 2020, Aragão et al., 2018; Feldpausch et al., 2016; Li et al., 2008; Marengo et al., 2016). Such conditions can lead to increased tree mortality, reduced net primary productivity, and decreased trace gas emissions such as VOCs due to biomass reduction (Aleixo et al., 2019, Yanez Serrano et al., 2020). Spatial and temporal rainfall patterns are governed by complex interactions between climate and landscape perturbations, including deforestation, fire, and drought (Haghtalab et al., 2020). These changes can have profound effects on the dry season length, which affects the atmospheric chemistry above the rainforest (MacKenzie et al., 2011). There is significant uncertainty regarding the effects of CO_2 increase and CO_2 fertilization, and measurements are currently taking place to investigate this critical issue (Lapola, 2018). If global warming is kept below 2°C, less than 2% of assemblages globally are projected to undergo abrupt exposure events of more than 20% of their constituent species; however, the risk accelerates with the magnitude of warming, threatening 15% of assemblages at 4°C, with similar levels of risk in protected and unprotected areas (Trisos et al., 2020).

Increases in forest areas are being discussed as one of the strategies to mitigate climate change. This would involve reforestation, forest restoration, afforestation, or capturing CO_2 from the atmosphere via BECCS (bioenergy with carbon capture and storage) (IPCC SRCCL, 2019, IPCC SR1.5, 2018, Bastin et al., 2019). Bastin et al. (2019) propose an extra forest coverage of $9{\cdot}10^6$ km^2 as a global tree restoration potential that could store 205 Pg of carbon in the long-term perspective. They estimate this significant potential increase from their estimate of the total forest area of $28{\cdot}10^6$ km^2, differing from the estimate of $40{\cdot}10^6$ km^2 by Pan et al., 2011. Bastin et al. claim that the extra $9{\cdot}10^6$ km^2 will not impact urban or cropland, while IPCC SRCCL, 2019, state a need to increase crop area to provide food security for our increasing population. BECCS is being analyzed as a mitigation strategy that could remove CO_2 from the atmosphere at a scale of up to 11.3 Pg CO_2 a^{-1} in 2050, doubling the present CO_2 removal by global forests. For such a large-scale BECCS deployment, many technological issues must be worked out. In addition, these policies of large-scale BECCS implementation will need careful management between reducing tropical deforestation, increase in food production areas, and bioenergy production (Fuss et al., 2018).

Tropical and boreal forests have quite different feedback mechanisms and different sensitivity to warming or change in precipitation. ***Figure 6.1*** shows a

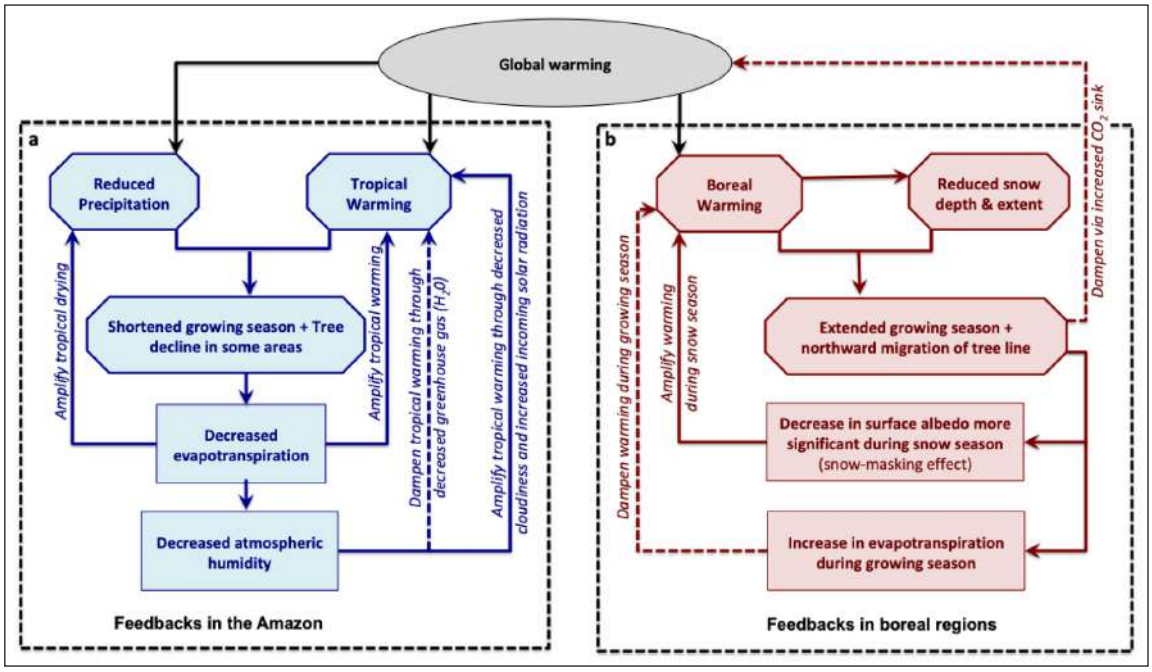

Figure 6.1 Schematic illustration of the processes through which the effects of global warming in the **a)** Amazon (left panel, blue boxes, and arrows) and **b)** boreal regions (right panel, red boxes, and arrows) feedback on the regional climate change (Jia et al., 2019, IPCC SRCCL, 2019).

schematic illustration of the processes through which the effects of global warming in tropical and boreal forests feedback on the regional climate change. Feedbacks are very different in each ecosystem. In boreal regions, the feedback depends on the season, although global warming has positive feedback in high latitude forests. Dashed lines illustrate negative feedbacks, while solid lines indicate positive feedbacks (IPCC SRCCL 2019).

6.1. FEEDBACKS IN BOREAL FORESTS

Boreal forests play a crucial role in the Earth's carbon balance, storing 272 ± 23 Pg carbon, or 32% of the world's total forest carbon stock (Pan et al., 2011). Understanding the mechanisms regulating carbon exchange in the boreal forest ecosystems is crucial from a climate change perspective. Besides the rather noticeable effect of changing green mass in the ecosystem's CO_2 balance, chains of complex interactions between the ecosystem and atmosphere have been identified (Kulmala et al., 2013b). Here we focus on two carbon-based Continental Biosphere-Atmosphere-Cloud-Climate (COBACC) feedback loops in boreal forests and our current qualitative understanding of the physical processes behind these loops.

Schematics of the loops are shown in ***Figure 6.1.1***. A CO_2 increase may cause an increase in the GPP of an ecosystem, an effect known as CO_2 fertilization (CO_2 – GPP link in ***Figure 6.1.1***). The GPP is one of the ingredients of the carbon dioxide flux fixed by an ecosystem, thus characterizing the ecosystem's photosynthetic activity (see section 4.2). The NEE and GPP are related by GPP=NEE-Rec, where Rec is the ecosystem respiration. Rec is the sum of above-ground biomass respiration and CO_2 efflux from the soil surface (including root respiration). Due to CO_2 fertilization, NEE in boreal and temperate forests increases on average by 0.45 g C m^{-2} a^{-1} per ppm increase of CO_2 in the atmosphere (Fernández-Martínez et al., 2017), however as the authors show, the estimate ranges from 0.2 to 0.6 C m^{-2} a^{-1} ppm^{-1} depending on methodology. Photosynthesis is responsible for the carbon supply to the plants, necessary for their regular metabolism and function. Some types of plants have special carbon storages to allocate part of the carbon received in the process of photosynthesis. Plants can use this stored carbon and the carbon from de novo photosynthesis to produce BVOC (Ghirardo et al., 2010). Enhanced photosynthesis may lead to increased BVOC emissions (GPP – BVOC link in ***Figure 6.1.1***).

In addition, an increase in CO_2 concentration in the atmosphere leads to a temperature increase due to the enhanced greenhouse effect (CO_2 – T link in ***Figure 6.1.1***). This temperature increases boost emissions of many BVOCs (mono- and sesquiterpenes, for instance) through mechanisms associated with evapotranspiration (Grote et al., 2013). An exponentially growing dependence of BVOC emissions on temperature is observed for the emissions using carbon from the storage pool (Tingey et al., 1980). The emissions were processing carbon from de novo photosynthesis (e.g., isoprene) decrease after some threshold value of temperature because high temperatures (>40–45°C) destroy the photosynthetic apparatus of plants (Monson et al., 1992). However, such high temperatures are rarely observed at middle and high latitudes, and therefore all emissions in boreal forests generally grow with temperature (T-BVOC link in ***Figure 6.1.1***).

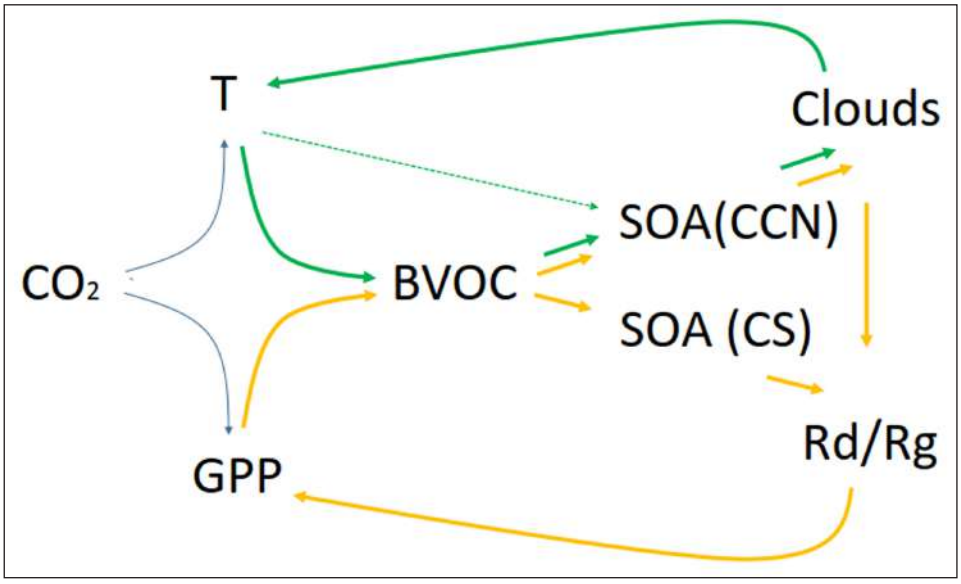

Figure 6.1.1 Schematic of the carbon-based Continental Biosphere-Atmosphere-Cloud-Climate COBACC feedback loops. The temperature-related feedback loop is in green color, while the GPP-related feedback loop is in orange. CO_2 – concentration of carbon dioxide, GPP – gross primary production, BVOC – biogenic volatile organic compounds, SOA – secondary organic aerosol, CS – condensation sink, CCN – cloud condensation nuclei, R_d/R_g – fraction of diffuse radiation in global radiation, T – temperature. For an explanation regarding the colors and arrows, please see the text.

Note that both temperature-related and GPP-related loops in ***Figure 6.1.1*** share an important BVOC-aerosol link. BVOCs are oxidized in the atmosphere to form low-volatility and extremely low-volatility organic vapors (Hallquist et al., 2009). These vapors contribute to the process of new particle formation and growth (Ehn, 2014), which has two important consequences. One is an increase in the number of particles able to act as cloud condensation nuclei (BVOC-CCN link in ***Figure 6.1.1***), and the other is an increase in the condensation sink (BVOC – CS link in ***Figure 6.1.1***). Condensation sink (CS) is a parameter proportional to aerosol surface area and mainly sensitive to the aerosol particles' increase in size (Lehtinen et al., 2004, Ezhova et al., 2018a). The link between BVOC and SOA has been investigated using different approaches. Particles inside an air mass moving over land are constantly growing because organic vapors produced from BVOCs emitted by forests condense onto existing aerosol particles. The increase in total aerosol mass with time over land has been demonstrated by Tunved et al. (2006b) and Liao et al. (2014). With this approach, the authors showed that aerosol growth in boreal forests is a process essentially non-local in space and time. Besides, whereas the aerosol characteristics are measured, the monoterpene emission (Loreto et al., 1998) are parameterized by Tunved et al. (2006b) and Liao et al. (2014). Kulmala et al. (2014a) proposed a different approach to the BVOC-SOA link based on in-situ atmospheric observations. The authors considered CS as a function of the particle growth rate at the smallest particle sizes (GR), calculated from the particle number size distribution. The GR is larger for higher concentrations of BVOCs and organic vapors, and CS increased with GR. This approach reduced the data set to only NPF days, which can be relatively rare in summer (Dada et al., 2017), and abundant only in parts of the boreal forest. One more approach accounting for the BVOCs effect links temperature to aerosols (dashed line in ***Figure 6.1.1***). Sporre et al. (2020) analyzed the significant differences in the aerosol radiative response to BVOC changes using three Earth system models and found that different chemical mechanisms for SOA production is the reason of different model responses. The increase in CCN with temperature was demonstrated by Paasonen et al. (2013) based on atmospheric observations from eleven sites in different parts of the world. While recent measurements at two remote forest sites in British Columbia, Canada, showed almost daily NPF (Andreae et al., 2019), a long-term study at the ZOTTO site in Siberia found only 11 nucleation events were observed over three years, indicating that homogeneous nucleation followed by condensational growth is not a major process maintaining the aerosol population in that region (Wiedensohler et al., 2019).

The next step of the feedback loop is from CCN to clouds. The effect of aerosols on cloud cover is not well established and is itself subject to various complex feedbacks (see also section 6.2). However, the first indirect effect (Twomey, 1977) has been confirmed by many studies (Rosenfeld et al., 2014). Cloud albedo (reflection of solar radiation) increases when the number of cloud droplets increases at constant liquid water content (Twomey, 1977), resulting in a cooling of the atmosphere due to the increase in reflected radiation (clouds-T link in ***Figure 6.1.1***). Thus, the temperature-related COBACC feedback loop (shown in green in ***Figure 6.1.1***) represents negative feedback on temperature.

The GPP-related loop (shown in orange in ***Figure 6.1.1***) includes two effects on solar radiation related to secondary organic aerosol, namely particles acting as CCN and increasing aerosol loading (CS). The CS-related link corresponds to the "clear-sky" part of the GPP-related loop, whereas the CCN-related link corresponds to the 'cloudy' part. In what follows, we focus mainly on photosynthetically active radiation (PAR), which corresponds to the range of wavelengths between 400 and 700 nm in the solar radiation spectrum. Incoming PAR consists of direct and diffuse radiation. Direct radiation comes from the sun's direction, whereas diffuse radiation (i.e., sunlight scattered by molecules, particles, and droplets in the atmosphere) comes from all other directions. An increase in aerosol loading under a clear sky, as well as clouds present in the sky, leads to an increase in the diffuse fraction of solar radiation due to larger light scattering (SOA-R_d/R_g links in ***Figure 6.1.1***). Under a clear sky and at low aerosol loading, PAR is mainly direct radiation. Under this condition, only the upper part of the canopies of forest ecosystems can get enough light for effective photosynthesis, especially in dense canopies when the diffuse fraction of radiation increases, more incoming radiation arrives from different angles. As a result, more light photons penetrate the canopy and can be captured and used for photosynthesis (Gu et al., 2002, Niyogi et al., 2004). This leads to an increase in light use efficiency (LUE) – a parameter quantifying the amount of carbon dioxide taken up by an ecosystem per unit of absorbed PAR. At the same time, an increase in the diffuse fraction of radiation is the consequence of an increase in scattering and reflecting agents (aerosol particles and clouds) in the atmosphere, which also scatter part of the incoming radiation back into space. Therefore, the total incoming radiation reaching the surface decreases when the diffuse fraction of solar radiation increases. A large increase in diffuse fraction usually leads to a decrease in GPP because such a strong radiation decrease makes light a limiting factor for photosynthesis. However, at moderate aerosol burdens, a moderate increase in diffuse radiation may lead to an increase in ecosystem GPP (R_d/R_g – GPP link in ***Figure 6.1.1***) due to the effect of diffuse radiation fertilization on forests (see also section 4.6).

At remote sites in boreal and hemiboreal forests, on clear days, aerosol loading (CS) can lead to an increase

in the diffuse fraction of solar radiation from 10% (clean atmosphere, clear days) to ~ 27% (high aerosol loading, clear days) (Ezhova et al., 2018b, see also section 4.6). The corresponding DRF effect estimated from observations is a 6–14% increase in GPP. The largest increase, up to 10–30% for different ecosystems compared to clean atmosphere and clear sky conditions, is associated with some particular types of clouds, e.g., cumulus clouds (Freedman et al., 2001; Alton, 2008, Pedruzo-Bagazgoitia et al., 2017). At the same time, optically thick clouds reduce the GPP of an ecosystem (Pedruzo-Bagazgoitia et al., 2017). Therefore, the 'clear sky' or CS-related part of the feedback loop results in positive feedback for GPP, while the 'cloudy sky' or CCN-associated effect for GPP may be negative or positive.

Two recent modeling studies simulating the global effect of aerosols on GPP reported opposite results. In the Norwegian Earth System Model (NorESM), an increased aerosol loading, and the resulting higher cloud cover and lower temperatures resulted in a very slight decrease of global GPP (Sporre et al., 2019). In contrast, a simulation using the Joint UK Land Environment Simulator (JULES), which did not include the effects of biogenic SOA on cloud albedo and lifetime and aerosol-induced reductions in temperature, yielded a significant increase in primary productivity (Rap et al., 2018).

6.2. FEEDBACKS FOR TROPICAL FORESTS

Tropical forests are of global importance for atmospheric carbon levels and climate (Covey et al., 2021, Andreae et al., 2015). They have been estimated to hold 471 ± 93 Pg of carbon, about 55% of the carbon inventory in the world's forests (Pan et al., 2011). In contrast to boreal forests, where most carbon is present in the organic soil, 56% of carbon is stored in the biomass and 32% in the soil in tropical forests. There is an ongoing debate about the net carbon flux between tropical forests and the atmosphere, with some studies indicating a small net carbon uptake and others a net carbon loss (e.g., Pan et al., 2011; Gloor et al., 2012; Baccini et al., 2017; Schimel et al., 2015; Brienen et al., 2015). This disagreement is significant because the net carbon flux is the difference between two large gross fluxes. The carbon emissions largely result from deforestation, and the carbon uptake is due to forest growth, likely supported by the increasing CO_2 concentration in the atmosphere. Consequently, any change in the processes that affect atmosphere-biosphere interactions can result in large changes in the net carbon transfer between the tropical forests and the atmosphere, with substantial repercussions for atmospheric CO_2 levels and global climate (Lewis, 2006; Chambers and Silver, 2004).

Humid tropical forests are vulnerable to climate and land-use change (Saatchi et al., 2021). Several recent works show that rainforest's response to heat and drying varies across the continents, and vulnerabilities are widespread. Forests in the Americas exhibit extensive vulnerability to these stressors, while in Africa, forests show relative resilience to climate, and in Asia reveal more vulnerability to land use and fragmentation. (Vancutsem et al., 2021, Feng et al., 2021, Hubau et al., 2020, Qin et al., 2021, Saatchi et al., 2021, Sullivan et al., 2020).

Rainfall in the tropics depends on the large-scale atmospheric circulation and moisture sources, such as evaporation from the ocean surface. In Amazonia, an analysis of precipitation data from 1920 to 2010 shows five stations with increasing trends and 12 sites with decreasing or no trend (Satyamurty et al., 2010). Changing sea surface temperatures and shifts in the location and extent of the ITCZ (Intertropical Convergent Zone) are a result of global climate change (Schneider et al., 2014; Heffernan, 2016). In particular, a reduction in anthropogenic aerosol global emissions has been proposed to change the north-south gradient of sea surface temperature in the North Atlantic, which would cause increased droughts in the Amazon Basin (Cox et al., 2008). This, in turn, would affect the carbon budget of the Amazon Forest and facilitate fires in drier areas of the basin, etc., with regional and large-scale effects on the climate system. Climate modeling indicates a displacement north of the ITCZ of about 1 degree from 2025 to 2049 (Acosta Navarro et al., 2017). Such displacement is directly connected to changes in anthropogenic aerosol emissions but is difficult to distinguish in observations due to natural variability (Allen et al., 2015). However, Ridley et al., 2015, find, through investigations of a 456-year speleothem record, strong observational evidence for a southward displacement with increasing aerosol concentrations in the northern hemisphere. They also claim that differentiating between anthropogenic aerosol forcing, global differential increase in temperature, and century-scale natural variability is a complex scientific issue.

Increasing temperatures and drought have been predicted to cause a reduction of the tropical land carbon uptake in the coming decades (Sitch et al., 2008, Aragão et al., 2008). This feedback has been validated observationally. Its magnitude was shown to have doubled over the last five decades (Wang et al., 2014), probably related to prevailing drier conditions in the more recent decades. This highlights the important couplings between the water and carbon cycles in the tropics. Evapotranspiration provides a large component of the atmospheric moisture over the Amazon, becoming increasingly more important towards the western part of the basin (Spracklen et al., 2012; Molina et al., 2019). Deforestation and increasing atmospheric CO_2 both act to reduce evapotranspiration, reducing the amount of water available for rainfall in the western Amazon Basin and adversely impacting rainforest resilience (Zemp et al., 2017). This effect even extends beyond the

Amazon Basin into the Rio de la Plata region, for which Amazonian evapotranspiration is a vital moisture source (Camponogara et al., 2014; Zemp et al., 2014).

The impact of the changes in the water cycle on the Amazonian biogeochemistry is discussed in several recent papers, e.g., Aleixo et al., 2019, who found that over the past 50 years, a large increase in tree mortality occurred associated with changes in precipitation. Covey et al., 2021, reviews the forest biogeochemistry in a rapidly changing Amazon. They find that the majority of anthropogenic impacts act to increase the radiative effect potential of the rapidly changing Amazon Basin.

Droughts cause most mortality in pioneer species, which tend to be less drought-tolerant compared to late-successional high wood density tree species and thus are particularly vulnerable. Variability in drought-induced mortality followed the rhythm of El Niño events. Storms were found to particularly affect large trees of late-successional species, which are usually thought to be most resistant to storms. Non-linear responses to heat anomalies are found, with mortality increasing rapidly above 29.5°C. This points to a possible Achilles heel of these forests concerning climate change (Gloor et al., 2019). Phillips et al. 2009 already had shown a strong association between the drought of 2005 and carbon cycling, when forests with a water deficit increase of 100-mm lost 0.53 kg C m^{-2} of above-ground biomass carbon. A tropical forest study from Borneo and Amazonia (Philipps et al., 2010), with 119 monitoring sites, found a large increase in mortality rate associated with a decrease in precipitation. This is important because most climate models from the Coupled Model Intercomparison Project Phase 5 (CMIP5) and Coupled Model Intercomparison Project Phase 6 (CMIP6) show a potential reduction in precipitation in eastern Amazonia, and a 7-years drought experiments in Amazonia confirms these findings (da Costa et al., 2010). In addition to the increase in temperature, it has been observed that climate extremes strongly affect the functioning of tropical ecosystems. Bathiany et al. (2018) show that climate models predict increasing temperature variability in the tropics, with stronger and more frequent heatwaves, with the Amazon as a particular hotspot of concern. Brando et al. (2019) show an explicit dependency between precipitation and aboveground live biomass for the Congo, Amazon, and Southeast Asia. ***Figure 6.2.1*** shows

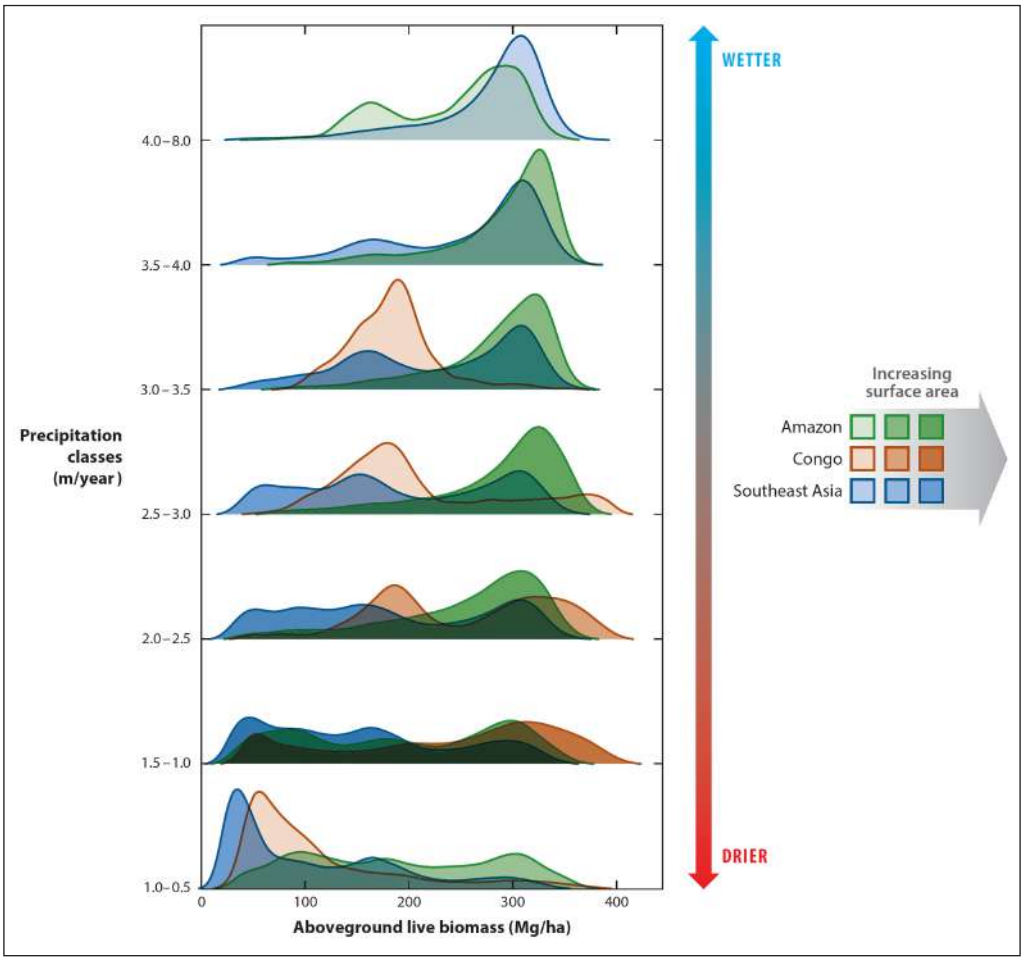

Figure 6.2.1 Relative density distributions of aboveground biomass in living woody plants per 1981–2017 mean annual precipitation class for the tropical forest in the Amazon, Congo Basin, and Southeast Asia. The color shading is proportional to 30 m × 30 m pixels in each of the relative density plots. Thus, the more solid the color is, the greater the number of pixels and the larger the area in that precipitation class, while the less solid color represents fewer pixels and smaller areas. Figure from Brando et al. (2019).

the dependence of aboveground live biomass versus precipitation for tropical forests. For drier regions, the peak of aboveground live biomass is less than 10 kg m^{-2}. For wetter forests, the peak in above-ground biomass is about 30 kg m^{-2}. This clearly shows the link between carbon cycling and precipitation regimes. It also indicates that droughts have reduced forest carbon uptake and stocks by elevating tree mortality, increasing autotrophic respiration, and promoting wildfires (Brando et al., 2019; Yang et al., 2018).

Vapor pressure deficit, or VPD, is the difference between moisture in the air and how much moisture air can hold when it is saturated. From a plant's perspective, the VPD is the difference between the vapor pressure inside the leaf and the vapor pressure of the outside air. Atmospheric vapor pressure deficit is a critical variable linked to plant photosynthesis and water use. Increased VPD reduces global vegetation growth. The synthesis of four global climate datasets reveals a sharp increase in VPD after the late 1990s (Yuan et al., 2019). Increases in VPD recently observed in Amazonia were attributed to elevated GHG levels and biomass burning aerosols, reducing water availability due to less precipitation (Barkhordarian et al., 2019). ***Figure 6.2.2*** shows that the increase in VPD was strong in Southeast and Northwest Amazonia and amplified during the three drought years of 2005, 2010, and 2015.

The forest interacts with the climate system also by influencing the atmospheric aerosol burden. In its undisturbed state, the tropical forest supports relatively low aerosol particle concentrations, on the order of about 150–250 cm^{-3} during the wet season (Andreae et al., 2009, Pöschl et al., 2010; Pöhlker et al., 2019, see also section 3.2–3.3). These concentrations are similar to those over the tropical oceans, which has given rise to the "green ocean" (Roberts et al., 2001; Williams et al., 2002). According to this concept, the low CCN particle concentrations over the pristine tropical continents lead to cloud and rainfall properties that resemble those over the oceans, with a dominance of cloud droplet growth to raindrop size via collision and coagulation (Rosenfeld et al., 2008, 2014, see also section 3.4 and 5).

The processes that maintain this aerosol population over the tropical forest are still not fully understood (Kulmala et al., 2011). The type of nucleation event that yields large numbers of small particles, and which has been suggested to account for a significant source of particles over the boreal forest and in polluted environments, has rarely been observed over the unpolluted Amazon Forest, despite years of intense observations at several sites (Andreae et al., 2015; Rizzo et al., 2013, 2018; Wimmer et al., 2018; see also section 4.4). This is most likely due to the very low concentrations of SO_2 in the unpolluted tropical boundary layer, which do not yield enough H_2SO_4 vapor concentrations to enable particle nucleation (Andreae et al., 1990; Ekman et al., 2008).

Instead, a likely source of the aerosol particles in the tropical boundary layer appears to be nucleation and initial growth of particles in the upper troposphere (UT) above ca. 8 km, which are transported down into the planetary boundary layer (PBL) by downdrafts associated with convective storms (Wang et al., 2016). Extensive aircraft measurements over the Amazon Basin have shown extremely high concentrations of small (<80 nm diameter) particles in the altitude range between 8 and 15 km altitude, sometimes exceeding 60,000 cm^{-3} (Andreae et al., 2018). Based on their size and spatial distribution,

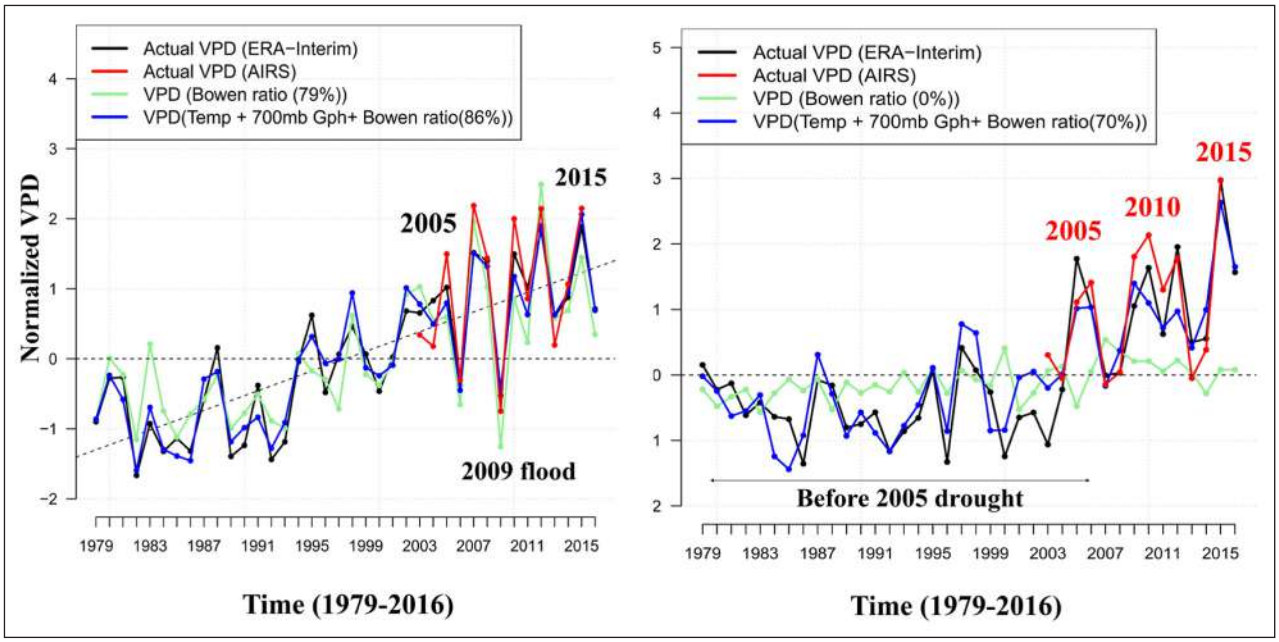

Figure 6.2.2 Vapor pressure deficit (VPD) in Southeast (left) and Northwest Amazonia (right) from 1979 to 2016 measured through various techniques. Adapted from Barkhordarian et al., 2019.

these particles must have formed relatively recently in the UT and grown to detectable sizes over periods of a few hours to a couple of days. Trajectory analyses indicate that the particles formed in the outflow plumes from deep convective storms, which had been stripped of pre-existing aerosol (CS) by precipitation scavenging but retained substantial concentrations of biogenic VOCs from the PBL. The combination of BVOC from convective transport, NO_x from lightning, and high solar actinic flux in the UT provides a highly reactive chemical environment, where highly oxidized organic molecules (HOMs) with very low volatilities can be produced (Zhao et al., 2020). Given the very low temperatures and low condensation sink in the UT, these molecules may be able to nucleate even without the involvement of H_2SO_4 vapors. As discussed in section 4.4 and ***Figure 4.4.1***, the production of NPF in the free troposphere could be a more general feature of forests. These findings have been integrated into a conceptual model of the aerosol life cycle over the tropical continents shown in ***Figure 6.2.3***, which has recently been confirmed by a numerical model (Zhu et al., 2019).

In this concept, the emission of BVOCs by the forest provides the source material both for the condensational growth of aerosol particles in the boundary layer and for the nucleation of new particles in the UT. Deep convection also plays a dual role, removing the pre-existing particles by precipitation scavenging and providing the source material for new particle formation in the UT, thus being a crucial part of creating and removing particles. This leads to a multitude of potential feedback, as the aerosol concentration affects the dynamics of the convective clouds, which determines the scavenging efficiency and the intensity of upward transport of aerosol precursors and the downward transport of newly formed particles from the UT into the PBL. Consequently, a simple relationship between BVOC emissions and CCN concentrations in the PBL has been proposed above for the boreal forest. It cannot be expected to apply to the tropical forest.

Williamson et al., 2019 recently observed a large source of CCN from new particle formation in the tropical FT as part of the NASA Atmospheric Tomography Mission (Atom). They observed intense NPF at high altitudes in tropical convective regions over both Pacific and Atlantic oceans. Together with the results of chemical-transport models, the findings indicate that NPF prevails at all longitudes as a global-scale band in the tropical upper troposphere, covering about 40 percent of Earth's surface (Williamson et al., 2019). This NPF in the tropical upper

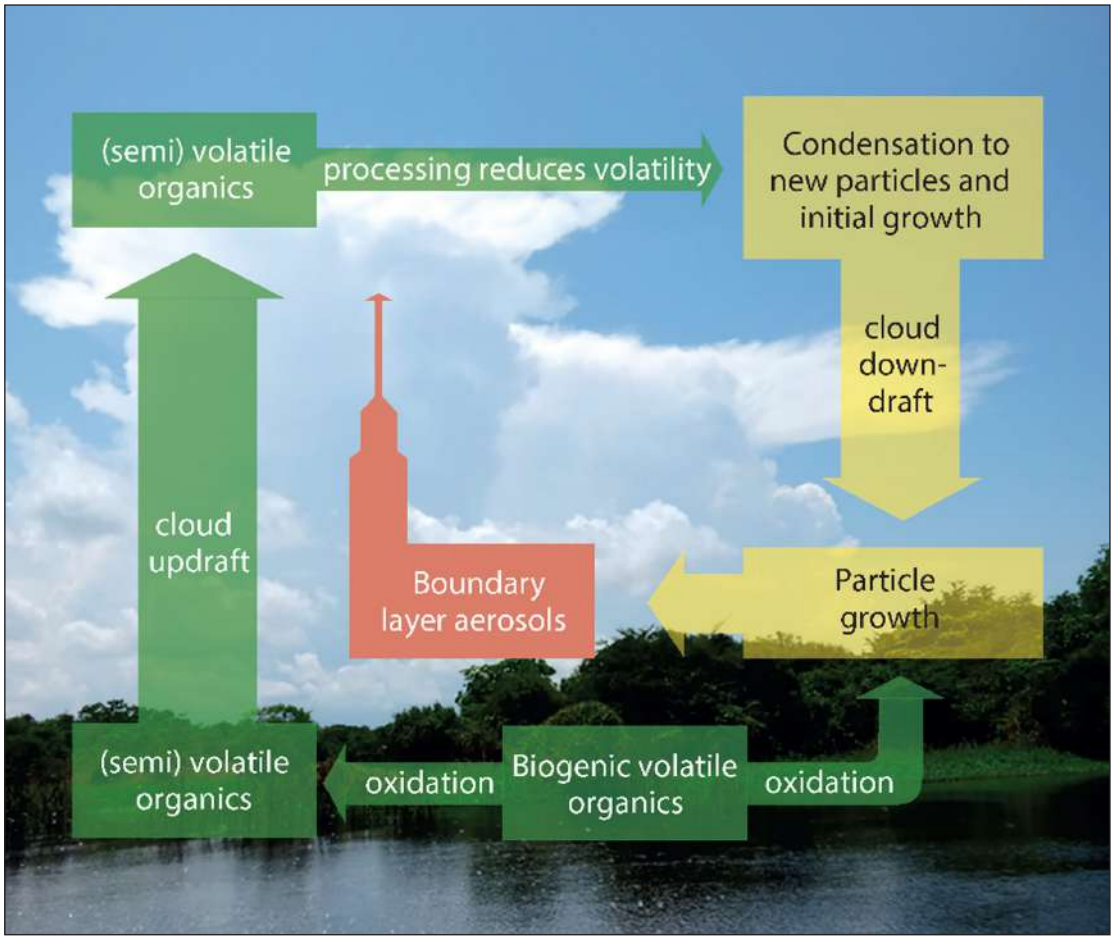

Figure 6.2.3 Conceptual model of the aerosol life cycle over the Amazon Basin relating VOC emissions from the forest with vertical cloud transport and production of new particles in the upper troposphere.

troposphere can be a globally significant source of CCN to the lower troposphere, where CCN can affect cloud properties. The production of CCN as new particles descend towards the surface is not adequately captured in global models, as discussed in section 4.4.

The biogeochemical feedback of natural aerosols changes is not limited to the Amazonian region since large-scale impacts could be expected (Mahowald et al., 2005). Scott et al., 2018b estimated feedbacks based on a combination of observations and model calculations. The extra-tropical aerosol-climate feedback is estimated to be –0.14 Wm^{-2} K^{-1} for landscape fire aerosol, greater than the –0.03 $Wm^{-2}K^{-1}$ estimated for biogenic SOA. They also estimated extratropical feedback associated with an indirect aerosol radiative feedback of -0.06 ± 0.03 $W m^{-2} K^{-1}$. It is important to point out that response in CCN concentrations changes at a certain supersaturation does not necessarily result in the same change in cloud droplet number concentration since the process is nonlinear (Sporre et al., 2020). These estimates of natural aerosol – climate feedbacks are applicable for the present day. They may differ in future climates due to uncertainties in the amount and type of vegetation, altering both BVOC and fire emissions.

Anthropogenic pollution from vegetation fires and fossil fuels emissions results in dramatic changes in the atmospheric environment over the tropical forest. Aerosol concentrations can increase tenfold or more, and the addition of NO_x and VOCs from combustion changes the atmospheric oxidation pathways and self-cleansing mechanisms (Artaxo et al., 2002, 2013; Roberts et al., 2003; Talbot et al., 1988; Andreae et al., 2002, 2015; Pöhlker et al., 2018 Martin et al., 2010; Trebs et al., 2012; Kuhn et al., 2010). The most apparent result of the transformation of photochemical pathways as a result of pollution is an increase in ozone concentrations during the burning season, which is observed both in the Amazon and the Congo Forest (Kirchhoff et al., 1990; Bela et al., 2015; Rummel et al., 2007; Andreae et al., 1992; Cros et al., 1988; Andreae et al., 2002, 2015). Ozone is known to damage plants, reducing primary productivity and crop yields (Ashmore et al., 2005; Fishman et al., 2010; Tai et al., 2014)), and consequently diminishing the terrestrial carbon sink (Sitch et al., 2007; Pacifico et al., 2015). Like elevated CO_2, higher ozone levels lead to stomatal closure, which affects evapotranspiration. As a result, the increased tropospheric ozone concentrations affect the climate both through the direct radiate effect by ozone and via the indirect forcing through its impact on the land-carbon and water cycles.

As discussed above, for the boreal forest, increasing aerosol levels over the tropical forest, especially from biomass burning, cause a decrease in photosynthetically active radiation (PAR) and an increase in the ratio of diffuse to direct solar radiation. This affects photosynthesis and GPP (Schafer et al., 2002, 2008; Artaxo et al., 2009; Artaxo et al., 2013; see also section 4.6). On the other hand, biomass smoke may reduce rainfall, which would reduce forest productivity (Liu et al., 2020, Chambers and Artaxo, 2017, Martin et al., 2016). In addition, the ozone produced by the smoke pollution would also have a negative impact on productivity (Pacifico et al., 2015). The aerosol-driven increase in cloud optical thickness can also cause a reduction in GPP (see section 6.1), counteracting the clear-sky positive aerosol effect on GPP.

As discussed in section 5, aerosol concentrations can profoundly affect cloud and precipitation properties in the tropics. Changes in the atmospheric aerosol burden can indirectly affect the forest biota by changing rainfall distribution and characteristics. Regional or seasonal reduction in rainfall can cause or aggravate droughts, which impact carbon uptake by the forest, the allocation of carbon to different components of the vegetation, and tree mortality (Doughty et al., 2015a, 2015b; Yang et al., 2018). High CCN concentrations have also been shown to increase storm intensity, resulting in higher updraft and downdraft velocities, increased hail, and more frequent lightning (Andreae et al., 2004; Rosenfeld et al., 2006, 2008, 2011, 2014; Williams and Satori, 2004; Machado et al., 2018; Wang et al., 2018). More intense storms can dramatically affect the forest ecosystem: Hail can cause extensive tree damage, and lightning is a frequent source of forest fires. While lightning would not normally be expected to cause fires in moist tropical forests, it may ignite tropical forests stressed by drought, either due to climate change or during El Niño events. Under these conditions, fires can cause high levels of tree mortality in tropical forests (Silva et al., 2018), which can ultimately induce a tipping point, where the forest ecosystem irreversibly transitions into savanna vegetation (Nepstad et al., 2008; Cochrane et al., 1999; Barlow and Peres, 2008). Severe downdrafts have been implicated as a major cause of tree mortality in Amazonia by creating large areas of downed trees, sometimes involving several thousand trees on more than 10 ha (Chambers et al., 2013). This has been proposed to be a major mechanism of ecosystem disturbance and succession in Amazonia, with large implications for the forest carbon budget (Chambers et al., 2013). If the changing aerosol burden in Amazonia affects the intensity of downdrafts from convective storms, this effect could provide a further feedback mechanism.

Land use and climate change affect how fires develop. There are three broad types of fire in the Amazon (***Figure 6.2.4***). There are deforestation fires, fires in areas that have been previously cleared, and fires that invade standing forests, either for the first time when flames are mostly restricted to the understorey or repeated events, resulting in more intense fires. Different types of fires have different drivers, as illustrated in the conceptual framework for fire feedback in Amazonia showed in

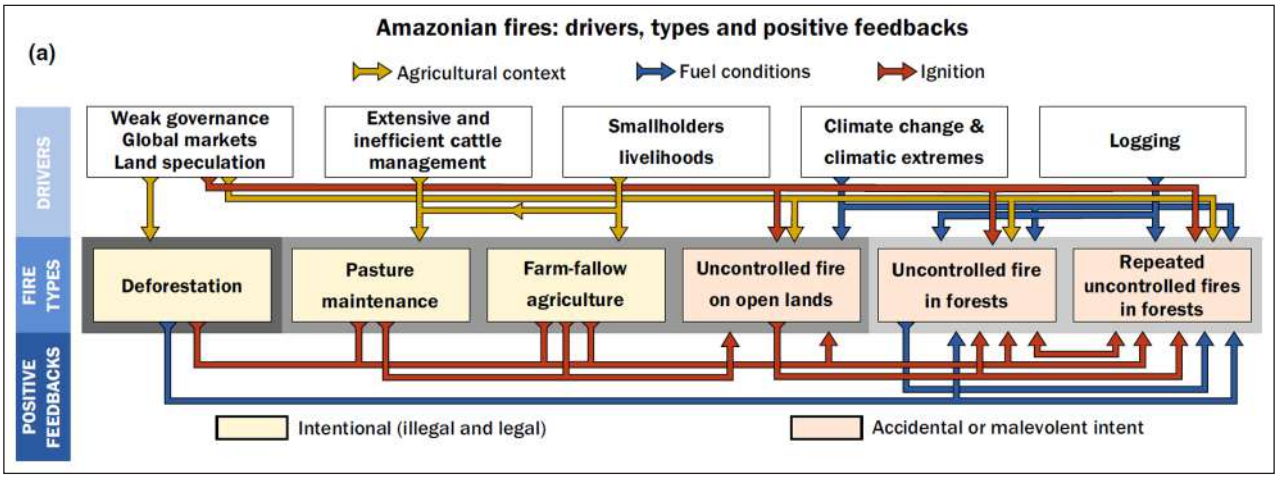

Figure 6.2.4 Conceptual framework for fire feedback in Amazonia, with the different fire types associated with the different ecosystem and human-induced drivers (Barlow et al., 2019).

Figure 6.2.4, with weak governance leading to more deforestation fires. Climate change makes forests hotter and drier, thus more likely to sustain large uncontrolled fires (Brando et al., 2019).

It is important to discuss the possibility of a tropical forest "tipping point" where the forests could not sustain a net carbon accumulation anymore and start losing carbon to the atmosphere (Lovejoy and Nobre 2018, Steffen et al., 2015, 2018, Gatti et al., 2021). Tropical ecosystems are undergoing unprecedented degradation rates from deforestation, fire, and drought disturbances and are more exposed to climate extremes (Bathiany et al., 2018). The collective effects of these disturbances threaten to shift large portions of tropical ecosystems such as Amazon forests into the savanna-like structure via tree loss, functional changes, and the emergence of fire (a process called savannization) (Stark et al., 2020). Changes from forest states to a more open savanna-like structure can affect local microclimates, surface energy fluxes, and biosphere-atmosphere interactions. Where might the tipping point be for deforestation-generated degradation of the hydrological cycle? The work of Sampaio et al., 2007 indicated that at about 40% of deforestation in Amazonia (in 2021, the deforested area is at about 19%), central, southern, and eastern Amazonia would experience diminished rainfall and a lengthier dry season, predicting a shift to savanna vegetation to the east. Sullivan et al., 2020 estimated that at a canopy temperature of 32.2°C tropical forests could start to lose carbon to the atmosphere. Reducing precipitation and increased temperature is possibly already making parts of eastern Amazonia a carbon source (Gatti et al., 2021) due to forest degradation and impacts of deforestation on regional precipitation. More research is needed to deal with the critical question of where a tropical forest tipping point could be. Tropical forests are sensitive to climate extremes that are increasing rapidly (IPCC, 2021). As discussed in sections 4.2 and 6.2, the large amount of carbon stored in tropical forests could partially go to the atmosphere, enhancing the greenhouse effect. This is certainly a scenario we would like to avoid.

Recent data document an increase in tree mortality due to extreme drought events makes the ecosystem carbon-neutral, instead of a significant carbon sink 15–20 years ago. Another factor limiting carbon sequestration is high temperatures. Such photosystems could be affected (Aleixo et al., 2019; Sastry and Barua 2017; Gloor, 2019). However, other approaches show different results, as Smith et al., 2020 show consistent, negative sensitivity of gross ecosystem productivity (GEP) to vapor pressure deficit (VPD) but little direct response to temperature. Importantly, in the mesocosm at low VPD, GEP persisted up to 38°C, a temperature exceeding projection for tropical forests in 2100 (IPCC 2013). If elevated CO_2 mitigates VPD-induced stomatal limitation through enhanced water-use efficiency as hypothesized, tropical forest photosynthesis may have a margin of resilience to future warming. In recent work, Staal et al., 2020 explores the hysteresis of tropical forests in the 21st century and showed that forest-rainfall feedback expands the geographic range of possible forest distributions, especially in the Amazon. The Amazon Forest could partially recover from complete deforestation. Still, it may lose that resilience later this century, while the Congo Forest currently lacks resilience but is predicted to gain it under climate change (Staal et al., 2020).

7. CONCLUSIONS AND PERSPECTIVES

From the extensive analysis and discussions above, we will in the following extract the most important conclusions and give some perspective on the results. It is possible to conclude that tropical and boreal forests are critical components of the global climate system These ecosystems are rapidly changing as a result of climate change and human activities, with important

climate feedbacks. This review shows that the interaction between these critical ecosystems and the atmosphere affects the atmospheric composition, the global carbon balance, and the hydrological cycle, which further impact cloud formation, precipitation, radiation balance, and climate. It also shows that the future carbon and water cycles depend strongly on how these forest ecosystems develop. The quantitative knowledge of feedbacks is critical to quantify the impacts of the anthropogenic and climatic forcing on these forest ecosystems. The proposed large-scale reforestation and afforestation success will depend on how they are implemented.

Long-term holistic and integrated observations of the critical parameters in the major biogeochemical cycles, i.e., water, energy, carbon, and trace components, are unfortunately too sparse. There are only three sites in the global forests that can present such critical data, ATTO in central Amazonia, SMEAR II at Hyytiälä in southern Finland, and ZOTTO in central Siberia. Many other sites measure some critical parameters but most often in an uncoordinated way and not on a long-term basis. Very few continental areas are so remote that the anthropogenic influence does not seriously affect essential aspects of the atmospheric composition and properties, at least in some seasons. In this review, ATTO and ZOTTO sites are considered representative of undisturbed tropical and boreal forests. Still, anthropogenic pollution occasionally affects both sites, as discussed in several sections in this review. This points towards two fundamental aspects. Firstly, the fact that possibly no pristine forest areas are left on Earth. Even though humans may not directly touch the forest, they are affected by long-range polluted air masses, and a global anthropogenically perturbed climate, altering our possibility to study an undisturbed interaction between the natural forest and the atmosphere. The other aspect is that long-term data are only available from two remote sites, one in the tropics and one in the boreal continental region. Given the expected variability in biodiversity and different air masses reaching the whole tropical and boreal forests, it is important to have a much larger number of observational sites, similar to what we have for basic meteorological operational observations.

The links through processes and feedback loops between the ecosystems and the atmosphere and its functions, shown in this review, make it clear that relevant parameters in both systems must be observed simultaneously over a long time. Without more observation sites and a comprehensive observation system, it is challenging to understand how a nonlinear, complex, and strongly variable ecosystem will react to a changing climate and all anthropogenic land-use change drivers. In a changing climate, biodiversity will also change, and species respond differently to different stress. CO_2 uptake, evapotranspiration rates, VOC emissions, PBAP emissions, drought tolerance, sensitivity to temperature, and radiation are just a few of the critical paraments that will be affected by a changing climate and biodiversity.

In terms of meteorology, tropical and boreal forests are very different. They differ strongly in temperature, solar radiation, precipitation, evapotranspiration, albedo, cloud structure and cover, convection, etc. In Amazonia and most tropical forests, meteorology is influenced by changes in the ITCZ position. In Amazonia, where the southern part is influenced by the Southern Atlantic and the north by the Tropical Atlantic, giving dry and wet seasons with strongly varying convective activity manifested in the variation in precipitation providing wet and dry seasons. On the other hand, the boreal forest is controlled by the amount of radiation inflow, which changes temperature, giving winter and summertime. In the continental boreal forest, there is a very large temperature seasonality with strong convection during summer and stratified air during winter when the frozen ground and the biosphere on hold give a low water transport to the atmosphere producing low precipitation. There are regions with a substantial influence of frontal activity, in particular in winter. Meteorology in both systems is influenced by biophysical processes modifying fundamental climate drivers, e.g., water vapor flux, radiation, and biogenic sources of CCN. These drivers are affected by natural variations, land-use changes, and anthropogenic influences on atmospheric composition. The precipitation of both forest systems is influenced by emissions of PBAP and BVOC compounds. Climate change is now affecting both systems by changing temperature, precipitation, and circulation patterns. For the tropics, the general circulation is most likely manifested by a northward moving ITCZ affecting the hydrological circulation (see chapter 6.2). While the boreal is zone is moving north due to changing climate.

The essential difference between the tropical and the boreal meteorological systems is water availability, giving much more precipitation in the tropics. The biosphere processes the water, so in principle, the amount of precipitation downwind of the ecosystem is regulated by the water vapor processing by the biosphere, leading to water transport to other regions. In the case of Amazonia, the tropical Atlantic is the primary source of water vapor. The increase in sea surface temperature in the tropical Atlantic has probably increased the precipitation but followed by a decreased evapotranspiration observed through a change of carbon uptake to zero and an observed long-term increase of vapor pressure deficit over the Amazonas implicate a significant change in the forest – atmosphere interaction in the Amazonas and possibly in other tropical forests (see chapter 6.2).

During the winter in the boreal zone, the ground is frozen, the biosphere is put on hold, and the water transport to the atmosphere is very low. The atmosphere

over the continental part of the boreal region is strongly stratified, with stratus clouds yielding comparably low amounts of precipitation. Shallow clouds dominate the tropical dry season as the strong convection moves north with the ITCZ. There is still convective activity but very much less than during the wet season. The water processed by the forest is still very important, and CCN availability will affect both systems but differently.

The cloud formation, structure, and development are different due to the different water vapor and CCN amounts and meteorological conditions that promote convection, such as available Convective Available Potential Energy (CAPE). Besides the different natural circumstances, clouds are consequently transformed by land-use change, aerosols from biomass burning emissions, long-range transport pollution, and all these factors are geographically inhomogeneous and cause a variation within both the tropical and boreal forests.

Forest emissions, formation, and deposition of trace gases and aerosols are key in regulating their atmospheric concentrations. Concentrations of trace gases in boreal and tropical forest regions are controlled by biogenic forest sources, atmospheric gas and liquid phase chemistry, meteorology, forest fires, and long-range transport. NOx and SO2 concentrations are very low in tropical forests, but they are important in controlling the SOA production pathway and particle formation even at low concentrations. CO_2 emissions and uptake are governed by the photosynthesis and respiration processes and canopy interactions. Emissions of CH_4 are significant in flooded natural areas in tropical forests and released by permafrost melting in boreal forests. CO is controlled by long-range transport of forest fire emissions as well as pollution. Trends for CO_2 and CH_4 follow the global values. The VOC emissions also regulate the atmospheric oxidation capacity. OH reactivity is controlled mainly through VOC emissions and reaction pathways and is key to the atmospheric lifetime of many species. Ozone increases in concentration and ozone damage can significantly reduce the CO_2 uptake.

Biogenic emissions (BVOC) dominate global VOC emissions and are highly sensitive to insect herbivory, droughts, forestry operations, weather extremes, land use, and climate change. Our limited understanding of the processes controlling the specific responses makes it difficult to compare and contrast tropical and boreal ecosystems quantitatively. However, the BVOC emissions in the boreal and the tropical forest seem dominated by monoterpenes and isoprene, respectively. A multitude of other unknown BVOCs is also emitted by vegetation. BVOC emissions from forests tend to be dominated by foliar emissions. The role of ecosystem disturbances in determining emission variations should be a priority for future research efforts. Despite large uncertainties, existing emission models have been shown to give reasonably good estimates of the emissions of the major compounds. Still, a large number of unidentified VOCs are emitted.

Organic primary and secondary aerosols dominate the aerosol composition, with 70 to 85% of PM_1 mass for tropical and boreal forests. In Amazonia, sulfates, nitrates, and BC show very low concentrations, while background continental boreal sites have 2–3 times higher SO2, sulfate, nitrates, and BC concentrations. Amazonian aerosols are mostly biogenic in terms of sources, through direct primary aerosol particle emissions and SOA produced from forest gaseous precursors. The boreal forest shows a similar composition because a secondary aerosol dominated by organics characterizes it. However, it originates from monoterpene-driven chemistry compared to an isoprene-driven one in the tropical forest. In the tropical dry season and boreal late spring and summer, biomass burning dominates the aerosol composition, with higher OC and BC. Biomass burning emissions significantly impact aerosol composition and concentrations in tropical and boreal forests, increasing aerosol number concentrations by 5 to 12 in Amazonia and 3 to 6 at the ZOTTO tower. During the Amazonian wet season and most of the year in the boreal zone, the aerosol size distributions show evidence of cloud processes that indicate the cloud processing, i.e., the cloud liquid phase chemistry on the atmospheric composition. However, anthropogenic pollution influences the boreal forest atmosphere, especially during winter. Anthropogenic emissions in Amazonia have been shown to affect atmospheric chemistry, producing strongly increased SOA concentrations. However, dust, African biomass burning, and volcanic emissions, as well as Atlantic marine aerosols, affect the Amazon. This illustrates that long-distance transported aerosols, natural and anthropogenic, are significantly affecting atmospheric and ecosystem processes in pristine regions.

The aerosol optical properties significantly influence the climate effects and are strongly dependent on biomass burning. The Amazonian wet-season averages of both scattering and absorption coefficients are close to the boreal background clean-season averages. The Amazonian dry-season averages show strongly absorbing aerosols due to large-scale biomass burning emissions and are at the same level as the winter-season averages at all boreal sites. AERONET monitoring sites with long time series in Canadian and Siberia boreal forests and Amazonia show clear similarities in the high values of AOD. Also, they indicate that biomass burning is the primary driving force for the peak concentrations. The dry-season AOD over Amazonia is recently increasing after a drastic drop during the period 2003–2013. However, it should be noted that the AOD peak values over Canada and Russia have also increased during the last 10 years, reaching a similar magnitude as present Amazon measurements. The boreal fires are probably

dominated by natural fires, while the fires in Amazon are anthropogenic due to human driven deforestation and land clearing. The biomass burning emissions also control most of the aerosol radiative effect changes over these forest ecosystems. Biomass burning season intensity in the tropics varies with large-scale meteorological forcing such as ENSO, while it is closely related to high-temperature draught periods in the boreal. Extensive biomass burning has an unexpected effect on the radiation balance. Observational and modeling studies showed that net ecosystem exchange could be enhanced by 30% in tropical forests and 10% in boreal forests at high observed values of AOD due to the increased flux of diffuse radiation.

Primary bioaerosol particle (PBAP) emissions, composition, and properties depend on the seasonal characteristics of tropical and boreal forests. Still, similarities can also be found, e.g., that PBAP dominates the coarse mode mass concentrations in both forest systems, and the composition is mostly organic. Boreal forests show pronounced seasonal PBAP cycles, whereas, in tropical forests, only moderate seasonal changes in total aerosol number concentration were measured. They are low in numbers but can act as efficient CCN and INP, directly influencing cloud formation and development. In terms of diurnal cycles, tropical and boreal forest systems display similar distinctive patterns, with the highest PBAP values during the night. Important to note that PBAP are often active as INP. The influence of the IN on precipitation is unknown and is potentially an important factor in future climate change.

The aerosol size distribution in the tropical and the boreal forests are regulated by similar processes, but the different seasonality and meteorological conditions make the aerosol size distribution different in both ecosystems. New particle formation (NPF) and subsequent condensational growth are important sources of CCN in both systems. NPF events in the boundary layer are common in some boreal sites, such as the SMEAR II at Hyytiälä in Finland, and have been observed in all continents and urban to remote locations. However, the actual formation mechanism for the originating stable particles, in the size range 2–3 nm, that grow further through condensation is not well known. Even though NPF in the boundary layer is found in remote places like the Arctic and Antarctica, it is almost absent in Amazonia and at the ZOTTO site in central Siberia. It is unclear why NPF is not observed at ZOTTO under relatively similar conditions as at SMEAR II. Likely, low SO_2 concentrations at the remote ZOTTO site, combined with elevated levels of aged pollution aerosol from long-range transport acting as CS, impede NPF in remote Siberia. Air pollutant concentrations are considerably higher in Finland, but the NPF occurs almost only in Arctic air masses arriving from the north, i.e., clean marine air. ATTO and ZOTTO show remarkable similarities in a low number of NPF in the boundary layer, but also signs of cloud processing are evident at both sites, with a pronounced Hoppel minimum in the size distribution. In Amazonia, strong new particle formation was observed in the upper troposphere and provides an interesting interaction between forest emissions, convection, cloud transport and processing, and particle formation and aging at high altitudes. These particles are organic, and after aging, they may be brought back to the ground by downdrafts and replenish the aerosols and CCN concentrations in the lower troposphere. Nature has developed very complex mechanisms to sustain the aerosol population in tropical forests, which are not fully understood.

Hygroscopic properties affect the particle size, optical properties, and the ability to act as CCN. Typically, inorganic compounds are strongly hygroscopic, while organics are less hygroscopic. The mainly isoprene-driven Amazonian organic aerosol is slightly less hygroscopic than the boreal monoterpene-driven SOA. Even such minor differences can have a significant effect on the radiation balance. However, the primary influence on hygroscopicity is due to inorganic compounds, such as sulfates, which are often anthropogenic, influencing forested areas within the range from significant source areas, e.g., the Eurasian boreal forest. A natural aging process that might affect the hygroscopic properties of the natural aerosol in both the tropical and the boreal is the processing by clouds and subsequent new particle formation and growth in the subsiding air, providing an aged boundary layer aerosol.

Cloud formation and development, including the formation of rain, are a highly complex chain of processes. However, current global and regional climate models do not typically include explicit convective cloud microphysics and hence lack the ability to represent the majority of the effects proposed to be of importance for the impact of forest aerosols on clouds and climate. However, the recent development of advanced aerosol-aware convection parameterizations and the increasing availability of (near) global cloud-resolving modeling will help close this gap in the medium to long term. Even though process-based observations on a limited number of clouds show a strong CCN effect on cloud development, e.g., cloud invigoration, it is not clear that the results from such studies are applicable to cloud-field, regional, or even global scales, for which moisture and energy budgets are of crucial importance. Such budgetary constraints may be the underlying mechanism of the concept of "buffering." As the net aerosol effective radiative forcing from aerosol-cloud interactions is negative, the net radiative effect of forest aerosol on the global radiation balance is likely to be negative but highly uncertain due to the above-mentioned limitations in global climate models used to quantify these effects. This once more brings forward aerosol-cloud interaction as a major issue in climate modeling uncertainties.

Aerosols, clouds, and precipitation properties are strongly coupled through a series of processes. However, the existence of a large number of confounding factors affecting the hydrological cycle makes it difficult to establish causality from purely observational studies. Due to sparse precipitation monitoring networks in tropical areas, it is difficult to observe any changes in precipitation patterns. Future work should employ large-domain and global Large Eddy Simulations/Cloud Resolving Models simulations with prognostic aerosols to facilitate comparison with observations. This approach could provide more robust assessments of the effect of forest aerosols on clouds, precipitation, and climate.

Boreal and tropical forests store large amounts of carbon and are critical in the global carbon cycle, being responsible for about 13% of global CO_2 emissions (mainly through tropical deforestation) and absorption of anthropogenic emissions of CO_2 (29%), thus having a significant effect on atmospheric CO_2 concentrations and the global climate. Until a few years ago, Amazonia was absorbing carbon at a rate of about 50 g C $m^{-2}a^{-1}$, primarily due to the CO_2 fertilization effect. Tropical forests make an approximately neutral contribution to the global carbon cycle, with intact and recovering forests taking in as much carbon as is released through deforestation and degradation.

Boreal forests are carbon sinks, absorbing about 80 g C $m^{-2}a^{-1}$, but the large spatial variability and rapid climate change make it difficult to estimate the large-scale boreal forest carbon budget. The CO_2, CH_4, and H_2O flux magnitudes are relatively smaller in boreal forests than in tropical forests. Given the distinguishing climatic and environmental characteristics in boreal and tropical regions, fluxes of boreal forests have a more substantial seasonal variability than tropical forests. Fewer tree species exist in boreal forests, which are typically nitrogen-limited, whereas tropical forests have a greater species diversity and are phosphorus-limited. It is essential to develop new and improved methods to assess forest carbon balance through 1) Forest inventory plots; 2) Atmospheric CO_2 inversions; 3) Satellite measurements; 4) Modelling approaches. Satellites can estimate forest area, carbon stocks using Lidar and passive microwave remote sensing, and GHG concentrations with good accuracy for CO_2.

Forest Net Ecosystem Exchange (NEE) is very sensitive to rainfall amounts, thus changes in the hydrological cycle affect the CO_2 exchange and, most likely other emissions, particles as gases, which are closely dependent on meteorological changes. Tropical forests are a major global source of N_2O due to their high rate of nitrogen turnover. Tropical soils emit N_2O and CH_4 and increases in global temperature can change these fluxes.

Tropical flooded areas, as well as boreal regions with shrinking permafrost, are significant sources of CH_4. Emissions of CO and O_3 precursors from biomass burning are vital in regulating oxidative processes in the atmosphere (Tuet et al., 2019). NO_x emissions from biomass burning and urban areas regulate the pathway of VOC oxidation. SO_2 is important to NPF even at very low concentrations.

A fundamental lesson from the last years of Earth System research is the understanding that ecosystem feedback processes are crucial for responding to anthropogenic perturbations in any biogeochemical cycle and thus for the climate system. As forests cover such a large part of the Earth, they greatly influence the climate systems. For example, they provide an important link in the hydrological cycle, CCN, and thermodynamic conditions for the cloud systems. This includes precipitation formation over large areas, also outside the actual forested regions. The feedback loops presented in this review are quite sensitive to the effects of disturbances in essential components, such as SO_2 and O_3 due to pollution, changing thermodynamic conditions due to land-use changes, changing large-scale circulation changes induced by emissions elsewhere, changing precipitation and temperature in the forests. In conclusion, the forest feedback loops form an intricate and complex tangle of process chains regulating the climate. Even though we do not fully see all connections, large-scale land-use changes or atmospheric composition changes can drastically affect biodiversity and climate and have large-scale effects on our society.

The tropics are rapidly changing due to human interventions. In addition to the effects of climate change in tropical regions, land-use change, and urbanization are rapidly increasing, generating strong impacts in the ecosystem processes. Climate change in the tropics is expected to increase temperatures and further alter precipitation patterns, as more frequent and intense droughts are combined with elevated temperatures that are already being observed. Such conditions can lead to increased tree mortality, reduced net primary productivity, and decreased trace gas emissions such as VOCs due to biomass reduction.

Climate change affects the boreal forest and the chemistry of its atmosphere through increasing CO_2 concentrations, higher temperatures, enhanced UV radiation, and changes in precipitation patterns (including drought), to name the most important factors. In general, BVOC emissions are expected to increase, which has important impacts on climate and atmospheric chemistry feedback, including OH reactivity. Given the important role BVOC emissions and their oxidation play in new particle formation and growth, it could modify the aerosol particle formation processes and cloud optical thickness. Due to the complex and non-linear interactions between weather, vegetation, and people, future fire severity and intensity are difficult to determine. Still, we can expect fire seasons to continue the lengthening trend (see section 4.5).

Terrestrial ecosystems are key in their role to sequester atmospheric CO_2, and the iNDC (intended National Determined Contribution) of several countries aims to reforest large areas. We emphasize that photosynthesis is still the main process to remove CO_2 from the atmosphere at the necessary scale. The IPCC 1.5 SR makes this clear and recognizes that large-scale reforestation and afforestation are essential to achieve the Paris Agreement goals. It is also important to emphasize that anthropogenic pollution is second to biomass burning emissions in boreal and tropical forests concerning aerosol optical depth. The drivers for biomass burning are, of course, different for boreal and tropical forests. The deforestation of tropical areas has been increasing over the last few years. Higher temperatures and an increase in climate extremes can only worsen this critical issue, together with public policies that favor deforestation. Considering the complexity, sensitivity, and possible climate tipping points in these ecosystems, it is of utmost importance that our remaining forests' anthropogenic use and change are based on careful management techniques based on the best scientific knowledge. This also calls for much more extensive observations of the forests and their biodiversity and the atmospheric composition and climate, which provide the conditions that can make our tropical and boreal forests sustainable. Recent work from Cooper et al., 2020 shows that regime shifts occur disproportionately faster in larger ecosystems, and regime shifts can abruptly affect hydrological, climatic, and terrestrial systems, leading to degraded ecosystems and impoverished societies. A thorough understanding of ecosystem-atmosphere interactions in these two critical biomes is crucial to improving our knowledge of the future ecosystem feedbacks under a changing climate.

A thorough understanding of ecosystem-atmosphere interactions in these two critical biomes is crucial to improve our knowledge about the future ecosystem feedbacks under a changing climate. Ecosystem feedback processes are essential for both boreal and tropical forests but very difficult to quantify. The complex relationship between GPP, BVOC, SOA, CCN, INP, clouds, radiation, temperature, and CO_2 show multiple pathways for boreal forests, and only some of these branches can be quantified. Feedback to increasing temperature and changes in the hydrological cycle must provide models with critical processes to obtain more reliable forecasts of how the climate and forests will develop. With climate change and deforestation pressures accelerating, the future of Amazonia becomes uncertain.

In the preceding paragraphs, we have shown that both boreal and tropical forests are vital components in the climate system, with numerous couplings with the cycles of water, energy, carbon, trace gases, and aerosols. Understanding how this system operates at present and projecting how it will respond to a global and regional change in the future will require research into these interactions and feedbacks, many of which are at present only hypothetical. Importantly, however, it will require integrating these processes and linkages into Earth System Models that can represent these complex interactions. Recent modeling studies with more sophisticated representations of the biological components have shown that changing community ecology plays a vital role in driving BVOC emissions (Wang et al., 2018). Due to land-use conversion, tropical and boreal forests worldwide are also changing significantly.

Several countries, e.g., Brazil, have commitments to reduce deforestation and reforest large areas to fulfill their Nationally Determined Contributions (NDC) under the Paris Agreement. In the case of Brazil, in addition to stopping illegal deforestation, the country is committed to reforesting 120 000 km^2 by 2025. Therefore, integration with socio-economic and political drivers changing the forest environment is essential.

This review finds solid arguments for the following statements.

- Forests are vital ecosystems that interact strongly with climate in a complex set of non-linear mechanisms. Forests are critical in regulating the global carbon cycle. Observations show that the carbon stock has decreased in the Amazonian forest because of the increase in tree mortality. Deforestation pressures are very strong in most tropics and are responsible for about 13% of global CO_2 emissions in 2018.
- The hydrological cycle is changing in the Amazon and most likely in all the tropical regions due to a climate-change-induced shift of the ITCZ position, causing changes in the precipitation patterns temporally and spatially. There are first indications that ecosystem responses further strengthen the change in hydrological cycles by decreased precipitation in the outflow regions of the Amazon. The boreal zone shows rapidly increasing temperatures and more extended drought periods, severely increasing the risk for forest fires.
- Observations and modeling studies show that the carbon cycle is changing in the Amazon, with the ecosystem going from a carbon sink to carbon neutrality. This is most likely due to the climate change-induced hydrological cycle changes and subsequent ecosystem change, with increased tree mortality. This strengthens the concern that the Amazon Forest could be on a transition path to a savannah ecosystem, but how far away we are from a possible tipping point is unknown. The tropical region could have been turned into a potentially global CO_2 source by biomass burning and deforestation. Increasing amounts of boreal forest

fires have been observed, decreasing the total carbon sink in the boreal zone.

- The ongoing ecosystem changes are most likely affecting atmospheric chemistry, changing both trace gas and aerosol content by changes in the emissions of primary particles and BVOC. The BVOC emissions are the major precursor of the fine particles (SOA) and control the CCN population over forested areas, with possible strong effects on cloud formation and development. However, no consensus has been reached whether these aerosol-cloud interaction processes will have any large-scale effects, which energy and moisture budget limitations may buffer. The interactions between the forest, clouds, and convection have played an essential role in new particle formation in Amazonia, thus providing new tropospheric CCN.
- Biomass burning dominates the atmospheric composition during the dry and warm periods in both boreal and tropical forests. This can be observed through increased aerosol concentrations in both the continental boreal and tropical forests. In the continental boreal, most likely due to changing natural conditions, enhanced by climate change. In the tropics, due to increased anthropogenic land clearing for agriculture and forestry. This increases carbon emissions and provides significant changes in the hydrological cycle through aerosol-cloud effects. It thus enhances climate change on all scales.
- Several important feedback mechanisms between forest functioning and climate can be identified in boreal and tropical forests. Some of these are positive feedbacks that could boost climate change. Quantification of these feedbacks is still a challenge due to the complex nonlinear interactions. The positive feedback, such as reducing carbon uptake by the increase in temperature, is critical in tropical forests. It is essential to work on better quantification of possible tipping points.
- Tropical forest degradation is being responsible for enhanced CO_2 emissions. This is transforming the tropical forests from a carbon sink a few years ago to a carbon source. An increase in temperatures, climate extremes, and reduced precipitation are stressing the tropical forests. This is also happening in Northern Amazonian pristine areas but is stronger in areas close to deforested regions in the South-eastern Amazon region. As global warming progresses, this tropical forest degradation will increase, releasing more carbon into the atmosphere.
- The observations yielding these harsh and essential results are unfortunately limited to few observational sites. Still, fortuitously we have ten or more years of records for a few critical sites, in addition to remote sensing observations. More observations following all the seasonal cycles of hydrological, carbon, and other biogeochemical cycles, as well as biodiversity and other ecosystem parameters, in a holistic manner, will substantially increase our ability to establish useful and reliable models for projections into the future. This will provide society with a chance not to go blindly into an unknown world of possibly degrading global agriculture and forestry and of disappearing forests and natural areas, which are critical in maintaining the essential ecosystem services.

ACKNOWLEDGEMENTS

We would like to thank the Department of Environmental Sciences, University of Stockholm, for supporting a guest visit for PA and HC H travel to Brazil that allowed this review to be written. We would like to thank the Large-Scale Biosphere-Atmosphere Program (LBA), coordinated by the National Institute for Amazonian Research (INPA), and all partner institutions and contributors for the use and availability of data, logistical support, and infrastructure during field activities at several sites in Amazonia, including the Amazon Tall Tower Observatory (ATTO). M. O. Andreae, U. Pöschl, C. Pöhlker, M. Pöhlker, M. Sörgel, F. Ditas, B. A. Holanda, V. Després, B. Weber, and E. Mikhailov acknowledge substantial long-term funding and support by the Max Planck Society (MPG) for ATTO, ZOTTO and related campaigns and investigations (ACRIDICON-CHUVA, AMAZE-08). P. Artaxo acknowledges funding from FAPESP project 2017/17047-0, INCT-Climate Change Project Phase 2 (Grants FAPESP 2014/50848-9, CNPq 465501/2014-1, CAPES/FAPS Nº 16/2014), and RCGI Research Center for Greenhouse Gas Innovation, FAPESP project 2020/15230-5, and Funding from Shell. J. Kesselmeier thanks the Max Planck Society for continuous support and acknowledges the funding of the ATTO project by the German Federal Ministry of Education and Research (BMBF contract 01LB1001A). E.G.A. was funded by a BMBF scholarship. F. Bender acknowledges funding from the Swedish Research Council (project 2018-04274).

J. Rinne acknowledges funding from Swedish Research Council for Sustainable Development (2017-01474). Marco A. M. Franco acknowledges a scholarship from CNPq, project 169842/2017-7, for supporting his Ph.D. studies at the University of São Paulo, São Paulo, Brazil, and CAPES, project 88887.368025/2019-00, for supporting a sandwich doctorate at Max-Planck-Institut für Chemie, Mainz, Germany. L. A. Machado acknowledges a grant from FAPESP 2015/14497-0. The data described in Sect. 3 were obtained within the Russian Science Foundation (grant agreement No. 18-17-00076). Barbosa acknowledges the support of FAPESP grants 2016/18866-2 and 2018/16608-1, and grant 308682/20173 from Conselho Nacional de Desenvolvimento Científico e Tecnológico (CNPq). J. Kesselmeier thanks the Max

Planck Society for continuous support and acknowledges the funding of the ATTO project by the German Federal Ministry of Education and Research (BMBF contract 01LB1001A). E.G.A. thanks BMBF grants. BW appreciates the support of the Max Planck Society and the University of Graz and would like to thank Paul Crutzen for awarding her a Nobel Laureate fellowship. GM would like to thank the UK Natural Environment Research Council (NERC) for funding Amazonian measurements under the Brazil–UK Network for Investigation of Amazonian Atmospheric Composition and Impacts on Climate project (NE/I030178/1) and Bornean measurements under the Oxidant and Photochemical Particle Processes above a Southeast Asian tropical rainforest (OP3; NE/0021171/1) and the Aerosol Coupling in the Earth System (ACES; NE/E011217/1) projects. P. Zieger acknowledges funding from the Swedish Research Council (project 2018-05045). James N. Smith acknowledges CAPES/CNPq through the Ciência Sem Fronteiras (Brazilian Science Mobility Program) grant. P. Stier acknowledges funding from the European Research Council (ERC) project RECAP and the FORCeS project under the European Union's Horizon 2020 research and innovation program with grant agreements No 724602 and 821205, respectively, the UK NERC A-CURE project (NE/P013406/1) and from the Alexander von Humboldt Foundation.

COMPETING INTERESTS

The authors have no competing interests to declare.

AUTHOR AFFILIATIONS

Paulo Artaxo *orcid.org/0000-0001-7754-3036*
Institute of Physics, University of São Paulo, Rua do Matão 1371, CEP 05508-090, São Paulo, Brazil; RCGI Research Center for Greenhouse Gas Innovation, POLI-USP, São Paulo, Brazil

Hans-Christen Hansson *orcid.org/0000-0001-7794-2889*
Dep of Environmental Science & Bolin Centre for Climate Research, Stockholm University, Stockholm, Sweden

Meinrat O. Andreae *orcid.org/0000-0003-1968-7925*
Max Planck Institute for Chemistry, Mainz, Germany; Scripps Institution of Oceanography, University of California San Diego, La Jolla, USA

Jaana Bäck *orcid.org/0000-0002-6107-667X*
Institute for Atmospheric and Earth System Research INAR / Forest Sciences, Faculty of Agriculture and Forestry, University of Helsinki, Finland

Eliane Gomes Alves *orcid.org/0000-0001-5245-1952*
Department of Biogeochemical Processes, Max Planck Institute for Biogeochemistry, Jena, Germany

Henrique M. J. Barbosa *orcid.org/0000-0002-4027-1855*
Institute of Physics, University of São Paulo, Rua do Matão 1371, CEP 05508-090, São Paulo, Brazil

Frida Bender *orcid.org/0000-0003-4867-4007*
Department of Meteorology and Bolin Centre for Climate Research, Stockholm University, Stockholm, Sweden

Efstratios Bourtsoukidis *orcid.org/0000-0001-5578-9414*
Max Planck Institute for Chemistry, Mainz, Germany; Climate and Atmosphere Research Center (CARE-C), The Cyprus Institute, 20 Konstantinou Kavafi Street, 2121, Nicosia, Cyprus

Samara Carbone *orcid.org/0000-0002-3397-1183*
Universidade de Uberlândia, Uberlândia, Brazil

Jinshu Chi *orcid.org/0000-0001-5688-8895*
Department of Forest Ecology and Management, Swedish University of Agricultural Sciences, Umeå, Sweden

Stefano Decesari *orcid.org/0000-0001-6486-3786*
Institute of Atmospheric Sciences and Climate, CNR, Bologna, Italy

Viviane R. Després *orcid.org/0000-0002-5590-984X*
Institute of Molecular Physiology, Johannes Gutenberg University, Mainz, Germany

Florian Ditas *orcid.org/0000-0003-3824-9373*
Department of Multiphase Chemistry, Max Planck Institute for Chemistry, Mainz, Germany

Ekaterina Ezhova *orcid.org/0000-0003-2770-9143*
Institute for Atmospheric and Earth System Research/Physics, Faculty of Science, University of Helsinki, Helsinki, Finland

Sandro Fuzzi *orcid.org/0000-0002-5275-2381*
Institute of Atmospheric Sciences and Climate, CNR, Bologna, Italy

Niles J. Hasselquist *orcid.org/0000-0003-2777-0163*
Department of Forest Ecology and Management, Swedish University of Agricultural Sciences, Umeå, Sweden

Jost Heintzenberg *orcid.org/0000-0002-6445-0030*
Leibniz-Institute for Tropospheric Research, Leipzig, Germany

Bruna A. Holanda *orcid.org/0000-0003-3444-0912*
Department of Multiphase Chemistry, Max Planck Institute for Chemistry, Mainz, Germany

Alex Guenther *orcid.org/0000-0001-6283-8288*
University of California, Irvine, CA, USA

Hannele Hakola *orcid.org/0000-0002-9711-9053*
Finnish Meteorological Institute, Climate Research Programme, Helsinki, Finland

Liine Heikkinen *orcid.org/0000-0001-7837-967X*
Institute for Atmospheric and Earth System Research/Physics, Faculty of Science, University of Helsinki, Helsinki, Finland

Veli-Matti Kerminen *orcid.org/0000-0002-0706-669X*
Institute for Atmospheric and Earth System Research/Physics, Faculty of Science, University of Helsinki, Helsinki, Finland

Jenni Kontkanen *orcid.org/0000-0002-5373-3537*
Institute for Atmospheric and Earth System Research/Physics, Faculty of Science, University of Helsinki, Helsinki, Finland

Radovan Krejci *orcid.org/0000-0002-9384-9702*
Dep of Environmental Science & Bolin Centre for Climate Research, Stockholm University, Stockholm, Sweden

Markku Kulmala *orcid.org/0000-0003-3464-7825*
Institute for Atmospheric and Earth System Research/Physics, Faculty of Science, University of Helsinki, Helsinki, Finland

Jost V. Lavric *orcid.org/0000-0003-3610-9078*
Department of Biogeochemical Processes, Max Planck Institute for Biogeochemistry, Jena, Germany

Gerrit de Leeuw *orcid.org/0000-0002-1649-6333*
KNMI (Royal Netherlands Meteorological Institute), De Bilt, The Netherlands

Katrianne Lehtipalo *orcid.org/0000-0002-1660-2706*
Institute for Atmospheric and Earth System Research/Physics, Faculty of Science, University of Helsinki, Helsinki, Finland;

Finnish Meteorological Institute, Climate Research Programme, Helsinki, Finland

Luiz Augusto T. Machado *orcid.org/0000-0002-8243-1706*
Institute of Physics, University of São Paulo, Rua do Matão 1371, CEP 05508-090, São Paulo, Brazil; Department of Biogeochemical Processes, Max Planck Institute for Biogeochemistry, Jena, Germany; RCGI Research Center for Greenhouse Gas Innovation, POLI-USP, São Paulo, Brazil

Gordon McFiggans *orcid.org/0000-0002-3423-7896*
Atmospheric and Environmental Sciences, University of Manchester, Manchester, UK

Marco Aurelio M. Franco *orcid.org/0000-0002-2279-7722*
Institute of Physics, University of São Paulo, Rua do Matão 1371, CEP 05508-090, São Paulo, Brazil; RCGI Research Center for Greenhouse Gas Innovation, POLI-USP, São Paulo, Brazil

Bruno Backes Meller *orcid.org/0000-0002-3511-3940*
Institute of Physics, University of São Paulo, Rua do Matão 1371, CEP 05508-090, São Paulo, Brazil

Fernando G. Morais *orcid.org/0000-0002-7207-4450*
Institute of Physics, University of São Paulo, Rua do Matão 1371, CEP 05508-090, São Paulo, Brazil

Claudia Mohr *orcid.org/0000-0002-3291-9295*
Dep of Environmental Science & Bolin Centre for Climate Research, Stockholm University, Stockholm, Sweden

William Morgan *orcid.org/0000-0003-0984-5774*
Atmospheric and Environmental Sciences, University of Manchester, Manchester, UK

Mats B. Nilsson *orcid.org/0000-0003-3765-6399*
Department of Forest Ecology and Management, Swedish University of Agricultural Sciences, Umeå, Sweden

Matthias Peichl *orcid.org/0000-0002-9940-5846*
Department of Forest Ecology and Management, Swedish University of Agricultural Sciences, Umeå, Sweden

Tuukka Petäjä *orcid.org/0000-0002-1881-9044*
Institute for Atmospheric and Earth System Research/Physics, Faculty of Science, University of Helsinki, Helsinki, Finland

Maria Praß *orcid.org/0000-0003-4263-5859*
Department of Multiphase Chemistry, Max Planck Institute for Chemistry, Mainz, Germany

Christopher Pöhlker *orcid.org/0000-0001-6958-425X*
Department of Multiphase Chemistry, Max Planck Institute for Chemistry, Mainz, Germany

Mira L. Pöhlker *orcid.org/0000-0001-6852-0756*
Department of Multiphase Chemistry, Max Planck Institute for Chemistry, Mainz, Germany

Ulrich Pöschl *orcid.org/0000-0003-1412-3557*
Department of Multiphase Chemistry, Max Planck Institute for Chemistry, Mainz, Germany

Celso Von Randow *orcid.org/0000-0003-1045-4316*
Instituto Nacional de Pesquisas Espaciais, INPE, São José dos Campos, Brazil

Ilona Riipinen *orcid.org/0000-0001-9085-2319*
Dep of Environmental Science & Bolin Centre for Climate Research, Stockholm University, Stockholm, Sweden

Janne Rinne *orcid.org/0000-0003-1168-7138*
Department of Physical Geography and Ecosystem Sciences, Lund University, Sweden

Luciana V. Rizzo *orcid.org/0000-0002-1748-6997*
Federal University of São Paulo, Campus Diadema, São Paulo, S.P., Brazil

Daniel Rosenfeld *orcid.org/0000-0002-0784-7656*
Institute of Earth Sciences, The Hebrew University of Jerusalem, Israel

Maria A. F. Silva Dias *orcid.org/0000-0001-8591-6090*
Department of Atmospheric Sciences, IAG-USP, University of São Paulo, Brazil

Larisa Sogacheva *orcid.org/0000-0003-3455-8638*
Finnish Meteorological Institute, Climate Research Programme, Helsinki, Finland

Philip Stier *orcid.org/0000-0002-1191-0128*
Atmospheric, Oceanic and Planetary Physics, Department of Physics, University of Oxford, UK

Erik Swietlicki *orcid.org/0000-0003-2031-0404*
Department of Physics, Lund University, Lund, Sweden

Matthias Sörgel *orcid.org/0000-0003-1745-8221*
Max Planck Institute for Chemistry, Mainz, Germany

Peter Tunved *orcid.org/0000-0001-7471-3458*
Dep of Environmental Science & Bolin Centre for Climate Research, Stockholm University, Stockholm, Sweden

Aki Virkkula *orcid.org/0000-0003-4874-7552*
Institute for Atmospheric and Earth System Research/Physics, Faculty of Science, University of Helsinki, Helsinki, Finland; Finnish Meteorological Institute, Climate Research Programme, Helsinki, Finland

Jian Wang *orcid.org/0000-0002-4515-9782*
Center for Aerosol Science and Engineering, Department of Energy, Environmental and Chemical Engineering, Washington University in St. Louis, St. Louis, USA

Bettina Weber *orcid.org/0000-0002-5453-3967*
Department of Multiphase Chemistry, Max Planck Institute for Chemistry, Mainz, Germany; Department of Biology, University of Graz, Graz, Austria

Ana Maria Yáñez-Serrano *orcid.org/0000-0001-6408-5961*
Center for Ecological Research and Forestry Applications (CREAF), Bellaterra, Spain; Global Ecology Unit, CREAF-CSIC-UAB, Bellaterra, Spain

Paul Zieger *orcid.org/0000-0001-7000-6879*
Dep of Environmental Science & Bolin Centre for Climate Research, Stockholm University, Stockholm, Sweden

Eugene Mikhailov *orcid.org/0000-0001-5736-0996*
St. Petersburg State University, 7/9 Universitetskaya nab, St. Petersburg, 199034, Russia; Max Planck Institute for Chemistry, Mainz, Germany

James N. Smith *orcid.org/0000-0003-4677-8224*
University of California, Irvine, CA, USA

Jürgen Kesselmeier *orcid.org/0000-0002-4446-534X*
Department of Multiphase Chemistry, Max Planck Institute for Chemistry, Mainz, Germany

REFERENCES

Aalto, J., Kolari, P., Hari, P., Kerminen, V.-M., Schiestl-Aalto, P., and co-authors. 2014. New foliage growth is a significant, unaccounted source for volatiles in boreal evergreen forests, *Biogeosciences*, **11**, 1331–1344. DOI: *https://doi.org/10.5194/bg-11-1331-2014*

Aalto J., Porcar-Castell, A., Atherton, J., Kolari, P., Pohja, T. And co-authors. 2015. Onset of photosynthesis in spring speeds up monoterpene synthesis and leads to emission bursts. *Plant Cell Environ*, **38**, 2299–2312. DOI: *https://doi.org/10.1111/pce.12550*

Aaltonen, H., J. Aalto, P. Kolari, M. Pihlatie, J. Pumpanen, and co-authors, 2013. Continuous VOC flux measurements on boreal forest floor, *Plant Soil*, **369**, 241–256. DOI: *https://doi.org/10.1007/s11104-012-1553-4*

Aaltonen, V., E. Rodriguez, S. Kazadzis, A. Arola, V. Amiridis, and co-authors, 2012. On the variation of aerosol properties over Finland based on the optical columnar measurements. *Atm. Res.,* **116**, 46–55. DOI: *https://doi.org/10.1016/j.atmosres.2011.07.014*

Abatzoglou, John T. and A. Park Williams. Impact of anthropogenic climate change on wildfire across western US forests, 2016, *PNAS* **113** (42) 11770–11775. DOI: *https://doi.org/10.1073/pnas.1607171113*

Abel, S., Highwood, E. J., Haywood, J. M., & Stringer, M. A. (2005). The direct radiative effect of biomass burning over southern Africa. *Atmos. Chem. Phys*., **5**, 1999–2018. DOI: *https://doi.org/10.5194/acp-5-1999-2005*

Achard, F., and Coauthors, Determination of tropical deforestation rates and related carbon losses from 1990 to 2010, 2014, *Glob. Chang. Biol*., **20**, 2540–2554. DOI: *https://doi.org/10.1111/gcb.12605*

Ackerman, A. S., O. B. Toon, D. E. Stevens, A. J. Heymsfield, V. Ramanathan, and E. J. Welton. 2000. Reduction of tropical cloudiness by soot, *Science*, **288**, 1042–1047. DOI: *https://doi.org/10.1126/science.288.5468.1042*

Acosta Navarro, J. C., Ekman, A., M., L., Pausata, F., S., R., Lewinshcal, A., Varma, V., and coauthors. 2017. Future Response of Temperature and Precipitation to Reduced Aerosol Emissions as Compared with Increased Greenhouse Gas Concentrations. *J. Climate*, **30**, 939–954. DOI: *https://doi.org/10.1175/JCLI-D-16-0466.1*

Acosta Navarro, J. C., Smolander, S., Struthers, H., Zorita, E., L. Ekman, and co-authors, 2014. Global emissions of terpenoid VOCs from terrestrial vegetation in the last millennium, *J. Geophys. Res. Atmos*., **119**, 6867–6885. DOI: *https://doi.org/10.1002/2013JD021238*

Adachi, Kouji, Naga Oshima, Zhaoheng Gong, Suzane de Sá, Adam P Bateman, and co-authors, 2020. Mixing states of Amazon-basin aerosol particles transported over long distances using transmission electron microscopy. *Atmos. Chem. Phys*., **20**, 11923–11939. DOI: *https://doi.org/10.5194/acp-20-11923-2020*

Adesina, A. J., Kumar, K. R., & Sivakumar, V. 2015. Variability in aerosol optical properties and radiative forcing over Gorongosa (18.97°S, 34.35°E) in Mozambique. *Meteorol. Atmospheric Phys*., **127**, 217–228. DOI: *https://doi.org/10.1007/s00703-014-0352-2*

Aguiar, A.P.D. et al., 2016. Land use change emission scenarios: anticipating a forest transition process in the Brazilian Amazon. *Glob Chang Biol*, **22**, 1821–1840. DOI: *https://doi.org/10.1111/gcb.13134*

Ahlm, L., Nilsson, E. D., Krejci, R., Mårtensson, E. M., Vogt, M., and Artaxo, P. 2009. Aerosol number fluxes over the Amazon rain forest during the wet season, *Atmos. Chem. Phys*., **9**, 9381–9400. DOI: *https://doi.org/10.5194/acp-9-9381-2009*

Ahlm, L., Nilsson, E. D., Krejci, R., Mårtensson, E. M., Vogt, M., and Artaxo, P. 2010. A comparison of dry and wet season aerosol number fluxes over the Amazon rain forest, *Atmos. Chem. Phys.,* **10**, 3063–3079. DOI: *https://doi.org/10.5194/acp-10-3063-2010*

Äijälä M., Daellenbach K., Canonaco F. et al. 2019. Constructing a data-driven receptor model for organic and inorganic aerosol – A synthesis analysis of eight mass spectrometric data sets from a boreal forest site. *Atmos. Chem. Phys*., **19,** 3645–3672. DOI: *https://doi.org/10.5194/acp-19-3645-2019*

Äijälä, M., Heikkinen, L., Fröhlich, R., Canonaco, F., Prévôt, A. S. H., and co-authors, 2017. Resolving anthropogenic aerosol pollution types – deconvolution and exploratory classification of pollution events, *Atmos. Chem. Phys.,* **17**, 3165–3197. DOI: *https://doi.org/10.5194/acp-17-3165-2017*

Ainsworth, E.A., Craig R. Yendrek, Stephen Sitch, William J. Collins, Lisa D. Emberson, 2012, The Effects of Tropospheric Ozone on Net Primary Productivity and Implications for Climate Change, *Annu. Rev. Plant Biol*., 63, 637–661. DOI: *https://doi.org/10.1146/annurev-arplant-042110-103829*

Akagi, S. K., R. J. Yokelson, C. Wiedinmyer, M. J. Alvarado, J. S. Reid, and co-authors, 2011: Emission factors for open and domestic biomass burning for use in atmospheric models. Atmos. Chem. Phys., 11, 4039–4072. DOI: *https://doi.org/10.5194/acp-11-4039-2011*

Albrecht, B. A. 1989, Aerosols, Cloud Microphysics, and Fractional Cloudiness, *Science,* **245**, 1227–1230. DOI: *https://doi.org/10.1126/science.245.4923.1227*

Albrecht, R. I., Morales, C. A., Silva Dias, M. A. F., 2011. Electrification of precipitating systems over the Amazon: Physical processes of thunderstorm development. J. Geophys. Res. Atmos. **116**, D08209. DOI: *https://doi.org/10.1029/2010JD014756*

Alcantara, C. R., Silva Dias, M. A.F., Souza, E. P.; and Cohen, J. 2011. Verification of the role of the low-level jets in Amazon squall lines. *Atmos. Res.,* **100**, 36–44. DOI: *https://doi.org/10.1016/j.atmosres.2010.12.023*

Alden C.B., Miller J.B., Gatti L. V., et al. 2016. Regional atmospheric CO_2 inversion reveals seasonal and geographic differences in Amazon net biome exchange. *Glob Chang Biol* **22**, 3427–43. DOI: *https://doi.org/10.1111/gcb.13305*

Aleixo, Izabela, Darren Norris, Lia Hemerik, Antenor Barbosa, Eduardo Prata, and co-authors, 2019. *Nat. Clim. Change*. DOI: *https://doi.org/10.1038/s41558-019-0458-0*

Aliaga, D., Sinclair, V. A., Andrade, M., Artaxo, P., Carbone, S, and co-authors, 2021. Identifying source regions of air masses sampled at the tropical high-altitude site of Chacaltaya using WRF-FLEXPART and cluster analysis, *Atmos. Chem. Phys. Discuss*. in review, 2021. DOI: *https://doi.org/10.5194/acp-2021-126*

Allan, J. D., Alfarra, M. R., Bower, K. N., Coe, H., Jayne, J. T, and co-authors, 2006. Size and composition measurements of background aerosol and new particle growth in a Finnish

forest during QUEST 2 using an Aerodyne Aerosol Mass Spectrometer, *Atmos. Chem. Phys.*, **6**, 315–327. DOI: *https://doi.org/10.5194/acp-6-315-2006*

Allan, J.D., W. T. Morgan, E. Darbyshire, M. J. Flynn, P. I. Williams, and co-authors, 2014. Airborne Observations of IEPOX-Derived Isoprene SOA in the Amazon during SAMBBA. *Atmos. Chem. Phys*., **14**, 11393–11407. DOI: *https://doi.org/10.5194/acp-14-11393-2014*

Allen, M. R., and W. J. Ingram. 2002. Constraints on future changes in climate and the hydrologic cycle, *Nature*, **419** (6903), 224–232. DOI: *https://doi.org/10.1038/nature01092*

Allen, R. J., Evan, A. T., & Booth, B. B. B. 2015. Interhemispheric Aerosol Radiative Forcing and Tropical Precipitation Shifts during the Late Twentieth Century, *J. Clim.,* **28** (20), 8219–8246. DOI: *https://doi.org/10.1175/JCLI-D-15-0148.1*

Alton, P.B., 2008, Reduced carbon sequestration in terrestrial ecosystems under overcast skies compared to clear skies, *Agric. For. Meteorol*., **148**, 10, 2008, 1641–1653. DOI: *https://doi.org/10.1016/j.agrformet.2008.05.014*

Alves et al., 2012. Organic compounds in aerosols from selected European sites: Biogenic versus anthropogenic sources, *Atmos. Environ*. **59**, 243–255. DOI: *https://doi.org/10.1016/j.atmosenv.2012.06.013*

Alves, E. G., Jardine, K., Tota, J., Jardine, A., Yãnez-Serrano, and co-authors, 2016. Seasonality of isoprenoid emissions from a primary rainforest in central Amazonia, *Atmos. Chem. Phys*., **16**, 3903–3925. DOI: *https://doi.org/10.5194/acp-16-3903-2016*

Alves, E. G., Tóta, J., Turnipseed, A., Guenther, A. B., Vega Bustillos, and co-authors, 2018. Leaf phenology as one important driver of seasonal changes in isoprene emissions in central Amazonia, *Biogeosciences*, **15**, 4019–4032. DOI: *https://doi.org/10.5194/bg-15-4019-2018*

Amaral e Silva, A., Braga, Matheus Quintão, Ferreira, J., Juste dos Santos, and co-authors, 2020. Anthropic activities, and the Legal Amazon: Estimative of impacts on forest and regional climate for 2030, *Remote Sens. Appl. Soc. Environ*., **18**, 100304. DOI: *https://doi.org/10.1016/j.rsase.2020.100304*

Amaral, J. H. F., Melack, J. M., Barbosa, P. M., MacIntyre, S., Kasper, D, and co-authors, 2020. Carbon dioxide fluxes to the atmosphere from waters within flooded forests in the Amazon basin. Journal of Geophysical Research: *Biogeosciences*, **125**, e2019JG005293. DOI: *https://doi.org/10.1029/2019JG005293*

Amiro, B.D., 2001. Paired-tower measurements of carbon and energy fluxes following disturbance in the boreal forest. *Global Change Biol.,* **7**(3): 253–268. DOI: *https://doi.org/10.1046/j.1365-2486.2001.00398.x*

Andela, N., and coauthors, 2017: A human-driven decline in global burned area. *Science*, **356**, 1356–1362. DOI: *https://doi.org/10.1126/science.aal4108*

Andreae, M. O., 1991. Biomass burning: Its history, use and distribution and its impact on environmental quality and global climate, in Global Biomass Burning: Atmospheric, Climatic and Biospheric Implications, edited by J. S. Levine, pp. 3–21, MIT Press, Cambridge, Mass.

Andreae, M. O. 2001a. The Biosphere: Pilot or passenger on spaceship Earth? In: Heinen D, In: Hoch S., In: Krafft T. In: Moss C, In: Welschhoff A, eds. Contributions to Global Change Research. German National Committee on Global Change Research, Bonn, 59–66.

Andreae, M. O., Acevedo, O. C., Araújo, A., Artaxo, P. and co-authors, 2015. The Amazon Tall Tower Observatory (ATTO): overview of pilot measurements on ecosystem ecology, meteorology, trace gases, and aerosols, *Atmos. Chem. Phys*., **15**(18), 10723–10776. DOI: *https://doi.org/10.5194/acp-15-10723-2015*

Andreae, M. O., Afchine, A., Albrecht, R., Holanda, B. A., Artaxo, P., and co-authors, 2018. Aerosol characteristics and particle production in the upper troposphere over the Amazon Basin. *Atmos Chem Phys*, **18**, 921–961, 2018. DOI: *https://doi.org/10.5194/acp-18-921-2018*

Andreae, M. O., and Andreae, T. W. 1988. The cycle of biogenic sulfur-compounds over the Amazon basin 1. Dry season, *J. Geophys. Res*., **93**, 1487–1497. DOI: *https://doi.org/10.1029/JD093iD02p01487*

Andreae, M. O., Andreae, T. W., and Ditas, F., 2019. How frequent is new particle formation in the boundary layer over the remote temperate-boreal forest? American Geophysical Union Fall Meeting 2019. San Francisco. DOI: *https://doi.org/10.1002/essoar.10501148.1*

Andreae, M. O., Artaxo, P., Beck, V., Bela, M., Freitas, S., and co-authors, 2012. Carbon monoxide and related trace gases and aerosols over the Amazon Basin during the wet and dry seasons, *Atmos. Chem. Phys.,* **12**, 6041–6065. DOI: *https://doi.org/10.5194/acp-12-6041-2012*

Andreae, M. O., Artaxo, P., Brandão, C., Carswell, F. E., Ciccioli, P., and co-authors, 2002. Biogeochemical cycling of carbon, water, energy, trace gases and aerosols in Amazonia: The LBA-EUSTACH experiments: *J. Geophys. Res.*, **107**, 8066. DOI: *https://doi.org/10.1029/2001JD000524*

Andreae, M. O., Artaxo, P; Fischer, H.; Freitas, S. R., Lelieveld, J.; Dias, and co-authors, 2001; Transport of biomass burning smoke to the upper troposphere by deep convection in the equatorial region. *J. Geophys. Res.,* **28**, 951–954. DOI: *https://doi.org/10.1029/2000GL012391*

Andreae, M.O., Berresheim, H., Bingemer, H., Jacob, D. J., Lewis, and co-authors, 1990. THE ATMOSPHERIC SULFUR CYCLE OVER THE AMAZON BASIN .2. WET SEASON, *J. Geophys. Res.,* **95**, 16813–16824. DOI: *https://doi.org/10.1029/JD095iD10p16813*

Andreae, M. O., Chapuis, A., Cros, B., Fontan, J., Helas, G., and co-authors, 1992. Ozone and Aitken nuclei over equatorial Africa: Airborne observations during DECAFE 88. *J. Geophys. Res*., **97**, 6137–6148. DOI: *https://doi.org/10.1029/91JD00961*

Andreae, M.O. and Gelencsér, A. 2006. Black carbon or brown carbon? The nature of light-absorbing carbonaceous aerosols, *Atmos. Chem. Phys.,* **6**, 3131–3148. DOI: *https://doi.org/10.5194/acp-6-3131-2006*

Andreae, M.O., D. Rosenfeld, P. Artaxo, A. A. Costa, G. P. Frank, and co-authors, 2004. Smoking rain clouds over the Amazon. *Science,* **303**, 1337–1342. DOI: *https://doi.org/10.1126/science.1092779*

Anselmo, E. M., C. Schumacher and L.A. T. Machado. 2019. The Amazonian Low-level Jet and its Connection to Convective Cloud Organization. *Mon. Wea. Rev*., **148**, 1–42. DOI: *https://doi.org/10.1175/MWR-D-19-0414.1*

Ansmann, A., and coauthors, 2018. Extreme levels of Canadian wildfire smoke in the stratosphere over central Europe on 21–22 August 2017. *Atmos. Chem. Phys*., **18**, 11831–11845. DOI: *https://doi.org/10.5194/acp-18-11831-2018*

Ansmann, A., H. Baars, M. Tesche, D. Müller, D. Althausen and co-authors, 2009. Dust and smoke transport from Africa to South America: Lidar profiling over Cape Verde and the Amazon rainforest, *Geophys. Res. Lett.,* **36**, L11802. DOI: *https://doi.org/10.1029/2009GL037923*

Anttila, P., & Tuovinen, J. P. 2010. Trends of primary and secondary pollutant concentrations in Finland in 1994–2007. *Atmos Environ,* **44**(1), 30–41. DOI: *https://doi.org/10.1016/j.atmosenv.2009.09.041*

Aragão, L. E. O. C., Anderson, L. O., Fonseca, M. G., Rosan, T. M., Vedovato, L. B., and co-authors, 2018. 21st Century drought-related fires counteract the decline of Amazon deforestation carbon emissions., *Nat. Commun*., **9**(1), 536. DOI: *https://doi.org/10.1038/s41467-017-02771-y*

Aragão, L.E.O.C., Poulter, B., Barlow, J.B., Anderson, L.O., Malhi, Y., and co-authors, 2014. Environmental change and the carbon balance of Amazonian forests. *Biol. Rev.* **89**, 913–931. DOI: *https://doi.org/10.1111/brv.12088*

Aragão, L. E. O. C., Yadvinder M., Nicolas B., Andre Lima, Yosio Shimabukuro and co-authors, 2008. Interactions between rainfall, deforestation, and fires during recent years in the Brazilian Amazonia. *Philos. Trans. R. Soc. Lond., B, Biol. Sci*., **363**(1498), 1779–1785. DOI: *https://doi.org/10.1098/rstb.2007.0026*

Arana, A., Loureiro, A. L., Barbosa, H. M. J., Van Grieken, R. and Artaxo, P. 2014. Optimized energy dispersive X-ray fluorescence analysis of atmospheric aerosols collected at pristine and perturbed Amazon Basin sites, *X-Ray Spectrom*., **43**(4), 228–237. DOI: *https://doi.org/10.1002/xrs.2544*

Araújo, A.C., Nobre, A.D., Kruijt, B., Elbers, J.A., Dallarosa, R.G., and co-authors, 2002. Comparative measurements of carbon dioxide fluxes from two nearby towers in a central Amazonian rainforest: The Manaus LBA site. *J. Geophys. Res. Atmos*. **107**, 1–20. DOI: *https://doi.org/10.1029/2001JD000676*

Archibald, S., C. E. R. Lehmann, J. L. Gómez-Dans, and R. A. Bradstock, 2013: Defining pyromes and lobal syndromes of fire regimes. *Proc. Natl. Acad. Sci.,* **110**, 6442–6447. DOI: *https://doi.org/10.1073/pnas.1211466110*

Arneth, A.; Niinemets, U.; Pressley, S.; Back, J.; Hari, P, and co-authors, 2007. Process-based estimates of terrestrial ecosystem isoprene emissions: incorporating the effects of a direct CO_2-isoprene interaction. *Atmos. Chem. Phys.,* **7**, 31–53. DOI: *https://doi.org/10.5194/acp-7-31-2007*

Arnott, W. P., Hamasha, K., Moosmüller, H., Sheridan, P. J., and Ogren, J. A. 2005. Towards aerosol light-absorption measurements with a 7-wavelength aethalometer: Evaluation with a photoacoustic instrument and 3-wavelength nephelometer, *Aerosol Sci. Tech*., **39**, 17–29. DOI: *https://doi.org/10.1080/027868290901972*

Artaxo, P., 2012. Break down boundaries in climate research. World View Section, *Nature* **481**, 239. DOI: *https://doi.org/10.1038/481239a*

Artaxo, P. and Hansson, H.-C. 1995. Size Distribution of Biogenic Aerosol Particles, *Atmos. Environ*., **29**(3), 393–402. DOI: *https://doi.org/10.1016/1352-2310(94)00178-N*

Artaxo, P.; Maenhaut, W.; Storms, H.; Van Grieken, R.;1990. Aerosol characteristics and sources for the Amazon basin during the wet season, *J. Geophys. Res. Atmos*, **95**, D10, 16971–16985. DOI: *https://doi.org/10.1029/JD095iD10p16971*

Artaxo, P., J. V. Martins, M. A. Yamasoe, A. S. Procópio, T. M. Pauliquevis, and co-authors, 2002. Physical and chemical properties of aerosols in the wet and dry season in Rondônia, Amazonia. *J. Geophys. Res. Atmos*, **107**, D20, 8081–8095. DOI: *https://doi.org/10.1029/2001JD000666*

Artaxo, P., Rizzo, L. V., Brito, J. F., Barbosa, H. M. J., Arana, A., and co-authors, 2013. Atmospheric aerosols in Amazonia and land use change: from natural biogenic to biomass burning conditions, *Faraday Discuss*., **165**, 203. DOI: *https://doi.org/10.1039/c3fd00052d*

Artaxo, P., Rizzo, L. V., Paixão, M., de Lucca, S., Oliveira, and co-authors, 2009. Aerosol particles in Amazonia: Their composition, role in the radiation balance, cloud formation and nutrient cycles, in Amazonia and Global Change, edited by M. Keller, M. Bustamante, J. Gash, & P. Dias, pp. 233–250, American Geophysical Union, Washington, DC. DOI: *https://doi.org/10.1029/2008GM000778*

Artaxo, P.; Storms, H.; Bruynseels, F.; Van Grieken, R.; Maenhaut, W. 1988. Composition and sources of aerosols from the Amazon Basin. *J. Geophys. Res. Atmos*, **93**, 1605–1615. DOI: *https://doi.org/10.1029/JD093iD02p01605*

Ashmore, M. R., 2005. Assessing the future global impacts of ozone on vegetation: Plant Cell Environ., **28**, 949–964. DOI: *https://doi.org/10.1111/j.1365-3040.2005.01341.x*

Asmi, E., Kivekäs, N., Kerminen, V.-M., Komppula, M., Hyvärinen, A.-P., and co-authors, 2011. Secondary new particle formation in Northern Finland Pallas site between the years 2000 and 2010, *Atmos. Chem. Phys*., **11**, 12959–12972. DOI: *https://doi.org/10.5194/acp-11-12959-2011*

Assis T. O., Aguiar APD de, Randow C. von, and co-authors, 2020. CO_2 emissions from forest degradation in Brazilian Amazon. *Environ Res Lett* **15**: 104035. DOI: *https://doi.org/10.1088/1748-9326/ab9cfc*

Aubin, I., L. Boisvert-Marsh, H. Kebli, D. McKenney, J. Pedlar, and co-authors, 2018. Tree vulnerability to climate change: improving exposure-based assessments using traits as indicators of sensitivity. *Ecosphere* **9**(2):e02108. DOI: *https://doi.org/10.1002/ecs2.2108*

Avissar, Roni and David Werth. 2005. Global Hydroclimatological Teleconnections Resulting from Tropical Deforestation. *J. Hydrometeor.*, **6**, 134–145. DOI: *https://doi.org/10.1175/JHM406.1*

Baars, H., Ansmann, A., Althausen, D., Engelmann, R., Artaxo, P., and co-authors, 2011. Further evidence for significant smoke transport from Africa to Amazonia. *Geophys. Res. Lett.* **38**, 1–6. DOI: *https://doi.org/10.1029/2011GL049200*

Baars, H., Ansmann, A., Althausen, D., Engelmann, R., Heese, B., and co-authors, 2012. Aerosol profiling with lidar in the Amazon Basin during the wet and dry season. *J. Geophys. Res.* **117**, 1–16. DOI: *https://doi.org/10.1029/2012JD018338*

Baccini, A., Walker, W., Carvalho, L., Farina, M., Sulla-Menashe, D., and co-authors, 2017. Tropical forests are a net carbon source based on aboveground measurements of gain and loss. *Science* **358**, 230–34. DOI: *https://doi.org/10.1126/science.aam5962*

Bäck, J., Aalto, J., Henriksson, M., Hakola, H., He, Q., et al. 2012. Chemodiversity of a Scots pine stand and implications for terpene air concentrations. *Biogeosciences* **9**, 689–702. DOI: *https://doi.org/10.5194/bg-9-689-2012*

Bäck, J., Neuvonen, S., and Huttunen, S. 1994. Pine needle growth and fine structure after prolonged acid rain treatment in the subarctic. *Plant Cell Environ.* **17**, 1009–21. DOI: *https://doi.org/10.1111/j.1365-3040.1994.tb02024.x*

Baker, B., Bai, J. H., Johnson, C., Cai, Z. T., Li, Q. J., et al. 2005. Wet and dry season ecosystem level fluxes of isoprene and monoterpenes from a southeast Asian secondary forest and rubber tree plantation. *Atmos. Environ.* **39**, 381–90. DOI: *https://doi.org/10.1016/j.atmosenv.2004.07.033*

Bakwin, P. S., Wofsy, S. C., Song-Miao Fan, Keller, M., Trumbore, S. E., et al. 1990. Emission of nitric oxide (NO) from tropical forest soils and exchange of NO between the forest canopy and atmospheric boundary layers. *J. Geophys. Res.* **95**. DOI: *https://doi.org/10.1029/JD095iD10p16755*

Baldocchi, D., Chu, H., and Reichstein, M. 2018. Inter-annual variability of net and gross ecosystem carbon fluxes: A review. *Agric. For. Meteorol.* **249**, 520–33. DOI: *https://doi.org/10.1016/j.agrformet.2017.05.015*

Barber, V. A., Juday, G. P., and Finney, B. P. 2000. Reduced growth of Alaskan white spruce in the twentieth century from temperature-induced drought stress. *Nature* **405**, 668–73. DOI: *https://doi.org/10.1038/35015049*

Barkhordarian, A., Saatchi, S. S., Behrangi, A., Loikith, P. C., and Mechoso, C. R. 2019. A Recent Systematic Increase in Vapor Pressure Deficit over Tropical South America. *Sci. Rep.* **9**, 1–12. DOI: *https://doi.org/10.1038/s41598-019-51857-8*

Barkley, M. P., Palmer, P. I., De Smedt, I., Karl, T., Guenther, A., et al. 2009. Regulated large-scale annual shutdown of Amazonian isoprene emissions? *Geophys. Res. Lett.* **36**, 1–5. DOI: *https://doi.org/10.1029/2008GL036843*

Barkley, M. P., Palmer, P. I., Ganzeveld, L., Arneth, A., Hagberg, D., et al. 2011. Can a "state of the art" chemistry transport model simulate Amazonian tropospheric chemistry? *J. Geophys. Res.* **116**, 1–28. DOI: *https://doi.org/10.1029/2011JD015893*

Barlow, J., Berenguer, E., Carmenta, R., and França, F. 2019. Clarifying Amazonia's burning crisis. *Glob. Chang. Biol.* **26**, 319–21. DOI: *https://doi.org/10.1111/gcb.14872*

Barlow, J., and Peres, C. A. 2008. Fire-mediated dieback and compositional cascade in an Amazonian forest. *Philos. Trans. R. Soc. Lond. B. Biol. Sci.* **363**, 1787–94. DOI: *https://doi.org/10.1098/rstb.2007.0013*

Barnett, T. P., Adam, J. C., and Lettenmaier, D. P. 2005. Potential impacts of a warming climate on water availability in snow-dominated regions. *Nature* **438**, 303–9. DOI: *https://doi.org/10.1038/nature04141*

Barr, A. G., Griffis, T. J., Black, T. A., Lee, X., Staebler, R. M., et al. 2002. Comparing the carbon budgets of boreal and temperate deciduous forest stands. *Can. J. For. Res.* **32**, 813–22. DOI: *https://doi.org/10.1139/x01-131*

Basso, L. S., Gatti, L. V., Gloor, M., Miller, J. B., Domingues, L. G., et al. 2016. Seasonality and interannual variability of CH_4 fluxes from the eastern Amazon Basin inferred from atmospheric mole fraction profiles. *J. Geophys. Res.* **121**, 168–84. DOI: *https://doi.org/10.1002/2015JD023874*

Bastin, J. F., Finegold, Y., Garcia, C., Mollicone, D., Rezende, M., et al. 2019. The global tree restoration potential. *Science* **364**, 76–79. DOI: *https://doi.org/10.1126/science.aax0848*

Bateman, A. P., Bertram, A. K., and Martin, S. T. 2015. Hygroscopic influence on the semisolid-to-liquid transition of secondary organic materials. *J. Phys. Chem. A* **119**, 4386–95. DOI: *https://doi.org/10.1021/jp508521c*

Bateman, A. P., Gong, Z., Harder, T. H., De Sá, S. S., Wang, B., et al. 2017. Anthropogenic influences on the physical state of submicron particulate matter over a tropical forest. *Atmos. Chem. Phys.* **17**, 1759–73. DOI: *https://doi.org/10.5194/acp-17-1759-2017*

Bateman, A. P., Gong, Z., Liu, P., Sato, B., Cirino, G., et al. 2016. Sub-micrometre particulate matter is primarily in liquid form over Amazon rainforest. *Nat. Geosci.* **9**, 34–37. DOI: *https://doi.org/10.1038/ngeo2599*

Bathiany, S., Dakos, V., Scheffer, M., and Lenton, T. M. 2018. Climate models predict increasing temperature variability in poor countries. *Sci. Adv.* **4**, 1–10. DOI: *https://doi.org/10.1126/sciadv.aar5809*

Bauer, H., Giebl, H., Hitzenberger, R., Kasper-Giebl, A., Reischl, G., et al. 2003. Airborne bacteria as cloud condensation nuclei. *J. Geophys. Res.* **108**, 1–5. DOI: *https://doi.org/10.1029/2003JD003545*

Beck, H. E., Zimmermann, N. E., McVicar, T. R., Vergopolan, N., Berg, A., et al. 2018. Present and future köppen-geiger climate classification maps at 1-km resolution. *Sci. Data* **5**, 1–12. DOI: *https://doi.org/10.1038/sdata.2018.214*

Beck, V., Chen, H., Gerbig, C., Bergamaschi, P., Bruhwiler, L., et al. 2012. Methane airborne measurements and comparison to global models during BARCA. *J. Geophys. Res.* **117**, 1–16. DOI: *https://doi.org/10.1029/2011JD017345*

Beck, V., Gerbig, C., Koch, T., Bela, M. M., Longo, K. M., et al. 2013. WRF-Chem simulations in the Amazon region during wet and dry season transitions: Evaluation of methane models and wetland inundation maps. *Atmos. Chem. Phys.* **13**, 7961–82. DOI: *https://doi.org/10.5194/acp-13-7961-2013*

Beer, C., Reichstein, M., Tomelleri, E., Ciais, P., Jung, M., et al. 2010. Terrestrial gross carbon dioxide uptake: Global distribution and covariation with climate. *Science* **329**, 834–38. DOI: *https://doi.org/10.1126/science.1184984*

Bekryaev, R. V., Polyakov, I. V., and Alexeev, V. A. 2010. Role of polar amplification in long-term surface air temperature variations and modern arctic warming. *J. Clim.* **23**, 3888–3906. DOI: *https://doi.org/10.1175/2010JCLI3297.1*

Bela, M. M., Longo, K. M., Freitas, S. R., Moreira, D. S., Beck, V., et al. 2015. Ozone production and transport over the Amazon Basin during the dry-to-wet and wet-to-dry transition seasons. *Atmos. Chem. Phys.* **15**, 757–82. DOI: *https://doi.org/10.5194/acp-15-757-2015*

Ben-Ami, Y., Koren, I., Rudich, Y., Artaxo, P., Martin, S. T., et al. 2010. Transport of North African dust from the Bodélé depression to the Amazon Basin: A case study. *Atmos. Chem. Phys.* **10**, 7533–44. DOI: *https://doi.org/10.5194/acp-10-7533-2010*

Bender, F. A. M., Ramanathan, V., and Tselioudis, G. 2012. Changes in extratropical storm track cloudiness 1983–2008: Observational support for a poleward shift. *Clim. Dyn.* **38**, 2037–53. DOI: *https://doi.org/10.1007/s00382-011-1065-6*

Bergh, J., Nilsson, U., Allen, H. L., Johansson, U., and Fahlvik, N. 2014. Long-term responses of Scots pine and Norway spruce stands in Sweden to repeated fertilization and thinning. *For. Ecol. Manage.* **320**, 118–28. DOI: *https://doi.org/10.1016/j.foreco.2014.02.016*

Betts, A. K., and Ball, J. H. 1997. Albedo over the boreal forest. *J. Geophys. Res.* **102**, 28901–9. DOI: *https://doi.org/10.1029/96JD03876*

Betts, A. K., Ball, J. H., and McCaughey, J. H. 2001. Near-surface climate in the boreal forest. *J. Geophys. Res.* **106**, 33529–41. DOI: *https://doi.org/10.1029/96JD03876*

Betts, A. K., Gatti, L. V., Cordova, A. M., Silva Dias, M. A. F., and Fuentes, J. D. 2002. Transport of ozone to the surface by convective downdrafts at night. *J. Geophys. Res.* **107**, LBA 13-1-LBA 13-6. DOI: *https://doi.org/10.1029/2000JD000158*

Bianchi, F., Kurtén, T., Riva, M., Mohr, C., Rissanen, M. P., et al. 2019. Highly Oxygenated Organic Molecules (HOM) from Gas-Phase Autoxidation Involving Peroxy Radicals: A Key Contributor to Atmospheric Aerosol. *Chem. Rev.* **119**, 3472–3509. DOI: *https://doi.org/10.1021/acs.chemrev.8b00395*

Bianchi, F., Sinclair, V. A., Aliaga, D., Zha, Q., Scholz, W., et al. 2021. The SALTENA experiment: Comprehensive observations of aerosol sources, formation and processes in the South American Andes. *Bull. Amer. Meteor.* **1**, 1–46. DOI: *https://doi.org/10.1175/BAMS-D-20-0187.1*

Bianchi, F., Trostl, J., Junninen, H., Frege, C., Henne, S., et al. 2016. New particle formation in the free troposphere: A question of chemistry and timing. *Science* **352**, 1109–12. DOI: *https://doi.org/10.1126/science.aad5456*

Bison, J. V., Cardoso-Gustavson, P., de Moraes, R. M., da Silva Pedrosa, G., Cruz, L. S., et al. 2018. Volatile organic compounds and nitric oxide as responses of a Brazilian tropical species to ozone: the emission profile of young and mature leaves. *Environ. Sci. Pollut. Res.* **25**, 3840–48. DOI: *https://doi.org/10.1007/s11356-017-0744-1*

Blundo, C., Carilla, J., Grau, R., Malizia, A., Malizia, L., et al. 2021. Taking the pulse of Earth's tropical forests using networks of highly distributed plots. *Biol. Conserv.* **260**, 108849. DOI: *https://doi.org/10.1016/j.biocon.2020.108849*

Boiyo, R., Kumar, K. R., and Zhao, T. 2018. Spatial variations and trends in AOD climatology over East Africa during 2002–2016: a comparative study using three satellite data sets. *Int. J. Climatol.* **38**, e1221–40. DOI: *https://doi.org/10.1002/joc.5446*

Boiyo, R., Kumar, K. R., Zhao, T., and Guo, J. 2019. A 10-Year Record of Aerosol Optical Properties and Radiative Forcing Over Three Environmentally Distinct AERONET Sites in Kenya, East Africa. *J. Geophys. Res.* **124**, 1596–1617. DOI: *https://doi.org/10.1029/2018JD029461*

Bonan, G. B. 2008. Forests and climate change: Forcings, feedbacks, and the climate benefits of forests. *Science* **320**, 1444–49. DOI: *https://doi.org/10.1126/science.1155121*

Bonan, G. B., Pollard, D., and Thompson, S. L. 1992. Effects of boreal forest vegetation on global climate. *Nature* **359**, 716–18. DOI: *https://doi.org/10.1038/359716a0*

Bonan, G. B., and Shugart, H. H. 1989. Environmental factors and ecological processes in boreal forests. *Annu. Rev. Ecol. Evol. Syst.* 1–28. DOI: *https://doi.org/10.1146/annurev.es.20.110189.000245*

Bond, T. C., Doherty, S. J., Fahey, D. W., Forster, P. M., Berntsen, T., et al. 2013. Bounding the role of black carbon in the climate system: A scientific assessment. *J. Geophys. Res.* **118**, 5380–5552. DOI: *https://doi.org/10.1002/jgrd.50171*

Bond-Lamberty, B., Peckham, S. D., Ahl, D. E., and Gower, S. T. 2007. Fire as the dominant driver of central Canadian boreal forest carbon balance. *Nature* **450**, 89–92. DOI: *https://doi.org/10.1038/nature06272*

Borma, L. S., Da Rocha, H. R., Cabral, O. M., Von Randow, C., Collicchio, E., et al. 2009. Atmosphere and hydrological controls of the evapotranspiration over a floodplain forest in the Bananal Island region, Amazonia. *J. Geophys. Res.* **114**, 1–12. DOI: *https://doi.org/10.1029/2007JG000641*

Botía, S., Gerbig, C., Marshall, J., Lavric, J. V., Walter, D., et al. 2020. Understanding nighttime methane signals at the Amazon Tall Tower Observatory (ATTO). *Atmos. Chem. Phys.* **20**, 6583–6606. DOI: *https://doi.org/10.5194/acp-20-6583-2020*

Bourgeois, Q., Ekman, A. M. L., and Krejci, R. 2015. Aerosol transport over the andes from the amazon basin to the remote Pacific Ocean: A multiyear CALIOP assessment. *J. Geophys. Res.* **120**, 8411–25. DOI: *https://doi.org/10.1002/2015JD023254*

Bourtsoukidis, E., Behrendt, T., Yañez-Serrano, A. M., Hellén, H., Diamantopoulos, E., et al. 2018. Strong sesquiterpene emissions from Amazonian soils. *Nat. Commun.* **9**, 1–11. DOI: *https://doi.org/10.1038/s41467-018-04658-y*

Bourtsoukidis, E., Bonn, B., Dittmann, A., Hakola, H., Hellén, H., et al. 2012. Ozone stress as a driving force of sesquiterpene emissions: A suggested parameterisation. *Biogeosciences* **9**, 4337–52. DOI: *https://doi.org/10.5194/bg-9-4337-2012*

Bowman, D. M. J. S., Balch, J., Artaxo, P., Bond, W. J., Cochrane, M. A., et al. 2011. The human dimension of fire regimes on Earth. *J. Biogeogr.* **38**, 2223–36. DOI: *https://doi.org/10.1111/j.1365-2699.2011.02595.x*

Boy, M., Thomson, E. S., Navarro, J. C. A., Arnalds, O., Batchvarova, E., et al. 2019. Interactions between the atmosphere, cryosphere, and ecosystems at northern high latitudes. *Atmos. Chem. Phys.* **19**, 2015–61. DOI: *https://doi.org/10.5194/acp-19-2015-2019*

Brando, P. M., Balch, J. K., Nepstad, D. C., Morton, D. C., Putz, F. E., et al. 2014. Abrupt increases in Amazonian tree mortality due to drought-fire interactions. *Proc. Natl. Acad. Sci. U. S. A.* **111**, 6347–52. DOI: *https://doi.org/10.1073/pnas.1305499111*

Brando, P. M., Paolucci, L., Ummenhofer, C. C., Ordway, E. M., Hartmann, H., et al. 2019. Droughts, Wildfires, and Forest Carbon Cycling: A Pantropical Synthesis. *Annu. Rev. Earth Planet. Sci.* **47**, 555–81. DOI: *https://doi.org/10.1146/annurev-earth-082517-010235*

Brando, P. M., Soares-Filho, B., Rodrigues, L., Assunção, A., Morton, D., et al. 2020. The gathering firestorm in southern Amazonia. *Sci. Adv.* **6**, 1–9. DOI: *https://doi.org/10.1126/sciadv.aay1632*

Brassard, B. W., and Chen, H. Y. H. 2006. Stand structural dynamics of North American boreal forests. *CRC. Crit. Rev. Plant Sci.* **25**, 115–37. DOI: *https://doi.org/10.1080/07352680500348857*

Brienen, R. J. W., Phillips, O. L., Feldpausch, T. R., Gloor, E., Baker, T. R., et al. 2015. Long-term decline of the Amazon carbon sink. *Nature* **519**, 344–48. DOI: *https://doi.org/10.1038/nature14283*

Brioude, J., Cooper, O. R., Feingold, G., Trainer, M., Freitas, S. R., et al. 2009. Effect of biomass burning on marine stratocumulus clouds off the California coast. *Atmos. Chem. Phys.* **9**, 8841–56. DOI: *https://doi.org/10.5194/acp-9-8841-2009*

Brito, J., Rizzo, L. V., Morgan, W. T., Coe, H., Johnson, B., et al. 2014. Ground-based aerosol characterization during the South American Biomass Burning Analysis (SAMBBA) field experiment. *Atmos. Chem. Phys.* **14**, 12069–83. DOI: *https://doi.org/10.5194/acp-14-12069-2014*

Bryan, N. C., Christner, B. C., Guzik, T. G., Granger, D. J., and Stewart, M. F. 2019. Abundance and survival of microbial aerosols in the troposphere and stratosphere. *ISME J.* **13**, 2789–99. DOI: *https://doi.org/10.1038/s41396-019-0474-0*

Buenrostro Mazon, S., Riipinen, I., Schultz, D. M., Valtanen, M., Maso, M. D., et al. 2009. Classifying previously undefined days from eleven years of aerosol-particle-size distribution data from the SMEAR II station, Hyytiälä, Finland. *Atmos. Chem. Phys.* **9**, 667–76. DOI: *https://doi.org/10.5194/acp-9-667-2009*

Bullock, E. L., Woodcock, C. E., Souza, C., and Olofsson, P. 2020. Satellite-based estimates reveal widespread forest degradation in the Amazon. *Glob. Chang. Biol.* **26**, 2956–69. DOI: *https://doi.org/10.1111/gcb.15029*

Bunn, A. G., Goetz, S. J., Kimball, J. S., and Zhang, K. 2007. Northern high-latitude ecosystems respond to climate change. *Eos (Washington. DC).* **88**, 333–35. DOI: *https://doi.org/10.1029/2007EO340001*

Burgos, M. A., Andrews, E., Titos, G., Alados-Arboledas, L., Baltensperger, U., et al. 2019. A global view on the effect of water uptake on aerosol particle light scattering. *Sci. Data 2019 61* **6**, 1–19. DOI: *https://doi.org/10.1038/s41597-019-0158-7*

Burleyson, C. D., Feng, Z., Hagos, S. M., Fast, J., Machado, L. A. T., et al. 2016. Spatial Variability of the Background Diurnal Cycle of Deep Convection around the GoAmazon2014/5 Field Campaign Sites. *J. Appl. Meteorol. Climatol.* **55**, 1579–98. DOI: *https://doi.org/10.1175/JAMC-D-15-0229.1*

Burrows, S. M., Butler, T., Jöckel, P., Tost, H., Kerkweg, A., et al. 2009a. Bacteria in the global atmosphere – Part 2: Modeling of emissions and transport between different ecosystems. *Atmos. Chem. Phys.* **9**, 9281–97. DOI: *https://doi.org/10.5194/acp-9-9281-2009*

Burrows, S. M., Elbert, W., Lawrence, M. G., and Pöschl, U. 2009b. Bacteria in the global atmosphere – Part 1: Review and synthesis of literature data for different ecosystems. *Atmos. Chem. Phys.* **9**, 9263–80. DOI: *https://doi.org/10.5194/acp-9-9263-2009*

Butt, E. W., Conibear, L., Reddington, C. L., Darbyshire, E., Morgan, W. T., et al. 2020. Large air quality and human health impacts due to amazon forest and vegetation fires. *Environ. Res. Commun.* **2**, 1–18. DOI: *https://doi.org/10.1088/2515-7620/abb0db*

Buzorius, G., Rannik, Ü., Mäkelä, J. M., Keronen, P., Vesala, T., et al. 2000. Vertical aerosol fluxes measured by the eddy covariance method and deposition of nucleation mode particles above a Scots pine forest in southern Finland. *J. Geophys. Res.* **105**, 19905–16. DOI: *https://doi.org/10.1029/2000JD900108*

Buzorius, G., Rannik, Ü., Mäkelä, J. M., Vesala, T., and Kulmala, M. 1998. Vertical aerosol particle fluxes measured by eddy covariance technique using condensational particle counter. *J. Aerosol Sci.* **29**, 157–71. DOI: *https://doi.org/10.1016/S0021-8502(97)00458-8*

Byrne, M. P., Pendergrass, A. G., Rapp, A. D., and Wodzicki, K. R. 2018. Response of the Intertropical Convergence Zone to Climate Change: Location, Width, and Strength. *Curr. Clim. Chang. Reports* **4**, 355–70. DOI: *https://doi.org/10.1007/s40641-018-0110-5*

Camarinha-Neto, G. F., Cohen, J. C. P., Dias, C. Q., Sörgel, M., Cattanio, J. H., et al. 2021. The friagem event in the central Amazon and its influence on micrometeorological variables and atmospheric chemistry. *Atmos. Chem. Phys.* **21**, 339–56. DOI: *https://doi.org/10.5194/acp-21-339-2021*

Camponogara, G., Silva Dias, M. A. F., and Carrió, G. G. 2014. Relationship between Amazon biomass burning aerosols and rainfall over the la Plata Basin. *Atmos. Chem. Phys.* **14**, 4397–4407. DOI: *https://doi.org/10.5194/acp-14-4397-2014*

Camponogara, G., Da Silva Dias, M. A. F., and Carrió, G. G. 2018. Biomass burning CCN enhance the dynamics of a mesoscale convective system over the la Plata Basin: A numerical approach. *Atmos. Chem. Phys.* **18**, 2081–96. DOI: *https://doi.org/10.5194/acp-18-2081-2018*

Canadell, J. G., and Schulze, E. D. 2014. Global potential of biospheric carbon management for climate mitigation. *Nat. Commun.* **5**, 1–12. DOI: *https://doi.org/10.1038/ncomms6282*

Carvalho, A., Monteiro, A., Flannigan, M., Solman, S., Miranda, A. I., et al. 2011. Forest fires in a changing climate and their impacts on air quality. *Atmos. Environ.* **45**, 5545–53. DOI: *https://doi.org/10.1016/j.atmosenv.2011.05.010*

Cavalli, F., Facchini, M. C., Decesari, S., Emblico, L., Mircea, M., et al. 2006. Size-segregated aerosol chemical composition at a boreal site in southern Finland, during the QUEST project. *Atmos. Chem. Phys.* **6**, 993–1002. DOI: *https://doi.org/10.5194/acp-6-993-2006*

Cecchini, M. A., Machado, L. A. T., Andreae, M. O., Martin, S. T., Albrecht, R. I., et al. 2017. Sensitivities of Amazonian clouds to aerosols and updraft speed. *Atmos. Chem. Phys.* **17**, 10037–50. DOI: *https://doi.org/10.5194/acp-17-10037-2017*

Cecchini, M. A., Machado, L. A. T., and Artaxo, P. 2014. Droplet Size Distributions as a function of rainy system type and Cloud Condensation Nuclei concentrations. *Atmos. Res.* **143**, 301–12. DOI: *https://doi.org/10.1016/j.atmosres.2014.02.022*

Cecchini, M. A., Machado, L. A. T., Comstock, J. M., Mei, F., Wang, J., et al. 2016. Impacts of the Manaus pollution plume on the microphysical properties of Amazonian warm-phase clouds in the wet season. *Atmos. Chem. Phys.* **16**, 7029–7041. DOI: *https://doi.org/10.5194/acp-16-7029-2016*

Cerully, K. M., Raatikainen, T., Lance, S., Tkacik, D., Tiitta, P., et al. 2011. Aerosol hygroscopicity and CCN activation kinetics in a boreal forest environment during the 2007 EUCAARI campaign. *Atmos. Chem. Phys.* **11**, 12369–86. DOI: *https://doi.org/10.5194/acp-11-12369-2011*

Chakrabarty, R. K., Gyawali, M., Yatavelli, R. L. N., Pandey, A., Watts, A. C., et al. 2016. Brown carbon aerosols from burning of boreal peatlands: Microphysical properties, emission factors, and implications for direct radiative forcing. *Atmos. Chem. Phys.* **16**, 3033–40. DOI: *https://doi.org/10.5194/acp-16-3033-2016*

Chambers, J. Q., and Artaxo, P. 2017. Deforestation size influences rainfall. *Nat. Clim. Chang.* **7**, 175–76. DOI: *https://doi.org/10.1038/nclimate3238*

Chambers, J. Q., Higuchi, N., Tribuzy, E. S., and Trumbore, S. E. 2001. Carbon sink for a century. *Nature* **410**, 429–429. DOI: *https://doi.org/10.1038/35068624*

Chambers, J. Q., Negron-Juarez, R. I., Marra, D. M., Di Vittorio, A., Tews, J., et al. 2013. The steady-state mosaic of disturbance and succession across an old-growth Central Amazon forest landscape. *Proc. Natl. Acad. Sci. U. S. A.* **110**, 3949–54. DOI: *https://doi.org/10.1073/pnas.1202894110*

Chambers, J. Q., and Silver, W. L. 2004. Some aspects of ecophysiological and biogeochemical responses of tropical forests to atmospheric change. *Philos. Trans. R. Soc. Lond. B. Biol. Sci.* **359**, 463–76. DOI: *https://doi.org/10.1098/rstb.2003.1424*

Chand, D., Guyon, P., Artaxo, P., Schmid, O., Frank, G. P., et al. 2006. Optical and physical properties of aerosols in the boundary layer and free troposphere over the Amazon Basin during the biomass burning season. *Atmos. Chem. Phys.* **6**, 2911–25. DOI: *https://doi.org/10.5194/acp-6-2911-2006*

Chang, E. K. M., Lee, S., and Swanson, K. L. 2002. Storm track dynamics. *J. Clim.* **15**, 2163–83. DOI: *https://doi.org/10.1175/1520-0442(2002)015<02163:STD>2.0.CO;2*

Chapin, F. S., Sturm, M., Serreze, M. C., McFadden, J. P., Key, J. R., et al. 2005. Role of land-surface changes in arctic summer warming. *Science* **310**, 657–60. DOI: *https://doi.org/10.1126/science.1117368*

Chapman, W. L., and Walsh, J. E. 1993. Recent variations of sea ice and air temperature in high latitudes. *Bull. Amer. Meteor.* **74**, 33–47. DOI: *https://doi.org/10.1175/1520-0477(1993)074<0033:RVOSIA>2.0.CO;2*

Chen, Q., Farmer, D. K., Rizzo, L. V., Pauliquevis, T., Kuwata, M., et al. 2015. Submicron particle mass concentrations and sources in the Amazonian wet season (AMAZE-08). *Atmos. Chem. Phys.* **15**, 3687–3701. DOI: *https://doi.org/10.5194/acp-15-3687-2015*

Chen, Q., Farmer, D. K., Schneider, J., Zorn, S. R., Heald, C. L., et al. 2009. Mass spectral characterization of submicron biogenic organic particles in the Amazon Basin. *Geophys. Res. Lett.* **36**, L20806. DOI: *https://doi.org/10.1029/2009GL039880*

Chen, Y., Morton, D. C., Andela, N., van der Werf, G. R., Giglio, L., et al. 2017. A pan-tropical cascade of fire driven by El Niño/Southern Oscillation. *Nat. Clim. Chang.* **7**, 906–11. DOI: *https://doi.org/10.1038/s41558-017-0014-8*

Chen, X., Quéléver, L. L. J., Fung, P. L., Kesti, J., Rissanen, M. P., et al. 2018. Observations of ozone depletion events in a Finnish boreal forest. *Atmos. Chem. Phys.* **18**, 49–63. DOI: *https://doi.org/10.5194/acp-18-49-2018*

Chi, J., Nilsson, M. B., Kljun, N., Wallerman, J., Fransson, J. E. S., et al. 2019. The carbon balance of a managed boreal landscape measured from a tall tower in northern Sweden. *Agric. For. Meteorol.* **274**, 29–41. DOI: *https://doi.org/10.1016/j.agrformet.2019.04.010*

Chi, X., Winderlich, J., Mayer, J. C., Panov, A. V., Heimann, M., et al. 2013. Long-term measurements of aerosol and carbon monoxide at the ZOTTO tall tower to characterize polluted and pristine air in the Siberian taiga. *Atmos. Chem. Phys.* **13**, 12271–98. DOI: *https://doi.org/10.5194/acp-13-12271-2013*

China, S., Burrows, S. M., Wang, B., Harder, T. H., Weis, J., et al. 2018. Fungal spores as a source of sodium salt particles in the Amazon basin. *Nat. Commun.* **9**, 4793. DOI: *https://doi.org/10.1038/s41467-018-07066-4*

China, S., Wang, B., Weis, J., Rizzo, L., Brito, J., et al. 2016. Rupturing of Biological Spores As a Source of Secondary Particles in Amazonia. *Environ. Sci. Technol.* **50**, 12179–86. DOI: *https://doi.org/10.1021/acs.est.6b02896*

Ciais, P., Bombelli, A., Williams, M., Piao, S. L., Chave, J., et al. 2011. The carbon balance of Africa: synthesis of recent research studies. *Philos. Trans. R. Soc. A Math. Phys. Eng. Sci.* **369**, 2038–57. DOI: *https://doi.org/10.1098/rsta.2010.0328*

Cirino, G., Brito, J., Barbosa, H. M. J., Rizzo, L. V., Tunved, P., et al. 2018. Observations of Manaus urban plume evolution and interaction with biogenic emissions in GoAmazon 2014/5. *Atmos. Environ.* **191**, 513–24. DOI: *https://doi.org/10.1016/j.atmosenv.2018.08.031*

Cirino, G. G., Souza, R. A. F., Adams, D. K., and Artaxo, P. 2014. The effect of atmospheric aerosol particles and clouds on net ecosystem exchange in the Amazon. *Atmos. Chem. Phys.* **14**, 6523–43. DOI: *https://doi.org/10.5194/acp-14-6523-2014*

Claeys, M., Graham, B., Vas, G., Wang, W., Vermeylen, R., et al. 2004. Formation of Secondary Organic Aerosols Through Photooxidation of Isoprene. *Science* **303**, 1173–76. DOI: *https://doi.org/10.1126/science.1092805*

Claeys, M., Kourtchev, I., Pashynska, V., Vas, G., Vermeylen, R., et al. 2010. Polar organic marker compounds in atmospheric aerosols during the LBA-SMOCC 2002 biomass burning experiment in Rondônia, Brazil: Sources and source processes, time series, diel variations and size distributions. *Atmos. Chem. Phys.* **10**, 9319–31. DOI: *https://doi.org/10.5194/acp-10-9319-2010*

Clarke, A. D., Kapustin, V. N., Eisele, F. L., Weber, R. J., and McMurry, P. H. 1999. Particle production near marine clouds: Sulfuric acid and predictions from classical binary nucleation. *Geophys. Res. Lett.* **26**, 2425–28. DOI: *https://doi.org/10.1029/1999GL900438*

Clarke, A. D., Varner, J. L., Eisele, F., Mauldin, R. L., Tanner, D., et al. 1998. Particle production in the remote marine atmosphere: Cloud outflow and subsidence during ACE 1. *J. Geophys. Res.* **103**, 16397–409. DOI: *https://doi.org/10.1029/97JD02987*

Cochrane, M. A., Alencar, A., Schulze, M. D., Souza, C. M., Nepstad, D. C., et al. 1999. Positive feedbacks in the fire dynamic of closed canopy tropical forests. *Science* **284**, 1832–35. DOI: *https://doi.org/10.1126/science.284.5421.1832*

Cohen, J. C. P., Silva Dias, M. A. F., and Nobre, C. A. 1995. Environmental Conditions Associated with Amazonian Squall Lines: A Case Study. *Mon. Weather Rev.* **123**, 3163–74. DOI: *https://doi.org/10.1175/1520-0493(1995)123<3163:ECAWAS>2.0.CO;2*

Collaud Coen, M., Weingartner, E., Apituley, A., Ceburnis, D., Fierz-Schmidhauser, R., et al. 2010. Minimizing light absorption measurement artifacts of the Aethalometer: evaluation of five correction algorithms. *Atmos. Meas. Tech.* **3**, 457–74. DOI: *https://doi.org/10.5194/amt-3-457-2010*

Cooper, G. S., Willcock, S., and Dearing, J. A. 2020. Regime shifts occur disproportionately faster in larger ecosystems. *Nat. Commun.* **11**, 1–10. DOI: *https://doi.org/10.1038/s41467-020-15029-x*

Corrigan, A. L., Russell, L. M., Takahama, S., Äijälä, M., Ehn, M., et al. 2013. Biogenic and biomass burning organic aerosol in a boreal forest at Hyytiälä, Finland, during HUMPPA-COPEC 2010. *Atmos. Chem. Phys.* **13**, 12233–56. DOI: *https://doi.org/10.5194/acp-13-12233-2013*

Coursolle, C., Giasson, M. A., Margolis, H. A., and Bernier, P. Y. 2012. Moving towards carbon neutrality: CO_2 exchange of a black spruce forest ecosystem during the first 10 years of recovery after harvest. *Can. J. For. Res.* **42**, 1908–18. DOI: *https://doi.org/10.1139/x2012-133*

Covey, K., Soper, F., Pangala, S., Bernardino, A., Pagliaro, Z., et al. 2021. Carbon and Beyond: The Biogeochemistry of Climate in a Rapidly Changing Amazon. *Front. For. Glob. Chang.* **4**, 11. DOI: *https://doi.org/10.3389/ffgc.2021.618401*

Cox, P. M., Harris, P. P., Huntingford, C., Betts, R. A., Collins, M., et al. 2008. Increasing risk of Amazonian drought due to decreasing aerosol pollution. *Nature* **453**, 212–15. DOI: *https://doi.org/10.1038/nature06960*

Crippa, M., Canonaco, F., Lanz, V. A., Äijälä, M., Allan, J. D., et al. 2014. Organic aerosol components derived from 25 AMS data sets across Europe using a consistent ME-2 based source apportionment approach. *Atmos. Chem. Phys.* **14**, 6159–76. DOI: *https://doi.org/10.5194/acp-14-6159-2014*

Cronn, D. R., and Nutmagul, W. 1982. Analysis of atmospheric hydrocarbons during winter MONEX. *Tellus* **34**, 159–65. DOI: *https://doi.org/10.3402/tellusa.v34i2.10798*

Cros, B., Delmas, R., Nganga, D., Clairac, B., and Fontan, J. 1988. Seasonal trends of ozone in equatorial Africa: Experimental evidence of photochemical formation. *J. Geophys. Res.* **93**, 8355–66. DOI: *https://doi.org/10.1029/JD093iD07p08355*

Crutzen, P. J., Williams, J., Pöschl, U., Hoor, P., Fischer, H., et al. 2000. High spatial and temporal resolution measurements of primary organics and their oxidation products over the tropical forests of Surinam. *Atmos. Environ.* **34**, 1161–65. DOI: *https://doi.org/10.1016/S1352-2310(99)00482-3*

Crutzen, S. P. J., Coffey, M. T., Delany, A. C., Greenberg, J., Haagenson, P., et al. 1985. OBSERVATIONS OF AIR COMPOSITION IN BRAZIL BETWEEN THE EQUATOR AND 20°S DURING THE DRY. *Acta Amaz.* **15**, 77–119. DOI: *https://doi.org/10.1590/1809-43921985152119*

da Costa, A. C. L., Galbraith, D., Almeida, S., Portela, B. T. T., da Costa, M., et al. 2010. Effect of 7 yr of experimental drought on vegetation dynamics and biomass storage of an eastern Amazonian rainforest. *New Phytol.* **187**, 579–91. DOI: *https://doi.org/10.1111/j.1469-8137.2010.03309.x*

da Rocha, H. R., Manzi, A. O., Cabral, O. M., Miller, S. D., Goulden, M. L., et al. 2009. Patterns of water and heat flux across a biome gradient from tropical forest to savanna in brazil. *J. Geophys. Res.* **114**, 0–12. DOI: *https://doi.org/10.1029/2007JG000640*

Dada, L., Paasonen, P., Nieminen, T., Buenrostro Mazon, S., Kontkanen, J., et al. 2017. Long-term analysis of clear-sky new particle formation events and nonevents in Hyytiälä. *Atmos. Chem. Phys.* **17**, 6227–41. DOI: *https://doi.org/10.5194/acp-17-6227-2017*

Daellenbach, K., Kourtchev, I., Vogel, A., Bruns, E., Jiang, J., et al. 2019. Impact of anthropogenic and biogenic sources on the seasonal variation in the molecular composition of urban organic aerosols: A field and laboratory study using ultra-high-resolution mass spectrometry. *Atmos. Chem. Phys.* **19**, 5973–91. DOI: *https://doi.org/10.5194/acp-19-5973-2019*

Dal Maso, M., Kulmala, M., Riipinen, I., Wagner, R., Hussein, T., et al. 2005. Formation and growth of fresh atmospheric aerosols: Eight years of aerosol size distribution data from SMEAR II, Hyytiälä, Finland. *Boreal Environ. Res.* **10**, 323–36.

Dal Maso, M., and Sogacheva, L. 2007. Aerosol particle formation events at two Siberian stations inside the boreal forest. *Nucleation Atmos. Aerosols* 840–44. DOI: *https://doi.org/10.1007/978-1-4020-6475-3*

Dal Maso, M., Sogacheva, L., Aalto, P. P., Riipinen, I., Komppula, M., et al. 2007. Aerosol size distribution measurements at four Nordic field stations: Identification, analysis and trajectory analysis of new particle formation bursts. *Tellus B* **59**, 350–61. DOI: *https://doi.org/10.1111/j.1600-0889.2007.00267.x*

Darbyshire, E., Morgan, W. T., Allan, J. D., Liu, D., Flynn, M. J., et al. 2019. The vertical distribution of biomass burning pollution over tropical South America from aircraft in situ measurements during SAMBBA. *Atmos. Chem. Phys.* **19**, 5771–90. DOI: *https://doi.org/10.5194/acp-19-5771-2019*

Davidson, E. A., and Artaxo, P. 2004. Globally significant changes in biological processes of the Amazon Basin: results of the Large-scale Biosphere–Atmosphere Experiment. *Glob. Chang. Biol.* **10**, 519–29. DOI: *https://doi.org/10.1111/j.1529-8817.2003.00779.x*

Davidson, E. A., De Araüjo, A. C., Artaxo, P., Balch, J. K., Brown, I. F., et al. 2012. The Amazon basin in transition. *Nature* **481**, 321–28. DOI: *https://doi.org/10.1038/nature10717*

de Oliveira, G., Chen, J. M., Stark, S. C., Berenguer, E., Moutinho, P., et al. 2020. Smoke pollution's impacts in Amazonia. *Science* **369**, 634–35. DOI: *https://doi.org/10.1126/science.abd5942*

de Oliveira, B. F. A., de Carvalho, L. V. B., Mourão, D. de S., da Costa Mattos, R. de C. O., de Castro, H. A., et al. 2018. Environmental Exposure Associated with Oxidative Stress Biomarkers in Children and Adolescents Residents in Brazilian Western Amazon. *J. Environ. Prot.* **09**, 347–67. DOI: *https://doi.org/10.4236/jep.2018.94023*

de Sá, S. S., Palm, B. B., Campuzano-Jost, P., Day, D. A., Hu, W., et al. 2018. Urban influence on the concentration and composition of submicron particulate matter in central Amazonia. *Atmos. Chem. Phys.* **18**, 12185–206. DOI: *https://doi.org/10.5194/acp-18-12185-2018*

de Sá, S. S., Palm, B. B., Campuzano-Jost, P., Day, D. A., Newburn, M. K., et al. 2017. Influence of urban pollution on the production of organic particulate matter from isoprene epoxydiols in central Amazonia. *Atmos. Chem. Phys.* **17**, 6611–29. DOI: *https://doi.org/10.5194/acp-17-6611-2017*

de Sá, S. S., Rizzo, L. V., Palm, B. B., Campuzano-Jost, P., Day, D. A., et al. 2019. Contributions of biomass-burning, urban, and biogenic emissions to the concentrations and light-absorbing properties of particulate matter in central Amazonia during the dry season. *Atmos. Chem. Phys.* **19**, 7973–8001. DOI: *https://doi.org/10.5194/acp-19-7973-2019*

Decesari, S., Fuzzi, S., Facchini, M. C., Mircea, M., Emblico, L., et al. 2006. Characterization of the organic composition of aerosols from Rondônia, Brazil, during the LBA-SMOCC 2002 experiment and its representation through model compounds. *Atmos. Chem. Phys.* **6**, 375–402. DOI: *https://doi.org/10.5194/acp-6-375-2006*

Delort, A. M., Vaïtilingom, M., Amato, P., Sancelme, M., Parazols, M., et al. 2010. A short overview of the microbial population in clouds: Potential roles in atmospheric chemistry and nucleation processes. *Atmos. Res.* **98**, 249–60. DOI: *https://doi.org/10.1016/j.atmosres.2010.07.004*

Dengel, S., Grace, J., Aakala, T., Hari, P., Newberry, S. L., et al. 2013. Spectral characteristics of pine needles at the limit of tree growth in subarctic Finland. *Plant Ecol. Divers.* **6**, 31–44. DOI: *https://doi.org/10.1080/17550874.2012.754512*

Després, V., Huffman, Ja., Burrows, S. M., Hoose, C., Safatov, A., et al. 2012. Primary biological aerosol particles in the atmosphere: a review. *Tellus B* **64**, 1–58. DOI: *https://doi.org/10.3402/tellusb.v64i0.15598*

Di Lorenzo, R. A., Place, B. K., VandenBoer, T. C., and Young, C. J. 2018. Composition of Size-Resolved Aged Boreal Fire Aerosols: Brown Carbon, Biomass Burning Tracers, and Reduced Nitrogen. *ACS Earth Space Chem.* **2**, 278–85. doi: *10.1021/acsearthspacechem.7b00137*.

Dias-Junior, C. Q., Dias, N. L., Fuentes, J. D., and Chamecki, M. 2017. Convective storms and non-classical low-level jets during high ozone level episodes in the Amazon region: An ARM/GOAMAZON case study. *Atmos. Environ.* **155**, 199–209. DOI: *https://doi.org/10.1016/j.atmosenv.2017.02.006*

Díaz, S., Zafra-Calvo, N., Purvis, A., Verburg, P. H., Obura, D., et al. 2020. Set ambitious goals for biodiversity and sustainability. *Science* **370**, 411–13. DOI: *https://doi.org/10.1126/science.abe1530*

Diedhiou, A., Machado, L. A. T., and Laurent, H. 2010. Mean kinematic characteristics of synoptic easterly disturbances over the Atlantic. *Adv. Atmos. Sci.* **27**, 483–99. DOI: *https://doi.org/10.1007/s00376-009-9092-5*

Doerr, S. H., and Santín, C. 2016. Global trends in wildfire and its impacts: Perceptions versus realities in a changing world. *Philos. Trans. R. Soc. Lond. B. Biol. Sci.* **371**, 20150345. DOI: *https://doi.org/10.1098/rstb.2015.0345*

Donohoe, A., Marshall, J., Ferreira, D., Armour, K., and McGee, D. 2014. The Interannual Variability of Tropical Precipitation and Interhemispheric Energy Transport. *J. Clim.* **27**, 3377–92. DOI: *https://doi.org/10.1175/JCLI-D-13-00499.1*

dos Santos, M. J., Dias, M. A. F. S., and Freitas, E. D. 2014. Influence of local circulations on wind, moisture, and precipitation close to Manaus city, Amazon region, Brazil. *J. Geophys. Res.* **119**, 13,233-13,249. DOI: *https://doi.org/10.1002/2014JD021969*

Doughty, C. E., Metcalfe, D. B., Girardin, C. A. J., Amézquita, F. F., Cabrera, D. G., et al. 2015a. Drought impact on forest carbon dynamics and fluxes in Amazonia. *Nature* **519**, 78–82. DOI: *https://doi.org/10.1038/nature14213*

Doughty, C. E., Metcalfe, D. B., Girardin, C. A.J., Amezquita, F. F., Durand, L., et al. 2015b. Source and sink carbon dynamics and carbon allocation in the Amazon basin. *Global Biogeochem. Cycles* **29**, 645–55. DOI: *https://doi.org/10.1002/2014GB005028*

Dunn, A. L., Barford, C. C., Wofsy, S. C., Goulden, M. L., Daube, B. C., et al. 2007. A long-term record of carbon exchange in a boreal black spruce forest: means, responses to interannual variability, and decadal trends. *Glob. Chang. Biol.* **13**, 577–90. DOI: *https://doi.org/10.1111/j.1365-2486.2006.01221.x*

Dusek, U., Covert, D. S., Wiedensohler, A., Neusüss, C., Weise, D., et al. 2003. Cloud condensation nuclei spectra derived from size distributions and hygroscopic properties of the aerosol in coastal south-west Portugal during ACE-2. *Tellus B* **55**, 35–53. DOI: *https://doi.org/10.3402/tellusb.v55i1.16357*

Dusek, U., Frank, G. P., Curtius, J., Drewnick, F., Schneider, J., et al. 2010. Enhanced organic mass fraction and decreased hygroscopicity of cloud condensation nuclei (CCN) during new particle formation events. *Geophys. Res. Lett.* **37**, 3804. DOI: *https://doi.org/10.1029/2009GL040930*

Ebben, C. J., Martinez, I. S., Shrestha, M., Buchbinder, A. M., Corrigan, A. L., et al. 2011a. Contrasting organic aerosol particles from boreal and tropical forests during HUMPPA-COPEC-2010 and AMAZE-08 using coherent vibrational spectroscopy. *Atmos. Chem. Phys.* **11**, 10317–29. DOI: *https://doi.org/10.5194/acp-11-10317-2011*

Ebben, C. J., Shrestha, M., Martinez, I. S., Corrigan, A. L., Frossard, A. A., et al. 2012. Organic Constituents on the Surfaces of Aerosol Particles from Southern Finland, Amazonia, and California Studied by Vibrational Sum Frequency Generation. *J. Phys. Chem. A* **116**, 8271–90. DOI: *https://doi.org/10.1021/jp302631z*

Ebben, C. J., Zorn, S. R., Lee, S. B., Artaxo, P., Martin, S. T., et al. 2011b. Stereochemical transfer to atmospheric aerosol particles accompanying the oxidation of biogenic volatile organic compounds. *Geophys. Res. Lett.* **38**, 1–5. DOI: *https://doi.org/10.1029/2011GL048599*

Echalar, F., Artaxo, P., Martins, J. V., Yamasoe, M., Gerab, F., et al. 1998. Long-term monitoring of atmospheric aerosols in the Amazon Basin: Source identification and apportionment. *J. Geophys. Res.* **103**, 31849–64. DOI: *https://doi.org/10.1029/98JD01749*

Eck, T. F., Holben, B. N., Reid, J. S., O'Neill, N. T., Schafer, J. S., et al. 2003. High aerosol optical depth biomass burning events: A comparison of optical properties for different source regions. *Geophys. Res. Lett.* **30**, 1–4. DOI: *https://doi.org/10.1029/2003GL017861*

Ehn, M., Petäjä, T., Aufmhoff, H., Aalto, P., Hämeri, K., et al. 2007. Hygroscopic properties of ultrafine aerosol particles in the boreal forest: Diurnal variation, solubility and the influence of sulfuric acid. *Atmos. Chem. Phys.* **7**, 211–22. DOI: *https://doi.org/10.5194/acp-7-211-2007*

Ehn, M., Thornton, J. A., Kleist, E., Sipilä, M., Junninen, H., et al. 2014. A large source of low-volatility secondary organic aerosol. *Nature* **506**, 476–79. DOI: *https://doi.org/10.1038/nature13032*

Ekman, A. M. L., Engström, A., and Söderberg, A. 2011. Impact of two-way aerosol-cloud interaction and changes in aerosol size distribution on simulated aerosol-induced deep convective cloud sensitivity. *J. Atmos. Sci.* **68**, 685–98. DOI: *https://doi.org/10.1175/2010JAS3651.1*

Ekman, A. M. L., Krejci, R., Engström, A., Ström, J., de Reus, M., et al. 2008. Do organics contribute to small particle formation in the Amazonian upper troposphere? *Geophys. Res. Lett.* **35**, L17810. DOI: *https://doi.org/10.1029/2008GL034970*

Ekström, S., Nozière, B., Hultberg, M., Alsberg, T., Magnér, J., et al. 2010. A possible role of ground-based microorganisms on cloud formation in the atmosphere. *Biogeosciences* **7**, 387–94. DOI: *https://doi.org/10.5194/bg-7-387-2010*

Elbert, W., Taylor, P. E., Andreae, M. O., and Pöschl, U. 2007. Contribution of fungi to primary biogenic aerosols in the atmosphere: Wet and dry discharged spores, carbohydrates, and inorganic ions. *Atmos. Chem. Phys.* **7**, 4569–88. DOI: *https://doi.org/10.5194/acp-7-4569-2007*

Erb, K. H., Kastner, T., Plutzar, C., Bais, A. L. S., Carvalhais, N., et al. 2018. Unexpectedly large impact of forest management and grazing on global vegetation biomass. *Nature* **553**, 73–76. DOI: *https://doi.org/10.1038/nature25138*

Ezhova, E., Kerminen, V. M., Lehtinen, K. E. J., and Kulmala, M. 2018a. A simple model for the time evolution of the condensation sink in the atmosphere for intermediate Knudsen numbers. *Atmos. Chem. Phys.* **18**, 2431–42. DOI: *https://doi.org/10.5194/acp-18-2431-2018*

Ezhova, E., Ylivinkka, I., Kuusk, J., Komsaare, K., Vana, M., et al. 2018b. Direct effect of aerosols on solar radiation and gross primary production in boreal and hemiboreal forests. *Atmos. Chem. Phys.* **18**, 17863–81. DOI: *https://doi.org/10.5194/acp-18-17863-2018*

Falkovich, A. H., Graber, E. R., Schkolnik, G., Rudich, Y., Maenhaut, W., et al. 2005. Low molecular weight organic acids in aerosol particles from Rondônia, Brazil, during the biomass-burning, transition and wet periods. *Atmos. Chem. Phys.* **5**, 781–97. DOI: *https://doi.org/10.5194/acp-5-781-2005*

Fan, J., Comstock, J. M., and Ovchinnikov, M. 2010. The cloud condensation nuclei and ice nuclei effects on tropical anvil characteristics and water vapor of the tropical tropopause layer. *Environ. Res. Lett.* **5**, 044005. DOI: *https://doi.org/10.1088/1748-9326/5/4/044005*

Fan, J., Leung, L. R., Rosenfeld, D., Chen, Q., Li, Z., et al. 2013. Microphysical effects determine macrophysical response for aerosol impacts on deep convective clouds. *Proc. Natl. Acad. Sci. U. S. A.* **110**, E4581–90. DOI: *https://doi.org/10.1073/pnas.1316830110*

Fan, J., Rosenfeld, D., Zhang, Y., Giangrande, S. E., Li, Z., et al. 2018. Substantial convection and precipitation enhancements by ultrafine aerosol particles. *Science* **359**, 411–18. DOI: *https://doi.org/10.1126/science.aan8461*

FAO, 2015. Global Forest Resources Assessment 2015. UN Food and Agriculture Organization, Rome, Italy. ISBN 978-92-5-108826-5, 253 pg.

FAO, 2018: The state of world's forests 2018 – Forest pathways to sustainable development. FAO, Rome, 139 pp, ISBN 978-92-5-130561-4. *http://www.fao.org/publications/sofo/en/*.

Farmer, D. K., Chen, Q., Kimmel, J. R., Docherty, K. S., Nemitz, E., et al. 2013. Chemically resolved particle fluxes over tropical and temperate forests. *Aerosol Sci. Technol.* **47**, 818–30. DOI: *https://doi.org/10.1080/02786826.2013.791022*

Fauset, S., Johnson, M. O., Gloor, M., Baker, T. R., Monteagudo M., A., et al. 2015. Hyperdominance in Amazonian forest carbon cycling. *Nat. Commun.* **6**, 6857. DOI: *https://doi.org/10.1038/ncomms7857*

Feldpausch, T. R., Phillips, O. L., Brienen, R. J. W., Gloor, E., Lloyd, J., et al. 2016. Amazon forest response to repeated droughts. *Global Biogeochem. Cycles* **30**, 964–82. DOI: *https://doi.org/10.1002/2015GB005133*

Feng, L., Palmer, P. I., Bösch, H., Parker, R. J., Webb, A. J., et al. 2017. Consistent regional fluxes of CH_4 and CO_2 inferred from GOSAT proxy XCH_4:XCO_2 retrievals, 2010–2014. *Atmos. Chem. Phys.* **17**, 4781–97. DOI: *https://doi.org/10.5194/acp-17-4781-2017*

Feng, X., Merow, C., Liu, Z., Park, D. S., Roehrdanz, P. R., et al. 2021. How deregulation, drought and increasing fire impact Amazonian biodiversity. *Nature* **597**, 516–21. DOI: *https://doi.org/10.1038/s41586-021-03876-7*

Fernández-Martínez, M., Vicca, S., Janssens, I. A., Ciais, P., Obersteiner, M., et al. 2017. Atmospheric deposition, CO_2, and change in the land carbon sink. *Sci. Rep.* **7**, 9632. DOI: *https://doi.org/10.1038/s41598-017-08755-8*

Finessi, E., Decesari, S., Paglione, M., Giulianelli, L., Carbone, C., et al. 2012. Determination of the biogenic secondary organic aerosol fraction in the boreal forest by NMR spectroscopy. *Atmos. Chem. Phys.* **12**, 941–59. DOI: *https://doi.org/10.5194/acp-12-941-2012*

Fishman, J., Creilson, J. K., Parker, P. A., Ainsworth, E. A., Vining, G. G., et al. 2010. An investigation of widespread ozone damage to the soybean crop in the upper Midwest determined from ground-based and satellite measurements. *Atmos. Environ.* **44**, 2248–56. DOI: *https://doi.org/10.1016/j.atmosenv.2010.01.015*

Fitzjarrald, D. R., R. K. Sakai, O. L. L. Moraes, R. C. de Oliveira, O. C. Acevedo, M. J. et al. 2008. Spatial and temporal rainfall variability near the Amazon-Tapajós confluence. *J. Geophys. Res.* **113**, 1–17. DOI: *https://doi.org/10.1029/2007JG000596*

Fitzjarrald, D. R., Stormwind, B. L., Fisch, G., and Cabral, O. M. R. 1988. Turbulent transport observed just above the Amazon forest. *J. Geophys. Res.* **93**, 1551–63. DOI: *https://doi.org/10.1029/JD093iD02p01551*

Flannigan, M. D., Krawchuk, M. A., De Groot, W. J., Wotton, B. M., and Gowman, L. M. 2009. Implications of changing climate for global wildland fire. *Int. J. Wildl. Fire* **18**, 483–507. DOI: *https://doi.org/10.1071/WF08187*

Forkel, M., Carvalhais, N., Rödenbeck, C., Keeling, R., Heimann, M., et al. 2016. Enhanced seasonal CO_2 exchange caused by amplified plant productivity in northern ecosystems. *Science* **351**, 696–99. DOI: *https://doi.org/10.1126/science.aac4971*

Formenti, P., Andreae, M. O., Lange, L., Roberts, G., Cafmeyer, J., et al. 2001. Saharan dust in Brazil and Suriname during the Large-Scale Biosphere-Atmosphere Experiment in Amazonia (LBA) – Cooperative LBA Regional Experiment (CLAIRE) in March 1998. *J. Geophys. Res.* **106**, 14919–34. DOI: *https://doi.org/10.1029/2000JD900827*

Formenti, P., Rajot, J. L., Desboeufs, K., Caquineau, S., Chevaillier, S., et al. 2008. Regional variability of the composition of mineral dust from western Africa: Results from the AMMA SOP0/DABEX and DODO field campaigns. *J. Geophys. Res.* **113**, D00C13. DOI: *https://doi.org/10.1029/2008JD009903*

Fraund, M., Pham, D. Q., Bonanno, D., Harder, T. H., Wang, B., et al. 2017. Elemental Mixing State of Aerosol Particles Collected in Central Amazonia during GoAmazon2014/15, *Atmosphere*, **8**, 173. DOI: *https://doi.org/10.3390/atmos8090173*

Freedman, J. M., D. R. Fitzjarrald, K. E. Moore, and R. K. Sakai. 2001. Boundary Layer Clouds and Vegetation–Atmosphere Feedbacks. *J. Clim.* **14**, 180–97. DOI: *https://doi.org/10.1175/1520-0442(2001)013<0180:BLCAVA>2.0.CO;2*

Freire, L. S., Gerken, T., Ruiz-Plancarte, J., Wei, D., Fuentes, J. D., et al. 2017. Turbulent mixing and removal of ozone within an Amazon rainforest canopy. *J. Geophys. Res.* **122**, 2791–2811. DOI: *https://doi.org/10.1002/2016JD026009*

Freitas, S. R., Longo, K. M., Silva Dias, M. A. F., Silva Dias, P. L., Chatfield, R., et al. 2005. Monitoring the transport of biomass burning emissions in South America. *Environ. Fluid Mech.* **5**, 135–67. DOI: *https://doi.org/10.1007/s10652-005-0243-7*

Freitas, S. R., Panetta, J., Longo, K. M., Rodrigues, L. F., Moreira, D. S., et al. 2017. The Brazilian developments on the Regional Atmospheric Modeling System (BRAMS 5.2): An integrated environmental model tuned for tropical areas. *Geosci. Model Dev.* **10**, 189–222. DOI: *https://doi.org/10.5194/gmd-10-189-2017*

Freud, E., Rosenfeld, D., Andreae, M. O., Costa, A. A., and Artaxo, P. 2008a. Robust relations between CCN and the vertical evolution of cloud drop size distribution in deep convective clouds. *Atmos. Chem. Phys.* **8**, 1661–75. DOI: *https://doi.org/10.5194/acp-8-1661-2008*

Freud, E., Ström, J., Rosenfeld, D., Tunved, P., and Swietlicki, E. 2008b. Anthropogenic aerosol effects on convective cloud microphysical properties in southern Sweden. *Tellus B* **60**, 286–97. DOI: *https://doi.org/10.1111/j.1600-0889.2007.00337.x*

Friedlingstein, P., Jones, M. W., O'Sullivan, M., Andrew, R. M., Hauck, J., et al. 2019. Global carbon budget 2019. *Earth Syst. Sci. Data* **11**, 1783–1838. DOI: *https://doi.org/10.5194/essd-11-1783-2019*

Fröhlich-Nowoisky, J., Burrows, S. M., Xie, Z., Engling, G., Solomon, P. A., et al. 2012. Biogeography in the air: Fungal diversity over land and oceans. *Biogeosciences* **9**, 1125–36. DOI: *https://doi.org/10.5194/bg-9-1125-2012*

Fröhlich-Nowoisky, J., Hill, T. C. J., Pummer, B. G., Yordanova, P., Franc, G. D. et al. 2015. Ice nucleation activity in the widespread soil fungus Mortierella alpina, *Biogeosciences*, **12**, 1057–1071. DOI: *https://doi.org/10.5194/bg-12-1057-2015*

Fröhlich-Nowoisky, J., Kampf, C. J., Weber, B., Huffman, J. A., Pöhlker, C., et al. 2016. Bioaerosols in the Earth system: Climate, health, and ecosystem interactions. *Atmos. Res.* **182**, 346–76. DOI: *https://doi.org/10.1016/j.atmosres.2016.07.018*

Fu, R., Yin, L., Li, W., Arias, P. A., Dickinson, R. E., et al. 2013. Increased dry-season length over southern Amazonia in recent decades and its implication for future climate projection. *Proc. Natl. Acad. Sci. U. S. A.* **110**, 18110–15. DOI: *https://doi.org/10.1073/pnas.1302584110*

Fuhrer, J., Skärby, L., and Ashmore, M. R. 1997. Critical levels for ozone effects on vegetation in Europe. *Environ. Pollut.* **97**, 91–106. DOI: *https://doi.org/10.1016/S0269-7491(97)00067-5*

Fuss, S., Lamb, W. F., Callaghan, M. W., Hilaire, J., Creutzig, F., et al. 2018. Negative emissions – Part 2: Costs, potentials and side effects. *Environ. Res. Lett.* **13**, 063002. DOI: *https://doi.org/10.1088/1748-9326/aabf9f*

Fuzzi, S., Decesari, S., Facchini, M. C., Cavalli, F., Emblico, L., et al. 2007. Overview of the inorganic and organic composition of size-segregated aerosol in Rondônia, Brazil, from the biomass-burning period to the onset of the wet season. *J. Geophys. Res.* **112**, D01201. DOI: *https://doi.org/10.1029/2005JD006741*

Gabey, A. M., Gallagher, M. W., Whitehead, J., Dorsey, J. R., Kaye, P. H., et al. 2010. Measurements and comparison of primary biological aerosol above and below a tropical forest canopy using a dual channel fluorescence spectrometer. *Atmos. Chem. Phys.* **10**, 4453–66. DOI: *https://doi.org/10.5194/acp-10-4453-2010*

Gabey, A., Stanley, W., Gallagher, M., and Kaye, P. H. 2011. The fluorescence properties of aerosol larger than 0.8 μm in urban and tropical rainforest locations, *Atmos. Chem. Phys.*, **11**, 5491–5504. DOI: *https://doi.org/10.5194/acp-11-5491-2011*

Gatti, L. V., Basso, L. S., Miller, J. B., Gloor, M., Gatti Domingues, L., et al. 2021. Amazonia as a carbon source linked to deforestation and climate change. *Nature* **595**, 388–93. DOI: *https://doi.org/10.1038/s41586-021-03629-6*

Gatti, L. V., Gloor, M., Miller, J. B., Doughty, C. E., Malhi, Y., et al. 2014. Drought sensitivity of Amazonian carbon balance revealed by atmospheric measurements. *Nature* **506**, 76–80. DOI: *https://doi.org/10.1038/nature12957*

Gatti, L. V., Miller, J. B., D'amelio, M. T. S., Martinewski, A., Basso, L. S., et al. 2010. Vertical profiles of CO_2 above eastern Amazonia suggest a net carbon flux to the atmosphere and balanced biosphere between 2000 and 2009. *Tellus B* **62**, 581–94. DOI: *https://doi.org/10.1111/j.1600-0889.2010.00484.x*

Gauthier, S., Bernier, P., Kuuluvainen, T., Shvidenko, A. Z., and Schepaschenko, D. G. 2015. Boreal forest health and global change. *Science* **349**, 819–22. DOI: *https://doi.org/10.1126/science.aaa9092*

Gedney, N., Cox, P. M., and Huntingford, C. 2004. Climate feedback from wetland methane emissions. *Geophys. Res. Lett.* **31**, L20503. DOI: *https://doi.org/10.1029/2004GL020919*

Gerken, T., Chamecki, M., and Fuentes, J. D. 2017. Air-Parcel Residence Times Within Forest Canopies. *Boundary-Layer Meteorol.* **165**, 29–54. DOI: *https://doi.org/10.1007/s10546-017-0269-7*

Gerken, T., Wei, D., Chase, R. J., Fuentes, J. D., Schumacher, C., et al. 2016. Downward transport of ozone rich air and implications for atmospheric chemistry in the Amazon rainforest. *Atmos. Environ.* **124**, 64–76. DOI: *https://doi.org/10.1016/j.atmosenv.2015.11.014*

Geron, C., Guenther, A., Greenberg, J., Loescher, H. W., Clark, D., et al. 2002. Biogenic volatile organic compound emissions from a lowland tropical wet forest in Costa Rica. *Atmos. Environ.* **36**, 3793–3802. DOI: *https://doi.org/10.1016/S1352-2310(02)00301-1*

Geron, C., Owen, S., Guenther, A., Greenberg, J., Rasmussen, R., et al. 2006. Volatile organic compounds from vegetation in southern Yunnan Province, China: Emission rates and some potential regional implications. *Atmos. Environ.* **40**, 1759–73. DOI: *https://doi.org/10.1016/j.atmosenv.2005.11.022*

Gettelman, A., Morrison, H., Santos, S., Bogenschutz, P., and Caldwell, P. M. 2015. Advanced two-moment bulk microphysics for global models. Part II: Global model

solutions and aerosol-cloud interactions. *J. Clim.* **28**, 1288–1307. DOI: *https://doi.org/10.1175/JCLI-D-14-00103.1*

Ghimire, R. P., Markkanen, J. M., Kivimäenpää, M., Lyytikäinen-Saarenmaa, P., and Holopainen, J. K. 2013. Needle removal by pine sawfly larvae increases branch-level VOC emissions and reduces below-ground emissions of scots pine. *Environ. Sci. Technol.* **47**, 4325–32. DOI: *https://doi.org/10.1021/es4006064*

Ghirardo, A., K. Koch, R. Taipale, I. Zimmer, J.-P. Schnitzler et al. 2010. Determination of de novo and pool emissions of terpenes from four common boreal/alpine trees by 13 CO_2 labeling and PTR-MS analysis. *Plant Cell Environ.* **33**, 781–792. DOI: *https://doi.org/10.1111/j.1365-3040.2009.02104.x*

Giangrande, S. E., Feng, Z., Jensen, M. P., Comstock, J. M., Johnson, K. L., et al. 2017. Cloud characteristics, thermodynamic controls and radiative impacts during the Observations and Modeling of the Green Ocean Amazon (GoAmazon2014/5) experiment. *Atmos. Chem. Phys.* **17**, 14519–41. DOI: *https://doi.org/10.5194/acp-17-14519-2017*

Gibson, M. D., Pierce, J. R., Waugh, D., Kuchta, J. S., Chisholm, L., et al. 2013. Identifying the sources driving observed PM2.5 temporal variability over Halifax, Nova Scotia, during BORTAS-B. *Atmos. Chem. Phys.* **13**, 7199–7213. DOI: *https://doi.org/10.5194/acp-13-7199-2013*

Giglio, L., Randerson, J. T., and Van Der Werf, G. R. 2013. Analysis of daily, monthly, and annual burned area using the fourth-generation global fire emissions database (GFED4). *J. Geophys. Res.* **118**, 317–28. DOI: *https://doi.org/10.1002/jgrg.20042*

Gilardoni, S., Vignati, E., Marmer, E., Cavalli, F., Belis, C., et al. 2011. Sources of carbonaceous aerosol in the Amazon basin. *Atmos. Chem. Phys.* **11**, 2747–64. DOI: *https://doi.org/10.5194/acp-11-2747-2011*

Gilbert, G. S., and Reynolds, D. R. 2005. Nocturnal fungi: Airborne spores in the canopy and understory of a tropical rain forest. *Biotropica* **37**, 462–64. DOI: *https://doi.org/10.1111/j.1744-7429.2005.00061.x*

Glicker, H. S., Lawler, M. J., Ortega, J., De Sá, S. S., Martin, S. T., et al. 2019. Chemical composition of ultrafine aerosol particles in central Amazonia during the wet season. *Atmos. Chem. Phys.* **19**, 13053–66. DOI: *https://doi.org/10.5194/acp-19-13053-2019*

Gloor, E. 2019. The fate of Amazonia. *Nat. Clim. Chang.* **9**, 355–56. DOI: *https://doi.org/10.1038/s41558-019-0465-1*

Gloor, M., Barichivich, J., Ziv, G., Brienen, R., Schöngart, J., et al. 2015. Recent Amazon climate as background for possible ongoing and future changes of Amazon humid forests. *Global Biogeochem. Cycles* **29**, 1384–99. DOI: *https://doi.org/10.1002/2014GB005080*

Gloor, M., Brienen, R. J. W., Galbraith, D., Feldpausch, T. R., Schöngart, J., et al. 2013. Intensification of the Amazon hydrological cycle over the last two decades. *Geophys. Res. Lett.* **40**, 1729–33. DOI: *https://doi.org/10.1002/grl.50377*

Gloor, M., Gatti, L., Brienen, R., Feldpausch, T. R., Phillips, O. L., et al. 2012. The carbon balance of South America: A review of the status, decadal trends and main determinants. *Biogeosciences* **9**, 5407–30. DOI: *https://doi.org/10.5194/bg-9-5407-2012*

Gonçalves, K. dos S., Winkler, M. S., Benchimol-Barbosa, P. R., de Hoogh, K., Artaxo, P. E., et al. 2018. Development of non-linear models predicting daily fine particle concentrations using aerosol optical depth retrievals and ground-based measurements at a municipality in the Brazilian Amazon region. *Atmos. Environ.* **184**, 156–65. DOI: *https://doi.org/10.1016/j.atmosenv.2018.03.057*

González, N. J. D., Borg-Karlson, A. K., Artaxo, P., Guenther, A., Krejci, R., et al. 2014. Primary and secondary organics in the tropical Amazonian rainforest aerosols: Chiral analysis of 2-methyltetraols. *Environ. Sci. Process. Impacts* **16**, 1413–21. DOI: *https://doi.org/10.1039/c4em00102h*

Gouveia, D. A., Barja, B., Barbosa, H. M. J., Seifert, P., Baars, H., et al. 2017. Optical and geometrical properties of cirrus clouds in Amazonia derived from 1 year of ground-based lidar measurements. *Atmos. Chem. Phys.* **17**, 3619–36. DOI: *https://doi.org/10.5194/acp-17-3619-2017*

Grabowski, W. W. 2015. Untangling microphysical impacts on deep convection applying a novel modeling methodology. *J. Atmos. Sci.* **72**, 2446–64. DOI: *https://doi.org/10.1175/JAS-D-14-0307.1*

Grabowski, W. W., and Morrison, H. 2016. Untangling microphysical impacts on deep convection applying a novel modeling methodology. Part II: Double-moment microphysics. *J. Atmos. Sci.* **73**, 3749–70. DOI: *https://doi.org/10.1175/JAS-D-15-0367.1*

Grace, J., Mitchard, E., and Gloor, E. 2014. Perturbations in the carbon budget of the tropics. *Glob. Chang. Biol.* **20**, 3238–55. DOI: *https://doi.org/10.1111/gcb.12600*

Graham, B., Guyon, P., Maenhaut, W., Taylor, P. E., Ebert, M., et al. 2003b. Composition and diurnal variability of the natural Amazonian aerosol. *J. Geophys. Res.* **108**. DOI: *https://doi.org/10.1029/2003JD004049*

Graham, B., Guyon, P., Taylor, P. E., Artaxo, P., Maenhaut, W., et al. 2003a. Organic compounds present in the natural Amazonian aerosol: Characterization by gas chromatography-mass spectrometry. *J. Geophys. Res.* **108**, 4766. DOI: *https://doi.org/10.1029/2003JD003990*

Graham, B., Mayol-Bracero, O. L., Guyon, P., Roberts, G. C., Decesari, S., et al. 2002. Water-soluble organic compounds in biomass burning aerosols over Amazonia 1. Characterization by NMR and GC-MS. *J. Geophys. Res.* **107**, LBA 14-1-LBA 14-16. DOI: *https://doi.org/10.1029/2001JD000336*

Grant, L. D., and van den Heever, S. C. 2015. Cold pool and precipitation responses to aerosol loading: Modulation by dry layers. *J. Atmos. Sci.* **72**, 1398–1408. DOI: *https://doi.org/10.1175/JAS-D-14-0260.1*

Grantham, H. S., Duncan, A., Evans, T. D., Jones, K. R., Beyer, H. L., et al. 2020. Anthropogenic modification of forests means only 40% of remaining forests have high ecosystem integrity. *Nat. Commun.* **11**, 5978. DOI: *https://doi.org/10.1038/s41467-020-19493-3*

Greenberg, J. P. 1999. Biogenic volatile organic compound emissions in central Africa during the Experiment for the Regional Sources and Sinks of Oxidants (EXPRESSO) biomass burning season. *J. Geophys. Res.* **104**, 30659–71. DOI: *https://doi.org/10.1029/1999JD900475*

Greenberg, J. P., Guenther, A. B., Pétron, G., Wiedinmyer, C., Vega, O., et al. 2004. Biogenic VOC emissions from forested Amazonian landscapes. *Glob. Chang. Biol.* **10**, 651–62. DOI: *https://doi.org/10.1111/j.1365-2486.2004.00758.x*

Gregory, P. H. 1978. Distribution of airborne pollen and spores and their long distance transport. *Pure Appl. Geophys. PAGEOPH* **116**, 309–15. DOI: *https://doi.org/10.1007/BF01636888*

Greve, P., Orlowsky, B., Mueller, B., Sheffield, J., Reichstein, M., et al. 2014. Global assessment of trends in wetting and drying over land. *Nat. Geosci.* **7**, 716–21. DOI: *https://doi.org/10.1038/ngeo2247*

Griscom, B. W., Adams, J., Ellis, P. W., Houghton, R. A., Lomax, G., et al. 2017. Natural climate solutions. *Proc. Natl. Acad. Sci. U. S. A.* **114**, 11645–50. DOI: *https://doi.org/10.1073/pnas.1710465114*

Grote, R., Monson, R. K., and Niinemets, Ü. 2013. Leaf-level models of constitutive and stress-driven volatile organic compound emissions, 315–355, in Biology, Controls and Models of Tree Volatile Organic Compound Emissions, ed. U. Niinemets and R.K. Monson, Springer, 2013, ISBN 978-94-017-8384-2. DOI: *https://doi.org/10.1007/978-94-007-6606-8*

Gryspeerdt, E., Stier, P., and Partridge, D. G. 2014. Links between satellite-retrieved aerosol and precipitation. *Atmos. Chem. Phys.* **14**, 9677–94. DOI: *https://doi.org/10.5194/acp-14-9677-2014*

Gryspeerdt, E., Stier, P., White, B. A., and Kipling, Z. 2015. Wet scavenging limits the detection of aerosol effects on precipitation. *Atmos. Chem. Phys.* **15**, 7557–70. DOI: *https://doi.org/10.5194/acp-15-7557-2015*

Gu, D., Guenther, A. B., Shilling, J. E., Yu, H., Huang, M., Zhao, C., et al. 2017. Airborne observations reveal elevational gradient in tropical forest isoprene emissions, *Nat Commun*, **8**, 15541. DOI: *https://doi.org/10.1038/ncomms15541*

Gu, L., Baldocchi, D., Verma, S. B., Black, T. A., Vesala, T., et al. 2002. Advantages of diffuse radiation for terrestrial ecosystem productivity. *J. Geophys. Res.* **107**, D6. DOI: *https://doi.org/10.1029/2001JD001242*

Guenther, A. 1995. A global model of natural volatile organic compound emissions. *J. Geophys. Res.* **100**, 8873–92. DOI: *https://doi.org/10.1029/94JD02950*

Guenther, A. 1999. Isoprene emission estimates and uncertainties for the Central African EXPRESSO study domain. *J. Geophys. Res.* **104**, 30625–39. DOI: *https://doi.org/10.1029/1999JD900391*

Guenther, A. 2013. Biological and Chemical Diversity of Biogenic Volatile Organic Emissions into the Atmosphere. *ISRN Atmos. Sci.* **2013**, 1–27. DOI: *https://doi.org/10.1155/2013/786290*

Guenther, A. B., Jiang, X., Heald, C. L., Sakulyanontvittaya, T., Duhl, T., et al. 2012. The Model of Emissions of Gases and Aerosols from Nature version 2.1 (MEGAN2.1): an extended and updated framework for modeling biogenic emissions, *Geosci. Model Dev.*, **5**, 1471–1492. DOI: *https://doi.org/10.5194/gmd-5-1471-2012*

Guenther, A., Karl, T., Harley, P., Wiedinmyer, C., Palmer, P. I., et al. 2006. Estimates of global terrestrial isoprene emissions using MEGAN (Model of Emissions of Gases and Aerosols from Nature). *Atmos. Chem. Phys.* **6**, 3181–3210. DOI: *https://doi.org/10.5194/acp-6-3181-2006*

Guenther, A. B., Monson, R. K., and Fall, R. 1991. Isoprene and monoterpene emission rate variability: Observations with eucalyptus and emission rate algorithm development. *J. Geophys. Res.* **96**, 10799. DOI: *https://doi.org/10.1029/91JD00960*

Gunthe, S. S., King, S. M., Rose, D., Chen, Q., Roldin, P., et al. 2009. Cloud condensation nuclei in pristine tropical rainforest air of Amazonia: size-resolved measurements and modeling of atmospheric aerosol composition and CCN activity. *Atmos. Chem. Phys.* **9**, 7551–75. DOI: *https://doi.org/10.5194/acp-9-7551-2009*

Haapanala, S., Ekberg, A., Hakola, H., Tarvainen, V., Rinne, J., et al. 2009. Mountain birch – Potentially large source of sesquiterpenes into high latitude atmosphere. *Biogeosciences* **6**, 2709–18. DOI: *https://doi.org/10.5194/bg-6-2709-2009*

Haapanala, S., Hakola, H., Hellén, H., Vestenius, M., Levula, J., et al. 2012. Is forest management a significant source of monoterpenes into the boreal atmosphere? *Biogeosciences* **9**, 1291–1300. DOI: *https://doi.org/10.5194/bg-9-1291-2012*

Haapanala, S., Rinne, J., Pystynen, K. H., Hellén, H., Hakola, H., et al. 2006. Measurements of hydrocarbon emissions from a boreal fen using the REA technique. *Biogeosciences* **3**, 103–12. DOI: *https://doi.org/10.5194/bg-3-103-2006*

Haghtalab, N., Moore, N., Heerspink, B. P., and Hyndman, D. W. 2020. Evaluating spatial patterns in precipitation trends across the Amazon basin driven by land cover and global scale forcings. *Theor. Appl. Climatol.* **140**, 411–27. DOI: *https://doi.org/10.1007/s00704-019-03085-3*

Häkkinen, S. A. K., Äijälä, M., Lehtipalo, K., Junninen, H., Backman, J., et al. 2012. Long-term volatility measurements of submicron atmospheric aerosol in Hyytiälä, Finland. *Atmos. Chem. Phys.* **12**, 10771–86. DOI: *https://doi.org/10.5194/acp-12-10771-2012*

Hakola, H., Hellén, H., Hemmilä, M., Rinne, J., and Kulmala, M. 2012. In situ measurements of volatile organic compounds in a boreal forest. *Atmos. Chem. Phys.* **12**, 11665–78. DOI: *https://doi.org/10.5194/acp-12-11665-2012*

Hakola, H., Laurila, T., Lindfors, V., Hellén, H., Gaman A. et al. 2001. Variation of the VOC emission rates of birch species during the growing season. *Boreal Environ. Res.*, **6**, 237–249.

Hakola, H., Rinne, J., and Laurila, T. 1998. The hydrocarbon emission rates of tea-leafed willow (Salix phylicifolia), silver birch (Betula pendula) and European aspen (Populus tremula). *Atmos. Environ.* **32**, 1825–33. DOI: *https://doi.org/10.1016/S1352-2310(97)00482-2*

Hakola, H., Tarvainen, V., Bäck, J., Ranta, H., Bonn, B., et al. 2006. Seasonal variation of mono- and sesquiterpene emission rates of Scots pine. *Biogeosciences* **3**, 93–101. DOI: *https://doi.org/10.5194/bg-3-93-2006*

Hakola, H., Tarvainen, V., Laurila, T., Hiltunen, V., Hellén, H., et al. 2003. Seasonal variation of VOC concentrations above a boreal coniferous forest. *Atmos. Environ.* **37**, 1623–34. DOI: *https://doi.org/10.1016/S1352-2310(03)00014-1*

Hakola, H., Tarvainen, V., Praplan, A. P., Jaars, K., Hemmilä, M., et al. 2017. Terpenoid and carbonyl emissions from Norway spruce in Finland during the growing season. *Atmos. Chem. Phys.* **17**, 3357–70. DOI: *https://doi.org/10.5194/acp-17-3357-2017*

Hallquist, M., Wenger, J. C., Baltensperger, U., Rudich, Y., Simpson, D., et al. 2009. The formation, properties and impact of secondary organic aerosol: Current and emerging issues. *Atmos. Chem. Phys.* **9**, 5155–5236. DOI: *https://doi.org/10.5194/acp-9-5155-2009*

Hämeri, K., Väkevä, M., Aalto, P. P., Kulmala, M., Swietlicki, E., et al. 2001. Hygroscopic and CCN properties of aerosol particles in boreal forests. *Tellus B* **53**, 359–79. DOI: *https://doi.org/10.3402/tellusb.v53i4.16609*

Hanes, C. C., Wang, X., Jain, P., Parisien, M. A., Little, J. M., et al. 2019. Fire-regime changes in canada over the last half century. *Can. J. For. Res.* **49**, 256–69. DOI: *https://doi.org/10.1139/cjfr-2018-0293*

Hansen, J., Sato, M., and Ruedy, R. 1997. Radiative forcing and climate response. *J. Geophys. Res.* **102**, 6831–64. DOI: *https://doi.org/10.1029/96JD03436*

Hansen, M. C., Wang, L., Song, X. P., Tyukavina, A., Turubanova, S., et al. 2020. The fate of tropical forest fragments. *Sci. Adv.* **6**. DOI: *https://doi.org/10.1126/sciadv.aax8574*

Hantson, S., Arneth, A., Harrison, S. P., Kelley, D. I., Prentice, I. C., et al. 2016. The status and challenge of global fire modelling. *Biogeosciences*, **13**, 3359–3375. DOI: *https://doi.org/10.5194/bg-13-3359-2016*

Hari, P. and Kulmala, M., 2005. Station for Measuring Ecosystem–Atmosphere Relations (SMEAR II). *Bor. Env. Res.*, **10**, 315–322.

Harley, P., Vasconcellos, P., Vierling, L., Pinheiro, C. C. D., Greenberg, J., et al. Variation in potential for isoprene emissions among Neotropical forest sites. *Glob. Change Biol.*, **10**, 630–650, 2004. DOI: *https://doi.org/10.1111/j.1529-8817.2003.00760.x*

Harris, Z. M., Spake, R., and Taylor, G. 2015. Land use change to bioenergy: A meta-analysis of soil carbon and GHG emissions. *Biomass and Bioenergy*. **82**, 27–39. DOI: *https://doi.org/10.1016/j.biombioe.2015.05.008*

Harrison, S. P., Marlon, J. R., and Bartlein, P. J. 2010. Fire in the Earth System. *Chang. Clim. Earth Syst. Soc.* **324**, 21–48. DOI: *https://doi.org/10.1007/978-90-481-8716-4_3*

Heald, C. L., and Spracklen, D. V. 2009. Atmospheric budget of primary biological aerosol particles from fungal spores. *Geophys. Res. Lett.* **36**. DOI: *https://doi.org/10.1029/2009GL037493*

Healy, D. A., Huffman, J. A., O'Connor, D. J., Pöhlker, C., Pöschl, U., et al. 2014. Ambient measurements of biological aerosol particles near Killarney, Ireland: A comparison between real-time fluorescence and microscopy techniques. *Atmos. Chem. Phys.* **14**, 8055–69. DOI: *https://doi.org/10.5194/acp-14-8055-2014*

Heffernan, O. 2016. The mystery of the expanding tropics. *Nature* **530**, 20–22. DOI: *https://doi.org/10.1038/530020a*

Heikenfeld, M., White, B., Labbouz, L., and Stier, P. 2019. Aerosol effects on deep convection: The propagation of aerosol perturbations through convective cloud microphysics. *Atmos. Chem. Phys.* **19**, 2601–27. DOI: *https://doi.org/10.5194/acp-19-2601-2019*

Heikkinen, L., Äijälä, M., Riva, M., Luoma, K., Dällenbach, K., et al. 2020. Long-term sub-micrometer aerosol chemical composition in the boreal forest: Inter- And intra-annual variability. *Atmos. Chem. Phys.* **20**, 3151–80. DOI: *https://doi.org/10.5194/acp-20-3151-2020*

Heimann, M. 2002. The EUROSIBERIAN CARBONFLUX project. *Tellus B* **54**, 417–19. DOI: *https://doi.org/10.3402/tellusb.v54i5.16676*

Heimann, M. 2008. The Zotino Tall Tower Observatory (ZOTTO): A 300m tall tower for long-term atmospheric monitoring of biogeochemical changes in central Siberia, *Geop. Res. Abstr.* **10**, 2156–2202. Ref-ID: 1607-7962/gra/EGU2008-A-10738.

Heimann, M., Schulze, E.-D., Winderlich, J., Andreae, M. O., Chi, X., et al. 2014. The Zotino Tall Tower Observatory (ZOTTO): Quantifying large scale biogeochemical changes in Central Siberia. *Nova Acta Leopold*. **117**, 51–64.

Heinritzi, M., Dada, L., Simon, M., Stolzenburg, D., Wagner, A. C., et al. 2020. Molecular understanding of the suppression of new-particle formation by isoprene. *Atmos. Chem. Phys.* **20**, 11809–21. DOI: *https://doi.org/10.5194/acp-20-11809-2020*

Heintzenberg, J., and Birmili, W. 2010. Aerosols over the Siberian Forest: The ZOTTO project. *J. Cryog. Soc. Japan* **68**, 5–8.

Heintzenberg, J., Birmili, W., Otto, R., Andreae, M. O., Mayer, J.-C., et al. 2011. Aerosol particle number size distributions and particulate light absorption at the ZOTTO tall tower (Siberia), 2006–2009. *Atmos. Chem. Phys.* **11**, 8703–19. DOI: *https://doi.org/10.5194/acp-11-8703-2011*

Heintzenberg, J., Birmili, W., Seifert, P., Panov, A., Chi, X., et al. 2013. Mapping the aerosol over Eurasia from the Zotino tall tower. *Tellus B* **65**, 20062. DOI: *https://doi.org/10.3402/tellusb.v65i0.20062*

Heintzenberg, J., Birmili, W., Theiss, D., and Kisilyakhov, Y. 2008. The atmospheric aerosol over Siberia, as seen from the 300 m ZOTTO tower. *Tellus B* **60 B**, 276–85. DOI: *https://doi.org/10.1111/j.1600-0889.2007.00335.x*

Helin, A., Sietiö, O. M., Heinonsalo, J., Bäck, J., Riekkola, M. L., et al. 2017. Characterization of free amino acids, bacteria

and fungi in size-segregated atmospheric aerosols in boreal forest: Seasonal patterns, abundances and size distributions. *Atmos. Chem. Phys.* **17**, 13089–101. DOI: *https://doi.org/10.5194/acp-17-13089-2017*

Hellén, H., Praplan, A. P., Tykkä, T., Ylivinkka, I., Vakkari, V., et al. 2018. Long-term measurements of volatile organic compounds highlight the importance of sesquiterpenes for the atmospheric chemistry of a boreal forest. *Atmos. Chem. Phys.* **18**, 13839–63. DOI: *https://doi.org/10.5194/acp-18-13839-2018*

Hess, L.L., Melack, J.M., Novo, E.M.L.M., Barbosa, C.C.F., Gastil, M. 2003. Dual-season mapping of wetland inundation and vegetation for the central Amazon basin. *Remote Sens. Environ.* DOI: *https://doi.org/10.1016/j.rse.2003.04.001*

Hewitt, C. N., Lee, J. D., MacKenzie, A. R., Barkley, M. P., Carslaw, N., et al. 2010. Overview: oxidant and particle photochemical processes above a south-east Asian tropical rainforest (the OP3 project): introduction, rationale, location characteristics and tools. *Atmos. Chem. Phys.*, **10**, 169–99. DOI: *https://doi.org/10.5194/acp-10-169-2010*

Hjelmroos, M. 1991. Evidence of long-distance transport of Betula pollen. *Grana.* **30**, 215–228. DOI: *https://doi.org/10.1080/00173139109427802*

Hodgson, A., Morgan, W., O'Shea, S., Bauguitte, S., Allan, J., et al. 2017a. Near-field emission profiling of Rainforest and Cerrado fires in Brazil during SAMBBA 2012. *Atmos. Chem. Phys. Discuss.* **87**, 1–33. DOI: *https://doi.org/10.5194/acp-2016-1019*

Hoesly, R. M., Smith, S. J., Feng, L., Klimont, Z., Janssens-Maenhout, G., et al. 2018. Historical (1750–2014) anthropogenic emissions of reactive gases and aerosols from the Community Emissions Data System (CEDS). *Geosci. Model Dev.* **11**, 369–408. DOI: *https://doi.org/10.5194/gmd-11-369-2018*

Hoffmann, A. A., Hallas, R. J., Dean, J. A., and Schiffer, M. 2003. Low potential for climatic stress adaptation in a rainforest Drosophila species. *Science* **301**, 100–102. DOI: *https://doi.org/10.1126/science.1084296*

Holanda, B. A., Pöhlker, M. L., Walter, D., Saturno, J., Sörgel, M., et al. 2020. Influx of African biomass burning aerosol during the Amazonian dry season through layered transatlantic transport of black carbon-rich smoke. *Atmos. Chem. Phys.* **20**, 4757–85. DOI: *https://doi.org/10.5194/acp-20-4757-2020*

Holland, M. M., and Bitz, C. M. 2003. Polar amplification of climate change in coupled models. *Clim. Dyn.* **21**, 221–32. DOI: *https://doi.org/10.1007/s00382-003-0332-6*

Holst, T., Arneth, A., Hayward, S., Ekberg, A., Mastepanov, M., et al. 2010. BVOC ecosystem flux measurements at a high latitude wetland site. *Atmos. Chem. Phys.* **10**, 1617–34. DOI: *https://doi.org/10.5194/acp-10-1617-2010*

Hong, J., Äijälä, M., Häme, S. A. K., Hao, L., Duplissy, J., et al. 2017. Estimates of the organic aerosol volatility in a boreal forest using two independent methods. *Atmos. Chem. Phys.* **17**, 4387–99. DOI: *https://doi.org/10.5194/acp-17-4387-2017*

Hong, J., Häkkinen, S. A. K., Paramonov, M., Äijälä, M., Hakala, J., et al. 2014. Hygroscopicity, CCN and volatility properties of submicron atmospheric aerosol in a boreal forest environment during the summer of 2010. *Atmos. Chem. Phys.* **14**, 4733–48. DOI: *https://doi.org/10.5194/acp-14-4733-2014*

Hong, J., Kim, J., Nieminen, T., Duplissy, J., Ehn, M., et al. 2015. Relating the hygroscopic properties of submicron aerosol to both gas- and particle-phase chemical composition in a boreal forest environment. *Atmos. Chem. Phys.* **15**, 11999–9. DOI: *https://doi.org/10.5194/acp-15-11999-2015*

Hoppel, W. A., Frick, G. M., and Larson, R. E. 1986. Effect of nonprecipitating clouds on the aerosol size distribution in the marine boundary layer. *Geophys. Res. Lett.* **13**, 125–28. DOI: *https://doi.org/10.1029/GL013i002p00125*

Horel, J. D., Hahmann, A. N., and Geisler, J. E. 1989. An investigation of the Annual Cycle of Convective Activity over the Tropical Americas. *J. Clim.* **2**, 1388–1403. DOI: *https://doi.org/10.1175/1520-0442(1989)002<1388:AIOTAC>2.0.CO;2*

Hu, W. W., Campuzano-Jost, P., Palm, B. B., Day, D. A., Ortega, A. M., et al. 2015. Characterization of a real-time tracer for isoprene epoxydiols-derived secondary organic aerosol (IEPOX-SOA) from aerosol mass spectrometer measurements. *Atmos. Chem. Phys.* **15**, 11807–33. DOI: *https://doi.org/10.5194/acp-15-11807-2015*

Hubau, W., Lewis, S. L., Phillips, O. L., Affum-Baffoe, K., Beeckman, H., et al. 2020. Asynchronous carbon sink saturation in African and Amazonian tropical forests. *Nature* **579**, 80–87. DOI: *https://doi.org/10.1038/s41586-020-2035-0*

Huffman, J. A., Perring, A. E., Savage, N. J., Clot, B., Crouzy, B., et al. 2019. Real-time sensing of bioaerosols: Review and current perspectives. *Aerosol Sci. Technol.* **54**, 465–95. DOI: *https://doi.org/10.1080/02786826.2019.1664724*

Huffman, J. A., Perring, A. E., Savage, N. J., Clot, B., Crouzy, B., et al. 2020. Real-time sensing of bioaerosols: Review and current perspectives. *Aerosol Sci. Technol.* **54**, 465–95. DOI: *https://doi.org/10.1080/02786826.2019.1664724*

Huffman, J. A., Prenni, A. J., Demott, P. J., Pöhlker, C., Mason, R. H., et al. 2013. High concentrations of biological aerosol particles and ice nuclei during and after rain. *Atmos. Chem. Phys.* **13**, 6151–64. DOI: *https://doi.org/10.5194/acp-13-6151-2013*

Huffman, J. A., Sinha, B., Garland, R. M., Snee-Pollmann, A., Gunthe, S. S., et al. 2012. Size distributions and temporal variations of biological aerosol particles in the Amazon rainforest characterized by microscopy and real-time UV-APS fluorescence techniques during AMAZE-08. *Atmos. Chem. Phys.* **12**, 11997–19. DOI: *https://doi.org/10.5194/acp-12-11997-2012*

Huffman, J. A., Treutlein, B., and Pöschl, U. 2010. Fluorescent biological aerosol particle concentrations and size distributions measured with an Ultraviolet Aerodynamic Particle Sizer (UV-APS) in Central Europe. *Atmos. Chem. Phys.* **10**, 3215–33. DOI: *https://doi.org/10.5194/acp-10-3215-2010*

Huijnen, V., Wooster, M. J., Kaiser, J. W., Gaveau, D. L., Flemming, J., et al. 2016. Fire carbon emissions over maritime southeast Asia in 2015 largest since 1997. *Sci. Rep.* **6**, 1–8. DOI: *https://doi.org/10.1038/srep26886*

Hurrell, J. W. 1995. Decadal trends in the North Atlantic oscillation: Regional temperatures and precipitation. *Science* **269**, 676–79. DOI: *https://doi.org/10.1126/science.269.5224.676*

Hussein, T., Norros, V., Hakala, J., Petäjä, T., Aalto, P. P., et al. 2013. Species traits and inertial deposition of fungal spores. *J. Aerosol Sci.* **61**, 81–98. DOI: *https://doi.org/10.1016/j.jaerosci.2013.03.004*

Hüve, K., Christ, M. M., Kleist, E., Uerlings, R., Niinemets, Ü., et al. 2007. Simultaneous growth and emission measurements demonstrate an interactive control of methanol release by leaf expansion and stomata. *J. Exp. Bot.* **58**, 1783–93. DOI: *https://doi.org/10.1093/jxb/erm038*

Hyvärinen, A. P., Raatikainen, T., Komppula, M., Mielonen, T., Sundström, A. M., et al. 2011. Effect of the summer monsoon on aerosols at two measurement stations in Northern India-Part 2: Physical and optical properties. *Atmos. Chem. Phys.* **11**, 8283–94. DOI: *https://doi.org/10.5194/acp-11-8283-2011*

IPBES (2019): Summary for policymakers of the global assessment report on biodiversity and ecosystem services of the Intergovernmental Science-Policy Platform on Biodiversity and Ecosystem Services. S. Díaz, J. Settele, E. S. Brondízio, H. T. Ngo, M. Guèze, J. Agard, A. Arneth, P. Balvanera, K. A. Brauman, S. H. M. Butchart, K. M. A. Chan, L. A. Garibaldi, K. Ichii, J. Liu, S. M. Subramanian, G. F. Midgley, P. Miloslavich, Z. Molnár, D. Obura, A. Pfaff, S. Polasky, A. Purvis, J. Razzaque, B. Reyers, R. Roy Chowdhury, Y. J. Shin, I. J. Visseren-Hamakers, K. J. Willis, and C. N. Zayas (eds.). IPBES secretariat, Bonn, Germany. 56 pages. DOI: *https://doi.org/10.5281/zenodo.3553579*

IPCC, 2013: Climate Change 2013: The Physical Science Basis. Contribution of Working Group I to the Fifth Assessment Report of the Intergovernmental Panel on Climate Change [Stocker, T.F., D. Qin, G.-K. Plattner, M. Tignor, S.K. Allen, J. Boschung, A. Nauels, Y. Xia, V. Bex and P.M. Midgley (eds.)]. Cambridge University Press, Cambridge, United Kingdom and New York, NY, USA, 1535 pp.

IPCC, 2014: Climate Change 2014: Synthesis Report. Contribution of Working Groups I, II and III to the Fifth Assessment Report of the Intergovernmental Panel on Climate Change [Core Writing Team, R.K. Pachauri and L.A. Meyer (eds.)]. IPCC, Geneva, Switzerland, 151 pp.

IPCC, 2018: Summary for Policymakers. In: Global Warming of 1.5°C. An IPCC Special Report on the impacts of global warming of 1.5°C above pre-industrial levels and related global greenhouse gas emission pathways, in the context of strengthening the global response to the threat of climate change, sustainable development, and efforts to eradicate poverty [Masson-Delmotte, V., P. Zhai, H.-O. Pörtner, D. Roberts, J. Skea, P.R. Shukla, A. Pirani, W. Moufouma-Okia, C. Péan, R. Pidcock, S. Connors, J.B.R. Matthews, Y. Chen, X. Zhou, M.I. Gomis, E. Lonnoy, T. Maycock, M. Tignor, and T. Waterfield (eds.)]. World Meteorological Organization, Geneva, Switzerland, 32 pp.

IPCC, 2019: Summary for Policymakers. In: Climate Change and Land: an IPCC special report on climate change, desertification, land degradation, sustainable land management, food security, and greenhouse gas fluxes in terrestrial ecosystems [P.R. Shukla, J. Skea, E. Calvo Buendia, V. Masson-Delmotte, H.- O. Pörtner, D. C. Roberts, P. Zhai, R. Slade, S. Connors, R. van Diemen, M. Ferrat, E. Haughey, S. Luz, S. Neogi, M. Pathak, J. Petzold, J. Portugal Pereira, P. Vyas, E. Huntley, K. Kissick, M. Belkacemi, J. Malley, (eds.)].

IPCC, 2021: Climate Change 2021: The Physical Science Basis. Contribution of Working Group I to the Sixth Assessment Report of the Intergovernmental Panel on Climate Change [Masson-Delmotte, V., P. Zhai, A. Pirani, S.L. Connors, C. Péan, S. Berger, N. Caud, Y. Chen, L. Goldfarb, M.I. Gomis, M. Huang, K. Leitzell, E. Lonnoy, J.B.R. Matthews, T.K. Maycock, T. Waterfield, O. Yelekçi, R. Yu, and B. Zhou (eds.)]. Cambridge University Press.

Irwin, M., Robinson, N., Allan, J. D., Coe, H., and McFiggans, G. 2011. Size-resolved aerosol water uptake and cloud condensation nuclei measurements as measured above a Southeast Asian rainforest during OP3. *Atmos. Chem. Phys.* **11**, 11157–11174. DOI: *https://doi.org/10.5194/acp-11-11157-2011*

Isidorov, V. A., Zenkevich, I. G., and Ioffe, B. V. 1985. Volatile organic compounds in the atmosphere of forests. *Atmos. Environ.* **19**, 1–8. DOI: *https://doi.org/10.1016/0004-6981(85)90131-3*

Jäkel, E., Wendisch, M., Krisna, T. C., Ewald, F., Kölling, T., et al. 2017. Vertical distribution of the particle phase in tropical deep convective clouds as derived from cloud-side reflected solar radiation measurements. *Atmos. Chem. Phys.* **17**, 9049–66. DOI: *https://doi.org/10.5194/acp-17-9049-2017*

Janson, R., De Serves, C., and Romero, R. 1999. Emission of isoprene and carbonyl compounds from a boreal forest and wetland in Sweden. *Agric. For. Meteorol.* **98**–**99**, 671–81. DOI: *https://doi.org/10.1016/S0168-1923(99)00134-3*

Janson, R. W. 1993. Monoterpene emissions from Scots pine and Norwegian spruce. *J. Geophys. Res.* **98**, 2839–50. DOI: *https://doi.org/10.1029/92JD02394*

Jardine, A. B., Jardine, K. J., Fuentes, J. D., Martin, S. T., Martins, G., et al. 2015b. Highly reactive light-dependent monoterpenes in the Amazon. *Geophys. Res. Lett.* **42**, 1576–83. DOI: *https://doi.org/10.1002/2014GL062573*

Jardine, K., Chambers, J., Alves, E. G., Teixeira, A., Garcia, S., et al. 2014. Dynamic balancing of isoprene carbon sources reflects photosynthetic and photorespiratory responses to temperature stress. *Plant Physiol.* **166**, 2051–64. DOI: *https://doi.org/10.1104/pp.114.247494*

Jardine, K. J., Chambers, J. Q., Holm, J., Jardine, A. B., Fontes, C. G., et al. 2015a. Green leaf volatile emissions during

high temperature and drought stress in a central Amazon rainforest. *Plants* **4**, 678–90. DOI: *https://doi.org/10.3390/plants4030678*

Jardine, K. J., Jardine, A. B., Holm, J. A., Lombardozzi, D. L., Negron-Juarez, R. I., et al. 2017. Monoterpene "thermometer" of tropical forest-atmosphere response to climate warming. *Plant Cell Environ.* **40**, 441–52. DOI: *https://doi.org/10.1111/pce.12879*

Jardine, K., Yañez Serrano, A., Arneth, A., Abrell, L., Jardine, A., Artaxo, P., et al. 2011a. Ecosystem-scale compensation points of formic and acetic acid in the central Amazon. *Biogeosciences* **8**, 3709–20. DOI: *https://doi.org/10.5194/bg-8-3709-2011*

Jardine, K., Yañez Serrano, A., Arneth, A., Abrell, L., Jardine, A., Van Haren, J., et al. 2011b. Within-canopy sesquiterpene ozonolysis in Amazonia. *J. Geophys. Res.* **116**. DOI: *https://doi.org/10.1029/2011JD016243*

Jepsen, S. M., Molotch, N. P., Williams, M. W., Rittger, K. E., and Sickman, J. O. 2012. Interannual variability of snowmelt in the Sierra Nevada and Rocky Mountains, United States: Examples from two alpine watersheds. *Water Resour. Res.* **48**, 2. DOI: *https://doi.org/10.1029/2011WR011006*

Jia, G., Shevliakova, E., Artaxo, P., de Noblet-Ducoudré, N., Houghton, R., House, J., … Verchot, L. (2019). Land–climate interactions. In T. F. Stocker, D. Qin, G. -K. Plattner, M. Tignor, S. K. Allen, J. Boschung, P. M. Midgley (Eds.), Climate change and land: An IPCC special report on climate change, desertification, land degradation, sustainable land management, food security, and greenhouse gas fluxes in terrestrial ecosystems (pp. 571–657). Cambridge, UK; New York, NY: Cambridge University Press.

Jiang, H., Xue, H., Teller, A., Feingold, G., and Levin, Z. 2006. Aerosol effects on the lifetime of shallow cumulus. *Geophys. Res. Lett.* **33**, L14806. DOI: *https://doi.org/10.1029/2006GL026024*

Jimenez, J. L., Canagaratna, M. R., Donahue, N. M., Prevot, A. S. H., Zhang, Q., et al. 2009. Evolution of Organic Aerosols in the Atmosphere. *Science* **326**, 1525–29. DOI: *https://doi.org/10.1126/science.1180353*

Johansson, V., Lönnell, N., Rannik, Ü., Sundberg, S., and Hylander, K. 2016. Air humidity thresholds trigger active moss spore release to extend dispersal in space and time. *Funct. Ecol.* **30**, 1196–1204. DOI: *https://doi.org/10.1111/1365-2435.12606*

Johansson, V., Lönnell, N., Sundberg, S., and Hylander, K. 2014. Release thresholds for moss spores: The importance of turbulence and sporophyte length. *J. Ecol.* **102**, 721–29. DOI: *https://doi.org/10.1111/1365-2745.12245*

Johnson, B. T., Shine, K. P., and Forster, P. M. 2004. The semi-direct aerosol effect: Impact of absorbing aerosols on marine stratocumulus. *Q. J. R. Meteorol. Soc.* **130**, 1407–22. DOI: *https://doi.org/10.1256/qj.03.61*

Jolleys, M. D., Coe, H., McFiggans, G., Taylor, J. W., O'Shea, S. J., et al. 2015. Properties and evolution of biomass burning organic aerosol from Canadian boreal forest fires. *Atmos. Chem. Phys.* **15**, 3077–95. DOI: *https://doi.org/10.5194/acp-15-3077-2015*

Jolly, W. M., Cochrane, M. A., Freeborn, P. H., Holden, Z. A., Brown, T. J., et al. 2015. Climate-induced variations in global wildfire danger from 1979 to 2013. *Nat. Commun.* **6**. DOI: *https://doi.org/10.1038/ncomms8537*

Jones, A. M., and Harrison, R. M. 2004. The effects of meteorological factors on atmospheric bioaerosol concentrations – A review. *Sci. Total Environ.* **326**, 151–80. DOI: *https://doi.org/10.1016/j.scitotenv.2003.11.021*

Joung, Y. S., Ge, Z., and Buie, C. R. 2017. Bioaerosol generation by raindrops on soil. *Nat. Commun.* **8**. DOI: *https://doi.org/10.1038/ncomms14668*

Jung, M., Reichstein, M., Ciais, P., Seneviratne, S. I., Sheffield, J., et al. 2010. Recent decline in the global land evapotranspiration trend due to limited moisture supply. *Nature* **467**, 951–54. DOI: *https://doi.org/10.1038/nature09396*

Jung, M., Reichstein, M., Margolis, H. A., Cescatti, A., Richardson, A. D., et al. 2011. Global patterns of land-atmosphere fluxes of carbon dioxide, latent heat, and sensible heat derived from eddy covariance, satellite, and meteorological observations. *J. Geophys. Res.* **116**, 1–16. DOI: *https://doi.org/10.1029/2010JG001566*

Jurányi, Z., Gysel, M., Duplissy, J., Weingartner, E., Tritscher, T., et al. 2009. Influence of gas-to-particle partitioning on the hygroscopic and droplet activation behaviour of α-pinene secondary organic aerosol. *Phys. Chem. Chem. Phys.* **11**, 8091–97. DOI: *https://doi.org/10.1039/b904162a*

Juuti, S., Arey, J., and Atkinson, R. 1990. Monoterpene emission rate measurements from a Monterey pine. *J. Geophys. Res.* **95**, 7515. DOI: *https://doi.org/10.1029/JD095iD06p07515*

Kajos, M. K., Hakola, H., Holst, T., Nieminen, T., Tarvainen, V., et al. 2013. Terpenoid emissions from fully grown east Siberian Larix cajanderi trees. *Biogeosciences* **10**, 4705–19. DOI: *https://doi.org/10.5194/bg-10-4705-2013*

Kanawade, V. P., Jobson, B. T., Guenther, A. B., Erupe, M. E., Pressley, S. N., et al. 2011. Isoprene suppression of new particle formation in a mixed deciduous forest. *Atmos. Chem. Phys.* **11**, 6013–27. DOI: *https://doi.org/10.5194/acp-11-6013-2011*

Karl, T., Guenther, A., Turnipseed, A., Tyndall, G., Artaxo, P., et al. 2009. Rapid formation of isoprene photo-oxidation products observed in Amazonia. *Atmos. Chem. Phys.* **9**, 7753–67. DOI: *https://doi.org/10.5194/acp-9-7753-2009*

Karl, T., Guenther, A., Yokelson, R. J., Greenberg, J., Potosnak, M., et al. 2007. The tropical forest and fire emissions experiment: Emission, chemistry, and transport of biogenic volatile organic compounds in the lower atmosphere over Amazonia. *J. Geophys Res.* **112**, 1–17. DOI: *https://doi.org/10.1029/2007JD008539*

Karl, T., Potosnak, M., Guenther, A., Clark, D., Walker, J., et al. 2004. Exchange processes of volatile organic compounds above a tropical rain forest: Implications for modeling tropospheric chemistry above dense vegetation. *J. Geophys. Res.* **109**, 1–19. DOI: *https://doi.org/10.1029/2004JD004738*

Karlsson, P. E., Tang, L., Sundberg, J., Chen, D., Lindskog, A., et al. 2007. Increasing risk for negative ozone impacts on vegetation in northern Sweden. *Environ. Pollut.* **150**, 96–106. DOI: *https://doi.org/10.1016/j.envpol.2007.06.016*

Keeling, R. F., Graven, H. D., Welp, L. R., Resplandy, L., Bi, J., et al. 2017. Atmospheric evidence for a global secular increase in carbon isotopic discrimination of land photosynthesis. *Proc. Natl. Acad. Sci. U. S. A.* **114**, 10361–66. DOI: *https://doi.org/10.1073/pnas.1619240114*

Keller, M., Alencar, A., Asner, G. P., Braswell, B., Bustamante, M., et al. 2004. Ecological research in the Large-scale Biosphere-Atmosphere Experiment in Amazonia: Early results. *Ecol. Appl.* **14**. DOI: *https://doi.org/10.1890/03-6003*

Keller, M., and Lerdau, M. 1999. Isoprene emission from tropical forest canopy leaves. *Global Biogeochem. Cycles* **13**, 19–29. DOI: *https://doi.org/10.1029/1998GB900007*

Kenseth, C. M., Huang, Y., Zhao, R., Dalleska, N. F., Caleb Hethcox, J., et al. 2018. Synergistic O3 + OH oxidation pathway to extremely low-volatility dimers revealed in β-pinene secondary organic aerosol. *Proc. Natl. Acad. Sci. U. S. A.* **115**, 8301–6. DOI: *https://doi.org/10.1073/pnas.1804671115*

Keppler, F., Hamilton, J. T. G., Braß, M., and Röckmann, T. 2006. Methane emissions from terrestrial plants under aerobic conditions. *Nature* **439**, 187–91. DOI: *https://doi.org/10.1038/nature04420*

Kerminen, V. M., Chen, X., Vakkari, V., Petäjä, T., Kulmala, M., et al. 2018. Atmospheric new particle formation and growth: Review of field observations. *Environ. Res. Lett.* **13**, 1–38. DOI: *https://doi.org/10.1088/1748-9326/aadf3c*

Kerminen, V. M., Lihavainen, H., Komppula, M., Viisanen, Y., and Kulmala, M. 2005. Direct observational evidence linking atmospheric aerosol formation and cloud droplet activation. *Geophys. Res. Lett.* **32**, 1–4. DOI: *https://doi.org/10.1029/2005GL023130*

Kerminen, V. M., Paramonov, M., Anttila, T., Riipinen, I., Fountoukis, C., et al. 2012. Cloud condensation nuclei production associated with atmospheric nucleation: A synthesis based on existing literature and new results. *Atmos. Chem. Phys.* **12**, 12037–59. DOI: *https://doi.org/10.5194/acp-12-12037-2012*

Kesselmeier, J., Kuhn, U., Wolf, A., Andreae, M. O., Ciccioli, P., et al. 2000. Atmospheric volatile organic compounds (VOC) at a remote tropical forest site in central Amazonia. *Atmos. Environ.* **34**, 4063–72. DOI: *https://doi.org/10.1016/S1352-2310(00)00186-2*

Khain, A., Rosenfeld, D., and Pokrovsky, A. 2005. Aerosol impact on the dynamics and microphysics of deep convective clouds. *Q. J. R. Meteorol. Soc.* **131**, 2639–63. DOI: *https://doi.org/10.1256/qj.04.62*

Khairoutdinov, M., and Kogan, Y. 2000. A new cloud physics parameterization in a large-eddy simulation model of marine stratocumulus. *Mon. Weather Rev.* **128**, 229–43. DOI: *https://doi.org/10.1175/1520-0493(2000)128<0229:ANCPPI>2.0.CO;2*

Kilkki, J., Aalto, T., Hatakka, J., Portin, H., and Laurila, T. 2015. Atmospheric CO_2 observations at Finnish urban and rural sites. *Boreal Environ. Res.* **20**, 227–42.

Kipling, Z., Stier, P., Labbouz, L., and Wagner, T. 2017. Dynamic subgrid heterogeneity of convective cloud in a global model: Description and evaluation of the Convective Cloud Field Model (CCFM) in ECHAM6-HAM2. *Atmos. Chem. Phys.* **17**, 327–42. DOI: *https://doi.org/10.5194/acp-17-327-2017*

Kirchhoff, V. W. J. H., Da Silva, I. M. O., and Browell, E. V. 1990. Ozone measurements in Amazonia: dry season versus wet season. *J. Geophys. Res.* **95**. DOI: *https://doi.org/10.1029/JD095iD10p16913*

Kirkby, J., Duplissy, J., Sengupta, K., Frege, C., Gordon, H., et al. 2016. Ion-induced nucleation of pure biogenic particles. *Nature* **533**, 521–26. DOI: *https://doi.org/10.1038/nature17953*

Kljun, N., Black, T. A., Griffis, T. J., Barr, A. G., Gaumont-Guay, D., et al. 2007. Response of net ecosystem productivity of three boreal forest stands to drought. *Ecosystems* **10**, 1039–55. DOI: *https://doi.org/10.1007/s10021-007-9088-x*

Knorr, W., Arneth, A., and Jiang, L. 2016. Demographic controls of future global fire risk. *Nat. Clim. Chang.* **6**, 781–85. DOI: *https://doi.org/10.1038/nclimate2999*

Koch, D., and Del Genio, A. D. 2010. Black carbon semi-direct effects on cloud cover: Review and synthesis. *Atmos. Chem. Phys.* **10**, 7685–96. DOI: *https://doi.org/10.5194/acp-10-7685-2010*

Köhl, M., Lasco, R., Cifuentes, M., Jonsson, Ö., Korhonen, K. T., et al. 2015. Changes in forest production, biomass and carbon: Results from the 2015 UN FAO Global Forest Resource Assessment. *For. Ecol. Manage.* **352**, 21–34. DOI: *https://doi.org/10.1016/j.foreco.2015.05.036*

Köhler, H. 1936. The nucleus in and the growth of hygroscopic droplets. *Trans. Faraday Soc.* **32**, 1152–61. DOI: *https://doi.org/10.1039/TF9363201152*

Kolmonen, P., Sogacheva, L., Virtanen, T. H., de Leeuw, G., and Kulmala, M. 2016. The ADV/ASV AATSR aerosol retrieval algorithm: current status and presentation of a full-mission AOD dataset. *Int. J. Digit. Earth* **9**, 545–61. DOI: *https://doi.org/10.1080/17538947.2015.1111450*

Komppula, M., Sihto, S. L., Korhonen, H., Lihavainen, H., Kerminen, V. M., et al. 2006. New particle formation in air mass transported between two measurement sites in Northern Finland. *Atmos. Chem. Phys.* **6**, 2811–24. DOI: *https://doi.org/10.5194/acp-6-2811-2006*

Köppen, W. 1884. Die Wärmezonen der Erde, nach der Dauer der heissen, gemässigten und kalten Zeit und nach der Wirkung der Wärme auf die organische Welt betrachtet. *Meteorol. Zeitschrift* 215–26.

Koren, I., Kaufman, Y. J., Remer, L. A., and Martins, J. V. 2004. Measurement of the Effect of Amazon Smoke on Inhibition of Cloud Formation. *Science* **303**, 1342–45. DOI: *https://doi.org/10.1126/science.1089424*

Kortelainen, A., Hao, L., Tiitta, P., Jaatinen, A., Miettinen, P., et al. 2017. Sources of particulate organic nitrates in the boreal forest in Finland. *Boreal Environ. Res.* **22**, 13–26.

Köster, E., Köster, K., Berninger, F., Aaltonen, H., Zhou, X., et al. 2017. Carbon dioxide, methane and nitrous oxide fluxes from a fire chronosequence in subarctic boreal forests of Canada. *Sci. Total Environ.* **601**–**602**, 895–905. DOI: *https://doi.org/10.1016/j.scitotenv.2017.05.246*

Kourtchev, I., Fuller, S., Aalto, J., Ruuskanen, T. M., McLeod, M. W., et al. 2013. Molecular composition of boreal forest aerosol from Hyytiälä, Finland, using ultrahigh resolution mass spectrometry. *Environ. Sci. Technol.* **47**, 4069–79. DOI: *https://doi.org/10.1021/es3051636*

Kourtchev, I., Giorio, C., Manninen, A., Wilson, E., Mahon, B., et al. 2016. Enhanced volatile organic compounds emissions and organic aerosol mass increase the oligomer content of atmospheric aerosols. *Sci. Rep.* **6**. DOI: *https://doi.org/10.1038/srep35038*

Kourtchev, I., Ruuskanen, T., Maenhaut, W., Kulmala, M., and Claeys, M. 2005. Observation of 2-methyltetrols and related photo-oxidation products of isoprene in boreal forest aerosols from Hyytiälä, Finland. *Atmos. Chem. Phys.* **5**, 2761–70. DOI: *https://doi.org/10.5194/acp-5-2761-2005*

Kousky, V. E., and Gan, M. A. 1981. Upper tropospheric cyclonic vortices in the tropical South Atlantic. *Tellus* **33**, 538–51. DOI: *https://doi.org/10.3402/tellusa.v33i6.10775*

Kozii, N., Laudon, H., Ottosson-Löfvenius, M., and Hasselquist, N. J. 2017. Increasing water losses from snow captured in the canopy of boreal forests: A case study using a 30 year data set. *Hydrol. Process.* **31**, 3558–67. DOI: *https://doi.org/10.1002/hyp.11277*

Kozlova, E. A., and Manning, A. C. 2009. Methodology and calibration for continuous measurements of biogeochemical trace gas and O2 concentrations from a 300-m tall tower in central Siberia. *Atmos. Meas. Tech.* **2**, 205–20. DOI: *https://doi.org/10.5194/amt-2-205-2009*

Kozlova, E. A., Manning, A. C., Kisilyakhov, Y., Seifert, T., and Heimann, M. 2008. Seasonal, synoptic, and diurnal-scale variability of biogeochemical trace gases and O2 from a 300-m tall tower in central Siberia. *Global Biogeochem. Cycles* **22**. DOI: *https://doi.org/10.1029/2008GB003209*

Krawchuk, M. A., and Moritz, M. A. 2011. Constraints on global fire activity vary across a resource gradient. *Ecology* **92**, 121–32. DOI: *https://doi.org/10.1890/09-1843.1*

Krejci, R., Ström, J., de Reus, M., Hoor, P., Williams, J., et al. 2003. Evolution of aerosol properties over the rain forest in Surinam, South America, observed from aircraft during the LBA-CLAIRE 98 experiment. *J. Geophys. Res.* **108**, 4561. DOI: *https://doi.org/10.1029/2001JD001375*

Krejci, R., Ström, J., de Reus, M., Williams, J., Fischer, H., et al. 2005. Spatial and temporal distribution of atmospheric aerosols in the lowermost troposphere over the Amazonian tropical rainforest. *Atmos. Chem. Phys.* **5**, 1527–43. DOI: *https://doi.org/10.5194/acp-5-1527-2005*

Kristensson, A., Dal Maso, M., Swietlicki, E., Hussein, T., Zhou, J., et al. 2008. Characterization of new particle formation events at a background site in southern Sweden: Relation to air mass history. *Tellus B* **60 B**, 330–44. DOI: *https://doi.org/10.1111/j.1600-0889.2008.00345.x*

Kuhn, U., Ganzeveld, L., Thielmann, A., Dindorf, T., Schebeske, G., et al. 2010. Impact of Manaus City on the Amazon Green Ocean atmosphere: ozone production, precursor sensitivity and aerosol load. *Atmos. Chem. Phys* **10**, 9251–82. DOI: *https://doi.org/10.5194/acp-10-9251-2010*

Kuhn, U., Rottenberger, S., Biesenthal, T., Wolf, A., Schebeske, G., et al. 2002. Isoprene and monoterpene emissions of Amazonian tree species during the wet season: Direct and indirect investigations on controlling environmental functions. *J. Geophys. Res.* **107**, LBA 38-1-LBA 38-13. DOI: *https://doi.org/10.1029/2001JD000978*

Kulmala, M., Asmi, A., Lappalainen, H. K., Baltensperger, U., Brenguier, J. L., et al. 2011. General overview: European Integrated project on Aerosol Cloud Climate and Air Quality interactions (EUCAARI)-integrating aerosol research from nano to global scales. *Atmos. Chem. Phys.* **11**, 13061–143. DOI: *https://doi.org/10.5194/acp-11-13061-2011*

Kulmala, M., Hämeri, K., Aalto, P. P., Mäkelä, J. M., Pirjola, L., et al. 2001. Overview of the international project on biogenic aerosol formation in the boreal forest (BIOFOR). *Tellus B* **53**, 324–43. DOI: *https://doi.org/10.3402/tellusb.v53i4.16601*

Kulmala, M., Kontkanen, J., Junninen, H., Lehtipalo, K., Manninen, H. E., et al. 2013a. Direct observations of atmospheric aerosol nucleation. *Science* **339**, 943–46. DOI: *https://doi.org/10.1126/science.1227385*

Kulmala, M., Nieminen, T., Chellapermal, R., Makkonen, R., Bäck, J., et al. 2013b. Climate Feedbacks Linking the Increasing Atmospheric CO_2 Concentration, BVOC Emissions, Aerosols and Clouds in Forest Ecosystems. Pp. 489–508. DOI: *https://doi.org/10.1007/978-94-007-6606-8_17*

Kulmala, Markku, Nieminen, T., Nikandrova, A., Lehtipalo, K., Manninen, H. E., et al. 2014a. CO_2-induced terrestrial climate feedback mechanism: From carbon sink to aerosol source and back. *Boreal Environ. Res.* **19**, 122–31.

Kulmala, M., Petäjä, T., Ehn, M., Thornton, J., Sipilä, M., et al. 2014b. Chemistry of atmospheric nucleation: On the recent advances on precursor characterization and atmospheric cluster composition in connection with atmospheric new particle formation. *Annu. Rev. Phys. Chem.* **65**, 21–37. DOI: *https://doi.org/10.1146/annurev-physchem-040412-110014*

Kulmala, M., Reissell, A., Sipilä, M., Bonn, B., Ruuskanen, T. M., et al. 2006. Deep convective clouds as aerosol production engines: Role of insoluble organics. *J. Geophys. Res.* **111**, D17202. DOI: *https://doi.org/10.1029/2005JD006963*

Kulmala, M., Suni, T., Lehtinen, K. E. J., Dal Maso, M., Boy, M., et al. 2004a. A new feedback mechanism linking forests, aerosols, and climate. *Atmos. Chem. Phys.* **4**, 557–62. DOI: *https://doi.org/10.5194/acp-4-557-2004*

Kulmala, M., Vehkamäki, H., Petäjä, T., Dal Maso, M., Lauri, A., et al. 2004b. Formation and growth rates of ultrafine atmospheric particles: A review of observations. *J.*

Aerosol Sci. **35**, 143–76. DOI: *https://doi.org/10.1016/j.jaerosci.2003.10.003*

Kurbatova, J., Arneth, A., Vygodskaya, N. N., Kolle, O., Varlargin, A. V., et al. 2002. Comparative ecosystem–atmosphere exchange of energy and mass in a European Russian and a central Siberian bog I. Interseasonal and interannual variability of energy and latent heat fluxes during the snowfree period. *Tellus B* **54**, 497–513. DOI: *https://doi.org/10.3402/tellusb.v54i5.16683*

Kurtén, T., Kulmala, M., Dal Maso, M., Suni, T., Reissell, A., et al. 2003. Estimation of different forest-related contributions to the radiative balance using observations in southern Finland. *Boreal Environ. Res.* **8**, 275–85.

Kyrö, E. M., Väänänen, R., Kerminen, V. M., Virkkula, A., Petäjä, T., et al. 2014. Trends in new particle formation in eastern Lapland, Finland: Effect of decreasing sulfur emissions from Kola Peninsula. *Atmos. Chem. Phys.* **14**, 4383–96. DOI: *https://doi.org/10.5194/acp-14-4383-2014*

Labbouz, L., Kipling, Z., Stier, P., and Protat, A. 2018. How well can we represent the spectrum of convective clouds in a climate model? Comparisons between internal parameterization variables and radar observations. *J. Atmos. Sci.* **75**, 1509–24. DOI: *https://doi.org/10.1175/JAS-D-17-0191.1*

Lamarque, J. F., Bond, T. C., Eyring, V., Granier, C., Heil, A., et al. 2010. Historical (1850–2000) gridded anthropogenic and biomass burning emissions of reactive gases and aerosols: Methodology and application. *Atmos. Chem. Phys.* **10**, 7017–39. DOI: *https://doi.org/10.5194/acp-10-7017-2010*

Lambe, A. T., Onasch, T. B., Massoli, P., Croasdale, D. R., Wright, J. P., et al. 2011. Laboratory studies of the chemical composition and cloud condensation nuclei (CCN) activity of secondary organic aerosol (SOA) and oxidized primary organic aerosol (OPOA). *Atmos. Chem. Phys.* **11**, 8913–28. DOI: *https://doi.org/10.5194/acp-11-8913-2011*

Lambin, E. F., Geist, H. J., and Lepers, E. 2003. Dynamics of land-use and land-cover change in tropical regions. *Annu. Rev. Environ. Resour.* **28**, 205–41. DOI: *https://doi.org/10.1146/annurev.energy.28.050302.105459*

Lapola, D. M. 2018. Bytes and boots to understand the future of the Amazon forest. *New Phytol.* **219**, 845–47. DOI: *https://doi.org/10.1111/nph.15342*

Lappalainen, H. K., Kerminen, V. M., Petäjä, T., Kurten, T., Baklanov, A., et al. 2016. Pan-Eurasian Experiment (PEEX): Towards a holistic understanding of the feedbacks and interactions in the land-Atmosphere-ocean-society continuum in the northern Eurasian region. *Atmos. Chem. Phys.* **16**, 14421–61. DOI: *https://doi.org/10.5194/acp-16-14421-2016*

Larsen, J.A., 1980. The Boreal Ecosystem. Physiological ecology. Academic Press, New York, ISBN: 9781483269870, pp. 516.

Laurila, T., Hakola, H., and Lindfors, V. 1999. Biogenic VOCs in continental Northern Europe-concentrations and Photochemistry. *Phys. Chem. Earth, Part B Hydrol. Ocean. Atmos.* **24**, 689–93. DOI: *https://doi.org/10.1016/S1464-1909(99)00066-0*

Law, B. E., Goldstein, A. H., Anthoni, P. M., Unsworth, M. H., Panek, J. A., et al. 2001. Carbon dioxide and water vapor exchange by young and old ponderosa pine ecosystems during a dry summer. *Tree Physiol.* **21**, 299–308. DOI: *https://doi.org/10.1093/treephys/21.5.299*

Law, B.E., T. Arkebauer, J.L. Campbell, J. Chen et al., 2008. Terrestrial Carbon Observations: Protocols for Vegetation Sampling and Data Submission, Global Terrestrial Observing System, Rome, Italy. Available at *http://www.fao.org/gtos/*.

Le Quéré, C., Andrew, R. M., Canadell, J. G., Sitch, S., Ivar Korsbakken, J., et al. 2016. Global Carbon Budget 2016. *Earth Syst. Sci. Data* **8**, 605–49. DOI: *https://doi.org/10.5194/essd-8-605-2016*

Le Quéré, C., Andrew, R., Friedlingstein, P., Sitch, S., Hauck, J., et al. 2018. Global Carbon Budget 2018. *Earth Syst. Sci. Data* **10**, 2141–94. DOI: *https://doi.org/10.5194/essd-10-2141-2018*

Lee, A. K. Y., Abbatt, J. P. D., Leaitch, W. R., Li, S. M., Sjostedt, S. J., et al. 2016. Substantial secondary organic aerosol formation in a coniferous forest: Observations of both day- and nighttime chemistry. *Atmos. Chem. Phys.* **16**, 6721–33. DOI: *https://doi.org/10.5194/acp-16-6721-2016*

Lee, B. H., Lopez-Hilfiker, F. D., D'Ambro, E. L., Zhou, P., Boy, M., et al. 2018. Semi-volatile and highly oxygenated gaseous and particulate organic compounds observed above a boreal forest canopy. *Atmos. Chem. Phys.* **18**, 11547–62. DOI: *https://doi.org/10.5194/acp-18-11547-2018*

Lee, J., Morrison, I. K., Leblanc, J. D., Dumas, M. T., and Cameron, D. A. 2002. Carbon sequestration in trees and regrowth vegetation as affected by clearcut and partial cut harvesting in a second-growth boreal mixedwood. *For. Ecol. Manage.* **169**, 83–101. DOI: *https://doi.org/10.1016/S0378-1127(02)00300-6*

Lee, S.-H. 2003. Particle Formation by Ion Nucleation in the Upper Troposphere and Lower Stratosphere. *Science* **301**, 1886–89. DOI: *https://doi.org/10.1126/science.1087236*

Lee, S.-H. 2004. New particle formation observed in the tropical/subtropical cirrus clouds. *J. Geophys. Res.* **109**, D20209. DOI: *https://doi.org/10.1029/2004JD005033*

Lehmann, J., and Coumou, D. 2015. The influence of mid-latitude storm tracks on hot, cold, dry and wet extremes. *Sci. Rep.* **5**, 1-9. DOI: *https://doi.org/10.1038/srep17491*

Lehtinen, K. E. J., Korhonen, H., Dal Maso, M., and Kulmala, M. 2003. On the concept of condensation sink diameter. *Boreal Environ. Res.* **8**, 405–11.

Lehtinen, K. E. J., Rannik, Ü., Petäjä, T., Kulmala, M., and Hari, P. 2004. Nucleation rate and vapor concentration estimations using a least squares aerosol dynamics method. *J. Geophys. Res.* **109**, 1–5. DOI: *https://doi.org/10.1029/2004JD004893*

Lehtipalo, K., Yan, C., Dada, L., Bianchi, F., Xiao, M., et al. 2018. Multicomponent new particle formation from sulfuric

acid, ammonia, and biogenic vapors. *Sci. Adv.* **4**, 1–9. DOI: *https://doi.org/10.1126/sciadv.aau5363*

Leino, K., Lampilahti, J., Poutanen, P., Väänänen, R., Manninen, A., et al. 2019. Vertical profiles of sub-3nm particles over the boreal forest. *Atmos. Chem. Phys.* **19**, 2127–38. DOI: *https://doi.org/10.5194/acp-19-4127-2019*

Leino, K., Riuttanen, L., Nieminen, T., Väänänen, R., Pohja, T., et al. 2014. Biomass-burning smoke episodes in Finland from eastern European wildfires. *Boreal Environ. Res.* **19**, 275–92.

Lelieveld, J., Butler, T. M., Crowley, J. N., Dillon, T. J., Fischer, H., et al. 2008. Atmospheric oxidation capacity sustained by a tropical forest. *Nature* **452**, 737–40. DOI: *https://doi.org/10.1038/nature06870*

Lenton, T. M., Held, H., Kriegler, E., Hall, J. W., Lucht, W., et al. 2008. Tipping elements in the Earth's climate system. *Proc. Natl. Acad. Sci. U. S. A.* **105**, 1786–93. DOI: *https://doi.org/10.1073/pnas.0705414105*

Levin, I., Ciais, P., Langenfelds, R., Schmidt, M., Ramonet, M., et al. 2002. Three years of trace gas observations over the EuroSiberian domain derived from aircraft sampling — a concerted action. *Tellus B* **54**, 696–712. DOI: *https://doi.org/10.3402/tellusb.v54i5.16717*

Lewis, S. L. 2006. Tropical forests and the changing earth system. *Philos. Trans. R. Soc. Lond. B. Biol. Sci.* **361**, 195–210. DOI: *https://doi.org/10.1098/rstb.2005.1711*

Li, W., Fu, R., Juárez, R. I. N., and Fernandes, K. 2008. Observed change of the standardized precipitation index, its potential cause and implications to future climate change in the Amazon region. Pp. 1767–72 in *Philosophical Transactions of the Royal Society B: Biological Sciences*. Vol. **363**. DOI: *https://doi.org/10.1098/rstb.2007.0022*

Liao, L., dal Maso, M., Taipale, R., Rinne, J., Ehn, M., et al. 2011. Monoterpene pollution episodes in a forest environment: Indication of anthropogenic origin and association with aerosol particles. *Boreal Environ. Res.* **16**, 288–303.

Liao, L., Kerminen, V. M., Boy, M., Kulmala, M., and Dal Maso, M. 2014. Temperature influence on the natural aerosol budget over boreal forests. *Atmos. Chem. Phys.* **14**, 8295–8308. DOI: *https://doi.org/10.5194/acp-14-8295-2014*

Lihavainen, H., Asmi, E., Aaltonen, V., Makkonen, U., and Kerminen, V. M. 2015. Direct radiative feedback due to biogenic secondary organic aerosol estimated from boreal forest site observations. *Environ. Res. Lett.* **10**, 1–8. DOI: *https://doi.org/10.1088/1748-9326/10/10/104005*

Lihavainen, H., Kerminen, V. M., Tunved, P., Aaltonen, V., Arola, A., et al. 2009. Observational signature of the direct radiative effect by natural boreal forest aerosols and its relation to the corresponding first indirect effect. *J. Geophys. Res.* **114**, 1–7. DOI: *https://doi.org/10.1029/2009JD012078*

Lim, H., Oren, R., Palmroth, S., Tor-ngern, P., Mörling, T., et al. 2015. Inter-annual variability of precipitation constrains the production response of boreal Pinus sylvestris to nitrogen fertilization. *For. Ecol. Manage.* **348**, 31–45. DOI: *https://doi.org/10.1016/j.foreco.2015.03.029*

Lin, Y. H., Zhang, Z., Docherty, K. S., Zhang, H., Budisulistiorini, S. H., et al. 2012. Isoprene epoxydiols as precursors to secondary organic aerosol formation: Acid-catalyzed reactive uptake studies with authentic compounds. *Environ. Sci. Technol.* **46**, 250–58. DOI: *https://doi.org/10.1021/es202554c*

Lindfors V., Laurila T., Hakola H., Steinbrecher R., and Rinne J. 2000. Modeling speciated terpenoid emissions from the European boreal forest. *Atmos Environ.* **34**, 4983–4996. DOI: *https://doi.org/10.1016/S1352-2310(00)00223-5*

Lindner, M., Maroschek, M., Netherer, S., Kremer, A., Barbati, A., et al. 2010. Climate change impacts, adaptive capacity, and vulnerability of European forest ecosystems. *For. Ecol. Manage.* **259**, 698–709. DOI: *https://doi.org/10.1016/j.foreco.2009.09.023*

Liu, L., Cheng, Y., Wang, S., Wei, C., Pöhlker, M. L., et al. 2020. Impact of biomass burning aerosols on radiation, clouds, and precipitation over the Amazon: Relative importance of aerosol-cloud and aerosol-radiation interactions. *Atmos. Chem. Phys.* **20**, 13283–13301. DOI: *https://doi.org/10.5194/acp-20-13283-2020*

Liu, Y., Brito, J., Dorris, M. R., Rivera-Rios, J. C., Seco, R., et al. 2016. Isoprene photochemistry over the Amazon rainforest. *Proc. Natl. Acad. Sci. U. S. A.* **113**, 6125–30. DOI: *https://doi.org/10.1073/pnas.1524136113*

Liu, Y., Seco, R., Kim, S., Guenther, A. B., Goldstein, A. H., et al. 2018. Isoprene photo-oxidation products quantify the effect of pollution on hydroxyl radicals over Amazonia. *Sci. Adv.* **4**. DOI: *https://doi.org/10.1126/sciadv.aar2547*

Lloyd, J., Gloor, E. U., and Lewis, S. L. 2009. Are the dynamics of tropical forests dominated by large and rare disturbance events? *Ecol. Lett.* **12**. DOI: *https://doi.org/10.1111/j.1461-0248.2009.01326.x*

Lloyd, J., Kolle, O., Fritsch, H., De Freitas, S. R., Silva Dias, M. A. F., et al. 2007. An airborne regional carbon balance for Central Amazonia. *Biogeosciences* **4**, 759–68. DOI: *https://doi.org/10.5194/bg-4-759-2007*

Lloyd, J., Shibistova, O., Zolotoukhine, D., Kolle, O., Arneth, A., et al. 2002. Seasonal and annual variations in the photosynthetic productivity and carbon balance of a central Siberian pine forest. *Tellus B* **54**, 590–610. DOI: *https://doi.org/10.1034/j.1600-0889.2002.01487.x*

Löbs, N., Barbosa, C. G. G., Brill, S., Walter, D., DItas, F., et al. 2020. Aerosol measurement methods to quantify spore emissions from fungi and cryptogamic covers in the Amazon. *Atmos. Meas. Tech.* **13**, 153–64. DOI: *https://doi.org/10.5194/amt-13-153-2020*

Lohila, A., Aalto, T., Aurela, M., Hatakka, J., Tuovinen, J. P., et al. 2016. Large contribution of boreal upland forest soils to a catchment-scale CH_4 balance in a wet year. *Geophys. Res. Lett.* **43**, 2946–53. DOI: *https://doi.org/10.1002/2016GL067718*

Lohila, A., Minkkinen, K., Aurela, M., Tuovinen, J. P., Penttilä, T., et al. 2011. Greenhouse gas flux measurements in a forestry-drained peatland indicate a large carbon sink. *Biogeosciences* **8**, 3203–18. DOI: *https://doi.org/10.5194/bg-8-3203-2011*

Longo, K. M., Thompson, A. M., Kirchhoff, V. W. J. H., Remer, L. A., De Freitas, S. R., et al. 1999. Correlation between smoke and tropospheric ozone concentration in Cuiabá during Smoke, Clouds, and Radiation-Brazil (SCAR-B). *J. Geophys. Res.* **104**, 12113–29. DOI: *https://doi.org/10.1029/1999JD900044*

Loreto, F., Förster, A., Dürr, M., Csiky, O., and Seufert, G. 1998. On the monoterpene emission under heat stress and on the increased thermotolerance of leaves of Quercus ilex L. fumigated with selected monoterpenes. *Plant Cell Environ.* **21**, 101–7. DOI: *https://doi.org/10.1046/j.1365-3040.1998.00268.x*

Lovejoy, T. E., and Nobre, C. 2018. Amazon tipping point. *Sci. Adv.* **4**, eaat2340. DOI: *https://doi.org/10.1126/sciadv.aat2340*

Luoma, K., Virkkula, A., Aalto, P., Petäjä, T., and Kulmala, M. 2019a. Over a 10-year record of aerosol optical properties at SMEAR II. *Atmos. Chem. Phys.* **19**, 11363–82. DOI: *https://doi.org/10.5194/acp-19-11363-2019*

Lutz, A., Mohr, C., Le Breton, M., Lopez-Hilfiker, F. D., Priestley, M., et al. 2019. Gas to particle partitioning of organic acids in the boreal atmosphere. *ACS Earth Space Chem.* **3**, 1279–87. DOI: *https://doi.org/10.1021/acsearthspacechem.9b00041*

Luyssaert, S., Inglima, I., Jung, M., Richardson, A. D., Reichstein, M., et al. 2007. CO_2 balance of boreal, temperate, and tropical forests derived from a global database. *Glob. Chang. Biol.* **13**, 2509–37. DOI: *https://doi.org/10.1111/j.1365-2486.2007.01439.x*

Lynn, B. H., Khain, A. P., Dudhia, J., Rosenfeld, D., Pokrovsky, A., et al. 2005. Spectral (bin) microphysics coupled with a mesoscale model (MM5). Part I: Model description and first results. *Mon. Weather Rev.* **133**, 44–58. DOI: *https://doi.org/10.1175/MWR-2840.1*

Lyubovtseva, Y. S., Sogacheva, L., Dal Maso, M., Bonn, B., Keronen, P., et al. 2005. Seasonal variations of trace gases, meteorological parameters, and formation of aerosols in boreal forests. *Boreal Environ. Res.* **10**. DOI: *https://doi.org/10.2205/2007ES000260*

Ma, Z., Peng, C., Zhu, Q., Chen, H., Yu, G., and co-authors, 2012, Regional drought-induced reduction in the biomass carbon sink of Canada's boreal forests, *Proc. Natl. Acad. Sci. U. S. A,* **109**, 2423–2427. DOI: *https://doi.org/10.1073/pnas.1111576109*

Machacova, K., Bäck, J., Vanhatalo, A., Halmeenmäki, E., Kolari, P., and co-authors, 2016, Pinus sylvestris as a missing source of nitrous oxide and methane in boreal forest. *Scientific Reports*, **6**, 23410. DOI: *https://doi.org/10.1038/srep23410*

Machado, L. A. T., Calheiros, A. J. P., Biscaro, T., Giangrande, S., Silva Dias, M. A. F., and co-authors, 2018, Overview: Precipitation characteristics and sensitivities to environmental conditions during GoAmazon2014/5 and ACRIDICON-CHUVA, *Atmos. Chem. Phys.*, **18**, 6461–6482. DOI: *https://doi.org/10.5194/acp-18-6461-2018*

Machado, L. A. T.; Laurent H.; N. Dessay and I. Miranda, 2004, Seasonal and diurnal variability of convection over the Amazonia: A comparison of different vegetation types and large scale forcing. *Theoretical and Applied Climatology*, **78**, 61. DOI: *https://doi.org/10.1007/s00704-004-0044-9*

Machado, L. A. T.; Laurent, H.; Lima, A. A., 2002, Diurnal march of the convection observed during TRMM-WETAMC/LBA. *J. Geophys. Res. Atmos.*, **107**, 8064. DOI: *https://doi.org/10.1029/2001JD000338*

MacKenzie, A. R., Langford, B., Pugh, T. A. M., Robinson, N., Misztal, P. K., and co-authors, 2011, The atmospheric chemistry of trace gases and particulate matter emitted by different land uses in Borneo., *Philos. Trans. R. Soc. Lond. B. Biol. Sci.*, **366,** (1582), 3177–95. DOI: *https://doi.org/10.1098/rstb.2011.0053*

Maenhaut, W., Fernandez-Jimenez, M.-T., Rajta, I. and Artaxo, P., 2002, Two-year study of atmospheric aerosols in Alta Floresta, Brazil: Multielemental composition and source apportionment, *Nucl. Instruments Methods Phys.* Res. Sect. B Beam Interact. with Mater. Atoms, **189**, 243–248. DOI: *https://doi.org/10.1016/S0168-583X(01)01050-3*

Maenhaut, W., M. T. Fernandez-Jimenez, P. Artaxo, 1999, Long-term study of atmospheric aerosols in Cuiabá, Brazil: multielemental composition, sources, and source apportionment. *Journal of Aerosol Science*, **30**, S259–260. DOI: *https://doi.org/10.1016/S0021-8502(99)80141-4*

Mahowald, N., P. Artaxo, A. Baker, T. Jickells, G. Okin, J. Randerson, A. Townsend., 2005, Impacts of biomass burning emissions and land use change on Amazonian atmospheric phosphorus cycling and deposition. *Global Biogeochemical Cycles*, **19** (4). DOI: *https://doi.org/10.1029/2005GB002541*

Mäkelä, J.M., Aalto, P., Jokinen, V., Pohja, T., Nissinen, A., and co-authors, 1997. Observations of ultrafine aerosol particle formation and growth in boreal forest. *Geophys. Res. Lett.*, **24**(10), 1219–1222. DOI: *https://doi.org/10.1029/97GL00920*

Makkonen, R., Asmi, A., Kerminen, V.-M., Boy, M., Arneth, A., Guenther, A., and Kulmala, M., 2012, BVOC-aerosol-climate interactions in the global aerosol-climate model ECHAM5.5-HAM2, *Atmos. Chem. Phys.*, **12**, 10077–10096. DOI: *https://doi.org/10.5194/acp-12-10077-2012*

Makkonen, U. V., A., Hellén, H., Hemmilä, M., Sund, J., Äijälä, M., Ehn, M., Junninen, H. and co-authors, 2014, Semi-continuous gas and inorganic aerosol measurements at a boreal forest site: seasonal and diurnal cycles of NH_3, HONO and HNO_3, *Boreal Environment Research,* (supp. B), 311–328.

Malavelle, F. F., Haywood, J. M., Mercado, L. M., Folberth, G. A., Bellouin, N., Sitch, S., and Artaxo, P., 2019, Studying the impact of biomass burning aerosol radiative and climate effects on the Amazon rainforest productivity with an Earth system model, *Atmos. Chem. Phys.*, **19**, 1301–1326. DOI: *https://doi.org/10.5194/acp-19-1301-2019*

Malhi, Y., Aragão, L. E. O. C., Galbraith, D., Huntingford, C., Fisher, R., and co-authors, 2009, Exploring the likelihood and mechanism of a climate-change-induced dieback of the Amazon rainforest, *Proc. Natl. Acad. Sci. U. S. A*, **106**, 20610–20615. DOI: *https://doi.org/10.1073/pnas.0804619106*

Malhi, Y., D. D. Baldocchi and P. G. Jarvis, 1999, The carbon balance of tropical, temperate, and boreal forests. *Plant, Cell and Environment*, **22**, 715–740. DOI: *https://doi.org/10.1046/j.1365-3040.1999.00453.x*

Malhi, Y., Roberts, J. T., Betts, R. A., Killeen, T. J., Li, W. Nobre, C. A., 2008, Climate Change, Deforestation, and the Fate of the Amazon, *Science*, **319**, 5860, 169–172. DOI: *https://doi.org/10.1126/science.1146961*

Maljanen, M., Jokinen, H., Saari, A., Strommer, R. and Martikainen, P.J., 2006. Methane and nitrous oxide fluxes, and carbon dioxide production in boreal forest soil fertilized with wood ash and nitrogen. *Soil Use Manage*., **22**(2): 151–157. DOI: *https://doi.org/10.1111/j.1475-2743.2006.00029.x*

Manabe, S. & Wetherald, R., 1975, The effects of doubling the CO_2 concentration on the climate of a general circulation model. *J. Atmos. Sci.*, **32**, 3–15. DOI: *https://doi.org/10.1175/1520-0469(1975)032<0003:TEODTC>2.0.CO;2*

Manninen H.E., Bäck, J., Sihto-Nissilä S.-L., Huffman A., Pessi A.-M., and co-authors, 2014, Patterns in airborne pollen and other primary biological aerosol particles (PBAP), and their contribution to aerosol mass and number in a boreal forest, *Boreal Environment Research*, **19** (suppl. B), 383–405.

MapBiomas Amazonia, 2020, Collection 2.0 of annual maps of land cover, land use and land use 13 changes between 1985 to 2018 in the Pan Amazon. *https://amazonia.mapbiomas.org/*.

Marais, E. A., Jacob, D. J., Kurosu, T. P., Chance, K., Murphy, J. G.; and co-authors, 2012, Isoprene emissions in Africa inferred from OMI observations of formaldehyde columns. *Atmos. Chem. Phys*., **12**, (14), 6219–6235. DOI: *https://doi.org/10.5194/acp-12-6219-2012*

Marenco, F., Johnson, B., Langridge, J. M., Mulcahy, J., Benedetti, A., and co-authors, 2016, On the vertical distribution of smoke in the Amazonian atmosphere during the dry season, *Atmos. Chem. Phys*., **16**, 2155–2174. DOI: *https://doi.org/10.5194/acp-16-2155-2016*

Marengo, J. A.; Borma, L. S.; Rodriguez, D. A; Pinho, P.; Soares, W. R.; Alves, L. M. 2013, Recent Extremes of Drought and Flooding in Amazonia: Vulnerabilities and Human Adaptation. *American Journal of Climate Change*, **2**, p. 87–96. DOI: *https://doi.org/10.4236/ajcc.2013.22009*

Marengo, J. A, E.R. Williams, L. M Alves, W. R. Soares, D. A. Rodrigues, 2016, Extreme seasonal variations in the Amazon Basin: droughts and floods. In *Interaction between biosphere, atmosphere, and human land use in the Amazon basin* (eds Nagy, L. Forsberg, B. R., Artaxo, P.), Springer, 55–76. DOI: *https://doi.org/10.1007/978-3-662-49902-3_4*

Marlon, J. R., Kelly, R., Daniau, A-L., Vannière, B., Power, M.J. and co-authors, 2016, Reconstructions of biomass burning from sediment-charcoal records to improve data-model comparisons, *Biogeosciences*, **13**, 3225–3244. DOI: *https://doi.org/10.5194/bg-13-3225-2016*

Martin, S. T., Andreae, M. O., Althausen, D., Artaxo, P., Baars, H., and co-authors, 2010, An overview of the Amazonian Aerosol Characterization Experiment 2008 (AMAZE-08), *Atmos. Chem. Phys*., **10**(23), 11415–11438. DOI: *https://doi.org/10.5194/acp-10-11415-2010*

Martin, S. T., Andreae, M. O., Artaxo, P., Baumgardner, D., Chen, Q., and co-authors, 2010, Sources and properties of Amazonian aerosol particles, *Rev. Geophys*., **48**, Rg2002. DOI: *https://doi.org/10.1029/2008RG000280*

Martin, S. T., Artaxo, P., Machado, L. A. T., Manzi, A. O., Souza, R. A. F., and co-authors, 2016, Introduction: Observations and Modeling of the Green Ocean Amazon (GoAmazon2014/5), *Atmos. Chem. Phys*., **16**, 4785–4797. DOI: *https://doi.org/10.5194/acp-16-4785-2016*

Martin, S. T., Artaxo, P., Machado, L., Manzi, A. O., Souza, R. A. F., and co-authors, 2017, The Green Ocean Amazon Experiment (GoAmazon2014/5) Observes Pollution Affecting Gases, Aerosols, Clouds, and Rainfall over the Rain Forest, *Bulletin of the American Meteorological Society*, **98**, 981–997. DOI: *https://doi.org/10.1175/BAMS-D-15-00221.1*

Martinez, M., Harder, H., Kubistin, D., Rudolf, M., Bozem, H., and co-authors, 2010, Hydroxyl radicals in the tropical troposphere over the Suriname rainforest: airborne measurements, *Atmos. Chem. Phys*., **10**(8), 3759–3773. DOI: *https://doi.org/10.5194/acp-10-3759-2010*

Martins, J. V.; Artaxo, P.; Kaufman, Y. J.; Castanho, A. D.; Remer, L. A., 2009, Spectral absorption properties of aerosol particles from 350–2500nm. *Geophys. Res. Lett*., **36**, No. 13, L13810. DOI: *https://doi.org/10.1029/2009GL037435*

Martins, J. V., P. V. Hobbs, R. E. Weiss, P. Artaxo, 1998, Morphology and structure of smoke particles from biomass burning in Brazil. *J. Geophys. Res. Atmos*., **103**, D24, 32041–32050. DOI: *https://doi.org/10.1029/98JD02593*

Martins, J. V., A. Marshak, L. Remer, D. Rosenfeld, Y. J. Kaufman, R., and co-authors, 2011, Remote sensing the vertical profile of cloud droplet effective radius, thermodynamic phase, and temperature. *Atmospheric Chemistry and Physics*, **11**, 9485–9501, 2011. DOI: *https://doi.org/10.5194/acp-11-9485-2011*

Matricardi, E. A. T., Skole, D.L., Bueno Costa, O., Pedlowski M.A., and co-authors, 2020,Long-term forest degradation surpasses deforestation in the Brazilian Amazon, *Science*, **369,** (6509), 1378–1382. DOI: *https://doi.org/10.1126/science.abb3021*

Matthias-Maser, S., Obolkin, V., Khodzer, T., and Jaenicke, R., 2000, Seasonal variation of primary biological aerosol particles in the remote continental region of Lake Baikal/Siberia, *Atmos Environ*, **34**, 3805–3811. DOI; *https://doi.org/10.1016/S1352-2310(00)00139-4*

Mauldin, R. L., Berndt, T., Sipila, M., Paasonen, P., Petaja, T., Kim, S., Kulmala, M. ,2012, A new atmospherically relevant oxidant of sulphur dioxide. *Nature*, **488,** (7410), 193–196. DOI: *https://doi.org/10.1038/nature11278*

McFiggans, G., Artaxo, P., Baltensperger, U., Coe, H., Facchini, M. C., and co-authors, 2006, The effect of physical and chemical aerosol properties on warm cloud droplet activation, *Atmos. Chem. Phys.*, **6**, 2593–2649. DOI: *https://doi.org/10.5194/acp-6-2593-2006*

Mei, F., Wang, J., Comstock, J. M., Weigel, R., Krämer, M., and co-authors, 2020, Comparison of aircraft measurements during GoAmazon2014/5 and ACRIDICON-CHUVA, *Atmos. Meas. Tech.*, **13**, 661–684. DOI: *https://doi.org/10.5194/amt-13-661-2020*

Melack, J.M., Hess, L.L., Gastil, M., Forsberg, B.R., Hamilton, S.K., Lima, I.B.T., Novo, E.M.L.M., 2004. Regionalization of methane emissions in the Amazon Basin with microwave remote sensing. *Glob. Chang. Biol.,* **10**, 530–544. DOI: *https://doi.org/10.1111/j.1365-2486.2004.00763.x*

Melnikova, I., & Sasai, T. (2020). Effects of anthropogenic activity on global terrestrial gross primary production. *J. Geophys. Res. Biog.,* **125**, e2019JG005403. DOI: *https://doi.org/10.1029/2019JG005403*

Merikanto, J., Spracklen, D. V., Mann, G. W., Pickering, S. J. and Carslaw, K. S., 2009, Impact of nucleation on global CCN, *Atmos. Chem. Phys.*, **9**, 8601–8616. DOI: *https://doi.org/10.5194/acp-9-8601-2009*

Metzger, A., Verheggen, B., Dommen, J., Duplissy, J., Prevot, A. S. H., and co-authors, 2010, Evidence for the role of organics in aerosol particle formation under atmospheric conditions, *Proc. Natl. Acad. Sci. USA*, **107**, 6646–6651. DOI: *https://doi.org/10.1073/pnas.0911330107*

Meurer, K. H. E., Franko, U., Stange, C. F., Rosa, J. D., Madari, B. E. and Jungkunst, H. F., 2016, Direct nitrous oxide (N_2O) fluxes from soils under different land use in Brazil—a critical review, Environ. Res. Lett., 11(2), 023001. DOI: *https://doi.org/10.1088/1748-9326/11/2/023001*

Mikhailov, E. F., Mironov, G. N., Pöhlker, C., Chi, X., Krüger, M. L., and co-authors, 2015, Chemical composition, microstructure, and hygroscopic properties of aerosol particles at the Zotino Tall Tower Observatory (ZOTTO), Siberia, during a summer campaign, *Atmos. Chem. Phys.*, **15**, 8847–8869. DOI: *https://doi.org/10.5194/acp-15-8847-2015*

Mikhailov, E., Mironova, S., Mironov, G., Vlasenko, S., Panov, A., and co-authors, 2017, Long-term measurements (2010–2014) of carbonaceous aerosol and carbon monoxide at the Zotino Tall Tower Observatory (ZOTTO) in central Siberia, *Atmos. Chem. Phys.*, **17**, 14365–14392. DOI: *https://doi.org/10.5194/acp-17-14365-2017*

Mikhailov, E., S. Vlasenko, D. Rose, and U. Pöschl, 2013, Mass-based hygroscopicity parameter interaction model and measurement of atmospheric aerosol water uptake, *Atmos. Chem. Phys.*, **13**, 717–740. DOI: *https://doi.org/10.5194/acp-13-717-2013*

Miller, J. B., Gatti, L. V., d'Amelio, M. T. S., Crotwell, A. M., Dlugokencky, E. J., Bakwin, P., Artaxo, P., and Tans, P. P. , 2007, Airborne measurements indicate large methane emissions from the eastern Amazon basin, *Geophys. Res. Lett.*, **34**, L10809. DOI: *https://doi.org/10.1029/2006GL029213*

Minkkinen, K., Ojanen P., Penttilä, T., Aurela, M., Laurila, T., and co-authors, 2018, Persistent carbon sink at a boreal drained bog forest. *Biogeosciences*, **15** (11): 3603–3624. DOI: *https://doi.org/10.5194/bg-15-3603-2018*

Mitchard, E. T. A., 2018, The tropical forest carbon cycle and climate change. *Nature*, **559**, 26, 527–534. DOI: *https://doi.org/10.1038/s41586-018-0300-2*

Möhler, O., DeMott, P. J., Vali, G., and Levin, Z., 2007, Microbiology and atmospheric processes: the role of biological particles in cloud physics, *Biogeosciences*, **4**, 1059–1071. DOI: *https://doi.org/10.5194/bg-4-1059-2007*

Mohr, C., Lopez Hilfiker, F.D., Yli Juuti, T., Heitto, A., Lutz, A., and co-authors, 2017. Ambient observations of dimers from terpene oxidation in the gas phase: Implications for new particle formation and growth. *Geophys. Res. Lett.,* **44** (6), 2958–2966. DOI: *https://doi.org/10.1002/2017GL072718*

Moiseenko, K.B., Shtabkin, Y.A., Berezina, E.V., Skorokhod, A.I., 2018, Regional Photochemical Surface-Ozone Sources in Europe and Western Siberia, *Izv. Atmos. Ocean. Phys.*, **54**, 545. DOI: *https://doi.org/10.1134/S0001433818060105*

Molina, L., Broquet, G., Imbach, P., Chevallier, F., Poulter, B., and co-authors, 2015, On the ability of a global atmospheric inversion to constrain variations of CO_2 fluxes over Amazonia, *Atmos. Chem. Phys.*, **15**, 8423–8438. DOI: *https://doi.org/10.5194/acp-15-8423-2015*

Molina, M.J. and J.T. Allen, 2019, On the Moisture Origins of Tornadic Thunderstorms, *J. Climate,* **32**, 4321–4346. DOI: *https://doi.org/10.1175/JCLI-D-18-0784.1*

Mondal, N., and R. Sukumar, 2016: Fires in Seasonally Dry Tropical Forest: Testing the Varying Constraints Hypothesis across a Regional Rainfall Gradient. *PLoS One*, **11**, e0159691. DOI: *https://doi.org/10.1371/journal.pone.0159691*

Monson RK, Jaeger CH, Adams WW, Driggers EM, Silver GM, Fall R., 1992, Relationships among Isoprene Emission Rate, Photosynthesis, and Isoprene Synthase Activity as Influenced by Temperature, *Plant Physiology.* **98** ,3,1175–1180. DOI: *https://doi.org/10.1104/pp.98.3.1175*

Moran-Zuloaga, D., Ditas, F., Walter, D., Saturno, J., Brito, J., and co-authors, 2018, Long-term study on coarse mode aerosols in the Amazon rain forest with the frequent intrusion of Saharan dust plumes, *Atmos. Chem. Phys.*, **18**, 10055–10088. DOI: *https://doi.org/10.5194/acp-18-10055-2018*

Morgan, W. T., Allan, J. D., Bauguitte, S., Darbyshire, E., Flynn, M. J., and co-authors, 2020, Transformation and ageing of biomass burning carbonaceous aerosol over tropical South America from aircraft in situ measurements during SAMBBA, *Atmos. Chem. Phys.,* **20**, 5309–5326. DOI: *https://doi.org/10.5194/acp-20-5309-2020*

Morgan, W.T., Darbyshire, E., Spracklen, D.V., Artaxo P., and H. Coe, 2019, Non-deforestation drivers of fires are

increasingly important sources of aerosol and carbon dioxide emissions across Amazonia. *Scientific Reports*, **9**:16975. DOI: *https://doi.org/10.1038/s41598-019-53112-6*

Morin, X., Viner, D. & Chuine, I. (2008) Tree species range shifts at a continental scale: new predictive insights from a process-based model. *Journal of Ecology*, **96**, 784–79. DOI: *https://doi.org/10.1111/j.1365-2745.2008.01369.x*

Morris, C. E., Georgakopoulos, D. G., and Sands, D. C., 2004, Ice nucleation active bacteria and their potential role in precipitation, *J. Phys. IV*, **121**, 87–103. DOI: *https://doi.org/10.1051/jp4:2004121004*

Morris, C. E., Sands, D. C., Bardin, M., Jaenicke, R., Vogel, B., and co-authors, 2011, Microbiology and atmospheric processes: research challenges concerning the impact of airborne micro-organisms on the atmosphere and climate, *Biogeosciences*, **8**, 17–25. DOI: *https://doi.org/10.5194/bg-8-17-2011*

Mota, B. W., Pereira, J. M. C., Oom, D., Vasconcelos, M. J. P., and Schultz, M., 2006, Screening the ESA ATSR-2 World Fire Atlas (1997–2002), *Atmos. Chem. Phys*., **6**, 1409–1424. DOI: *https://doi.org/10.5194/acp-6-1409-2006*

Mouchel-Vallon, C., Lee-Taylor, J., Hodzic, A., Artaxo, P., Aumont, B., and co-authors, 2020, Impact of Urban Emissions on a Biogenic Environment during the wet season: Explicit Modeling of the Manaus Plume Organic Chemistry with GECKO-A, *Atmos. Chem. Phys*., **20** (10), 5995–6014. DOI: *https://doi.org/10.5194/acp-20-5995-2020*

Mukhin, V.A. and Voronin, P.Y., 2008. A new source of methane in boreal forests. *Applied Biochemistry and Microbiology*, **44**(3): 297–299. DOI: *https://doi.org/10.1134/S0003683808030125*

Muller, C. J., and P. A. O'Gorman, 2011, An energetic perspective on the regional response of precipitation to climate change, *Nat Clim Change*, **1**, 5, 266–271. DOI: *https://doi.org/10.1038/nclimate1169*

Müller L., Reinnig, M.-C., Naumann, K. H., Saathoff, H., Mentel, T. F., 2012, Formation of 3-methyl-1,2,3-butanetricarboxylic acid via gas phaseoxidation of pinonic acid – a mass spectrometric study of SOA aging, *Atmos. Chem. Phys*., **12**, 1483–1496. DOI: *https://doi.org/10.5194/acp-12-1483-2012*

Muller, J. F., Stavrakou, T., Wallens, S., De Smedt, I., Van Roozendael, M., and co-authors, 2008, Global isoprene emissions estimated using MEGAN, ECMWF analyses and a detailed canopy environment model. *Atmos Chem Phys*, **8**, (5), 1329–1341. DOI: *https://doi.org/10.5194/acp-8-1329-2008*

Murphy, B.N., Julin, J., Riipinen, I., & Ekman, A.M. L., 2015, Organic aerosol processing in tropical deep convective clouds: Development of a new model (CRM-ORG) and implications for sources of particle number. *J. Geophys. Res. Atmos*., **120**, 10441–10464. DOI: *https://doi.org/10.1002/2015JD023551*

Myhre, G., B. H. Samset, M. Schulz, Y. Balkanski, S. Bauer, and co-authors, 2013, Radiative forcing of the direct aerosol effect from AeroCom Phase II simulations, *Atmos. Chem. Phys*., **13**, 1853–1877. DOI: *https://doi.org/10.5194/acp-13-1853-2013*

Nagy, Lazlo, Bruce Forsberg, Paulo Artaxo, 2016, Ecological Studies: Analysis and Synthesis in *Interactions between Biosphere, Atmosphere and Human Land Use in the Amazon Basin*. Springer Verlag, Berlin, Pages: 478, Library of Congress Control Number:2016944616, Hard Cover ISBN 978-3-662-49902-3, 227. DOI: *https://doi.org/10.1007/978-3-662-49902-3*

Nascimento, J. P., Bela, M. M., Meller, B., Banducci, A. L., Rizzo, L. V., and co-authors, 2021, Aerosols from anthropogenic and biogenic sources and their interactions: modeling aerosol formation, optical properties and impacts over the central Amazon Basin, *Atmos. Chem. Phys*., **21**, 6755–6779, 2021. DOI: *https://doi.org/10.5194/acp-21-6755-2021*

Nemecek-Marshall, M., MacDonald, R. C., Franzen, J. J., Wojciechowski, C. L. & Fall, R., 1995: Methanol emission from leaves. *Plant Physiol*., **108**, 1359–1368. DOI: *https://doi.org/10.1104/pp.108.4.1359*

Nemitz, E., Artaxo, P., Cappa, C.D., Martin S. T. & J. L. Jimenez, 2013, Chemically Resolved Particle Fluxes Over Tropical and Temperate Forests, *Aerosol Science and Technology*, **47**:7, 818–830. DOI: *https://doi.org/10.1080/02786826.2013.791022*

Nepstad, D. C., Stickler, C. M., Soares, B., and Merry, F., 2008, Interactions among Amazon land use, forests, and climate: prospects for a near-term forest tipping point, *Philosophical Transactions of the Royal Society B-Biological Sciences*, **363**, 1737–1746. DOI: *https://doi.org/10.1098/rstb.2007.0036*

Nessler, R. Weingartner, E. Baltensperger U., 2005, Effect of humidity on aerosol light absorption and its implications for extinction and the single scattering albedo illustrated for a site in the lower free troposphere, *J. Aerosol Sci*., **36** (2005), 958–972. DOI: *https://doi.org/10.1016/j.jaerosci.2004.11.012*

Ni, X. and Groffman, P.M., 2018. Declines in methane uptake in forest soils. *Proc. Natl. Acad. Sci. U. S. A*, **115** (34): 8587–8590. DOI: *https://doi.org/10.1073/pnas.1807377115*

Nieminen, T., Asmi, A., Dal Maso, M., Aalto, P. P., Keronen, P., and co-authors, 2014, Trends in atmospheric new-particle formation: 16 years of observations in a boreal-forest environment, *Boreal Environment Research*, **19**, 191–214.

Nilsson, E. D., Paatero, J and Boy, M. , 2001, Effects of air masses and synoptic weather on aerosol formation in the continental boundary layer, *Tellus B Chem Phys Meteorol*, **53**, 462–478. DOI: *https://doi.org/10.1034/j.1600-0889.2001.530410.x*

Niyogi, D., Chang, H., Saxena, V. K., Holt, T., Alapaty, K. and co-authors, 2004, Direct observations of the effects of aerosol loading on net ecosystem CO_2 exchanges over different landscapes, *Geophys. Res. Lett*., **31**. DOI: *https://doi.org/10.1029/2004GL020915*

Nobre, CA, JA Marengo, WR Soares, 2019, *Climate Change Risks in Brazil*, Springer. ISBN 978-3-319-92880-7. DOI: *https://doi.org/10.1007/978-3-319-92881-4*

Nölscher, A. C., Yañez-Serrano, A. M., Wolff, S., de Araujo, A. C., Lavrič, J. V., Kesselmeier, J. and Williams, J. 2016. Unexpected seasonality in quantity and composition of Amazon rainforest air reactivity, *Nat. Commun*., **7**, 10383. DOI: *https://doi.org/10.1038/ncomms10383*

Nunes, A. M. P.; Silva Dias, M. A. F.; Anselmo, E. M.; Morales, C. A., 2016, Severe Convection Features in the Amazon Basin: A TRMM-Based 15-Year Evaluation. *Frontiers in Earth Science,* **4**, 2016/000037. DOI: *https://doi.org/10.3389/feart.2016.00037*

O'Dowd, C., Yoon, Y., Junkermann, W., Aalto, P., Kulmala, M., Lihavainen, H., and Viisanen, Y. 2009, Airborne measurements of nucleation mode particles II: boreal forest nucleation events, *Atmos. Chem. Phys*., **9**. DOI: *https://doi.org/10.5194/acpd-8-2821-2008*

Oberlander, E.A., Brenninkmeijer, C.A.M., Crutzen, P.J., Elansky, N.F., Golitsyn, G.S., and co-authors, 2002, Trace gas measurements along the Trans-Siberian railroad: The TROICA 5 expedition, *J. Geophys. Res. Atmos*., **107**. DOI: *https://doi.org/10.1029/2001JD000953*

Oki, T. and Kanae, S., 2006. Global hydrological cycles and world water resources. *Science*, **313**(5790): 1068–1072. DOI: *https://doi.org/10.1126/science.1128845*

Okin, G. S., N. Mahowald, O. A. Chadwick, P. Artaxo. 2004, Impact of desert dust on the biogeochemistry of phosphorus in terrestrial ecosystems. *Global Biogeochemical Cycles*, **18**, 2, GB2005. DOI: *https://doi.org/10.1029/2003GB002145*

Oliveira, P. E. S., Acevedo, O. C., Sörgel, M., Tsokankunku, A., Wolff, S., and co-authors, 2018, Nighttime wind and scalar variability within and above an Amazonian canopy, *Atmos. Chem. Phys*., **18**, 3083–3099. DOI: *https://doi.org/10.5194/acp-18-3083-2018*

Oliveira, P. H. F., Artaxo, P., Pires, C., De Lucca, S., Procopio, A., and co-authors, 2007, The effects of biomass burning aerosols and clouds on the CO_2 flux in Amazonia, *Tellus B Chem Phys Meteorol*, **59B**, 338–349. DOI: *https://doi.org/10.1111/j.1600-0889.2007.00270.x*

Ometto, J. P. A. D. Nobre, H. Rocha, P. Artaxo, L. Martinelli, 2005, Amazônia and the Modern Carbon Cycle: Lessons Learned. Invited manuscript no. OEC-JE-2004-0459. *Oecologia*, **143**, 4, 483–500. DOI: *https://doi.org/10.1007/s00442-005-0034-3*

Öquist, M.G., Bishop, K., Grelle, A., Klemedtsson, L., Kohler, S.J., and co-authors, 2014. The full annual carbon balance of boreal forests is highly sensitive to precipitation, *Environmental Science & Technology Letters*, **1**, 7, 315–319. DOI: *https://doi.org/10.1021/ez500169j*

Ordway, E. M., and G. P. Asner. 2020. Carbon declines along tropical forest edges correspond to heterogeneous effects on canopy structure and function. *Proceedings of the National Academy of Sciences USA,* **117,** 7863–7870. DOI: *https://doi.org/10.1073/pnas.1914420117*

Ovadnevaite, J., Zuend, A., Laaksonen, A., Sanchez, K.J., Roberts, G., and co-authors, 2017, Surface tension prevails over solute effect in organic-influenced cloud droplet activation. *Nature*, **546**, 637–641. DOI: *https://doi.org/10.1038/nature22806*

Paasonen, P., Asmi, A., Petäjä, T., Kajos, M. K., Äijälä, M, and co-authors, 2013, Warming-induced increase in aerosol number concentration likely to moderate climate change, *Nature Geosci*, **6**, 438–442. DOI: *https://doi.org/10.1038/ngeo1800*

Paasonen, P., Nieminen, T., Asmi, E., Manninen, H. E., Petäjä, T., and co-authors, 2010, On the roles of sulphuric acid and low-volatility organic vapours in the initial steps of atmospheric new particle formation, *Atmos. Chem. Phys*., **10**, 11223–11242. DOI: *https://doi.org/10.5194/acp-10-11223-2010*

Pacifico, F., Folberth, G. A., Sitch, S., Haywood, J. M., Rizzo, L. V., and co-authors, 2015, Biomass burning related ozone damage on vegetation over the Amazon forest: a model sensitivity study, *Atmos. Chem. Phys*., **15**, 2791–2804. DOI: *https://doi.org/10.5194/acp-15-2791-2015*

Page, S.E., Rieley, J.O., Banks, C.J., 2011. Global and regional importance of the tropical peatland carbon pool. *Glob. Chang. Biol*. DOI: *https://doi.org/10.1111/j.1365-2486.2010.02279.x*

Pajunoja, A., Lambe, A.T., Hakala, J., Rastak, N., Cummings, M.J., and co-authors, 2015, Adsorptive uptake of water by semisolid secondary organic aerosols, *Geophys. Res. Lett*., **42**, 3063–3068. DOI: *https://doi.org/10.1002/2015GL063142*

Palácios, R. da S., Artaxo, P. E., Cirino, G. G., Nakale, V., Morais, F. G., and co-authors, 2020, Long-term measurements of aerosol optical properties and radiative forcing (2011–2017) over Central Amazonia. Atmósfera. Retrieved from *https://www.revistascca.unam.mx/atm/index.php/atm/article/view/52892*.

Palm, B. B., de Sá, S. S., Day, D. A., Campuzano-Jost, P., Hu, W., and co-authors, 2018, Secondary organic aerosol formation from ambient air in an oxidation flow reactor in central Amazonia, *Atmos. Chem. Phys*., **18**, 467–493. DOI: *https://doi.org/10.5194/acp-18-467-2018*

Pan, Y. D., R. A. Birdsey, J. Y. Fang, R. Houghton, P. E. Kauppi, and co-authors, 2011, A large and persistent carbon sink in the World's forests. *Science*, **333**, 988–993. DOI: *https://doi.org/10.1126/science.1201609*

Pan, Y., Birdsey, R.A., Phillips, O.L., Jackson, R.B., 2013. The structure, distribution, and biomass of the world's forests. *Annu. Rev. Ecol. Evol. Syst.,* **44**, 593–622. DOI: *https://doi.org/10.1146/annurev-ecolsys-110512-135914*

Pandolfi, M., Alados-Arboledas, L., Alastuey, A., Andrade, M., Angelov, C., and co-authors, 2018, A European aerosol phenomenology – 6: scattering properties of atmospheric aerosol particles from 28 ACTRIS sites, *Atmos. Chem. Phys*., **18**, 7877–7911. DOI: *https://doi.org/10.5194/acp-18-7877-2018*

Pangala, S. R., Enrich-Prast, A., Basso, L. S., Peixoto, R. B., Bastviken, D., and co-authors, 2017, Large emissions from floodplain trees close the Amazon methane budget, *Nature*, **552**/230. DOI: *https://doi.org/10.1038/nature24639*

Paralovo, S. L., Barbosa, C.G.G., Carneiro, I.P.S., Kurzlop, P., Borillo, G.C., and co-authors, 2019, Observations of particulate matter, NO_2, SO_2, O_3, H_2S and selected VOCs at a semi-urban environment in the Amazon region, *Science of The Total Environment*, **650**, Part 1, 996–1006. DOI: *https://doi.org/10.1016/j.scitotenv.2018.09.073*

Paramonov, M., Aalto, P. P., Asmi, A., Prisle, N., Kerminen, V.- M., Kulmala, M., and Petäjä, T., 2013, The analysis of size-segregated cloud condensation nuclei counter (CCNC) data and its implications for cloud droplet activation, *Atmos. Chem. Phys.*, **13**, 10285–10301. DOI: *https://doi.org/10.5194/acp-13-10285-2013*

Paris, J.-D., Ciais, P., Nédélec, P., Ramonet, M., Belan, B. D., and co-authors, 2008, The YAK-AEROSIB transcontinental aircraft campaigns: new insights on the transport of CO_2, CO and O_3 across Siberia, *Tellus B Chem Phys Meteorol*, **60**, 551–568. DOI: *https://doi.org/10.1111/j.1600-0889.2008.00369.x*

Paris, J.-D., Stohl, A., Ciais, P., Nédélec, P., Belan, B. D., and co-authors, 2010, Source-receptor relationships for airborne measurements of CO_2, CO, and O_3 above Siberia: a cluster-based approach, *Atmos. Chem. Phys.*, **10**, 1671–1687. DOI: *https://doi.org/10.5194/acp-10-1671-2010*

Park, S.-B., Knohl, A., Lucas-Moffat, A.M., Migliavacca, M., Gerbig, C., Vesala, T., and co-authors, 2018, Strong radiative effect induced by clouds and smoke on forest net ecosystem productivity in central Siberia, *Agric. For. Meteorol.*, **250–251**, 376–387. DOI: *https://doi.org/10.1016/j.agrformet.2017.09.009*

Patade, S., Phillips, V. T. J., Amato, P., Bingemer, H. G., Burrows, S. M., and co-authors, 2021, Empirical formulation for multiple groups of primary biological ice nucleating particles from field observations over Amazonia, *Journal of the Atmospheric Sciences*, **79**, 1–25. DOI: *https://doi.org/10.1175/JAS-D-20-0096.1*

Patra, P.K., Canadell, J.G., Houghton, R.A., Piao, S.L., Oh, N.H., and co-authors, 2013, The carbon budget of South Asia. *Biogeosciences*. DOI: *https://doi.org/10.5194/bg-10-513-2013*

Pauliquevis, T., Lara, L. L., Antunes, M. L. and Artaxo, P., 2012, Aerosol and precipitation chemistry measurements in a remote site in Central Amazonia: The role of biogenic contribution. *Atmos. Chem. Phys.*, **12**, 4987–5015. DOI: *https://doi.org/10.5194/acp-12-4987-2012*

Paulot, F., Crounse, J. D., Kjaergaard, H. G., Kroll, J. H., Seinfeld, J. H., and Wennberg, P. O., 2019, Isoprene photooxidation: new insights into the production of acids and organic nitrates, *Atmos. Chem. Phys.*, **9**, 1479–1501. DOI: *https://doi.org/10.5194/acp-9-1479-2009*

Pausas, J.G., and Paula, S., 2012, Fuel shapes the fire–climate relationship: evidence from Mediterranean ecosystems. *Global Ecology and Biogeography*, **21**: 1074–1082. DOI: *https://doi.org/10.1111/j.1466-8238.2012.00769.x*

Pedruzo-Bagazgoitia, X., H.G. Ouwersloot, M. Sikma, C.C. van Heerwaarden, C.M. Jacobs, and J. Vilà-Guerau de Arellano, 2017, Direct and Diffuse Radiation in the Shallow Cumulus–Vegetation System: Enhanced and Decreased Evapotranspiration Regimes. *J. Hydrometeor.*, **18**, 1731–1748. DOI: *https://doi.org/10.1175/JHM-D-16-0279.1*

Peng, C.H., Ma Z., Lei, X., Zhu, Q., Chen, H., and co-authors, 2011, A drought-induced pervasive increase in tree mortality across Canada's boreal forests. *Nature Climate Change*, **1,** 9, 467–471. DOI: *https://doi.org/10.1038/nclimate1293*

Penuelas, J., Asensio, D., Tholl, D., Wenke, K., Rosenkranz, M., Piechulla, B., and Schnitzler, J. P., 2014, Biogenic volatile emissions from the soil, *Plant, Cell & Environment*, **37**, 1866–1891. DOI: *https://doi.org/10.1111/pce.12340*

Peñuelas, J., and Staudt, M. 2010. BVOCs and global change. *Trends Plant Sci.* **15**, 133–44. DOI: *https://doi.org/10.1016/j.tplants.2009.12.005*

Perry, K. D. and Hobbs, P. V., 1994, Further evidence for particle nucleation in clear-air adjacent to marine cumulus clouds, *J. Geophys. Res.*, **99**, 22803–22818. DOI: *https://doi.org/10.1029/94JD01926*

Petäjä, T., Kerminen, V.-M., Hämeri, K., Vaattovaara, P., Joutsensaari, J., and co-authors, 2005, Effects of SO2 oxidation on ambient aerosol growth in water and ethanol vapours, *Atmos. Chem. Phys.*, **5**, 767–779. Sref-ID:1680-324/acp/2005-5-767. DOI: *https://doi.org/10.5194/acp-5-767-2005*

Petäjä, T., Mauldin, III, R. L., Kosciuch, E., McGrath, J., Nieminen, T., and co-authors, 2009, Sulfuric acid and OH concentrations in a boreal forest site, *Atmos. Chem. Phys.*, **9**, 7435–7448. DOI: *https://doi.org/10.5194/acp-9-7435-2009*

Petters, M. D. and Kreidenweis, S. M., 2007, A single parameter representation of hygroscopic growth and cloud condensation nucleus activity, *Atmos. Chem. Phys.*, **7**, 1961–1971. DOI: *https://doi.org/10.5194/acp-7-1961-2007*

Phillips, O. L, Aragão, L.E.O.C., Lewis, S.L., Fisher, J.B., Lloyd, J., and co-authors, 2009, Drought sensitivity of the Amazon rainforest. *Science*, **323**, 5919, 1344–1347.

Pielke RA, Vidale PL. 1995. The boreal forest and the polar front. *J. Geophys. Res. Atmos.*, **100**, 25755. DOI: *https://doi.org/10.1029/95JD02418*

Pinto, D. M., Blande, J. D., Souza, S. R., Nerg, A.-M. and Holopainen, J. K., 2010, Plant Volatile Organic Compounds (VOCs) in Ozone (O3) Polluted Atmospheres: The Ecological Effects, *J. Chem. Ecol.*, **36**, 22–34. DOI: *https://doi.org/10.1007/s10886-009-9732-3*

Pirjola, L., Virkkula, A., Petäjä, T., Levula, J., Kukkonen, J. and Kulmala, M. (2015) Mobile ground-based measurements of aerosol and trace gases during a prescribed burning experiment in boreal forest in Finland, *Boreal Environ. Res.,* **20**, 105–119.

Pöhlker, C., J. Saturno, M. L. Krüger, J.-D. Förster, M. Weigand, and co-authors, 2014, Efflorescence upon humidification?

X-ray microspectroscopic in situ observation of changes in aerosol microstructure and phase state upon hydration, *Geophys. Res. Lett.*, **41**,3681–3689. DOI: *https://doi.org/10.1002/2014GL059409*

Pöhlker, C., K. T. Wiedemann, B. Sinha, M. Shiraiwa, S. S. Gunthe, and co-authors. 2012. Biogenic potassium salt particles as seeds for secondary organic aerosol in the Amazon. *Science*, **337**, 1075–1078. DOI: *https://doi.org/10.1126/science.1223264*

Pöhlker, C., Walter, D., Paulsen, H., Könemann, T., Rodríguez-Caballero, E., and co-authors. 2019. Land cover and its transformation in the backward trajectory footprint region of the Amazon Tall Tower Observatory. *Atmos. Chem. Phys.*, **19**, 8425–8470. DOI: *https://doi.org/10.5194/acp-19-8425-2019*

Pöhlker, M. L., Ditas, F., Saturno, J., Klimach, T., Hrabě de Angelis, I., and co-authors. 2018. Long-term observations of cloud condensation nuclei over the Amazon rain forest – Part 2: Variability and characteristics of biomass burning, long-range transport, and pristine rain forest aerosols: *Atmos. Chem. Phys.*, **18**, 10289–10331. DOI: *https://doi.org/10.5194/acp-18-10289-2018*

Pöhlker, M. L., Pöhlker, C., Ditas, F., Klimach, T., Hrabe de Angelis, I., and co-authors. 2016. Long-term observations of cloud condensation nuclei in the Amazon rain forest – Part 1: Aerosol size distribution, hygroscopicity, and new model parametrizations for CCN prediction, Atmos. Chem. Phys., **16**, 15709–15740. DOI: *https://doi.org/10.5194/acp-16-15709-2016*

Ponomarev, I. E., I. V. Kharuk, and J. K. Ranson, 2016: Wildfires Dynamics in Siberian Larch Forests. *For.*, **7**. DOI: *https://doi.org/10.3390/f7060125*

Pope, R. J., Arnold, S. R., Chipperfield, M. P., Reddington, C. L. S., Butt, E. W., Keslake, T. D., and co-authors, 2020, Substantial increases in Eastern Amazon and Cerrado biomass burning-sourced tropospheric ozone. *Geophys. Res. Lett.*, **47**, e2019GL084143. DOI: *https://doi.org/10.1029/2019GL084143*

Pöschl, U., Martin, S. T., Sinha, B., Chen, Q., Gunthe, S. S., and co-authors, 2010, Rainforest Aerosols as Biogenic Nuclei of Clouds and Precipitation in the Amazon, *Science*, **329**, 1513–1516. DOI: *https://doi.org/10.1126/science.1191056*

Pöschl, U., and Shiraiwa, M., 2015, Multiphase Chemistry at the Atmosphere-Biosphere Interface Influencing Climate and Public Health in the Anthropocene, *Chemical Reviews*, **115**, 4440–4475. DOI: *https://doi.org/10.1021/cr500487s*

Praplan AP, Tykkä T, Chen D, Boy M, Taipale D, and co-authors, 2019. Long-term total OH reactivity measurements in a boreal forest, *Atmospheric Chemistry and Physics*, **19**, 14431–14453. DOI: *https://doi.org/10.5194/acp-19-14431-2019*

Prass, M., Andreae, M. O., de Araùjo, A. C., Artaxo, P., Ditas, F., and co-authors, 2021, Bioaerosols in the Amazon rain forest: temporal variations and vertical profiles of Eukarya, Bacteria, and Archaea. *Biogeosciences*, **18**, 17, 4873–4887. DOI: *https://doi.org/10.5194/bg-18-4873-2021*

Prenni, A.J., Petters, M.D., Kreidenweis, S.M., Heald, C.L., and co-authors, 2009, Relative roles of biogenic emissions and Saharan dust as ice nuclei in the Amazon basin, *Nature Geosciences*, **2**, 402–405. DOI: *https://doi.org/10.1038/ngeo517*

Prenni, A. J., Tobo, Y., Garcia, E., DeMott, P. J., Huffman, J. A., and co-authors, 2013, The impact of rain on ice nuclei populations at a forested site in Colorado, *Geophys. Res. Lett.*, **40**, 227–231. DOI: *https://doi.org/10.1029/2012GL053953*

Procópio, A, S., P. Artaxo, Y. J. Kaufman, L. A. Remer, J. S. Schafer, B. N. Holben, 2004, Multiyear analysis of Amazonian biomass burning smoke radiative forcing of climate. *Geophys. Res. Lett.*, **31**, No. 3, pg. L03108 – L03112. DOI: *https://doi.org/10.1029/2003GL018646*

Procópio, A. S.; L. A. Remer, P. Artaxo, Y. J. Kaufman, B. N. Holben, Modeled spectral optical properties for smoke aerosols in Amazonia, 2003, *Geophys. Res. Lett.*, **30**, 24, 2265–2270. DOI: *https://doi.org/10.1029/2003GL018063*

Proske J.U., 2018, Characterization of Biological Ice Nucleating Particles in a Boreal Forest Environment, BSc thesis, Johann Wolfgang Goethe-University, Frankfurt.

Prospero, J. M., Blades, E., Mathison, G., and Naidu, R., 2005, Interhemispheric transport of viable fungi and bacteria from Africa to the Caribbean with soil dust, *Aerobiologia*, **21**, 1–19. DOI: *https://doi.org/10.1007/s10453-004-5872-7*

Prăvălie, R., 2018, Major perturbations in the Earth's forest ecosystems. Possible implications for global warming. *Earth*. DOI: *https://doi.org/10.1016/j.earscirev.2018.06.010*

Pugh, T.A.M., Arneth, A., Kautz, M. and co-authors, 2019a, Important role of forest disturbances in the global biomass turnover and carbon sinks. *Nat. Geosci.*, **12**, 730–735 (2019). DOI: *https://doi.org/10.1038/s41561-019-0427-2*

Pugh, T. A. M., Jones, C. D., Huntingford, C., Burton, C., Arneth, A., Brovkin, V., and co-authors, 2018. A large committed long-term sink of carbon due to vegetation dynamics. *Earth's Future*, **6**, 1413– 1432. DOI: *https://doi.org/10.1029/2018EF000935*

Pugh, T.A.M., Lindeskog, M., Smith, B., Poultere, B., Arneth, A., and co-authors, 2019b, Role of forest regrowth in global carbon sink dynamics, *Proc. Natl. Acad. Sci. U. S. A*, **116**, 10, 4382–4387. DOI: *https://doi.org/10.1073/pnas.1810512116*

Pugh, T. A. M., MacKenzie, A. R., Hewitt, C. N., Langford, B., Edwards, P. M., and co-authors, 2010, Simulating atmospheric composition over a South-East Asian tropical rainforest: performance of a chemistry box model, *Atmos Chem Phys*, **10**, 279–298. DOI: *https://doi.org/10.5194/acp-10-279-2010*

Pulliainen, J. Aurela, M., Laurila, T., Aalto, T., Takala, M., and co-authors, 2017. Early snowmelt significantly enhances boreal springtime carbon uptake. *Proc. Natl. Acad. Sci. U. S. A*, **114**, 42, 11081–11086. DOI: *https://doi.org/10.1073/pnas.1707889114*

Pye, H.O.T., D'Ambro, E.L., Lee, B.H., Schobesberger, S., Takeuchi, M., and co-authors, 2019, Anthropogenic enhancements to production of highly oxygenated molecules from autoxidation, *Proc. Natl. Acad. Sci. U. S. A*, *116*, 14, 6641–6646. DOI: *https://doi.org/10.1073/pnas.1810774116*

Querino, C. A. S., Smeets, C. J. P. P., Vigano, I., Holzinger, R., Moura, V., and co-authors, 2011, Methane flux, vertical gradient and mixing ratio measurements in a tropical forest, *Atmos. Chem. Phys*., **11**, 7943–7953. DOI: *https://doi.org/10.5194/acp-11-7943-2011*

Räisänen T., Ryyppö A. & Kellomäki S. 2008. Impact of timber felling on the ambient monoterpene concentration of a Scots pine (Pinus sylvestris L.) forest. *Atmos. Environ*., **42**, 6759–6766. DOI: *https://doi.org/10.1016/j.atmosenv.2008.05.035*

Ramanathan, V., P. J. Crutzen, J. T. Kiehl, and D. Rosenfeld (2001), Atmosphere – Aerosols, climate, and the hydrological cycle, *Science*, **294,** 5549, 2119–2124. DOI: *https://doi.org/10.1126/science.1064034*

Ramsay, R., Di Marco, C. F., Heal, M. R., Sörgel, M., Artaxo, P., and co-authors, 2021, Measurement and modelling of the dynamics of NH_3 surface–atmosphere exchange over the Amazonian rainforest, *Biogeosciences*, **18**, 9, 2809–2825. DOI: *https://doi.org/10.5194/bg-18-2809-2021*

Ramsay, R., Di Marco, C. F., Sörgel, M., Heal, M. R., Carbone, S., and co-authors, 2020, Concentrations and biosphere–atmosphere fluxes of inorganic trace gases and associated ionic aerosol counterparts over the Amazon rainforest, *Atmos. Chem. Phys*., **20**, 15551–15584. DOI: *https://doi.org/10.5194/acp-20-15551-2020*

Randerson, J. T., H. Liu, M. G. Flanner, S. D. Chambers, Y. Jin, and co-authors, 2006, The Impact of Boreal Forest Fire on Climate Warming. *Science*, **314**, 5802, 1130–1132. DOI: *https://doi.org/10.1126/science.1132075*

Randerson, J., G. R. van der Werf, L. Giglio, G. J. Collagtz, and P. S. Kasibhatla, 2015: Global Fire Emissions Data Base-*GFED*, version **4**. Oak Ridge, TN, USA.

Rantala, P., J. Aalto, R. Taipale, T. M. Ruuskanen & J. Rinne, 2015, Annual cycle of volatile organic compound exchange between a boreal pine forest and the atmosphere. *Biogeosciences*, **12**, 5753–5770. DOI: *https://doi.org/10.5194/bg-12-5753-2015*

Rao, V. B., and K. Hada, 1990, Characteristics of rainfall over Brazil: Annual variations and connections with the Southern Oscillation, *Theoretical and Applied Meteorology*, **42**, 2, 81–91. DOI: *https://doi.org/10.1007/BF00868215*

Rap, A., Scott, C. E., Reddington, C. L., Mercado, L., Ellis, R. J., and co-authors, 2018, Enhanced global primary production by biogenic aerosol via diffuse radiation fertilization, *Nat. Geosci*., **11**, 640–644. DOI: *https://doi.org/10.1038/s41561-018-0208-3*

Rap, A., D. V. Spracklen, L. Mercado, C. L. Reddington, J. M. Haywood, and co-authors, 2015, Fires increase Amazon forest productivity through increases in diffuse radiation, *Geophys. Res. Lett*., **42**. DOI: *https://doi.org/10.1002/2015GL063719*

Rasmussen, R. A., 1970, Isoprene: identified as a forest-type emission to the atmosphere. *Environmental Science and Technology*, **4**, 8, 667–671. DOI: *https://doi.org/10.1021/es60043a008*

Rastak, N., Pajunoja, A., Acosta Navarro, J. C., Ma, J., Song, M., and co-authors, 2017, Microphysical explanation of the RH-dependent water affinity of biogenic organic aerosol and its importance for climate, *Geophys. Res. Lett*., **44**, 5167–5177. DOI: *https://doi.org/10.1002/2017GL073056*

Raupp, C. F. M., and P. L. Silva Dias, 2009: Resonant wave interactions in the presence of a diurnally varying heat source. *Journal of the Atmospheric Sciences*, **66**, 3165–3183. DOI: *https://doi.org/10.1175/2009JAS2899.1*

Raupp, C. F. M., and P. L. Silva Dias, 2010, Interaction of equatorial waves through resonance with the diurnal cycle of tropical heating, *Tellus A*, **62A**, 706–718. DOI: *https://doi.org/10.1111/j.1600-0870.2010.00463.x*

Reddington, C. L., Morgan, W. T., Darbyshire, E., Brito, J., Coe, H., and co-authors, 2019, Biomass burning aerosol over the Amazon: analysis of aircraft, surface and satellite observations using a global aerosol model, *Atmos. Chem. Phys*., **19**, 9125–9152. DOI: *https://doi.org/10.5194/acp-19-9125-2019*

Reddington, C. L., D. V. Spracklen, P. Artaxo, D. A. Ridley, L. V. Rizzo, and A. Arana, 2016: Analysis of particulate emissions from tropical biomass burning using a global aerosol model and long-term surface observations. *Atmos. Chem. Phys*., **16**. DOI: *https://doi.org/10.5194/acp-16-11083-2016*

Reinmuth-Selzle, K., Kampf, C. J., Lucas, K., Lang-Yona, N., Fröhlich-Nowoisky, and co-authors, 2017, Air pollution and climate change effects on allergies in the Anthropocene: Abundance, interaction, and modification of allergens and adjuvants, *Environmental Science & Technology*, 51, 4119–4141. DOI: *https://doi.org/10.1021/acs.est.6b04908*

Reponen T., Grinshpun S.A., Conwell K.L., Wiest J. & Anderson M., 2001, Aerodynamic versus physical size of spores: measurement and implication for respiratory deposition, *Grana*, **40**, 119–125. DOI: *https://doi.org/10.1080/00173130152625851*

Restrepo-Coupe, N., da Rocha, H.R., Hutyra, L.R., da Araujo, A.C., Borma, L.S., and co-authors, 2013. What drives the seasonality of photosynthesis across the Amazon basin? A cross-site analysis of eddy flux tower measurements from the Brasil flux network. *Agric. For. Meteorol*., **182–183**. DOI: *https://doi.org/10.1016/j.agrformet.2013.04.031*

Reutter, P., Su, H., Trentmann, J., Simmel, M., Rose, D., and co-authors, 2009, Aerosol- and updraft-limited regimes of cloud droplet formation: influence of particle number, size and hygroscopicity on the activation of cloud condensation nuclei (CCN), *Atmos. Chem. Phys*., **9**, 7067–7080. DOI: *https://doi.org/10.5194/acp-9-7067-2009*

Ribaud, JF, Machado, LAT, Biscaro, 2019, T X-band dual-polarization radar-based hydrometeor classification for Brazilian tropical precipitation systems, *Atm. Measurement Tech*., **12**, 2, 811–837. DOI: *https://doi.org/10.5194/amt-12-811-2019*

Riccobono, F., Schobesberger, S., Scott, C. E., Dommen, J., Ortega, I. K., and co-authors, 2014, Oxidation Products of Biogenic Emissions Contribute to Nucleation of Atmospheric Particles, *Science*, **344**, 717–721. DOI: *https://doi.org/10.1126/science.1243527*

Richardson, A.D., Keenan, T.F., Migliavacca, M., Ryu, Y., Sonnentag, O., Toomey, M., and co-authors, 2013. Climate change, phenology, and phenological control of vegetation feedbacks to the climate system. *Agric. For. Meteorol.*, **169**, 156–173. DOI: *https://doi.org/10.1016/j.agrformet.2012.09.012*

Rickenbach, T., R. N. Ferreira, J. Halverson, and M. A. F. Silva Dias, 2002: Modulation of convection in the southwestern Amazon basin by extratropical stationary fronts. *J. Geophys. Res.*, **107**, 8040. DOI: *https://doi.org/10.1029/2000JD000263*

Ridley, H. E., Asmerom, Y., Baldini, J. U. L. Breitenbach, S. F. M., Aquino, and co-authors, 2015, Aerosol forcing of the position of the intertropical convergence zone since AD 1550, *Nature geoscience*, **8**, 3, 195–200. DOI: *https://doi.org/10.1038/ngeo2353*

Riemer, N., Ault, A. P., West, M., Craig, R. L., & Curtis, J. H., 2019, Aerosol mixing state: Measurements, modeling, and impacts. *Reviews of Geophysics*, **57**, 187–249. DOI: *https://doi.org/10.1029/2018RG000615*

Riipinen, I., Rastak, N., and Pandis, S. N., 2015, Connecting the solubility and CCN activation of complex organic aerosols: a theoretical study using solubility distributions, *Atmos. Chem. Phys.*, **15**, 6305–6322. DOI: *https://doi.org/10.5194/acp-15-6305-2015*

Rinne, J., J. Bäck & H. Hakola, 2009, Biogenic volatile organic compound emissions from Eurasian taiga: Current knowledge and future directions. *Boreal Environment Research*, **14**, 807–826.

Rinne, H.J.I., A.B. Guenther, J.P. Greenberg & P.C. Harley, 2002, Isoprene and monoterpene fluxes measured above Amazonian rainforest and their dependence on light and temperature. *Atmos Environ*, **36**, 2421–2426. DOI: *https://doi.org/10.1016/S1352-2310(01)00523-4*

Rinne, J., H. Hakola, T. Laurila & Ü. Rannik, 2000, Canopy scale monoterpene emissions of Pinus sylvestris dominated forests. *Atmos Environ*, **34**, 1099–1107. DOI: *https://doi.org/10.1016/S1352-2310(99)00335-0*

Rinne J., Ruuskanen T., Reissell A., Taipale R., Hakola H., and Kulmala M., 2005, On-line PTR-MS measurements of atmospheric concentrations of volatile organic compounds in a European boreal forest ecosystem. *Boreal Env. Res.*, **10**, 425–436.

Rinne, J., R. Taipale, T. Markkanen, T.M. Ruuskanen, H. Hellén, and co-authors, 2007, Hydrocarbon fluxes above a Scots pine forest canopy: measurements and modeling. *Atmos Chem Phys*, **7**, 3361–3372. DOI: *https://doi.org/10.5194/acp-7-3361-2007*

Rissler, J., Svenningsson, B., Fors, E.O., Bilde, M. and Swietlicki, E., 2010, An evaluation and comparison of cloud condensation nucleus activity models: Predicting particle critical saturation from growth at subsaturation, *J. Geophys. Res.*, **115**. DOI: *https://doi.org/10.1029/2010JD014391*

Rissler, J., Swietlicki, E., Zhou, J., Roberts, G., Andreae, M. and co-authors, 2004, Physical properties of the sub-micrometer aerosol over the Amazon rain forest during the wet-to-dry season transition-comparison of modeled and measured CCN concentrations, *Atmos. Chem. Phys.*, **4**, 2119–2143. DOI: *https://doi.org/10.5194/acp-4-2119-2004*

Rissler, J., Vestin, A., Swietlicki, E., Fisch, G., Zhou, J., and co-authors, 2006, Size distribution and hygroscopic properties of aerosol particles from dry-season biomass burning in Amazonia, *Atmos. Chem. Phys.*, **6**, 471–491. DOI: *https://doi.org/10.5194/acp-6-471-2006*

Riuttanen, L., Hulkkonen, M., Dal Maso, M., Junninen, H., & Kulmala, M., 2013, Trajectory analysis of atmospheric transport of fine particles, SO_2, NO_x and O_3 to the SMEAR II station in Finland in 1996-2008. *Atmos Chem Phys*, **13**, 2153–2164. DOI: *https://doi.org/10.5194/acp-13-2153-2013*

Riva, M., Heikkinen, L., Bell, D., Peräkylä, O., Zha, Q., and co-authors, 2019, Chemical transformations in monoterpene-derived organic aerosol enhanced by inorganic composition, *Climate and Atmospheric Science*, *2*, 2. DOI: *https://doi.org/10.1038/s41612-018-0058-0*

Rizzo, L. V., Artaxo, P., Karl, T., Guenther, A. B. and Greenberg, J., 2010, Aerosol properties, in-canopy gradients, turbulent fluxes, and VOC concentrations at a pristine forest site in Amazonia, *Atmos. Environ.*, **44**(4). DOI: *https://doi.org/10.1016/j.atmosenv.2009.11.002*

Rizzo, L. V., Artaxo, P., Müller, T., Wiedensohler, A., Paixão, M., and co-authors, 2013. Long term measurements of aerosol optical properties at a primary forest site in Amazonia. Atmos. Chem. Phys., **13**, 2391–2413. DOI: *https://doi.org/10.5194/acp-13-2391-2013*

Rizzo, L. V., Correia, A. L., Artaxo, P., Procópio, A. S., and Andreae, M. O., 2011, Spectral dependence of aerosol light absorption over the Amazon Basin, *Atmos. Chem. Phys.*, **11**, 8899–8912. DOI: *https://doi.org/10.5194/acp-11-8899-2011*

Rizzo, L, Roldin, P., Brito, J., Backman, J., Swietlicki, E., and co-authors, 2018, Multi-year statistical and modeling analysis of submicrometer aerosol number size distributions at a rain forest site, *Atmos. Chem. Phys.*, **18**, 10255–10274. DOI: *https://doi.org/10.5194/acp-18-10255-2018*

Rizzolo, J. A., Barbosa, C. G. G., Borillo, G. C., Godoi, A. F. L., Souza, R. A. F., and co-authors, 2017, Soluble iron nutrients in Saharan dust over the central Amazon rainforest, *Atmos. Chem. Phys.*, **17**, 2673–2687. DOI: *https://doi.org/10.5194/acp-17-2673-2017*

Roberts, M. C., M. O. Andreae, J. C. Zhou, and P. Artaxo, 2001, Cloud condensation nuclei in the Amazon Basin: "Marine" conditions over a continent? *Geophys. Res. Lett.*, **28**, 14, 2807–2810. DOI: *https://doi.org/10.1029/2000GL012585*

Roberts, G. C., Artaxo, P., Jingchuan, Z., Swietlicki, E., and Andreae, M. O., 2002, Sensitivity of CCN spectra on chemical and physical properties of aerosol: a case study from the Amazon Basin, *J. Geophys. Res.*, **107,** D20, LBA37-1-18. DOI: *https://doi.org/10.1029/2001JD000583*

Roberts, G. C., Nenes, A., Seinfeld, J. H., and Andreae, M. O., 2003, Impact of biomass burning on cloud properties in the Amazon Basin, *J. Geophys. Res.*, **108**, 4062. DOI: *https://doi.org/10.1029/2001JD000985*

Robinson N.H., Hamilton, J.F., Allan, J.D., Langford, B., Oram, D.E., 2011, Evidence for a significant proportion of Secondary Organic Aerosol from isoprene above a maritime tropical forest, *Atmos. Chem. Phys.*, **11**, 1039–1050. DOI: *https://doi.org/10.5194/acp-11-1039-2011*

Rogelj, J., Popp, A., Calvin, K.V., and co-authors, 2018, Scenarios towards limiting global mean temperature increase below 1.5 °C, *Nature Clim Change,* **8,** 325–332. DOI: *https://doi.org/10.1038/s41558-018-0091-3*

Roldin, P., Ehn, M., Kurtén, T., Olenius, T., Rissanen, M. P., and co-authors, 2019, The role of highly oxygenated organic molecules in the Boreal aerosol-cloud-climate system, *Nature Communications*, **10**, 4370. DOI: *https://doi.org/10.1038/s41467-019-12338-8*

Romanovsky V. E., Smith S. L., Christiansen H. H., 2010, Permafrost thermal state in the polar Northern Hemisphere during the International Polar Year 2007–2009: a synthesis. *Permafrost and Periglac. Process.*, **21**, 106–116. DOI: *https://doi.org/10.1002/ppp.689*

Romatschke, U., & Houze, R. A., Jr. (2010). Extreme Summer Convection in South America, *Journal of Climate*, **23**, 14, 3761–3791. DOI: *https://doi.org/10.1175/2010JCLI3465.1*

Roos, C. I., Bowman, D. M. J. S., Balch, J. K., Artaxo, P., Bond, W. J., and co-authors, 2014, Pyrogeography, historical ecology, and the human dimensions of fire regimes. *Journal of Biogeography,* **41**, 833–836. DOI: *https://doi.org/10.1111/jbi.12285*

Roosevelt, A. C., 2013, The Amazon and the Anthropocene: 13,000 years of human influence in a tropical rainforest. *Anthropocene,* **4**, 69–87. DOI: *https://doi.org/10.1016/j.ancene.2014.05.001*

Rose, D., Gunthe, S. S., Mikhailov, E., Frank, G. P., Dusek, U., and co-authors, 2008, Calibration and measurement uncertainties of a continuous-flow cloud condensation nuclei counter (DMT-CCNC): CCN activation of ammonium sulfate and sodium chloride aerosol particles in theory and experiment, *Atmos. Chem. Phys.*, **8**, 1153–1179. DOI: *https://doi.org/10.5194/acp-8-1153-2008*

Rose, D., Gunthe, S. S., Su, H., Garland, R. M., Yang, H., e al., 2011, Cloud condensation nuclei in polluted air and biomass burning smoke near the mega-city Guangzhou, China – Part 2: Size-resolved aerosol chemical composition, diurnal cycles, and externally mixed weakly CCN-active soot particles, *Atmos. Chem. Phys.*, **11**, 2817–2836. DOI: *https://doi.org/10.5194/acp-11-2817-2011*

Rose, D., Nowak, A., Achtert, P., Wiedensohler, A., Hu, M., e al., 2010, Cloud condensation nuclei in polluted air and biomass burning smoke near the mega-city Guangzhou, China – Part 1: Size-resolved measurements and implications for the modeling of aerosol particle hygroscopicity and CCN activity, *Atmos. Chem. Phys.*, **10**, 3365–3383. DOI: *https://doi.org/10.5194/acp-10-3365-2010*

Rosenfeld, D., Andreae, M. O., Asmi, A., Chin, M., de Leeuw, G., and co-authors, 2014, Global observations of aerosol-cloud-precipitation-climate interactions, *Rev. Geophys.*, **52**, 750–808. DOI: *https://doi.org/10.1002/2013RG000441*

Rosenfeld, D., and Bell, T. L., 2011, Why do tornados and hailstorms rest on weekends? *J. Geophys. Res.*, **116**, D20211. DOI: *https://doi.org/10.1029/2011JD016214*

Rosenfeld, D., U. Lohmann, G. B. Raga, C. D. O'Dowd, M. Kulmala, and co-authors, 2008, Flood or drought: How do aerosols affect precipitation? *Science*, **321**, 5894, 1309–1313. DOI: *https://doi.org/10.1126/science.1160606*

Rosenfeld, D., Woodley, W. L., Krauss, T. W., and Makitov, V., 2006, Aircraft microphysical documentation from cloud base to anvils of hailstorm feeder clouds in Argentina, *Journal of Applied Meteorology and Climatology*, **45**, 1261–1281. DOI: *https://doi.org/10.1175/JAM2403.1*

Röser, C., Montagnani, L., Schulze, E.-D., Mollicone, D., Kolle, O., and co-authors, 2002. Net CO_2 exchange rates in three different successional stages of the "Dark Taiga" of Central Siberia. *Tellus B Chem Phys Meteorol*, **54**, 642–654. DOI: *https://doi.org/10.1034/j.1600-0889.2002.01351.x*

Rottenberger, S., Kuhn, U., Wolf, A., Schebeske, G., Oliva, S. T., and co-authors, 2004, Exchange of short-chain aldehydes between Amazonian vegetation and the atmosphere, *Ecol. Appl.*, **14**, 4, S247–S262. DOI: *https://doi.org/10.1890/01-6027*

Ruehl, C. R., Davies, J. F., and Wilson, K. R. , 2016, An interfacial mechanism for cloud droplet formation on organic aerosols. *Science*, **351**, 1447–1450. DOI: *https://doi.org/10.1126/science.aad4889*

Rummel, U., Ammann, C., Kirkman, G. A., Moura, M. A. L., Foken, T., and co-authors, 2007, Seasonal variation of ozone deposition to a tropical rainforest in southwest Amazonia: *Atmos. Chem. Phys.*, **7**, 5415–5435. DOI: *https://doi.org/10.5194/acp-7-5415-2007*

Ruuskanen, T. M., Reissell, A., Keronen, P., Aalto, P. P., Laakso, and co-authors, 2003, Atmospheric trace gas and aerosol particle concentration measurements in Eastern Lapland, Finland 1992–2001. *Boreal Env. Res.*, **8**, 335–349. ISSN 1239-6095.

Saarikoski, S. M., T., Hillamo, R., Aalto, P. P., Kerminen, V-M., Kulmala, M., 2005, Physico-chemical characterization and mass closure of size-segregated atmospheric aerosols in Hyytiälä, Finland, *Boreal Environment Research*, **10**, 385–400.

Saatchi, S.S., Harris, N.L., Brown, S., Lefsky, M., Mitchard, E.T.A., and co-authors, 2011. Benchmark map of forest carbon stocks in tropical regions across three continents. *Proc. Natl. Acad. Sci. U. S. A.* DOI: *https://doi.org/10.1073/pnas.1019576108*

Saatchi, S., Marcos Longo, and co-authors, 2021, Detecting vulnerability of humid tropical forests to multiple stressors, *One Earth*, **4**, 7, 988–1003. DOI: *https://doi.org/10.1016/j.oneear.2021.06.002*

Saeki, T., Maksyutov, S., Sasakawa, M., Machida, T., Arshinov, M., and co-authors, 2013, Carbon flux estimation for Siberia by inverse modeling constrained by aircraft and tower CO_2 measurements, *J. Geophys. Res. Atmos.*, **118**, 1100– 1122. DOI: *https://doi.org/10.1002/jgrd.50127*

Saito M, Kim H-S, Ito A, Yokota T, Maksyutov S., 2016, Enhanced Methane Emissions during Amazonian Drought by Biomass Burning. *PLoS ONE*, **11**, 11, e0166039. DOI: *https://doi.org/10.1371/journal.pone.0166039*

Saleska, S. R., Miller, S. D., Matross, D. M., Goulden, M. L., Wofsy, S. C., and co-authors, 2003, Carbon in Amazon forests: unexpected seasonal fluxes and disturbance-induced losses, *Science*, **302**, 1554–1557. DOI: *https://doi.org/10.1126/science.1091165*

Sampaio, G., C. A. Nobre, M. H. Costa, P. Satyamurty, B. S. Soares-Filho, M. Cardoso, 2007, Regional climate change over eastern Amazonia caused by pasture and soybean cropland expansion. *Geophys. Res. Lett.*, **34**, L17709. DOI: *https://doi.org/10.1029/2007GL030612*

Santana, R. A., Dias-Júnior, C. Q., da Silva, J. T., Fuentes, J. D., do Vale, R. S., and co-authors, 2018, Air turbulence characteristics at multiple sites in and above the Amazon rainforest canopy, *Agric. For. Meteorol.*, **260–261**, 41–54. DOI: *https://doi.org/10.1016/j.agrformet.2018.05.027*

Šantl-Temkiv, T., Sikoparija, B., Maki, T., Carotenuto, F., Amato, P., and co-authors, 2019, Outdoor Bioaerosol Field Measurements: Challenges and Perspectives, *Aerosol Science & Technology*. **54**, 520–546, DOI: *https://doi.org/10.1080/02786826.2019.1676395*

Saraiva, I, M. A. F. Silva Dias, C. A. R. Morales, J. M. B. Saraiva, 2016, Regional variability of rainclouds in the Amazon basin seen by a network of weather radars. *Aceito. Journal of Applied Meteorology and Climatology*, **55**, 2657–2675. DOI: *https://doi.org/10.1175/JAMC-D-15-0183.1*

Sarkkola, S., Nieminen, M., Koivusalo, H., Laurén, A., Ahti, E., and co-authors, 2013, Domination of growing-season evapotranspiration over runoff makes ditch network maintenance in mature peatland forests questionable. *Mires Peat*, **11**, 11.

Sarrafzadeh M., Wildt, J., Pullinen, I., Springer, M., Kleist, E., Tillmann, R., and co-authors, 2016, Impact of NOX and OH on secondary organic aerosol formation from β-pinene photo-oxidation, *Atmos. Chem. Phys.*, **16**, 11237–11248. DOI: *https://doi.org/10.5194/acp-16-11237-2016*

Sasakawa, M., Machida, T., Tsuda, N., Arshinov, M., Davydov, D., and co-authors, 2013, Aircraft and tower measurements of CO_2 concentration in the planetary boundary layer and the lower free troposphere over southern taiga in West Siberia: Longterm records from 2002 to 2011, *J. Geophys. Res. Atmos.*, **118**, 9489– 9498. DOI: *https://doi.org/10.1002/jgrd.50755*

Sasakawa, M., Shimoyama, K., Machida, T., Tsuda, N., Suto, H., and co-authors, 2010, Continuous measurements of methane from a tower network over Siberia, *Tellus B Chem Phys Meteorol*, **62**, 403–416. DOI: *https://doi.org/10.1111/j.1600-0889.2010.00494.x*

Satoh, M., T. Matsuno, H. Tomita, H. Miura, T. Nasuno, and S. Iga, 2008, Nonhydrostatic icosahedral atmospheric model (NICAM) for global cloud resolving simulations, *J Comput Phys*, **227**, 7, 3486–3514. DOI: *https://doi.org/10.1016/j.jcp.2007.02.006*

Saturno, J., Ditas, F., Penning de Vries, M., Holanda, B.A., Pöhlker, M.L., and co-authors, 2018b, African volcanic emissions influencing atmospheric aerosol particles over the Amazon rain forest. *Atmos Chem Phys*, **18**, 10391–10405. DOI: *https://doi.org/10.5194/acp-18-10391-2018*

Saturno, J., Holanda, B.A., Pöhlker, C., Ditas, F., Wang, Q., and co-authors, 2018a, Black and brown carbon over central Amazonia: Long-term aerosol measurements at the ATTO site. *Atmos. Chem. Phys.*, **18**, 12817–12843. DOI: *https://doi.org/10.5194/acp-18-12817-2018*

Satyamurty, P., Anderson de Castro, A., Tota, J., da Silva Gularte, L. E., Ocimar Manzi, A., 2010, Rainfall trends in the Brazilian Amazon Basin in the past eight decades. *Theor Appl Climatol.,* **99**, 1–2. DOI: *https://doi.org/10.1007/s00704-009-0133-x*

Savage, N. J., and Huffman, J. A., 2018, Evaluation of a hierarchical agglomerative clustering method applied to WIBS laboratory data for improved discrimination of biological particles by comparing data preparation techniques, *Atmos. Meas. Tech.*, **11**, 4929–4942. DOI: *https://doi.org/10.5194/amt-11-4929-2018*

Savage, N. J., Krentz, C. E., Könemann, T., Han, T. T., Mainelis, G., and co-authors, 2017, Systematic characterization and fluorescence threshold strategies for the wideband integrated bioaerosol sensor (WIBS) using size-resolved biological and interfering particles, *Atmos. Meas. Tech.*, **10**, 4279–4302. DOI: *https://doi.org/10.5194/amt-10-4279-2017*

Savage, K., Moore, T.R. and Crill, P.M., 1997. Methane and carbon dioxide exchanges between the atmosphere and northern boreal forest soils. *J. Geophys. Res. Atmos.*, **102**, D24, 29279–29288. DOI: *https://doi.org/10.1029/97JD02233*

Sawakuchi, H. O., Bastviken, D., Sawakuchi, A. O., Krusche, A. V., Ballester, M. V. and Richey, J. E., 2014, Methane emissions from Amazonian Rivers and their contribution to the global methane budget. *Glob Change Biol.*, **20**, 2829–2840. DOI: *https://doi.org/10.1111/gcb.12646*

Saxton, J. E., Lewis, A. C., Kettlewell, J. H., Ozel, M. Z., Gogus, F., and co-authors, 2007, Isoprene and monoterpene measurements in a secondary forest in northern Benin, *Atmos Chem Phys*, **7**, 4095–4106. DOI: *https://doi.org/10.5194/acp-7-4095-2007*

Scaife, A.A., C.K. Folland, L.V. Alexander, A. Moberg, and J.R. Knight, 2008: European Climate Extremes and the North Atlantic Oscillation. *J. Climate*, **21**, 72–83. DOI: *https://doi.org/10.1175/2007JCLI1631.1*

Scandalios, J. G., 1993, Oxygen Stress and Superoxide Dismutases., *Plant Physiol.*, **101**, 1, 7–12, *http://www.ncbi.nlm.nih.gov/pubmed/12231660*. DOI: *https://doi.org/10.1104/pp.101.1.7*

Schafer, J. S., Eck, T. F., Holben, B. N., Artaxo, P., and Duarte, A. F. 2008. Characterization of the optical properties of atmospheric aerosols in Amazônia from long-term AERONET monitoring (1993–1995 and 1999–2006). *J. Geophys. Res.*, **113**, 1–16. DOI: *https://doi.org/10.1029/2007JD009319*

Schafer, J. S., Holben, B. N., Eck, T. F., Yamasoe, M. A., and Artaxo, P., 2002, Atmospheric effects on insolation in the Brazilian Amazon: Observed modification of solar radiation by clouds and smoke and derived single scattering albedo of fire aerosols: *J. Geophys. Res.*, **107**, 8074. DOI: *https://doi.org/10.1029/2001JD000428*

Schallhart, S., P. Rantala, M.K. Kajos, J. Aalto, I. Mammarella, and co-authors, 2018, Temporal variation of VOC fluxes measured with PTR-TOF above a boreal forest. *Atmos. Chem. Phys.*, **18**, 815–832. DOI: *https://doi.org/10.5194/acp-18-815-2018*

Schimel, D., B. B. Stephens, and J. B. Fisher, 2015, Effect of increasing CO_2 on the terrestrial carbon cycle. *Proc. Natl. Acad. Sci. U. S. A.*, **112**, 436–441. DOI: *https://doi.org/10.1073/pnas.1407302112*

Schiro, K. A. and Neelin, J. D., 2018, Tropical continental downdraft characteristics: mesoscale systems versus unorganized convection, *Atmos. Chem. Phys.*, **18**, 1997–2010. DOI: *https://doi.org/10.5194/acp-18-1997-2018*

Schlesinger, W.H. and Jasechko, S., 2014. Transpiration in the global water cycle. *Agric. For. Meteorol.*, **189–190**, 115–117. DOI: *https://doi.org/10.1016/j.agrformet.2014.01.011*

Schmale J, Henning S, Decesari S, Henzing B, Keskinen H, Sellegri K, and co-authors, 2018, Long-term cloud condensation nuclei number concentration, particle number size distribution and chemical composition measurements at regionally representative observatories, *Atmos Chem Phys.*, **18**, 4, 2853–2881. DOI: *https://doi.org/10.5194/acp-18-2853-2018*

Schmid, O., P. Artaxo, W. P. Arnott, D. Chand, L. V. Gatti, and co-authors, 2006, Spectral light absorption by ambient aerosols influenced by biomass burning in the Amazon Basin – I. Comparison and field calibration of absorption measurement techniques. *Atmospheric Chemistry and Physics*, **6**, 3443–3462. DOI: *https://doi.org/10.5194/acp-6-3443-2006*

Schneider, T., Bischoff, T., and Haug, G. H., 2014, Migrations, and dynamics of the intertropical convergence zone: *Nature*, **513**, 45–53. DOI: *https://doi.org/10.1038/nature13636*

Schneider, J., F. Freutel, S. R. Zorn, Q. Chen, D. K. Farmer, and co-authors, 2011, Mass-spectrometric identification of primary biological particle markers: indication for low abundance of primary biological material in the pristine submicron aerosol of Amazonia. *Atmospheric Chemistry and Physics*, **11**, 11415–11429. DOI: *https://doi.org/10.5194/acp-11-11415-2011*

Schobesberger, S., Väänänen, R., Leino, K., Virkkula, A., Backman, J., and co-authors, 2013, Airborne measurements over the boreal forest of southern Finland during new particle formation events in 2009 and 2010, *Boreal Env. Res.*, **18**, 145–163.

Schrod, J., Thomson, E. S., Weber, D., Kossmann, J., Pöhlker, C., and co-authors, 2020, Long-term deposition and condensation ice-nucleating particle measurements from four stations across the globe, *Atmos. Chem. Phys.*, **20**, 15983–16006. DOI: *https://doi.org/10.5194/acp-20-15983-2020*

Schuh G, Heiden AC, Hoffmann Th, Kahl J, Rockel P, Rudolph J, Wildt J., 1997, Emissions of Volatile Organic Compounds from Sunflower and Beech: Dependence on Temperature and Light Intensity, *J Atmos Chem,* **27**, 291–318. DOI: *https://doi.org/10.1023/A:1005850710257*

Schulz, C., Schneider, J., Amorim Holanda, B., Appel, O., Costa, A., and co-authors, 2018, Aircraft-based observations of isoprene-epoxydiol-derived secondary organic aerosol (IEPOX-SOA) in the tropical upper troposphere over the Amazon region, *Atmos. Chem. Phys.*, **18**, 14979–15001. DOI: *https://doi.org/10.5194/acp-18-14979-2018*

Schultz, MG, Schröder, S, Lyapina, O, Cooper, O. R. Galbally, I, and co-authors, 2017, Tropospheric Ozone Assessment Report: Database and metrics data of global surface ozone observations. *Elementa Science of the Anthropocene*, **5**, 58. DOI: *https://doi.org/10.1525/elementa.244*

Schumacher C.J., Pöhlker C., Aalto P., Hiltunen V., Petäjä T., and co-authors, 2013, Seasonal cycles of fluorescent biological aerosol particles in boreal and semi-arid forests of Finland and Colorado, *Atmos. Chem. Phys.*, **13**, 11987–12001. DOI: *https://doi.org/10.5194/acp-13-11987-2013*

Scott, A., 2000: The Pre-Quaternary history of fire. *Palaeogeogr. Palaeoclimatol. Palaeoecol.*, **164**, 281–45 329. DOI: *https://doi.org/10.1016/S0031-0182(00)00192-9*

Scott, C. E., S. R. Arnold, S. A. Monks, A. Asmi, P. Paasonen, and D. V. Spracklen, 2018b: Substantial large-scale feedbacks between natural aerosols and climate. *Nat. Geosci.*, **11**, 44–48. DOI: *https://doi.org/10.1038/s41561-017-0020-5*

Scott, C. E., Monks, S. A., Spracklen, D. V., Arnold, S. R., Forster, P. M., and co-authors, 2018a, Impact on short-lived climate forcers increases projected warming due to deforestation. *Nat. Comm.*, **9**, 157. DOI: *https://doi.org/10.1038/s41467-017-02412-4*

Seidl, R., Thom, D., Kautz, M., Martin-Benito, D., Peltoniemi, M., and co-authors, 2017, Forest disturbances under climate change. *Nature Climate Change,* **7**, 395–402. DOI: *https://doi.org/10.1038/nclimate3303*

Seifert, A., T. Heus, R. Pincus, and B. Stevens, 2015, Large-eddy simulation of the transient and near-equilibrium behavior of precipitating shallow convection, *J. Adv. Model. Earth Syst.*, **7**. DOI: *https://doi.org/10.1002/2015MS000489*

Sena, E. T. and Artaxo, P. , 2015. A novel methodology for large-scale daily assessment of the direct radiative forcing of smoke aerosols. *Atmos. Chem. Phys.*, **15**, 5471–5483. DOI: *https://doi.org/10.5194/acp-15-5471-2015*

Sena, E. T., P. Artaxo, and A. L. Correia, 2013, Spatial variability of the direct radiative forcing of biomass burning aerosols and the effects of land use change in Amazonia. *Atmospheric Chemistry and Physics*, **13**, 1261–1275, 2013. DOI: *https://doi.org/10.5194/acp-13-1261-2013*

Sena, E. T., Silva Dias, M. A. F., Carvalho, L. M. V., and Silva Dias, P. L. 2018. Reduced wet season length detected by satellite retrievals of cloudiness over Brazilian Amazonia: a new methodology. *Journal of Climate*, **31**, 9941–9964. DOI: *https://doi.org/10.1175/JCLI-D-17-0702.1*

Settele, J., R. Scholes, R. Betts, S. Bunn, P. Leadley, and co-authors, 2014, Terrestrial and inland water systems. In: *Climate Change 2014: Impacts, Adaptation, and Vulnerability. Part A: Global and Sectoral Aspects. Contribution of Working Group II to the Fifth Assessment Report of the Intergovernmental Panel on Climate Change* [eds; Field, C.B., V.R. Barros, D.J. Dokken, K.J. Mach, M.D. Mastrandrea, T.E. Bilir, M. Chatterjee, K.L. Ebi, Y.O. Estrada, R.C. Genova, B. Girma, E.S. Kissel, A.N. Levy, S. MacCracken, P.R. Mastrandrea, and L.L. White]. Cambridge University Press, Cambridge, United Kingdom and New York, NY, USA, pp. 271–359.

Sharkey, T.D., F. Loreto, D. Baldocchi, & A. Guenther, 1997, The BEMA-project – A North American perspective. *Atmos. Environ*., **31**, 251–255. DOI: *https://doi.org/10.1016/S1352-2310(97)00266-5*

Shibistova, O., Lloyd, J., Evgrafova, S., Savushkina, N., Zrazhevskaya, G., and co-authors, 2002, Seasonal and spatial variability in soil CO_2 efflux rates for a central Siberian Pinus sylvestris forest, *Tellus B: Chemical and Physical Meteorology*, **54**, 5,552–567. DOI: *https://doi.org/10.3402/tellusb.v54i5.16687*

Shilling, J. E., Pekour, M. S., Fortner, E. C., Artaxo, P., de Sá, S., and co-authors, 2018, Aircraft observations of the chemical composition and aging of aerosol in the Manaus urban plume during GoAmazon 2014/5, *Atmos. Chem. Phys*., **18**, 10773–10797. DOI: *https://doi.org/10.5194/acp-18-10773-2018*

Shiraiwa, M., Ying Li, Y., Tsimpidi, A.P., Karydis, V.A., Berkemeier, T., and co-authors, 2017, Global distribution of particle phase state in atmospheric secondary organic aerosols, *Nature Communications*, **8**, 15002. DOI: *https://doi.org/10.1038/ncomms15002*

Shrivastava M, Andreae MO, Artaxo P, and co-authors 2019. Urban pollution greatly enhances formation of natural aerosols over the Amazon rainforest. *Nature Communications*, **10**, 1046. DOI: *https://doi.org/10.1038/s41467-019-08909-4*

Shrivastava, M., Cappa, S.C., Fan, J., Goldstein, A.H., Guenther, A. B., and co-authors, 2017, Recent advances in understanding secondary organic aerosol: Implications for global climate forcing, *Rev. Geophys*., **55**, 2, 509–559. DOI: *https://doi.org/10.1002/2016RG000540*

Shtabkin, Y.A., Moiseenko, K.B., Skorokhod, A.I. and co-authors , 2016, Sources of and variations in tropospheric CO in Central Siberia: Numerical experiments and observations at the Zotino Tall Tower Observatory. *Izv. Atmos. Ocean. Phys.* **52**, 45–56. DOI: *https://doi.org/10.1134/S0001433816010096*

Sihto, S-L., J. Mikkilä, J. Vanhanen, M. Ehn, L. Liao, and co-authors, 2011, Seasonal variation of CCN concentrations and aerosol activation properties in boreal forest, *Atmos. Chem. Phys*., **11**, 13269–13285. DOI: *https://doi.org/10.5194/acp-11-13269-2011*

Sikma, M., Vilà Guerau de Arellano, J., Pedruzo Bagazgoitia, X., Voskamp, T., Heusinkveld, B. G., and co-authors. 2019. Impact of future warming and enhanced CO_2 on the vegetation cloud interaction. *J. Geophys. Res. Atmos*., **124**, 12,444–12,454. DOI: *https://doi.org/10.1029/2019JD030717*

Sikstrom, U. and Hokka, H., 2016. Interactions between soil water conditions and forest stands in boreal forests with implications for ditch network maintenance. *Silva Fennica*, **50**, 1. DOI: *https://doi.org/10.14214/sf.1416*

Siljamo P., Sofiev M., Severova E., Ranta H., Kukkonen J., and co-authors, 2008, Sources, impact, and exchange of early-spring birch pollen in the Moscow region and Finland, *Aerobiologia*, **24**, 211–230. DOI: *https://doi.org/10.1007/s10453-008-9100-8*

Silva Camila V. J., Aragão L. E. O. C., Barlow J., Espirito-Santo F., Young P. J., and co-authors, 2018, Drought-induced Amazonian wildfires instigate a decadal-scale disruption of forest carbon dynamics, *Phil. Trans. R. Soc. B*., **373**, 1760. DOI: *https://doi.org/10.1098/rstb.2018.0043*

Silva Dias, M. A. F., Avissar, R., and Silva Dias, P.L. 2009. Modeling the Regional and Remote Climatic Impact of Deforestation In *Amazonia and Global Change*, Geophysical Monographs Series, edited by M. Keller; M. Bustamante; J. Gash; P. Silva Dias, **186**, 255–264: American Geophysical Union. DOI: *https://doi.org/10.1029/2008GM000817*

Silva Dias M. A. F., P. L. Silva Dias, M. Longo, D. R. Fitzjarrald, A. S. Denning, 2004, River breeze circulation in Eastern Amazon: observations and modeling results. *Theoretical and Applied Climatology*, **6**, 78,1–3, 111–121. DOI: *https://doi.org/10.1007/s00704-004-0047-6*

Silva Dias, M.A.F., Rutledge, S., Kabat, P., Silva Dias, P. L., Nobre, C. A., and co-authors, 2002, Clouds and rain processes in a biosphere atmosphere interaction context in the Amazon Region. *J. Geophys. Res. Atmos*., **107**, 46.1–46.23. DOI: *https://doi.org/10.1029/2001JD000335*

Silva Dias, P. L., W. H., Schubert, and M. Demaria, 1983, Large-scale response of the tropical atmosphere to transient forcing, *J. Atmos. Sci*., **40**, 2689–2707. DOI: *https://doi.org/10.1175/1520-0469(1983)040<2689:LSROTT>2.0.CO;2*

Silva Junior, C. H. L., Aragão, L. E. O. C. Anderson, L. O., Fonseca, M. G. Shimabukuro, Y. E., and co-authors, 2020, Persistent collapse of biomass in Amazonian forest edges following deforestation leads to unaccounted carbon losses, *Sci Adv*, **6**, 40, eaaz8360. DOI: *https://doi.org/10.1126/sciadv.aaz8360*

Silva Junior, Celso H. L., Carvalho N., and co-authors, 2021, *Nature Geosciences*, **14**, 634–635. DOI: *https://doi.org/10.1038/s41561-021-00823-z*

Siméon, A., Waquet, F., Péré, J.-C., Ducos, F., Thieuleux, F., and co-authors, 2021 Combining POLDER-3 satellite observations and WRF-Chem numerical simulations to derive biomass burning aerosol properties over the Southeast Atlantic region, accepted to be published in *Atmos. Chem. Phys.*, preprint at. DOI: *https://doi.org/10.5194/acp-2021-256*

Simoneit, B.R.T., Schauer, J.J., Nolte, C.G., Oros, D.R., Elias, V.O., and co-authors, 1999, Levoglucosan, a tracer for cellulose in biomass burning and atmospheric particles, *Atmos Environ*, **33**, 2, 173–182. DOI: *https://doi.org/10.1016/S1352-2310(98)00145-9*

Sindelarova, K., Granier, C., Bouarar, I., Guenther, A., Tilmes, S., and co-authors, 2014, Global data set of biogenic VOC emissions calculated by the MEGAN model over the last 30 years, *Atmos. Chem. Phys.*, **14**, 9317–9341. DOI: *https://doi.org/10.5194/acp-14-9317-2014*

Siqueira, J. R., and L. A. T. Machado, 2004: Influence of frontal systems on the day-to-day convection variability over South America. *J. Climate*, **17**, 1754–1766. DOI: *https://doi.org/10.1175/1520-0442(2004)017<1754:IOTFSO>2.0.CO;2*

Sitch, S., Cox, P. M., Collins, W. J., and Huntingford, C., 2007, Indirect radiative forcing of climate change through ozone effects on the land-carbon sink, *Nature*, **448**, 791–U4. DOI: *https://doi.org/10.1038/nature06059*

Sitch, S., Huntingford, C., Gedney, N., Levy, P. E., Lomas, M., and co-authors, 2008, Evaluation of the terrestrial carbon cycle, future plant geography and climate-carbon cycle feedbacks using five Dynamic Global Vegetation Models (DGVMs), *Global Change Biology*, **14**, 2015–2039. DOI: *https://doi.org/10.1111/j.1365-2486.2008.01626.x*

Smith, M. N., Taylor, C.T., van Haren, J., Rosolem, R., Restrepo-Coupe, N., 2020, Empirical evidence for resilience of tropical forest photosynthesis in a warmer world. *Nature Plants*, **6**, 1225–1230. DOI: *https://doi.org/10.1038/s41477-020-00780-2*

Smith, P., and Co-authors, 2014: Agriculture, Forestry and Other Land Use (AFOLU). In *Climate Change 2014: Mitigation of Climate Change. Contribution of Working Group III to the Fifth Assessment Report of the Intergovernmental Panel on Climate Change*, Eds. O. Edenhofer, and co-authors, Cambridge University Press, Cambridge, United Kingdom and New York, NY, USA.

Soares J., Sofiev M., Hakkarainen J., 2015, Uncertainties of wild-land fires emission in AQMEII phase 2 case study. *Atmos. Environ.*, **115**, 3, 61–370. DOI: *https://doi.org/10.1016/j.atmosenv.2015.01.068*

Sofiev M., Siljamo P., Ranta H. & Rantio-Lehtimäki A., 2006, Towards numerical forecasting of long-range air transport of birch pollen: theoretical considerations and a feasibility study, *Int. J. Biometeorol.*, **50**, 392–402. DOI: *https://doi.org/10.1007/s00484-006-0027-x*

Sofiev, M., Vankevich, R., Lotjonen, M., Prank, M., Petukhov, V., Ermakova, T., and co-authors, 2009, An operational system for the assimilation of the satellite information on wild-land fires for the needs of air quality modelling and forecasting, *Atmos. Chem. Phys.*, **9**, 6833–6847. DOI: *https://doi.org/10.5194/acp-9-6833-2009*

Sogacheva, L., Kolmonen, P., Virtanen, T. H., Rodriguez, E., Saponaro, G., and de Leeuw, G., 2017, Post-processing to remove residual clouds from aerosol optical depth retrieved using the Advanced Along Track Scanning Radiometer, *Atmos. Meas. Tech.*, **10**, 491–505. DOI: *https://doi.org/10.5194/amt-10-491-2017*

Soja, A. J., Tchebakova, N.M., French, N,H.F., Flannigan, M.D., Shugart, H.H., and co-authors, 2007, Climate-induced boreal forest change: Predictions versus current observations. *Global and Planetary Change*, **56**, 274–296. DOI: *https://doi.org/10.1016/j.gloplacha.2006.07.028*

Song, X.-P., M. C. Hansen, S. V Stehman, P. V Potapov, A. Tyukavina, and co-authors, 2018: Global land change from 1982 to 2016. *Nature*, **560**, 7720, 639–643. DOI: *https://doi.org/10.1038/s41586-018-0411-9*

Soto-Garcia, L. L; Andreae, MO; Andreae, TW; Artaxo, P.; Maenhaut, W.; and co-authors, 2011, Evaluation of the carbon content of aerosols from the burning of biomass in the Brazilian Amazon using thermal, optical, and thermal-optical analysis methods. *Atmospheric Chemistry and Physics*, **11**, 9, 4425–4444. DOI: *https://doi.org/10.5194/acp-11-4425-2011*

Souza, F.F.C., Rissi, D.V., Pedrosa, F.O., and co-authors, 2019. Uncovering prokaryotic biodiversity within aerosols of the pristine Amazon forest. *Sci. Total Environ.* **688**. DOI: *https://doi.org/10.1016/j.scitotenv.2019.06.218*

Spirig, C.; Guenther, A.; Greenberg, J. P.; Calanca, P.; Tarvainen, V., 2004, Tethered balloon measurements of biogenic volatile organic compounds at a Boreal forest site. *Atmos Chem Phys*, **4**, 215–229. DOI: *https://doi.org/10.5194/acp-4-215-2004*

Sporre, M. K., Blichner, S. M., Karset, I. H. H., Makkonen, R., and Berntsen, T. K., 2019, BVOC–aerosol–climate feedbacks investigated using NorESM, *Atmos. Chem. Phys.*, **19**, 4763–4782. DOI: *https://doi.org/10.5194/acp-19-4763-2019*

Sporre, M. K., Blichner, S. M., Schrödner, R., Karset, I. H. H., Berntsen, T. K., and co-authors, 2020, Large difference in aerosol radiative effects from BVOC-SOA treatment in three Earth system models, *Atmos. Chem. Phys.*, **20**, 8953–8973. DOI: *https://doi.org/10.5194/acp-20-8953-2020*

Spracklen, D. V., Arnold, S. R., and Taylor, C. M., 2012, Observations of increased tropical rainfall preceded by air passage over forests: *Nature*, **489**, 282–285. DOI: *https://doi.org/10.1038/nature11390*

Spracklen, D. V., Bonn, B., and Carslaw, K. S., 2008, Boreal forests, aerosols and the impacts on clouds and climate, *Phil. T. R. Soc. A.*, **266**, 1–11. DOI: *https://doi.org/10.1098/rsta.2008.0201*

Spracklen, D. V., Carslaw, K. S., Kulmala, M., Kerminen, V. M., Mann, G. W., and Sihto, S. L., 2006, The contribution of boundary layer nucleation events to total particle concentrations on regional and global scales, *Atmos. Chem. Phys.*, **6**, 5631–5648. DOI: *https://doi.org/10.5194/acp-6-5631-2006*

Spracklen, D. V., K. S. Carslaw, J. Merikanto, G.W. Mann, C.L. Reddington, and co-authors, 2010, Explaining global surface aerosol number concentrations in terms of primary emissions and particle formation. *Atmospheric Chemistry and Physics*, **10**, 10, 4775–4793. DOI: *https://doi.org/10.5194/acp-10-4775-2010*

Staal, A., Fetzer, I., Wang-Erlandsson, L. and co-authors, 2020, Hysteresis of tropical forests in the 21st century. *Nature Commun*, **11**, 4978. DOI: *https://doi.org/10.1038/s41467-020-18728-7*

Stanley, W. R., Kaye, P. H., Foot, V. E., Barrington, S. J., Gallagher, M., and Gabey, A., 2011, Continuous bioaerosol monitoring in a tropical environment using a UV fluorescence particle spectrometer, *Atmospheric Science Letters*, **12**, 195–199. DOI: *https://doi.org/10.1002/asl.310*

Stark, S. C. D. D. Breshears, S. Aragón, J. C. Villegas, D. J. Law, M. N., and co-authors, 2020. Reframing tropical savannization: linking changes in canopy structure to energy balance alterations that impact climate. *Ecosphere*, **11**, 9, e03231. DOI: *https://doi.org/10.1002/ecs2.3231*

Staudt, M., and Bertin, N., 1998, Light and temperature dependence of the emission of cyclic and acyclic monoterpenes from holm oak (Quercus ilex L.) leaves, *Plant Cell and Environment*, **21**, 385–395. DOI: *https://doi.org/10.1046/j.1365-3040.1998.00288.x*

Stavrakou, T.; Müller, J.-F.; Bauwens, M.; De Smedt, I.; Van Roozendael, M.; Guenther, A., 2018, Impact of Short-Term Climate Variability on Volatile Organic Compounds Emissions Assessed Using OMI Satellite Formaldehyde Observations. *Geophys. Res. Lett.*, **45**, 16, 8681–8689. DOI: *https://doi.org/10.1029/2018GL078676*

Stavrakou, T., Muller, J. F., De Smedt, I., Van Roozendael, M., van der Werf, G. R., and co-authors, 2009, Evaluating the performance of pyrogenic and biogenic emission inventories against one decade of space-based formaldehyde columns. *Atmos Chem Phys*, **9**, 3, 1037–1060. DOI: *https://doi.org/10.5194/acp-9-1037-2009*

Steffen, W., Richardson, K., Rockström, J., Cornell, S. E., Fetzer, I., and co-authors, 2015, Planetary Boundaries: Guiding Human Development on a Changing Planet, *Science*, **347**, 6223. DOI: *https://doi.org/10.1126/science.1259855*

Steffen, W., Rockström, J., Richardson, K., Lenton, T. M., Folke, C., and co-authors, 2018, Trajectories of the Earth System in the Anthropocene, *Proceedings of the National Academy of Science*s, **115**, 33, 8252–9. DOI: *https://doi.org/10.1073/pnas.1810141115*

Stenberg, L., Haahti, K., Hökkä, H., Launiainen, S., Nieminenet, M., and co-authors, 2018, Hydrology of drained peatland forest: Numerical experiment on the role of tree stand heterogeneity and management. *Forests*, **9**, 10, 645. DOI: *https://doi.org/10.3390/f9100645*

Stephens, G. L., J. L. Li, M. Wild, C. A. Clayson, N. Loeb, and co-authors, 2012, An update on Earth's energy balance in light of the latest global observations, *Nat Geosci*, **5**, 10, 691–696. DOI: *https://doi.org/10.1038/ngeo1580*

Stevens, B., and G. Feingold, 2009, Untangling aerosol effects on clouds and precipitation in a buffered system, *Nature*, **461**, 7264, 607–613. DOI: *https://doi.org/10.1038/nature08281*

Stickler, A., Fischer, H., Bozem, H., Gurk, C., Schiller, C., and co-authors, 2007, Chemistry, transport, and dry deposition of trace gases in the boundary layer over the tropical Atlantic Ocean and the Guyanas during the GABRIEL field campaign, *Atmos. Chem. Phys.*, **7**, 14, 3933–3956. DOI: *https://doi.org/10.5194/acp-7-3933-2007*

Stocker, T. F., D. Qin, G.-K. Plattner, L. V. Alexander, S. K. Allen, and co-authors, 2013, Technical Summary, in *Climate Change 2013: The Physical Science Basis. Contribution of Working Group I to the Fifth Assessment Report of the Intergovernmental Panel on Climate Change*, edited by T. F. Stocker, and co-authors, Cambridge University Press, Cambridge, United Kingdom and New York, NY, USA.

Stocks, B.J., Fosberg, M.A., Lynham, T.J. and co-authors, 1998, Climate Change and Forest Fire Potential in Russian and Canadian Boreal Forests. *Climatic Change*, **38**, 1–13. DOI: *https://doi.org/10.1023/A:1005306001055*

Strömgren, M., Hedwall, P.O. and Olsson, B.A., 2016. Effects of stump harvest and site preparation on N_2O and CH_4 emissions from boreal forest soils after clear-cutting. *Forest Ecology and Management*, **371**, 15–22. DOI: *https://doi.org/10.1016/j.foreco.2016.03.019*

Sullivan, M. J. P., S. L. Lewis, K. Affum-Baffoe, C. Castilho, F. Costa, and co-authors, 2020, Long-term thermal sensitivity of Earth's tropical forests. *Science*, **368**, 6493, 869–874. DOI: *https://doi.org/10.1126/science.aaw7578*

Sundqvist, E., Mölder, M., Crill, P., Kljun, N. and Lindroth, A., 2015. Methane exchange in a boreal forest estimated by gradient method. *Tellus B Chem Phys Meteorol*, **67**, 1. DOI: *https://doi.org/10.3402/tellusb.v67.26688*

Suni, T., A. Guenther, H.C. Hansson, M. Kulmala, M.O. Andreae and co-authors, 2015, The significance of land–atmosphere interactions in the Earth system—iLEAPS achievements and perspectives. *Anthropocene*. DOI: *https://doi.org/10.1016/j.ancene.2015.12.001*

Surratt, J. D., Chan, A. W. H., Eddingsaas, N. C., Chan, M. N., Loza, and co-authors, 2010, Reactive intermediates revealed in secondary organic aerosol formation from isoprene, Proc. Natl. Acad. Sci. U.S.A., **107**, 15, 6640–6645. DOI: *https://doi.org/10.1073/pnas.0911114107*

Swap, R., Garstang, M., Greco, S., Talbot, R. and Kallberg, P., 1992, Saharan dust in the Amazon Basin, *Tellus B Chem Phys Meteorol*, **44**, 2, 133–149. DOI: *https://doi.org/10.1034/j.1600-0889.1992.t01-1-00005.x*

Swap, R. J., M. Garstang, S. A. Macko, P. D. Tyson, W. Maenhaut, and co-authors, 1996, The long-range transport of

southern African aerosols over the tropical South Atlantic, *J. Geophys. Res*., **101**, 23, 777– 23,791. DOI: *https://doi.org/10.1029/95JD01049*

Swietlicki, E., Hansson, H. C., Hämeri, K., Svenningsson, B., Massling, A., and co-authors, 2008, Hygroscopic properties of submicrometer atmospheric aerosol particles measured with HTDMA instruments in various environment– A review, *Tellus B*, **60**, 432. DOI: *https://doi.org/10.1111/j.1600-0889.2008.00350.x*

Tack A.J.M., Hakala J., Petäjä T., Kulmala M. & Laine A.-L., 2014, Genotype and spatial structure shape pathogen dispersal and disease dynamics at small spatial scales, *Ecology*, **95**, 703–714. DOI: *https://doi.org/10.1890/13-0518.1*

Tai, A. P. K., M. V. Martin, and C. L. Heald, 2014, Threat to future global food security from climate change and ozone air pollution. *Nature Climate Change*, **4**, 817–821. DOI: *https://doi.org/10.1038/nclimate2317*

Taipale, R., M.K. Kajos, J. Patokoski, P. Rantala, T.M. Ruuskanen & J. Rinne, 2011: Role of de novo biosynthesis in ecosystem scale monoterpene emissions from a boreal Scots pine forest. *Biogeosciences*, **8**, 2247–2255. DOI: *https://doi.org/10.5194/bg-8-2247-2011*

Takemura, T., T. Nakajima, O. Dubovik, B.N. Holben, and S. Kinne, 2002, Single-Scattering Albedo and Radiative Forcing of Various Aerosol Species with a Global Three-Dimensional Model, *J. Climate*, **15**, 333–352. DOI: *https://doi.org/10.1175/1520-0442(2002)015<0333:SSAARF>2.0.CO;2*

Talbot, R. W., Andreae, M. O., Andreae, T. W., and Harriss, R. C., 1988, Regional aerosol chemistry of the Amazon Basin during the dry season, *J. Geophys. Res*., **93**, 1499–1508. DOI: *https://doi.org/10.1029/JD093iD02p01499*

Tanaka, L.; Satiamurty , P., Machado, Luiz A. T., 2014, Diurnal variation of precipitation in central Amazon Basin, *International Journal of Climatology*, **34**, 13, 3574–3584. DOI: *https://doi.org/10.1002/joc.3929*

Tarasova, O. A., Brenninkmeijer, C. A. M., Assono, S. S., Elansky, N. F., Röckmann, T., & Braß, M., 2006, Atmospheric CH_4 along the trans-Siberian railroad (TROICA) and river Ob: Source identification using stable isotope analysis, *Atmospheric Environment*, **40**, 29, 5617– 5628. DOI: *https://doi.org/10.1016/j.atmosenv.2006.04.065*

Tarvainen, V., Hakola, H., Hellen, H., Bäck, J., Hari, P., and Kulmala, M., 2005, Temperature and light dependence of the VOC emissions of Scots pine, *Atmos. Chem. Phys*., **5**, 989–998, *http://www.atmos-chem-phys.net/5/989/2005/*. DOI: *https://doi.org/10.5194/acp-5-989-2005*

Tarvainen, V., H. Hakola, J. Rinne, H. Hellén, & S. Haapanala, 2007, Towards a comprehensive emission inventory of terpenoids from boreal ecosystems. *Tellus B Chem Phys Meteorol*, **59B**, 526–534. DOI: *https://doi.org/10.1111/j.1600-0889.2007.00263.x*

Taylor, T. C., McMahon, S. M., Smith, M. N., Boyle, B., Violle, C., and co-authors, 2018, Isoprene emission structures tropical tree biogeography and community assembly responses to climate, *New Phytologist*, **220**, 435–446. DOI: *https://doi.org/10.1111/nph.15304*

Textor, C., M. Schulz, S. Guibert, S. Kinne, Y. Balkanski, and co-authors, 2006, Analysis and quantification of the diversities of aerosol life cycles within AeroCom, *Atmos Chem Phys*, **6**, 1777–1813. DOI: *https://doi.org/10.5194/acp-6-1777-2006*

Thalman, R., de Sá, S. S., Palm, B. B., Barbosa, H. M. J., Pöhlker, M. L., and co-authors, 2017, CCN activity and organic hygroscopicity of aerosols downwind of an urban region in central Amazonia: seasonal and diel variations and impact of anthropogenic emissions, *Atmos. Chem. Phys*., **17**, 11779–11801. DOI: *https://doi.org/10.5194/acp-17-11779-2017*

Timokhina, A. V., Prokushkin, A. S., Panov, A. V., Kolosov, R. A., Sidenko, and co-authors, 2018, Interannual Variability of Atmospheric CO_2 Concentrations over Central Siberia from ZOTTO Data for 2009—2015, *Russ. Meteorol. Hydrol*., **43**, 288. DOI: *https://doi.org/10.3103/S1068373918050023*

Tingey, D.T., M. Manning, L.C. Grothaus, W.F. Burns, 1980, Influence of Light and Temperature on Monoterpene Emission Rates from Slash Pine, *Plant Physiol*., **65**, 797–801. DOI: *https://doi.org/10.1104/pp.65.5.797*

Titos, G., Cazorla, A., Zieger, P., Andrews, E., Lyamani, H. and co-authors, 2016, Effect of hygroscopic growth on the aerosol light-scattering coefficient: A review of measurements, techniques, and error sources, *Atmos Environ*, **141**, 494–507. DOI: *https://doi.org/10.1016/j.atmosenv.2016.07.021*

Toledano, C., V. Cachorro, M. Gausa, K. Stebel, V. Aaltonen, and co-authors, 2012, Overview of sun photometer measurements of aerosol properties in Scandinavia and Svalbard, *Atmos Environ*, 52,18–28. DOI: *https://doi.org/10.1016/j.atmosenv.2011.10.022*

Toledo Machado, L. A., Franco, M. A., Kremper, L. A., Ditas, F., Andreae, M. O., and co-authors, 2021, How weather events modify aerosol particle size distributions in the Amazon boundary layer, *Atmos. Chem. Phys. Discuss*., in review. DOI: *https://doi.org/10.5194/acp-2021-314*

Toll, V. Christensen, M., Quaas, J. and N. Bellouin, 2019, Weak average liquid-cloud-water response to anthropogenic aerosols, *Nature*, **572**, 51–55. DOI: *https://doi.org/10.1038/s41586-019-1423-9*

Tomaziello, A.C.N., Carvalho, L.M.V. & Gandu, A.W., Intraseasonal variability of the Atlantic Intertropical Convergence Zone during austral summer and winter, *Clim Dyn*, **47**, 1717–1733 (2016). DOI: *https://doi.org/10.1007/s00382-015-2929-y*

Tong, H., Zhang, Y., Filippi, A., Wang, T., Li, C., and co-authors, 2019, Radical Formation by Fine Particulate Matter Associated with Highly Oxygenated Molecules, *Environ. Sci. Technol*., **53**, 21, 12506–12518. DOI: *https://doi.org/10.1021/acs.est.9b05149*

Topping, D.O., Barley, M.H. and McFiggans, G., 2011, The sensitivity of Secondary Organic Aerosol component partitioning to the predictions of component properties – Part 2: Determination

of particle hygroscopicity and its dependence on "apparent" volatility, *Atmos. Chem. Phys.*, **11**, 7767–7779. DOI: *https://doi.org/10.5194/acp-11-7767-2011*

Topping, D. O., and McFiggans G., 2012, Tight coupling of particle size, number and composition in atmospheric cloud droplet activation, *Atmos. Chem. Phys.*, **12**, 3253–3260. DOI: *https://doi.org/10.5194/acp-12-3253-2012*

Trail, F., Gaffoor, I., and Vogel, S., 2005, Ejection mechanics and trajectory of the ascospores of Gibberella zeae (anamorph Fusarium graminearum), *Fungal Genet. Biol.*, **42**, 528–533. DOI: *https://doi.org/10.1016/j.fgb.2005.03.008*

Treat CC, Natali SM, Ernakovich J, Iversen CM, Lupascu M., and co-authors, 2015, A pan-Arctic synthesis of CH_4 and CO_2 production from anoxic soil incubations. *Glob Chang Biol.*, **21**, 7, 2787–2803. DOI: *https://doi.org/10.1111/gcb.12875*

Trebs, I., Mayol-Bracero, O. L., Pauliquevis, T., Kuhn, U., Sander, R., and co-authors, 2012, Impact of the Manaus urban plume on trace gas mixing ratios near the surface in the Amazon Basin: Implications for the NO-NO2-O3 photostationary state and peroxy radical levels, *J. Geophys. Res.*, **117**, D05307. DOI: *https://doi.org/10.1029/2011JD016386*

Trenberth, K.E., Smith, L., Qian, T., Dai, A., and Fasullo, J., 2007. Estimates of the global water budget and its annual cycle using observational and model data. *J. Hydrometeorol.*, **8**, 4, 758–769. DOI: *https://doi.org/10.1175/JHM600.1*

Trisos, C.H., Merow, C. & Pigot, A.L. 2020, The projected timing of abrupt ecological disruption from climate change. *Nature*, **580**, 496–501. DOI: *https://doi.org/10.1038/s41586-020-2189-9*

Trumbore, S., Brando, P., Hartmann, H., 2015. Forest health and global change. *Science*, **349**, 814–818. DOI: *https://doi.org/10.1126/science.aac6759*

Tuet, W., Liu, F., Alves, N., Fok, S., Artaxo, P., and co-authors, 2019, Chemical oxidative potential and cellular oxidative stress from biomass burning aerosol, *Environmental Science & Technology Letters*, **6**, 126–132, *https://pubs.acs.org/doi/pdf/10.1021/acs.estlett.9b00060*. DOI: *https://doi.org/10.1021/acs.estlett.9b00060*

Tunved, P., Hansson, H. C., Kerminen, V. M., Strom, J., Dal Maso, M., and co-authors, 2006a, High natural aerosol loading over boreal forests, *Science*, **312**, 261–263. DOI: *https://doi.org/10.1126/science.1123052*

Tunved, P., Hansson, H. C., Kulmala, M., Aalto, P., Viisanen, Y., and co-authors, 2003, One year boundary layer aerosol size distribution data from five nordic background stations, *Atmos Chem Phys*, **3**, 2183–2205. DOI: *https://doi.org/10.5194/acp-3-2183-2003*

Tunved, P., Korhonen, H., Strom, J., Hansson, H. C., Lehtinen, K. E. J., and Kulmala, M., 2006b, Is nucleation capable of explaining observed aerosol integral number increase during southerly transport over Scandinavia? *Tellus B*, **58**, 129–140. DOI: *https://doi.org/10.1111/j.1600-0889.2006.00176.x*

Turner, J. C. R., and Webster, J., 1995, Mushroom Spores – The Analysis of Bullers Drop, *Chem. Eng. Sci.*, **50**, 2359–2360. DOI: *https://doi.org/10.1016/0009-2509(95)00097-O*

Twohy, C. H., Clement, C. F., Gandrud, B. W., Weinheimer, A. J., Campos, and co-authors, 2002, Deep convection as a source of new particles in the midlatitude upper troposphere, *J. Geophys. Res.,* **107**, 21. DOI: *https://doi.org/10.1029/2001JD000323*

Twomey, S., 1974, Pollution and the planetary albedo, *Atmos Environ*, **8**, 1251–1256. DOI: *https://doi.org/10.1016/0004-6981(74)90004-3*

Twomey, S., 1977, The Influence of Pollution on the Shortwave Albedo of Clouds, *Journal of the Atmospheric Sciences*, **34**, 1149–1152. DOI: *https://doi.org/10.1175/1520-0469(1977)034<1149:TIOPOT>2.0.CO;2*

Tyukavina, A., Baccini, A., Hansen, M.C., Potapov, P.V., Stehman, S.V. and Co-authors, 2015: Aboveground carbon loss in natural and managed tropical forests from 2000 to 2012. *Environ. Res. Lett.*, **10**, 74002–74002. DOI: *https://doi.org/10.1088/1748-9326/10/7/074002*

Unger, N., K. Harper, Y. Zheng, N.Y. Kiang, I. Aleinov, and co-authors, 2013, Photosynthesis-dependent isoprene emission from leaf to planet in a global carbon-chemistry-climate model, *Atmos Chem Phys*, **13**, 10243–10269. DOI: *https://doi.org/10.5194/acp-13-10243-2013*

Vaananen, R., Kyro, E. M., Nieminen, T., Kivekas, N., Junninen, H., and co-authors, 2013, Analysis of particle size distribution changes between three measurement sites in northern Scandinavia, *Atmos Chem Phys*, **13**, 11887–11903. DOI: *https://doi.org/10.5194/acp-13-11887-2013*

Väkevä, M., Hämeri, K., and Aalto, P., 2002, Hygroscopic properties of nucleation mode and Aitken mode particles during nucleation bursts and in background air on the west coast of Ireland, *J. Geophys. Res.*, **107**, 8104. DOI: *https://doi.org/10.1029/2000JD000176*

Valentini, R., Arneth, A., Bombelli, A., Castaldi, S., Cazzolla Gatti, R., and co-authors, 2014. A full greenhouse gases budget of Africa: Synthesis, uncertainties, and vulnerabilities, *Biogeosciences*, **11**, 381–407. DOI: *https://doi.org/10.5194/bg-11-381-2014*

van der Laan-Luijkx, I. T., van der Velde, I. R., Krol, M. C., Gatti, L. V., Domingues, L. G., and co-authors, 2015, Response of the Amazon carbon balance to the 2010 drought derived with CarbonTracker South America, *Global Biogeochem. Cycles*, **29**, 7, 1092–1108. DOI: *https://doi.org/10.1002/2014GB005082*

van der Werf, G. R., Randerson, J. T., Giglio, L., Collatz, G. J., Mu, M., , and co-authors, 2010, Global fire emissions and the contribution of deforestation, savanna, forest, agricultural, and peat fires (1997–2009), *Atmos. Chem. Phys.*, **10**, 11707–11735. DOI: *https://doi.org/10.5194/acp-10-11707-2010*

van der Werf, G. R., Randerson, J.T., Giglio, L., van Leeuwen, T.T., Chen, Y., and Co-authors, 2017: Global fire emissions estimates during 1997 – 2016, *Earth Syst. Sci. Data*, **9**, 697–720. DOI: *https://doi.org/10.5194/essd-9-697-2017*

van Marle, M. J. E., R. D. Field, G. R. van der Werf, I. A. Estrada de Wagt, R. A. Houghton, and co-authors, 2017, Fire and deforestation dynamics in Amazonia (1973–2014),

Global Biogeochem. Cycles, **31**. DOI: *https://doi.org/10.1002/2016GB005445*

Vancutsem, C., Achard, F., Pekel, J.-F., Vieilledent, G., Carboni, S., and co-authors, 2021, Long-term (1990–2019) monitoring of forest cover changes in the humid tropics, *Sci. Adv.*, **7**, 10, eabe1603. DOI: *https://doi.org/10.1126/sciadv.abe1603*

Vanhatalo, A., T. Chan, J. Aalto, J.F. Korhonen, P. Kolari, and co-authors, 2015, Tree water relations can trigger monoterpene emissions from Scots pine stems during spring recovery. *Biogeosciences*, **12**, 5353–5363. DOI: *https://doi.org/10.5194/bg-12-5353-2015*

Vanhatalo, A., Ghirardo, A., Juurola, E., Schnitzler, J.-P., Zimmer, I., and co-authors, 2018, Long-term dynamics of monoterpene synthase activities, monoterpene storage pools and emissions in boreal Scots pine, *Biogeosciences*, **15**, 16, 5047–5060. DOI: *https://doi.org/10.5194/bg-15-5047-2018*

Veraverbeke, S., B. M. Rogers, M. L. Goulden, R. R. Jandt, C. E. Miller, and co-authors, 2017, Lightning as a major driver of recent large fire years in North American boreal forests, *Nat. Clim. Change*, **7**, 529. DOI: *https://doi.org/10.1038/nclimate3329*

Vesala, T., Haataja, J., Aalto, P., Altimir, N., Buzorius, G., and co-authors, 1998, Long-term field measurements of atmosphere-surface interactions in boreal forest combining forest ecology, micrometeorology, aerosol particle size and composition distribution with aerosol physics and atmospheric chemistry, *Trends in Heat, Mass & Momentum Transfer*, **4**, 17–35.

Vestenius M., Hellén H., Levula J., Kuronen P., Helminen K.J., and co-authors, 2014, Acidic reaction products of mono- and sesquiterpenes in atmospheric fine particles in a boreal forest, *Atmos. Chem. Phys.*, **14**, 7883–7893. DOI: *https://doi.org/10.5194/acp-14-7883-2014*

Virkkula, A., Backman, J., Aalto, P. P., Hulkkonen, M., Riuttanen, L., and co-authors., 2011, Seasonal cycle, size dependencies, and source analyses of aerosol optical properties at the SMEAR II measurement station in Hyytiälä, Finland, *Atmos. Chem. Phys.*, **11**, 4445–4468. DOI: *https://doi.org/10.5194/acp-11-4445-2011*

Virkkula, A., Levula, J., Pohja, T., Aalto, P.P., Keronen, P., and co-authors, 2014a, Prescribed burning of logging slash in the boreal forest in Finland: emissions and effects on meteorological quantities and soil properties, *Atmos. Chem. Phys.*, **14**, 4473–4502. DOI: *https://doi.org/10.5194/acp-14-4473-2014*

Virkkula, A., Pohja, T., Aalto, P.P., Keronen, P., Schobesberger, S., and co-authors, 2014b, Airborne measurements of aerosols and carbon dioxide during a prescribed fire experiment at a boreal forest site, *Boreal Environ. Res.*, **19 B**, 153–181.

Virtanen, A., Joutsensaari, J., Koop, T., Kannosto, J., Yli-Pirila, P., and co-authors, 2010, An amorphous solid state of biogenic secondary organic aerosol particles, *Nature*, **467**, 824–827. DOI: *https://doi.org/10.1038/nature09455*

Vivchar, A.V., Moiseenko, K.B., Shumskii, R.A. and co-authors, 2009, *Izv. Atmos. Ocean. Phys.*, 45, 302. DOI: *https://doi.org/10.1134/S0001433809030049*

von Randow, C., Manzi, A.O.O., Kruijt, B., Oliveira, P.J.C., Zanchi, F.B.B., and co-authors, 2004, Comparative measurements and seasonal variations in energy and carbon exchange over forest and pasture in Southwest Amazonia, *Theor. Appl. Climatol.*, **78**, 5–26. DOI: *https://doi.org/10.1007/s00704-004-0041-z*

von Randow, C., Zeri, M., Restrepo-Coupe, N., Muza, M.N., de Gonçalves, L.G.G., and co-authors, 2013, Inter-annual variability of carbon and water fluxes in Amazonian forest, Cerrado and pasture sites, as simulated by terrestrial biosphere models. *Agric. For. Meteorol.*, **182**, 145–155. DOI: *https://doi.org/10.1016/j.agrformet.2013.05.015*

Wang, D., Giangrande, S. E., Bartholomew, M. J., Hardin, J., Feng, Z., and co-authors, 2018, The Green Ocean: precipitation insights from the GoAmazon2014/5 experiment, *Atmos. Chem. Phys.*, **18**, 9121–9145. DOI: *https://doi.org/10.5194/acp-18-9121-2018*

Wang, J., Krejci, R., Giangrande, S., Kuang, C., Barbosa, H. M. J., and co-authors, 2016, Amazon boundary layer aerosol concentration sustained by vertical transport during rainfall, *Nature*, **539**, 7629, 416–419. DOI: *https://doi.org/10.1038/nature19819*

Wang, X., S. Piao, P. Ciais, P. Friedlingstein, R. B. Myneni, and co-authors, 2014, A two-fold increase of carbon cycle sensitivity to tropical temperature variations. *Nature*, **506**, 212–215. DOI: *https://doi.org/10.1038/nature12915*

Wang, Q., Saturno, J., Chi, X., Walter, D., Lavric, J., and co-authors, 2016, Modeling investigation of light absorbing aerosols in the central Amazon during the wet season. *Atmos. Chem. Phys.*, **16**, 14775–14794, 2016. DOI: *https://doi.org/10.5194/acp-16-14775-2016*

Wang, H., Tetzlaff, D., Dick, J.J. and Soulsby, C., 2017. Assessing the environmental controls on Scots pine transpiration and the implications for water partitioning in a boreal headwater catchment. *Agric. For. Meteorol.*, **240–241**, 58–66. DOI: *https://doi.org/10.1016/j.agrformet.2017.04.002*

Warneke, C., S.L. Luxembourg, J.A. de Gouw, H.J.I. Rinne, A.B. Guenther & R. Fall, 2002, Disjunct eddy covariance measurements of oxygenated volatile organic compound fluxes from an alfalfa field before and after cutting. *J. Geophys. Res. Atmos.*, **107**, D8, 4067. DOI: *https://doi.org/10.1029/2001JD000594*

Weber, J., Archer-Nicholls, S., Abraham, N. L., Shin, Y. M., Bannan, T. J., and co-authors, 2021, Improvements to the representation of BVOC chemistry–climate interactions in UKCA (v11.5) with the CRI-Strat 2 mechanism: incorporation and evaluation, *Geosci. Model Dev.*, **14**, 8, 5239–5268. DOI: *https://doi.org/10.5194/gmd-14-5239-2021*

Webster, J., and Weber, R. W. S., 2007: Introduction to fungi, 3rd edition ed., Cambridge University Press, New York.

Wei D, Fuentes JD, Gerken T, Trowbridge AM, Stoy PC, Chamecki M. 2019. Influences of nitrogen oxides and isoprene on ozone-temperature relationships in the Amazon rain forest. Atmos Environ 206, 280–292. DOI: *https://doi.org/10.1016/j.atmosenv.2019.02.044*

Wendisch, M., Pöschl, U., Andreae, M. O., Machado, L. A. T., Albrecht, R., and co-authors, 2016, The ACRIDICON-CHUVA campaign: Studying tropical deep convective clouds and precipitation over Amazonia using the new German research aircraft HALO. *Bulletin of the American Meteorological Society*, **97**, 10, 1885–1908. DOI: *https://doi.org/10.1175/BAMS-D-14-00255.1*

White, B., E. Gryspeerdt, P. Stier, H. Morrison, G. Thompson, and Z. Kipling, 2017, Uncertainty from the choice of microphysics scheme in convection-permitting models significantly exceeds aerosol effects, *Atmos Chem Phys*, **17**, 19, 12145–12175. DOI: *https://doi.org/10.5194/acp-17-12145-2017*

Whitehead, J., Darbyshire, E., Brito, J., Barbosa, H., Crawford, I., and co-authors, 2016, Biogenic cloud nuclei in the central Amazon during the transition from wet to dry season, *Atmos. Chem. Phys.*, **16**, 9727–9743. DOI: *https://doi.org/10.5194/acp-16-9727-2016*

Whitehead, J. D., Gallagher, M. W., Dorsey, J. R., Robinson, N., Gabey, A. M., and co-authors, 2010, Aerosol fluxes and dynamics within and above a tropical rainforest in South-East Asia, *Atmos. Chem. Phys.*, **10**, 9369–9382. DOI: *https://doi.org/10.5194/acp-10-9369-2010*

Wiedensohler, A., N. Ma, W. Birmili, J. Heintzenberg, F. Ditas, and co-authors, 2019, Infrequent new particle formation over the remote boreal forest of Siberia. *Atmospheric Environment*, **200**, 1, 167–169. DOI: *https://doi.org/10.1016/j.atmosenv.2018.12.013*

Williams, J., J. Crowley, H. Fischer, H. Harder, M. Martinez, and co-authors, 2011. The summertime Boreal Forest field measurement intensive (HUMPPA- COPEC-2010): an overview of meteorological and chemical influences. *Atmos Chem Phys*, **11**, 20, 10599–10618. DOI: *https://doi.org/10.5194/acp-11-10599-2011*

Williams, C.A., Gu, H., MacLean, R., Masek, J.G. and Collatz, G.J., 2016. Disturbance and the carbon balance of US forests: A quantitative review of impacts from harvests, fires, insects, and droughts. *Global and Planetary Change*, **143**, 66–80. DOI: *https://doi.org/10.1016/j.gloplacha.2016.06.002*

Williams, C.A., Reichstein, M., Buchmann, N., Baldocchi, D., Beer, C., and co-authors, 2012, Climate and vegetation controls on the surface water balance: Synthesis of evapotranspiration measured across a global network of flux towers. *Water Resour. Res.*, **48**, 5. DOI: *https://doi.org/10.1029/2011WR011586*

Williams, E., Rosenfeld, D., Madden, N., Gerlach, J., Gears, N., and co-authors, 2002, Contrasting convective regimes over the Amazon: Implications for cloud electrification, *J. Geophys. Res.*, **107**, 8082. DOI: *https://doi.org/10.1029/2001JD000380*

Williams, E. R., and Sátori, G., 2004, Lightning, thermodynamic and hydrological comparison of the two tropical continental chimneys, *Journal of Atmospheric and Solar-Terrestrial Physics*, **66**, 1213–1231. DOI: *https://doi.org/10.1016/j.jastp.2004.05.015*

Williamson, C.J., Kupc, A., Axisa, D. and co-authors, 2019, A large source of cloud condensation nuclei from new particle formation in the tropics. *Nature*, **574**, 399–403. DOI: *https://doi.org/10.1038/s41586-019-1638-9*

Wilson, C., M. Gloor, L. V. Gatti, J. B. Miller, S. A. Monks, and co-authors, 2016, Contribution of regional sources to atmospheric methane over the Amazon Basin in 2010 and 2011, *Global Biogeochem. Cycles*, **30**, 400–420. DOI: *https://doi.org/10.1002/2015GB005300*

Wimmer, D., Buenrostro Mazon, S., Manninen, H. E., Kangasluoma, J., Franchin, A., and co-authors. 2018. Ground-based observation of clusters and nucleation mode particles in the Amazon, *Atmos. Chem. Phys.*, **18**, 13245–13264. DOI: *https://doi.org/10.5194/acp-18-13245-2018*

Winderlich, J., Chen, H., Gerbig, C., Seifert, T., Kolle, O., and co-authors, 2010. Continuous low-maintenance CO_2/CH_4/H_2O measurements at the Zotino Tall Tower Observatory (ZOTTO) in Central Siberia. *Atmospheric Measurement Techniques*, **3**, 4, 1113–1128. DOI: *https://doi.org/10.5194/amt-3-1113-2010*

Winderlich, J., Gerbig, C., Kolle, O., Heimann, M., 2014, Inferences from CO_2 and CH_4 concentration profiles at the Zotino Tall Tower Observatory (ZOTTO) on regional summertime ecosystem fluxes. *Biogeosciences*, **11**, 7, 2055–2068. DOI: *https://doi.org/10.5194/bg-11-2055-2014*

Womack, A. M., Artaxo, P. E., Ishida, F. Y., Mueller, R. C., Saleska, S. R., and co-authors, 2015, Characterization of active and total fungal communities in the atmosphere over the Amazon rainforest, *Biogeosciences*, *12*, 6337–6349. DOI: *https://doi.org/10.5194/bg-12-6337-2015*

World Resources Institute – WRI, 2021 – Global Forest Pulse (*https://research.wri.org/gfr/forest-pulse*). Accessed on October 10, 2021.

Wotton, B M, M D Flannigan, and G. A. Marshall, 2017, Potential climate change impacts on fire intensity and key wildfire suppression thresholds in Canada. *Environ. Res. Lett.*, **12**, 095003. DOI: *https://doi.org/10.1088/1748-9326/aa7e6e*

Yamasoe, M. A., P. Artaxo, A. H. Miguel, A. G. Allen, 2000, Chemical composition of aerosol particles from direct emissions of biomass burning in the Amazon Basin: water-soluble species and trace elements. *Atmospheric Environment*, **34**, 1641–1653. DOI: *https://doi.org/10.1016/S1352-2310(99)00329-5*

Yan, C., J. Crowley, H. Fischer, H. Harder, M. Martinez, and co-authors, 2016, Source characterization of highly oxidized multifunctional compounds in a boreal forest environment using positive matrix factorization, *Atmos Chem Phys*, **16**, 19, 12715–12731. DOI: *https://doi.org/10.5194/acp-16-12715-2016*

Yan C., Dada L., Rose C., Jokinen T., Nie W., and co-authors. 2018. The role of H_2SO_4-NH_3 anion clusters in ion-induced aerosol nucleation mechanisms in the boreal forest, *Atmos. Chem. Phys*., **18**, 13231–13243. DOI: *https://doi.org/10.5194/acp-18-13231-2018*

Yáñez-Serrano, A.M., Bourtsoukidis, E., Alves, E., Bauwens, M., Stavrakou, T., and co-authors, 2020, Amazonian BVOC emissions under global change: a review of current research, and future directions Journal, *Global Change Biology*, **26**, 9, 4722–4751. DOI: *https://doi.org/10.1111/gcb.15185*

Yáñez-Serrano AM, Fasbender L, Kreuzwieser J, Dubbert D, Haberstroh S, and co-authors, 2018b. Volatile diterpene emission by two Mediterranean Cistaceae shrubs. *Scientific Reports*, **8**, 6855. DOI: *https://doi.org/10.1038/s41598-018-25056-w*

Yáñez-Serrano, A. M., Nölscher, A. C., Bourtsoukidis, E., Gomes Alves, E., Ganzeveld, L., and co-authors, 2018a, Monoterpene chemical speciation in a tropical rainforest variation with season, height, and time of day at the Amazon Tall Tower Observatory (ATTO), *Atmos. Chem. Phys*., **18**, 5, 3403–3418. DOI: *https://doi.org/10.5194/acp-18-3403-2018*

Yáñez-Serrano, A. M., Nölscher, A. C., Williams, J., Wolff, S., Alves, E. G., and co-authors, 2015, Diel and seasonal changes of biogenic volatile organic compounds within and above an Amazonian rainforest, *Atmos. Chem. Phys*., **15**, 6, 3359–3378. DOI: *https://doi.org/10.5194/acp-15-3359-2015*

Yang, Y., Saatchi, S. S., Xu, L., Yu, Y., Choi, S., and co-authors, 2018. Post-drought declines of the Amazon carbon sink, *Nature Communications*, **9**, 3172. DOI: *https://doi.org/10.1038/s41467-018-05668-6*

Yang Y, Shao M, Wang X, Nölscher AC, Kessel S, Guenther A, Williams J. 2016. Towards a quantitative understanding of total OH reactivity: A review. *Atmos Environ*, **134**, 147–161. DOI: *https://doi.org/10.1016/j.atmosenv.2016.03.010*

Yee, L. D., Isaacman-VanWertz, G., Wernis, R., Kreisberg, N.M., Glasius, M. , 2020, Natural and anthropogenically-influenced isoprene oxidation in the Southeastern U.S.A. and central Amazon, *Environ. Sci. Technol*., **54**, 10, 5980–5991. DOI: *https://doi.org/10.1021/acs.est.0c00805*

Yee, L. D., Isaacman-VanWertz, G., Wernis, R. A., Meng, M., Rivera, V., and co-authors, 2018, Observations of sesquiterpenes and their oxidation products in central Amazonia during the wet and dry seasons, *Atmos. Chem. Phys*., **18**, 14, 10433–10457. DOI: *https://doi.org/10.5194/acp-18-10433-2018*

Yin J., 2005, A consistent poleward shift of the storm tracks in simulations of the 21st century climate. *Geophys Res Lett*, **32**, L18701. DOI: *https://doi.org/10.1029/2005GL023684*

Yingjun L., J. Brito, M. Dorris, J. C. Rivera-Rios, R. Seco, and co-authors, 2016, Isoprene Photochemistry over the Amazon Rain Forest. *Proc. Natl. Acad. Sci. U. S. A*, **113**, 22, 6125–6130. DOI: *https://doi.org/10.1073/pnas.1524136113*

Yingjun L., R. Seco, S. Kim, A. Guenther, A. H. Goldstein, and co-authors, 2018, Isoprene photo-oxidation products quantify the effect of pollution on hydroxyl radicals over Amazonia. *Sciences Advances*, **4**, 4, eaar2547, 2018. DOI: *https://doi.org/10.1126/sciadv.aar2547*

Yli-Juuti, T., T. Nieminen, A. Hirsikko, P.P. Aalto, E. Asmi, and co-authors, 2011, Growth rates of nucleation mode particles in Hyytiälä during 2003–2009: variation with particle size, season, data analysis method and ambient conditions. *Atmos Chem Phys*, **11**, 12865–12886. DOI: *https://doi.org/10.5194/acp-11-12865-2011*

Yli-Panula E., Fekedulegn D.B., Green B.G. & Ranta H., 2009, Analysis of airborne Betula pollen in Finland, a 31-year perspective, *Int. J. Environ. Res. Public Health*, **6**, 1706–1723. DOI: *https://doi.org/10.3390/ijerph6061706*

Yttri, K. E., Simpson, D., J. Nojgaard, J.K., Kristensen, K., Genberg, J., and co-authors, 2011, Source apportionment of the summertime carbonaceous aerosol at Nordic rural background sites. *Atmos Chem Phys*, **11**, 13339–13357. DOI: *https://doi.org/10.5194/acp-11-13339-2011*

Yu, Z. Wang, J., Liu, S., Piao, S., Ciais, P., Running S.W., and co-authors, 2016, Decrease in winter respiration explains 25% of the annual northern forest carbon sink enhancement over the last 30 years. *Global Ecology and Biogeography*, **25**, 5, 586–595. DOI: *https://doi.org/10.1111/geb.12441*

Yu, F., Wang, Z., Luo, G., and Turco, R., 2008, Ion-mediated nucleation as an important global source of tropospheric aerosols, *Atmos. Chem. Phys*., **8**, 2537–2554. DOI: *https://doi.org/10.5194/acp-8-2537-2008*

Yuan, W., Zheng, Y., Piao, S., Ciais, P., Lombardozzi, D., Wang, Y, and co-authors, 2019, Increased atmospheric vapor pressure deficit reduces global vegetation growth, *Sci. Adv*., **5**, eaax1396. DOI: *https://doi.org/10.1126/sciadv.aax1396*

Yue, C., Ciais, P., Zhu, D., Wang, T., Peng, S., and co-authors, 2016. How have past fire disturbances contributed to the current carbon balance of boreal ecosystems? *Biogeosciences*, **13**, 3, 675–690. DOI: *https://doi.org/10.5194/bg-13-675-2016*

Zemp, D. C., Schleussner, C. F., Barbosa, H. M. J., and Rammig, A., 2017, Deforestation effects on Amazon forest resilience, *Geophys. Res. Lett*., **44**, 6182–6190. DOI: *https://doi.org/10.1002/2017GL072955*

Zemp, D. C., Schleussner, C. F., Barbosa, H. M. J., van der Ent, R. J., Donges, J. F., and co-authors, 2014, On the importance of cascading moisture recycling in South America, *Atmos. Chem. Phys*., **14**, 13,337–13,359. DOI: *https://doi.org/10.5194/acp-14-13337-2014*

Zeri, M., Sá, L.D.A., Manzi, A.O., Araújo, A.C., Aguiar, R.G., and co-authors, 2014, Variability of carbon and water fluxes following climate extremes over a tropical forest in southwestern Amazonia. *PLoS One*, **9**. DOI: *https://doi.org/10.1371/journal.pone.0088130*

Zhang, T., R. G. Barry, K. Knowles, J. A. Heginbottom & J. Brown, 1999, Statistics and characteristics of permafrost and ground-ice distribution in the Northern Hemisphere,

Polar Geography, **23**, 2, 132–154. DOI: *https://doi.org/10.1080/10889379909377670*

Zhang, F., Wang, Y., Peng, J., Ren, J., Collins, D., 2017, Uncertainty in predicting CCN activity of aged and primary aerosols. *J. Geophys. Res. Atmos.*, **122**, 723–11,736. DOI: *https://doi.org/10.1002/2017JD027058*

Zhao, D.F., Buchholz, A., Kortner, B., Schlag, P., Rubach, F., and co-authors, 2016, Cloud condensation nuclei activity, droplet growth kinetics, and hygroscopicity of biogenic and anthropogenic secondary organic aerosol (SOA), *Atmos. Chem. Phys.*, **16**, 1105–1121. DOI: *https://doi.org/10.5194/acp-16-1105-2016*

Zhao, B., Shrivastava, M., Donahue, N.M., Gordon, H., Schervish, M., and co-authors, 2020, High concentration of ultrafine particles in the Amazon free troposphere produced by organic new particle formation. *Proc. Natl. Acad. Sci. U. S. A*, **117**, 41, 25344–25351. DOI: *https://doi.org/10.1073/pnas.2006716117*

Zhou, P., Ganzeveld, L., Rannik, Ü., Zhou, L., Gierens, R., and co-authors, 2017, Simulating ozone dry deposition at a boreal forest with a multi-layer canopy deposition model, *Atmos Chem Phys*, **17**, 2, 1361–1379. DOI: *https://doi.org/10.5194/acp-17-1361-2017*

Zhou, J. C., Swietlicki, E., Hansson, H. C., and Artaxo, P., 2002, Submicrometer aerosol particle size distribution and hygroscopic growth measured in the Amazon rain forest during the wet season, *J. Geophys. Res.-Atmos.*, **107**, D20, 8055. DOI: *https://doi.org/10.1029/2000JD000203*

Zhu, J., Penner, J. E., Yu, F., Sillman, S., Andreae, M. O., and Coe, H., 2019, Decrease in radiative forcing by organic aerosol nucleation, climate, and land use change, *Nature Communications*, **10**, 423. DOI: *https://doi.org/10.1038/s41467-019-08407-7*

Zhu, T., D. Wang, R.L. Desjardins, J.I. Macpherson, 1999, Aircraft-based volatile organic compounds flux measurements with relaxed eddy accumulation, *Atmos. Environ.*, **33**, 1969–1979. DOI: *https://doi.org/10.1016/S1352-2310(98)00098-3*

Zhuang, Q., Lu, Y., Chen, M., 2012, An inventory of global N2O emissions from the soils of natural terrestrial ecosystems. *Atmos. Environ.*, **47**, 66–75. DOI: *https://doi.org/10.1016/j.atmosenv.2011.11.036*

Zieger, P, Aalto, P. P., Aaltonen, V., Äijälä, M., Backman, J., and co-authors, 2015. Low hygroscopic scattering enhancement of boreal aerosol and the implications for a columnar optical closure study. *Atmos Chem Phys*, **15**, 13, 7247–7267. DOI: *https://doi.org/10.5194/acp-15-7247-2015*

Zieger, P., Fierz-Schmidhauser, R., Gysel, M., Ström, J., Henne, S. and co-authors. 2010. Effects of relative humidity on aerosol light scattering in the Arctic. *Atmos Chem Phys*, **10**, 8, 3875–3890. DOI: *https://doi.org/10.5194/acp-10-3875-2010*

Zieger, P., Fierz-Schmidhauser, R., Poulain, L., Müller, T., Birmili, W and co-authors. E., 2014. Influence of water uptake on the aerosol particle light scattering coefficients of the Central European aerosol. *Tellus B Chem Phys Meteorol*, **66**, 1, 22716. DOI: *https://doi.org/10.3402/tellusb.v66.22716*

Zieger, P., Fierz-Schmidhauser, R., Weingartner, E. and Baltensperger, U., 2013. Effects of relative humidity on aerosol light scattering: results from different European sites. *Atmos. Chem. Phys.*, **13**, 21, 10609–10631. DOI: *https://doi.org/10.5194/acp-13-10609-2013*

Zieger, P., Weingartner, E., Henzing, J., Moerman, M., de Leeuw, G., and co-authors, 2011, Comparison of ambient aerosol extinction coefficients obtained from in-situ, MAX-DOAS and LIDAR measurements at Cabauw, *Atmos. Chem. Phys.*, **11**, 2603–2624. DOI: *https://doi.org/10.5194/acp-11-2603-2011*

Zimmerman, P. R., Greenberg, J. P., and Westberg, C. E., 1988, Measurements of Atmospheric Hydrocarbons and Biogenic Emission Fluxes in the Amazon Boundary-Layer, *J. Geophys. Res.-Atmos.*, **93**, 1407–1416. DOI: *https://doi.org/10.1029/JD093iD02p01407*

Zona, D., Gioli, B., Commane, R., Lindaas, J., Wofsy, S.W., 2016, Cold season emissions dominate the Arctic tundra methane budget. *Proc. Natl. Acad. Sci. U. S. A*, **113**, 1, 40–45. DOI: *https://doi.org/10.1073/pnas.1516017113*

Zuidema, P., Sedlacek, A. J., Flynn, C., Springston, S., Delgadillo, R., Zhang, J., and co-authors, 2018, The Ascension Island boundary layer in the remote southeast Atlantic is often smoky. *Geophys. Res. Lett.*, **45**, 4456–4465. DOI: *https://doi.org/10.1002/2017GL076926*

TO CITE THIS ARTICLE:
Artaxo, P, Hansson, H-C, Andreae, MO, Bäck, J, Alves, EG, Barbosa, HMJ, Bender, F, Bourtsoukidis, E, Carbone, S, Chi, J, Decesari, S, Després, VR, Ditas, F, Ezhova, E, Fuzzi, S, Hasselquist, NJ, Heintzenberg, J, Holanda, BA, Guenther, A, Hakola, H, Heikkinen, L, Kerminen, V-M, Kontkanen, J, Krejci, R, Kulmala, M, Lavric, JV, de Leeuw, G, Lehtipalo, K, Machado, LAT, McFiggans, G, Franco, MAM, Meller, BB, Morais, FG, Mohr, C, Morgan, W, Nilsson, MB, Peichl, M, Petäjä, T, Praß, M, Pöhlker, C, Pöhlker, ML, Pöschl, U, Von Randow, C, Riipinen, I, Rinne, J, Rizzo, LV, Rosenfeld, D, Dias, MAFS, Sogacheva, L, Stier, P, Swietlicki, E, Sörgel, M, Tunved, P, Virkkula, A, Wang, J, Weber, B, Yáñez-Serrano, AM, Zieger, P, Mikhailov, E, Smith, JN and Kesselmeier, J. 2022. Tropical and Boreal Forest – Atmosphere Interactions: A Review. *Tellus B: Chemical and Physical Meteorology*, 74(2022), 24–163. DOI: *https://doi.org/10.16993/tellusb.34*

Submitted: 15 February 2022 Accepted: 15 February 2022 Published: 25 March 2022